The evolution of the autoantibody response in Graves' disease

Hargreaves, Chantal

Awarding institution:
King's College London

Title: The evolution of the autoantibody response in Graves' disease

Author: Chantal Hargreaves

Take down policy

THE EVOLUTION OF THE AUTOANTIBODY RESPONSE IN

GRAVES' DISEASE

CHANTAL ELIZABETH HARGREAVES

Thesis submitted to King's College London in candidature for the degree

of

DOCTOR OF PHILOSOPHY

(PhD)

School of Medicine

Division of Diabetes and Nutritional Sciences

London

August, 2012

ABSTRACT

Graves' disease (GD) is an antibody-mediated autoimmune disease caused by thyroid stimulating antibodies (TSAbs) activating the thyrotropin receptor (TSHR). Both genetic and environmental factors contribute to pathogenesis and one such factor is the infectious agent, *Yersinia enterocolitica*. Two high affinity TSAbs, (KSAb1, IgG_{2b}/κ; KSAb2, IgG_{2a}/κ), developed from an experimental murine model of GD, share common germline Ig genes and thus are derived from the same precursor B cell clone which diversified through somatic hypermutation.

The shared germline genes were expressed as recombinant (r) Fab germline and did not display measurable binding to TSHR in three assay systems: radioreceptor assay, flow cytometry and cAMP stimulation bioassay. Hence the precursor B cell clone was not endowed with autoreactive potential. To assess the individual contribution of KSAb1's heavy and light chains to TSHR reactivity chimeric rFab constructs were created. The interaction and stimulation of TSHR was dependent on the mature heavy chain.

Significantly, antigen recognition studies of rFab germline, KSAb1 and KSAb2 showed binding to OmpA, OmpC and OmpF of *Y. enterocolitica.* Our findings raise the possibility that the clonal expansion of B cell populations that acquire autoreactivity in the periphery may be associated with the porin proteins of *Y. enterocolitica*.

CLAIMS OF ORIGINALITY

The work described in this thesis was carried out in the Department of Diabetes and Endocrinology, Division of Diabetes and Nutritional Sciences, King's College London. Unless stated, the experiments were carried out by the author.

The thesis entitled 'The Evolution of the Autoantibody Response in Graves' Disease' has not been submitted for a degree or other qualification at another university.

Chantal Hargreaves

August, 2012.

PRESENTATIONS AT INTERNATIONAL MEETINGS ARISING FROM THESIS

Hargreaves CE, Dunn-Walters D, Banga JP. Studies on rearranged germline antibody genes that predispose potentially autoreactive B cells to produce thyroid stimulating antibodies in Graves' disease: expression as recombinant Fab antibody for evaluation of antigen binding specificity.
Poster presentation at 14th International Thyroid Congress, Paris, France, 2010.

Hargreaves CE, Dunn-Walters D, Banga JP. Anti-TSHR autoantibodies in Graves' disease develop from non-autoreactive precursors.
Oral presentation at ESF-JSPS Frontier Science Conference Series for Young Poster presentation at Cutting Edge Immunology and its Clinical Application, Holland, 2011.

Hargreaves CE, Dunn-Walters D, Banga JP. (2011). Somatic hypermutation of the immunoglobulin H-chain variable-region of thyroid stimulating antibodies determines binding to the TSH-receptor.
Oral presentation at 35th European Thyroid Association Annual Meeting, Krakow, Poland. 2011.

ACKNOWLEDGEMENTS

ABBREVIATIONS

aa	Amino acid
AID	Activation induced deaminase
Aire	Autoimmune regulator
AITD	Autoimmune thyroid disease
APC	Antigen presenting cell
BAFF	B cell activating factor
BCR	B cell receptor
bp	Base pair
B_{reg}	Regulatory B cell
BSA	Bovine serum albumin
cAMP	Cyclic adenosine monophosphate
CDR	Complementarity determining region
CHO cell	Chinese hamster ovary cell
CIA	Collagen-induced arthritis
Cpm	Counts per minute
CSR	Class-switch recombination
cTEC	Cortical thymic epithelial cell
CTLA4	Cytotoxic T lymphocyte antigen 4
D	Diversity
DC	Dendritic cell
ECL	Electrochemiluminescence
FCS	Foetal calf serum
FDC	Follicular dendritic cell

FSH	Follicle stimulating hormone
FSHR	Follicle stimulating hormone receptor
GC	Germinal centre
GD	Graves' disease
GlcNAc	N-acetyl-glucosamine
GO	Graves' orbitopathy
HBSS	Hanks' buffered saline solution
HLA	Human leukocyte antigen
HPT	Hypothalamus-pituitary-thyroid
HT	Hashimoto's thyroiditis
hTSHR	Human TSHR
IA-2	Islet cell antigen-2
IBMX	Isobutyl-1-methylxanthine
Ig	Immunoglobulin
IGF1-R	Insulin like growth factor 1 receptor
IGHV	Immunoglobulin H-chain variable region gene
IGLV	Immunoglobulin L-chain variable region gene
IL	Interleukin
IPTG	Isopropyl β-D-1-thiogalactopyranoside
iT_{reg}	Induced regulatory T cell
J	Joining
κ	Kappa chain
LB	Luria Bertani

λ	Lambda chain
mAb	Monoclonal antibody
MFI	Mean fluorescence intensity
MHC	Major histocompatibility complex
mTEC	Medullary thymic epithelial cell
mTSHR	Murine TSHR
nT_{reg}	Natural regulatory T cell
Omp	Outer membrane porin
PRR	Pattern recognition receptor
PBS	Phosphate buffered saline
PE	Phycoerythrin
PSF	Penicillin, streptomycin, fungizone
RAG	Recombinase activating gene
rFab	Recombinant Fab
RSS	Recombination signal sequences
S	Switch region
SCID	Severe combined immunodeficiency
scFv	Single chain variable fragment
SDS-PAGE	Sodium dodecyl sulphate polyacrylamide gel electrophoresis
SHM	Somatic hypermutation
SLE	Systemic lupus erythematosus
T3	triiodothyronine
Tc	Cytotoxic T cell
TCR	T cell receptor

T$_{FH}$ cell	Follicular T helper cell
Tg	Thyroglobulin
T$_H$ cell	T helper cell
TPO	Thyroid peroxidase
T$_{reg}$	Regulatory T cell
TSAb	TSHR stimulating antibody
TSBAb	TSHR stimulating blocking antibody
TSH	Thyroid stimulating hormone
TSHR	Thyroid stimulating hormone receptor
V	Variable
Y. enterocolitica	*Yersinia enterocolitica*
YLB	Yersinia Luria Bertani
Yops	Yersinia outer proteins

Table of contents

3   CHAPTER THREE: Recombinant Fab expression and evaluation of germline genes of thyroid stimulating antibodies................................... 117

Figures and Tables

19

CHAPTER ONE

GENERAL INTRODUCTION

1 CHAPTER ONE: General introduction

1.1 Immunity

1.1.1 Innate immunity

The immune system is vital for protection against infection. It functions to eliminate potentially damaging pathogenic organisms and toxic substances from the body whilst avoiding autoimmune responses against the host's self antigens. There are two arms of the immune system: the innate and the adaptive responses (Chaplin, 2010).

The innate response is the first line of defence against pathogens (Pancer and Cooper, 2006), acting quickly but without conferring memory. Innate mechanisms include physical barriers such as the skin, mucous, cilia, the acid pH of the stomach and bacteriolytic enzymes in secretions such as tears. Cellular and humoral aspects of the innate immune system enhance physical barriers and intervene when they are breached. A limited number of innate immune receptors expressed on cells are encoded by germline genes and recognise molecular structures found in many pathogens but not in human cells. The innate receptors are termed pattern recognition receptors (PRRs) e.g. TLRs (Figure 4), and the microbial components are termed pathogen associated molecular patterns (Janeway, 1989).

Figure 1: Toll-like receptors and their ligands.

TLRs are PRRs expressed on the cell surface or intracellularly to respond to a diverse range of viral and bacterial products. The function of TLR10 is unknown. Certain TLRs such as TLR7 and TLR9 have been implicated in autoimmunity.
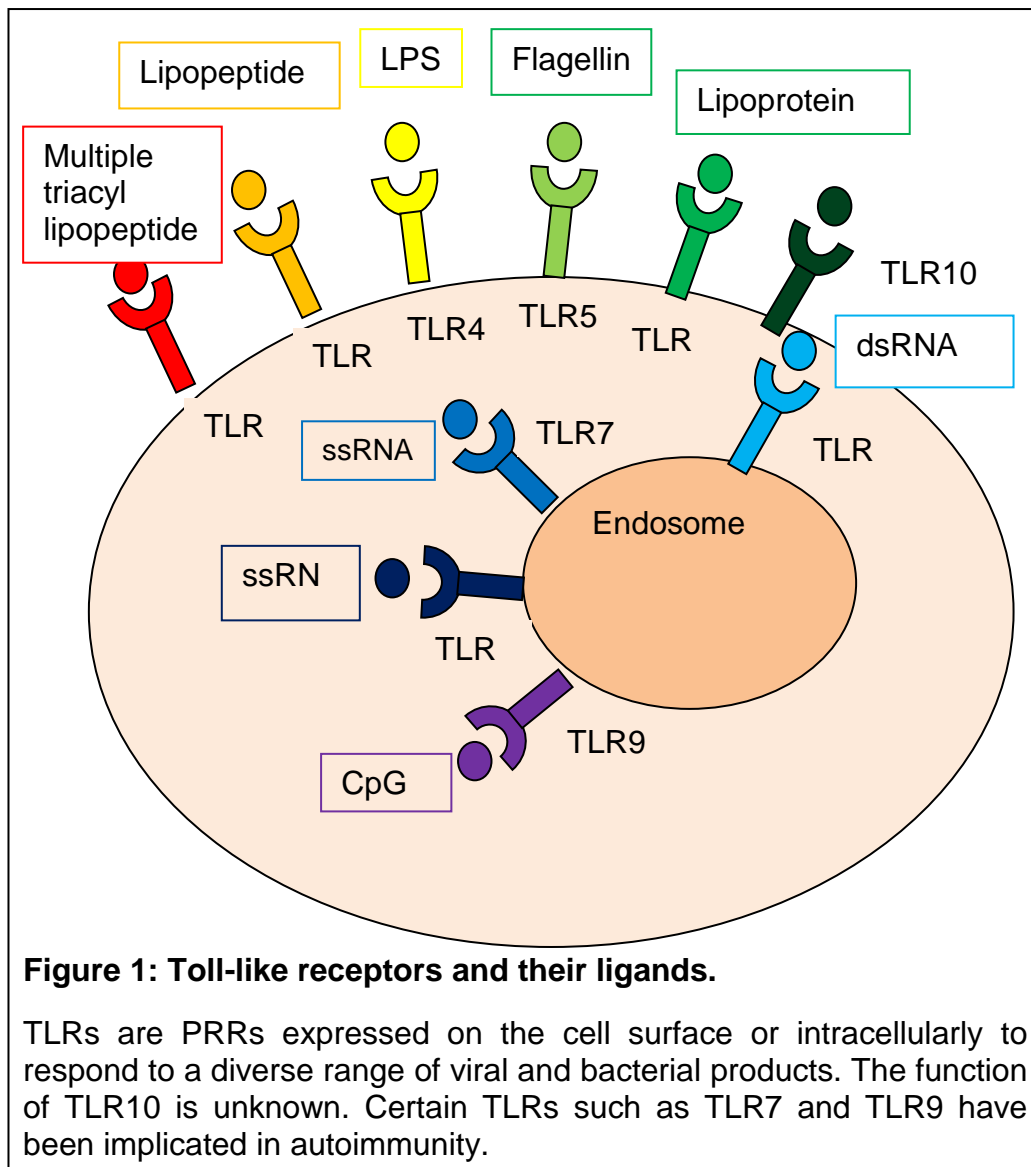
1.1.2 Adaptive immunity

The adaptive immune response is comprised of antigen-specific immune responses and thus is slower to develop than the innate response but generates long-lasting immunity (Pancer and Cooper, 2006). T and B cells comprise the adaptive immune response and recognise specific pathogens via their receptors, the T cell receptor (TCR) and the B cell receptor (BCR), or immunoglobulin (Ig), respectively (Boehm, 2011). Each TCR and BCR is generated by random somatic gene

rearrangements with genes chosen from many possible germline-encoded genes thus creating a huge repertoire of antigen specificities (Chaplin, 2010). Like the innate immune response, there are cellular and humoral arms of adaptive immunity. Specific proteins, antibodies, produced and secreted by B cells, mediate humoral adaptive immunity. The cellular arm of the adaptive immune response involves cytotoxic T (Tc) cells and helper T (T_H) cells and the release of pro-inflammatory cytokines.

1.1.3 Antigen presentation

Both B and T cells require the family of human leukocyte antigen (HLA) glycoproteins to recognise and respond to antigen. This region is encoded on chromosome 6p21, and represents the most gene-rich region of the human genome, with many important immunity-related genes expressed. HLA molecules or major histocompatibility molecules (MHC) molecules in mice, and are highly polymorphic.

HLA molecules are divided into 2 classes: HLA class I and HLA class II. HLA class I and class II proteins are both involved in antigen presentation, but differ in the peptides they present and the cells on which they are expressed (Neefjes et al., 2011). Cells expressing HLA class I present antigen to $CD8^+$ Tc cells, whilst cells expressing HLA class II present to $CD4^+$ T_H cells.

HLA class I molecules are heterodimeric proteins, formed of α-chain and β2-microglobulin, and are expressed on all nucleated cells and bind to intracellular antigenic peptides, typically from infected cells. HLA class I

molecules are encoded by three classical genes: HLA-A, -B and –C, with HLA-C being the least expressed of the three, three non-classical genes, HLA-E, -F and –G, and 12 pseudogenes (Shiina et al., 2009). The majority of peptides to be presented are degraded by the 26S proteasome after which they are transported by a transporter associated with antigen presentation to the endoplasmic reticulum. Here peptides may be trimmed to an approximate length of 8-10 amino acids, and are folded by tapasin protein and bound by stabilising chaperone proteins to allow loading onto HLA class I molecules. The HLA-peptide complex is then transported to the cell membrane for presentation (Neefjes et al., 2011).

HLA class II molecules are encoded for by three genes: -DRαβ, -DQα1β1 and –DPα1β1 (Shiina et al., 2009). Unlike HLA class I, the expression of HLA class II is more restricted; it is primarily expressed by professional APCs such as macrophages, dendritic cells (DCs) and B cells, but may be induced by IFN-γ stimulation of non-APCs. The majority of studies to understand the HLA class II pathway have involved HLA-DR, and the pathways for the other two genes may differ from that described here. HLA class II consists of transmembrane α- and β-chains paired with an invariant Ii chain. This complex is translocated to the late endosomal compartment where Ii is degraded and a residual class II associated Ii peptide (CLIP) is left in the HLA class II binding pocket. HLA-DM swaps CLIP for an exogenous peptide, degraded in the endosome, and the HLA class II/peptide complex is transported to the cell membrane for antigen presentation (Neefjes et al., 2011).

It is currently unknown why certain HLA alleles are associated with autoimmune disease for example, HLA-B27 is strongly associated with ankylosing spondylitis (Reveille, 2011), this may be due to the process of antigen presentation (Wucherpfennig and Sethi, 2011).

1.2   T cell development

Developing T cells in the thymus may be derived from one of two distinct lineages, defined by expression of either a γδ TCR or an αβ TCR, with both lineages derived from the same $CD4^-CD8^-$ precursor thymocytes. Thymocytes expressing an αβ TCR are most commonly found in the thymus and lymph nodes (Ciofani and Zúñiga-Pflücker, 2010) and will be discussed further with regard to their role in adaptive immunity and autoimmunity.

1.2.1   T cell central tolerance

T_H cells are $CD4^+$ and respond to antigen presented in the context of HLA class II molecules. Tc cells are $CD8^+$ and respond to antigen in the context of HLA class I molecules (Miller, 2011). Before leaving the thymus to enter the periphery, T cells must undergo rigorous positive and negative selection as part of central tolerance mechanisms to ensure a robust response to foreign antigens, and to prevent autoimmunity.

The thymus provides a specialised microenvironment for developing T cells and consists of a medulla region surrounded by a cortex (Ladi et al., 2006). The survival and antigen education of developing T cells are dependent on the presentation of self-antigen in the context of HLA class

I and HLA class II molecules expressed by cortical thymic epithelial cells (cTECs). Any $CD4^+CD8^+$ cells, derived from $CD4^-CD8^-$ cells, which do not engage in HLA contact, due to lack of or no affinity for antigen, die through lack of positive survival signals. Approximately 80-90% of thymocytes die by this mechanism. $CD4^+CD8^+$ cells which have an intermediate affinity for antigen receive positive selection signals from cTECs, commit to either the CD4 or CD8 lineage and migrate to the medulla by up-regulating the chemokine receptor, CCR7, to interact with DCs and medullary TECs (mTECs) (Klein et al., 2009; Ladi et al., 2006).

Negative selection occurs in the thymic medulla, where any T cell clones that recognise tissue-restricted self-antigens presented by mTECs, many under the control of the transcription factor, Aire (autoimmune regulator), are deleted (Derbinski et al., 2001). Deletion or mutation of the Aire gene results in severe organ-specific autoimmune disease in mice and humans, the autoimmune polyendocrine syndrome type 1 (Akirav et al., 2011; Mathis and Benoist, 2009). The self-antigens presented in the thymus may be derived from the bloodstream entering the thymus, resident thymic DCs or by DCs migrating there from the periphery (Klein et al., 2009; Li et al., 2009). This increases their presentation to thymocytes and increases tolerance induction (Koble and Kyewski, 2009)

The T cells emigrating from the thymus should only recognise foreign antigen when expressed in the context of a self-HLA molecule, be tolerant to self-antigen and should not respond in the periphery to cause autoimmune responses.

1.2.2 T cell peripheral tolerance

Central tolerance mechanisms are not infallible so control mechanisms exist in the periphery to prevent autoimmune disease.

Regulatory T cells (T$_{regs}$)

Natural (n) T$_{regs}$ develop alongside other conventional CD4$^+$ T cells, following intermediate to high affinity ligation of the TCR in the thymus. These cells are CD4$^+$ and express Foxp3 and CD25 (Sakaguchi et al., 2010; Sakaguchi et al., 1995; Wing and Sakaguchi, 2009). IL-2 has been shown to be an essential co-factor in nT$_{reg}$ development in the thymus, as has the NF-κB pathway (Feuerer et al., 2009). CD8$^+$ FoxP3$^+$ T$_{regs}$ have also been shown to exist to down-regulate CD4$^+$ T cell responses (Hu et al., 2011). T$_{regs}$ may also be induced (iT$_{regs}$) in the periphery through the plasticity of other subsets following exposure to certain chemicals and cytokines e.g. retinoic acid, TGF-β, vitamin D and indoleamine 2, 3-dioxygenase (Kushwah and Hu, 2011).

The importance of T$_{regs}$ is demonstrated by the severe proliferation of lymphocytes and multi-organ autoimmune disease observed in scurfy mice and immunodysregulation polyendocrinopathy and enteropathy, X-linked syndrome (known as IPEX syndrome) in humans, a monogenic disease caused by the deletion of the *foxp3* gene (Feuerer et al., 2009; Godfrey, 1991; Wildin et al., 2001). Similarly, altered numbers or function of T$_{regs}$ have been found and implicated in the development of numerous immune disorders (Buckner, 2010). Current *in vitro* assays used to measure the suppressive activity of T$_{regs}$ do not accurately reflect their

suppressive activity *in vivo*, so it is not known exactly how T$_{regs}$ interact with and control the responses of other cells. Further proposed T$_{reg}$ subsets include T$_H$1 T$_{regs}$, T$_H$2 T$_{regs}$ (Duhen et al., 2012) and DN T$_{regs}$ (Kushwah and Hu, 2011).

1.2.3 T cell activation

This discussion of T cell activation will focus on cell surface markers and their interactions rather than intracellular signalling events in the interest of brevity.

In the periphery, T cells require multiple signals and co-ligations to activate and respond to antigen. Signal 1 comes from peptide in the context of HLA engaging the TCR. It is thought that peptide-HLA complexes can sequentially engage multiple TCRs to amplify the signal and reach the necessary activation threshold. Signal 2 comes from ligation of accessory molecules, for example, CD28 on the T cell binding CD80/CD86 on the APC (Alegre et al., 2001). Signal 2 is likely a fine balance between pro- and anti-stimulatory signals and results in T cell proliferation and cytokine release. CD28 is constitutively expressed by resting and activated T cells and its ligands, CD80 and CD86, are expressed on activated APCs. CD28 increases TCR-mediated T cell survival, proliferation, cytokine release and ability to help B cells (Walker and Sansom, 2011). CD28 signalling may lower the TCR threshold necessary for T cell activation, possibly by decreasing the contact time with APCs (Iezzi et al., 1998). This contrasts with the function of cytotoxic T lymphocyte antigen 4 (CTLA4). A third signal comes from inflammatory

cytokines and determines the type of cell differentiation into T_H or Tc cells (Kalinski et al., 1999) (Figure 2, page 29).

Figure 2: T cell activation.

T cells are activated following multiple signals. Signal 1 is provided by the ligation of the TCR with its cognate antigen presented in the context of self-HLA expressed by an APC. Signal 2 is a fine-balance between the ligation of the pro-stimulatory molecule CD28 with CD80/CD86 and the anti-stimulatory molecule CTLA4 with two ligands, CD80/CD86. Signal 3 comes from the cytokine milieu and may determine the T cell subset differentiation. Figure is adapted from (Alegre et al., 2001).

CTLA4 competes with CD28 for CD80/CD86 binding to function as a negative regulator of T cell signalling (Walker and Sansom, 2011). It is up-regulated by T cells several days after activation in mice and humans (Linsley et al., 1992), and is constitutively expressed by resting and activated regulatory T cells (T_{regs}) (Read et al., 2000; Takahashi et al., 2000). CTLA4 has a higher affinity and avidity than CD28 for CD80/CD86; CTLA4-CD80 represents the strongest ligand interaction, CD28-CD86 the weakest (Collins et al., 2002) therefore CTLA4

antagonises CD28 binding. Variants in CTLA4 have also been implicated in multiple autoimmune diseases including type 1 diabetes (T1D), rheumatoid arthritis (RA) and GD (Karumuthil-Melethil et al., 2010; Liu et al., 2011; Takahashi and Kimura, 2010).

The T_H cell subsets mentioned in this thesis, their defining transcription factor and cytokines are summarised in Figure 3, page 30.

Figure 3: T helper cell subset differentiation.

Naive $CD4^+$ T cells (T_H0) may differentiate into numerous possible 'helper' subsets following antigenic challenge and depending on the cytokine milieu. T cell subsets are defined by their transcription factors and cytokines.
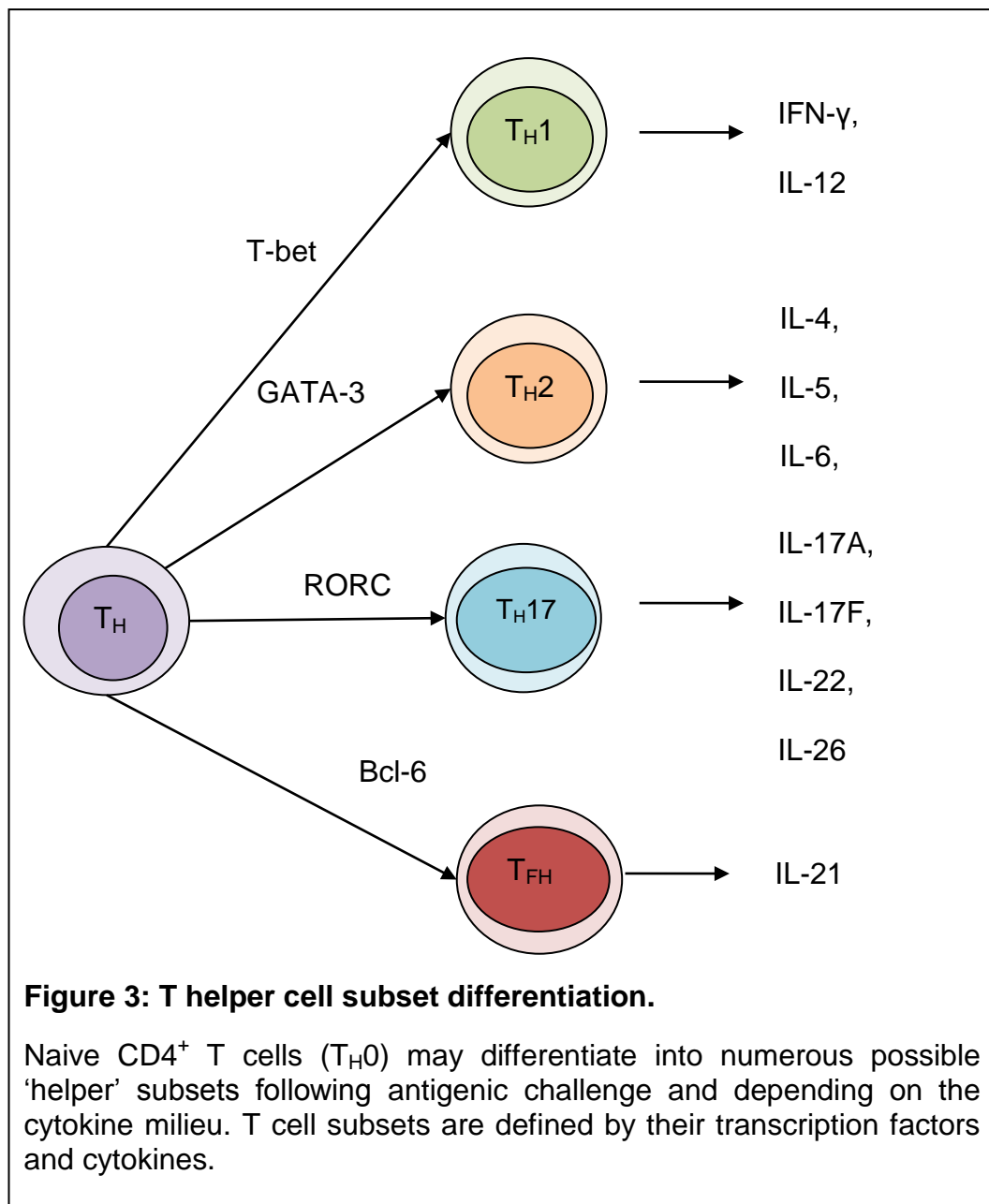
1.3 B cell development

B cells develop in the foetal liver and adult bone marrow from haematopoietic stem cells. In the periphery, B cells form an integral part of the humoral immune system by secreting antigen-specific antibody, acting as APCs and producing pro- and anti-inflammatory cytokines.

1.3.1 Antibody structure and subtypes

Antibody molecules belong to the Ig superfamily and consist of two glycosylated heavy (H)-chains and two non-glycosylated light (L)-chains, connected by disulphide bridges. H-chains comprise 3-4 constant (C) regions (C_H1-4), and one variable (V) region (V_H), whilst L-chains comprise one C-region (C_L) and one V-region (V_L). A hinge region links C_H1 and C_H2. H-chain has a molecular weight (MW) of 55 kDa, whilst an L-chain has a MW of 25 kDa.

The antigen binding, Fab, region of the antibody is formed of the entire L-chain with V_H and C_H1. The V-region of the Fab portion differs between the H- and L-chains. The V-region of the H-chain (immunoglobulin heavy chain Variable region; IGHV) is formed of three genes, Variable (V), Diversity (D) and Joining (J) genes, whilst the immunoglobulin light chain variable region (IGLV) is formed of the V and J genes, without a D gene. The V-region may also be subdivided into four framework (Fw) regions and three hypervariable complementarity determining regions (CDRs), with CDR 3 being the most variable and largest (Figure 4, page 32). The V gene encodes Fw 1-3 and CDRs 1-2 and the N-terminus of CDR3, the J gene segment continues CDR 3 and the complete Fw 4, the D gene

segment is found in CDR 3 between the C-terminus of the V gene and the N-terminus of the J gene (Figure 4) (Schroeder Jr and Cavacini, 2010).

The specific subtype of antibody is determined by the Fc portion, and may be IgM, IgD, IgA, IgE or IgG. IgG is the predominant antibody in serum and is further subdivided to IgG_1, IgG_2, IgG_3 and IgG_4 in humans, and IgG_1, IgG_{2a}, IgG_{2b} and IgG_3 in mice (Mix et al., 2006). IgM is the first antibody generated and is secreted in pentameric form, linked by a J chain; monomeric IgM has a lower affinity for antigen than the pentameric form (Weinstein et al., 2004). IgD's function is not fully understood (Chen and Cerutti, 2011). IgA is the main antibody found in mucosal locations. IgE is found in only trace amounts in serum but cause hypersensitivity reactions when bound to basophils causing their degranulation. (Weinstein et al., 2004).

Figure 4: Immunoglobulin G structure.

An IgG molecule contains two H-chains and two L-chains. The H-chain is encoded by V_H, D_H and J_H genes and 3-4 C_H genes. The L-chain is encoded by V_L and J_L genes. The Fab portion of the antibody is involved in antigen binding and the Fc portion is involved in signalling. CDRs shaded in light blue in the H and L chain V regions, Schroeder Jr and Cavacini, 2010.

1.3.2 VDJ recombination

To become functional, B cells must assemble and express a functional Ig molecule, from germline V, D and J genes. There are multiple VDJ genes to choose from and their random selection and rearrangement ensures a diverse cell population.

H-chain recombination

Recombination occurs firstly in the H-chain locus on chromosome 14q32, with D_H and J_H genes chosen at random and recombined together (Jung et al., 2006). The DJ_H gene segment is then combined with a randomly selected V_H gene. All other unused genes are excised as excision circles and a primary transcript is synthesised with a C-region gene.

All recombination events are under the control of the recombinase activating genes (RAG) 1 and 2. RAG 1 and 2 create double strand breaks at specific recombination signal sequences (RSSs), which are found at the 3` end of the V genes, 5` end of the J genes and both sides of the D genes. Which VDJ genes are selected and recombined is determined based on the RSSs that flank them, termed the 12/23 rule. RSSs may be either 12 or 23 base pairs (bp) long spacer sequences separating conserved heptamer or nonamer sequences; a gene flanked by a 12 bp RSS will be recombined with another gene segment flanked by a 23 bp RSS. Typically, RAG 1 will recognise e.g. the 12 bp spacer, RAG 2 then associates with RAG 1 and the same happens to the 23 bp spacer and a synaptic complex is formed (Schroeder Jr and Cavacini, 2010).

The RAG proteins nick a single strand of DNA at the heptamer sequence forming a hairpin loop, which is subsequently nicked again, and several nucleotides are removed from the end to create a 3' overhang. The overhang may be further modified for example by terminal deoxynucleotidyl transferase (TdT) which inserts non-germline encoded nucleotides at random, and is subsequently repaired (Figure 5) (Schroeder Jr and Cavacini, 2010). The random selection and rearrangement of VDJ genes is the first step in the creation of a diverse antigen receptor repertoire, known as recombinatorial diversity. Further junctional diversity is created by the random insertion of 'N' nucleotides at the junctions between VDJ genes by TdT. VDJ recombination is summarised in Figure 5.
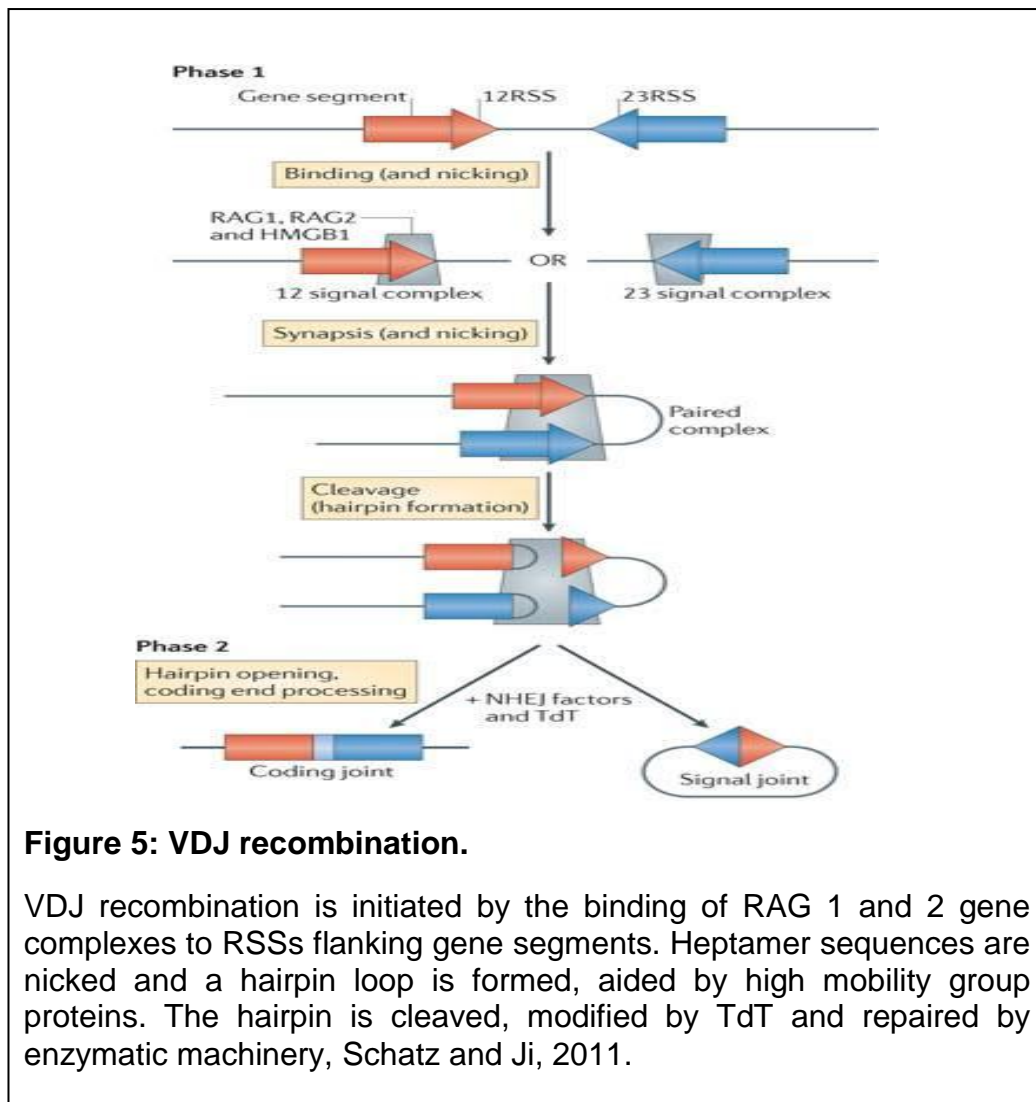
Figure 5: VDJ recombination.

VDJ recombination is initiated by the binding of RAG 1 and 2 gene complexes to RSSs flanking gene segments. Heptamer sequences are nicked and a hairpin loop is formed, aided by high mobility group proteins. The hairpin is cleaved, modified by TdT and repaired by enzymatic machinery, Schatz and Ji, 2011.

L-chain recombination

There are two types of L-chain: the κ chain locus encoded on chromosome 2p11 and the λ chain encoded on chromosome 22q11. Initial rearrangements begin at the L-chain κ locus and it is only if this locus proves unsuccessful and all possible Vκ and Jκ genes are exhausted, that the λ locus is rearranged. To ensure B cells express Ig with only one type of L-chain, non-productive κ genes are silenced by allelic exclusion (Gonzalez et al., 2007). The pairing of assembled functional H- and L-chains generates a surface IgM molecule and At this

developmental stage, immature B cells may now leave the bone marrow to recirculate through the secondary lymphoid organs to search for antigen (Pillai et al., 2011).

1.3.3 Germinal centre

B cells express CXCR5 to gain entry to the lymphoid organ follicles, in response to the expression of its ligand, CXCL13, expressed by follicular stromal cells (Gatto and Brink, 2010).

Germinal centre reaction

Antigen-specific B cells seed the GC following ligation of the B cell-expressed CD40 with CD40L expressed by activated T cells, as well as the action of cytokines secreted by T cells that promote B cell proliferation and differentiation. GCs are formed of a dark zone and light zone, named according to their histological appearance and are surrounded by outer and marginal zones (Figure 6, page 38). B cells become centroblasts in the dark zone, where they down-regulate their surface Ig and undergo rapid proliferation. Centroblasts express high levels of CXCR4, and its ligand, CXCL12, is in high abundance within the dark zone. Here they are close to the T cell zone where they receive help from T_{FH} cells; B cells express EB12 and CCR7 to distribute along this boundary, whilst T cells upregulate CXCR5 and Bcl-6 (Gatto and Brink, 2010; Vinuesa et al., 2005). Bcl-6 is the master regulator of GC localisation and prevents plasma cell differentiation by suppressing Blimp-1 expression (Crotty et al., 2010).

Centroblasts undergo the process of somatic hypermutation (SHM) to increase their affinity for cognate antigen. The enzyme, activation-induced deaminase (AID), is expressed primarily in the dark zone and demethylates deoxycytidine residues in IGHV and IGLV genes, which are excised by uracil DNA glycosylase. The excised uracil residues are replaced at random by an error-prone polymerase, which alters the specificity and affinity of the BCR for its antigen. This process of SHM may introduce mutations which decrease the BCR's affinity for antigen, or which introduce self-reactivity. The mutations may be silent or replacement: silent mutations do not alter the amino acid sequence of the BCR, whilst replacement mutations result in a change in amino acid and thus can have a dramatic impact on the structure and binding of the receptor. A high ratio of replacement to silent mutations indicates an antigen-driven response.

In the GC light zone, centroblasts become centrocytes mediated by CXCR5 and CXCL13 (Gatto and Brink, 2010). Light zone B cells are small and express surface Ig that they use to process antigen from FDCs and present to T_{FH} cells to elicit help (Figure 6, page 38). T_{FH} cells provide signals for differentiation and survival such as IL-21 (Zotos et al., 2010), CD40-CD40L and ICOS-ICOSL interactions. IL-21, in combination with anti-CD40 antibody, induces increased mitogenesis and differentiation into antibody-secreting cells *in vitro*. T cells stimulated by the TCR and ICOS secrete IL-10 which also acts to promote proliferation and differentiation of B cells (Vinuesa and Cyster, 2011; Vinuesa et al., 2005). In the absence of antigen-specific T_{FH} cells, centrocytes are

deleted and thus T cell help in GCs is a critical checkpoint for peripheral

B cell tolerance. GC B cells that fail to receive survival signals can be

rescued from apoptosis by CD40 ligation. Apoptotic cells are removed by

tingible body macrophages, as they may be immunogenic and promote

an autoreactive response to DNA antigens displayed as the B cell

apoptoses (Basten and Silveira, 2010).

Figure 6: Germinal centre reaction.

B cells encounter antigen in the follicle and become initially activated with T cell help. They undergo intense proliferation and SHM in the dark zone. In the light zone B cells with improved affinity for antigen receive survival and differentiation signals from FDCs and T_{FH} cells and undergo CSR to change their subtype. B cells then become either memory or plasma cells and leave the GC. Figure is adapted from Kuppers, 2003.

Class-switch recombination

As mentioned previously in Section 1.3.1, there are numerous subtypes

of antibody, defined by their Fc region. The light zone is also the location

38

where antibodies undergo class-switch recombination (CSR) to become IgA, IgE or IgG-expressing cells following cytokine stimulation. CSR occurs between switch (S) regions upstream of their paired C_H genes, except Cδ, located downstream of the VDJ_H segment. S regions are the specialised targets as CSR is eliminated in cells with deleted S regions. The C_H gene is part of a transcription unit, comprising an upstream intronic promoter, non-coding exon, S region, C_H gene and germline transcript. CSR is initiated from the intronic promoter and finishes at the 3' end of the C_H gene (Stavnezer et al., 2008). Like in the process of SHM, AID is an important enzyme, and acts in a similar manner (Muramatsu et al., 2000). It deaminates cytosines to convert them to uracil residues; these are removed to introduce DNA breaks in the donor (Sμ) and acceptor (downstream) S regions. Ku70 and Ku80 proteins bind to the ends of the DNA to allow end processing and joining (Stavnezer et al., 2008).

Ectopic GC

Follicular structures which resemble GCs and contain FDCs have been reported in the thymus of myasthenia gravis patients (Zuckerman et al., 2010), in chronically inflamed tissues such as the synovium in rheumatoid arthritis (Huizinga et al., 2009) and in murine SLE models (Nacionales et al., 2009). These structures are termed ectopic GCs.

Intrathyroidal lymphocytic infiltrates are a characteristic feature of GD pathogenesis. Suspended lymphocytes (McLachlan et al., 1983) and tissue sections (Warford et al., 1984) from GD thyroids have shown

varying degrees of infiltration between patients, without a striking difference in the proportions of B cell, T_H, Tc and APC compartments. Interestingly, stained thyroid tissue sections showed a diffuse T cell infiltrate whilst B cells tended to aggregate together (Warford et al., 1984). Ectopic GCs have been demonstrated in the thyroids of autoimmune thyroid diseases (AITD) patients, including those with GD. In Hashimoto's thyroiditis (HT), the ectopic structures are large and similar to the GCs observed in tonsils; however in GD the structures are small and similar to those in lymph nodes. There was a positive correlation between the presence of ectopic GC in thyroids and anti-thyroid antibody titre (Armengol et al., 2001).

As ectopic GCs are outside the traditional secondary lymphoid organs, they may be able to escape normal peripheral tolerance mechanisms more easily than typical GCs and thus contribute to or initiate the pathogenesis of autoimmune disease.

1.3.4 B cell tolerance

Tolerising B cells is important, not just for their functional roles in antibody secretion, antigen presentation and source of pro- and anti-inflammatory cytokines, but also because of the random nature of generating a diverse repertoire. The random nature of VDJ recombination and SHM inevitably leads to the development of autoreactive cells that must be removed or silenced. There are several overlapping tolerance mechanisms at several 'checkpoints' at which self-reactivity may be tested for and tolerance imposed.

1.3.4.1 B cell central tolerance

More than 50% of all early B cells in the bone marrow are poly- or autoreactive, yet only 5-20% of circulating mature B cells are autoreactive in healthy individuals (Wardemann et al., 2003).

B cell central tolerance is exerted within the bone marrow by deletion and receptor editing of B cells expressing receptors with a medium to high avidity for antigen. The earliest tolerance checkpoint may occur at the pro- to pre-B cell stage. Cells with autoreactive Ig H-chains may be removed by a poorly understood tolerance mechanism (Kohler et al., 2008). Pro-B cells with unproductive VDJ rearrangements that have exhausted all possible V_H alleles are deleted. Similarly, pre- or immature B cells expressing receptors with too high an avidity for antigen are also deleted. Self-reactive immature cells revert back to the pre-B cell stage, re-express the RAG genes and begin rearranging the L-chain locus as part of the receptor editing process (Pillai et al., 2011). New upstream V_K and downstream J_K genes are rearranged and replace the original self-reactive rearrangement. If the new rearrangement continues to recognise self-antigen then further rearrangements occur, if all possible κ genes are exhausted, then the κ locus is deleted and rearrangements begin at the λ locus. This process is mediated by the κ deleting element in humans (Siminovitch et al., 1985). Receptor editing is the predominant method of central tolerance within the bone marrow, with cells that remain autoreactive being clonally deleted (Halverson et al., 2004; Pelanda et al.,

1997). Defects in the receptor editing process have been demonstrated in SLE and type 1 diabetes patients (Panigrahi et al., 2008).

1.3.4.2 B cell peripheral tolerance

Due to the random nature of VDJ recombination and the large number of poly- and auto-reactive B cells produced in the bone marrow, it is unsurprising that some may escape central tolerance mechanisms. Indeed compared to naïve B cells, the memory B cell compartment is enriched with auto- and polyreactive clones (Tiller et al., 2007). Thus further tolerance mechanisms exist in the periphery (Figure 7, page 45).

Clonal deletion and anergy

Transitional B cells that react with high avidity to self-antigens in the secondary lymphoid organs are clonally deleted in a Bim-dependent manner. Cells with low avidity for self-antigen become anergic and acquire a T-3 phenotype (IgD^{hi} IgM^{lo} CD93^{+}) (Pillai et al., 2011). Anergic B cells cannot enter follicles and undergo apoptosis as the anergy is not reversible by ligation of co-stimulatory molecules or TLRs. Cells with very low avidity are ignored and do not receive survival signals, such as B cell activating factor (BAFF) (Basten and Silveira, 2010).

Survival signals

BAFF is a crucial survival factor for T and B cells. In the periphery autoreactive cells must compete with non-autoreactive cells for BAFF signals (Liu and Davidson, 2011; Stadanlick and Cancro, 2008). Experiments in transgenic mice show that BAFF levels control the

selection stringency after the T1 stage. Excess of BAFF has no effect prior to the T1 stage where it rescues anergic autoreactive cells, promoting their differentiation along the follicular and marginal zone pathways. Mature autoreactive B cells seem to have a greater need for BAFF for survival over non-autoreactive cells (Liu and Davidson, 2011).

In an induced murine model of GD (Gilbert et al., 2006a), soluble decoy receptors blocked BAFF binding and significantly reduced induced GD as shown by a decrease in anti-TSHR antibodies, indicating that BAFF is an important mediator of hyperthyroidism and BAFF blockade is an attractive therapeutic intervention (Gilbert et al., 2006c). More recently BAFF has been implicated in patients with GD and its complication Graves' orbitopathy (GO). Serum basal BAFF levels were significantly higher in GD patients compared to controls (Vannucchi et al., 2012).

Germinal centre tolerance checkpoints

The GC is a key peripheral checkpoint in B cell development; GC B cells have a pro-apoptotic phenotype, down-regulating Bcl-2 and up-regulating Bim, ensuring their deletion if they do not receive survival signals from T_{FH} cells. There may be a tolerance checkpoint after the GC reaction before cells can differentiate into plasma cells. In FcγRIIb-deficient mice, an accumulation of autoreactive GC B cells secreting somatically mutated antibody was observed. The authors suggest that FcγRIIb contributes to the removal of autoreactive B cells within the GC (Tiller et al., 2010), this may be because FcγRIIb is typically up-regulated by antigen-experienced B cells and it limits both the differentiation and reactivation of memory

cells and the survival of plasma B cells (Mackay et al., 2006; Xiang et al., 2007). The bone marrow plasma cell compartment has a significantly lower proportion of auto- or polyreactive B cells suggesting a tolerance checkpoint before plasma cells can enter the bone marrow (Scheid et al., 2011).

Regulatory B cells

A subset of B cells with suppressive capacity was first reported several decades ago (Zembala et al., 1976). In recent years there has been a renewed interest in this subset (Mauri and Bosma, 2012) which has resulted in the characterisation of IL-10-producing $CD5^{hi}$ $CD1d^{hi}$ B10 cells (Yanaba et al., 2008) and $CD19^{+}$ $CD24^{hi}$ $CD38^{hi}$ B_{regs} (Blair et al., 2010). These cells are capable of suppressing both B and T cells, possibly by the induction of $FoxP3^{+}$ T_{regs} (Carter et al., 2012). Selective knockout of B10 cells in chimeric mice resulted in exacerbated arthritis, decreased $FoxP3^{+}$ T_{regs} and increased T_H1 and T_H17 cells. Altered pro- and anti-inflammatory T cell ratios were only resolved on subsequent transfer of wildtype B10 cells (Carter et al., 2011). B cells presenting self-antigen in mice have been shown to be capable of inducing $FoxP3^{+}$ T_{regs} (Morlacchi et al., 2011; Zheng et al., 2010) rather than anergy or clonal deletion, which was induced by DCs presenting self-antigen (Morlacchi et al., 2011).

It is unknown whether clinical autoimmunity is a result of a breach in one or multiple tolerance checkpoints.

Figure 7: B cell development and tolerance checkpoints.

B cells develop initially in the bone marrow and migrate to the periphery following rearrangement of their BCR. Central and peripheral tolerance checkpoints are numbered. (1) Pro-B cells expressing unproductive rearrangements are deleted; (2) pre-B cells displaying high avidity antigen interactions are clonally deleted; (3) autoreactive immature B cells revert to the pre-B cell stage and undergo receptor editing; (4) transitional cells that react with high avidity are deleted and cells that react with low avidity are rendered anergic; additionally B cells must compete for survival factors such as BAFF; (5) marginal zone B cells contain B_{reg} populations; (6) unknown checkpoint for entry to bone marrow plasma cell compartment.

1.4 The thyroid gland

The thyroid gland functions to synthesise and secrete the hormones, thyroxine (T_4) and triiodothyronine (T_3). For this function, the thyroid stimulating hormone receptor (TSHR) in the basolateral membrane of thyroid follicular cells is ligated by its hormone, thyroid stimulating hormone (TSH), to trigger hormone synthesis and release. Iodine is an essential part of hormone formation and is transported as iodide into the thyroid follicular cell by the sodium iodide symporter expressed in the basolateral membrane. Efflux of iodide across the apical membrane and into colloid is likely to be mediated by the chloride exchanger, pendrin (Gillam et al., 2004). Thyroid peroxidase (TPO) oxidises iodine allowing it to bind tyrosyl groups of the scaffold molecule, thyroglobulin (Tg), in the presence of H_2O_2. TPO also catalyses the coupling of iodotyrosyl residues within the Tg molecule to form 3-monoiodotyrosine (MIT) and 3,5`-diiodothyrosine (DIT). Within the Tg molecule the prohormone, T_4, is formed following the coupling of two DIT molecules, whilst small amounts of the active hormone, T_3, are formed of one MIT molecule coupling with one DIT molecule (Dunn and Dunn, 2001) (Figure 8, page 47).

In the periphery, thyroid hormones enter target cells in a transporter-dependent fashion and T_4 is converted to active T_3 hormone where needed by type 2 iodothyronine deiodinase, whilst this conversion is prevented by type 3 iodothyronine deiodinase (Bianco and Kim, 2006). Active T_3 hormone binds to thyroid hormone nuclear receptors which regulate the relevant T_3-targeted genes which control such processes as

protein synthesis, metabolism, thermogenesis (Bassett and Williams, 2008) and prevents cretinism (Weetman, 1990).

Figure 8: Thyroid hormone synthesis.

To synthesis hormone, iodide is transported into the cell by the NIS and TPO catalyses its coupling to Tg. TPO further catalyses the iodotyrosol molecules within Tg, MIT and DIT, to form T4 and T3 hormones which are then released into the periphery.
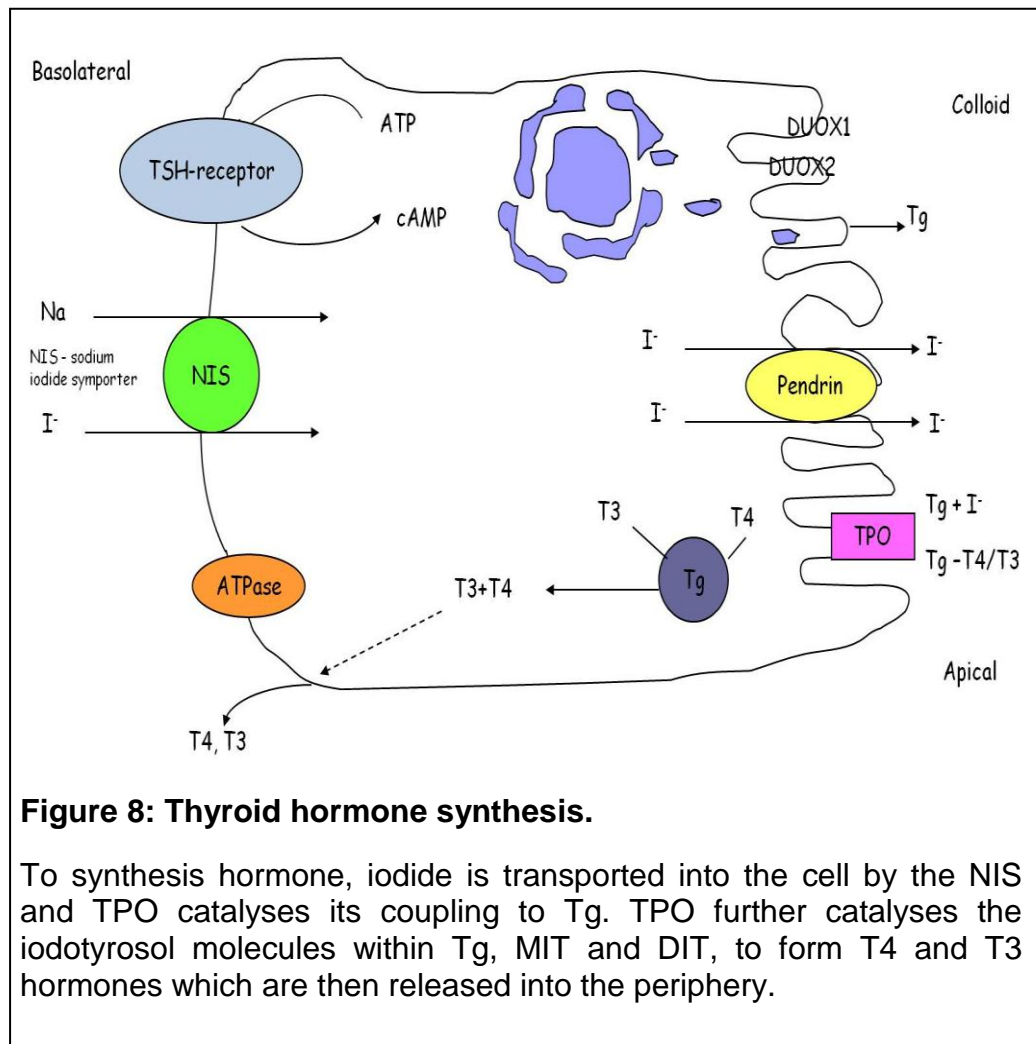
In euthyroid individuals thyroid hormone levels are regulated by a negative feedback loop of the hypothalamic-pituitary-thyroid axis, with ligation of TSH with the TSHR promoting thyroid hormone production whilst peripheral thyroid hormones negatively feedback to down-regulate thyroid releasing hormone and TSH production (Kopp, 2001).

1.5 Autoimmune thyroid disease

The thyroid gland is particularly susceptible to autoimmune processes and AITD represent the most common of the autoimmune diseases, affecting 2-5% of the Caucasian population (Simmonds and Gough, 2004a). The two main forms of AITD are GD and HT. Both conditions feature lymphocytic infiltration of the thyroid gland; however only in HT is the thyroid gland destroyed, as although GD thyroids develop foci of lymphocytes, the architecture of the gland remains intact. HT is characterised by goitre, hypothyroidism and autoantibodies against TPO and Tg antigens. The destruction of the thyroid follicles is a result of infiltrating Tc lymphocytes, and possibly death receptor-mediated apoptosis of thyroid cells (Stassi et al., 1999; Weetman, 2004b).

1.6 Thyroid autoantigens

The development of autoantibodies to thyroid components is a key feature of AITD, the autoantigens involved are long known and have been well characterised. The main autoantigens are Tg, TPO and TSHR. In HT autoantibodies to Tg and TPO develop, leading to the destruction of thyroid follicles and causing a hypoactive thyroid gland, while in GD agonist autoantibodies to the TSHR develop, causing a hyperactive thyroid (Simmonds and Gough, 2004b; Smith et al., 1988; Weetman, 2004a). However antibodies to all three autoantigens may be found in both GD and HT patients.

1.6.1 Thyroglobulin

Tg is expressed in the thyroid where it is the most abundant protein. It is the largest known autoantigen in the human body at 2749 aa (660 kDa) and anti-Tg antibodies were the first of the thyroid autoantibodies to be discovered (Campbell et al., 1956). Tg undergoes extensive post-translational modifications such as iodination. Indeed the level of iodination is related to the antigenicity of the molecule, with T cells only responding to iodinated Tg (Barin et al., 2005; Li and Carayanniotis, 2006). Tg is found in the peripheral blood but in its poorly iodinated, poorly antigenic form (Schneider et al., 1983). Furthermore, Tg has been implicated as an autoantigen in the extrathyroidal complication of GD, Graves' orbitopathy (GO). Tg was fist implicated in GO four decades ago (Kriss et al., 1967) and has recently been confirmed by a study showing Tg expression by fibroblasts in culture (Fernando et al., 2012).

1.6.2 Thyroid peroxidase

TPO is a large glycoprotein of 933 aa (107 kDa) found in the apical membrane of the thyroid follicular cell (Hadj-Kacem et al., 2009). It was the second thyroid autoantigen to be discovered following the seminal Tg findings. Antibodies to the thyroid microsomal antigen were shown to be anti-TPO antibodies (Banga et al., 1986; Czarnocka et al., 1985). Autoantibodies to TPO are found in the serum of AITD patients, are associated with complement fixation (Blanchin et al., 2003; Rebuffat et al., 2008; Weetman, 1990) and are markers of thyroid dysfunction (McLachlan and Rapoport, 2007).

1.6.3 Thyroid stimulating hormone receptor (TSHR)

The *tshr* gene is located on chromosome 14q13 and codes for a 764 amino acid (aa) protein. It is encoded by 13 exons and 12 introns (Kakinuma and Nagayama, 2002). The TSHR is expressed on the basolateral surface of thyroid follicular cells. A computer modelled structure of the TSHR is in Figure 9, page 52.

The TSHR belongs to the superfamily of G protein-coupled receptors, and forms a distinct subgroup of glycoprotein hormone-binding receptors with follicle stimulating hormone receptor (FSHR) and leutinising hormone receptor. The three receptors share approximately 70% amino acid similarity in their transmembrane domains and 39-45% similarity in their ectodomains (Kopp, 2001). Despite this similarity there is no cross-reactivity between the hormones and receptors. The TSHR is unique among this receptor family as it is a heterodimeric protein, comprising the A subunit and the B subunit (transmembrane domain), linked by disulphide bonds

Molecular cloning of the TSHR was achieved in 1989 and 1990 by three independent groups using various cloning methods (Frazier et al., 1990; Misrahi et al., 1990; Nagayama et al., 1989). The A-subunit is heavily glycosylated (40%) (Oda et al., 1999) and further comprises two cysteine-rich repeats flanking nine leucine-rich repeats in a horseshoe-shaped structure of α-helices and β-sheets arranged in parallel (Parmentier et al., 1989). The protein comprises a 21 aa leader sequence, a large A-subunit, seven transmembrane domains and an intracellular cytoplasmic

tail (Rapoport et al., 1998). The TSHR has an 8 aa insertion at its N-terminus (residues 38-45) and 50 aa at the C-terminus of the A-subunit (residues 316-366), the latter forms the proteolytic cleavage site of the receptor (Rapoport et al., 1998) not seen in the other receptors.

The TSHR undergoes intramolecular cleavage and shedding of the A-subunit (Loosfelt et al., 1992; Misrahi et al., 1994). The reasons for A-subunit shedding are as yet unknown. It has been suggested that release of the A-subunit into the blood may trigger autoimmunity in susceptible individuals (Chen et al., 2003; Mizutori et al., 2009). Confirmation of the antigenicity of the A-subunit comes from agonist anti-TSHR antibodies preferentially recognising the A-subunit rather than the full-length TSHR holoreceptor (Chen et al., 2003). Injection of mice with Ad-TSHR289 resulted in a greater incidence of experimental GD than mice immunised with holoreceptor (Chazenbalk et al., 2002; Chen et al., 2004; Gilbert et al., 2006b; Mizutori et al., 2009). It has been postulated that the shed A-subunit could trigger or enhance the anti-TSHR immune response in the periphery (Rapoport and McLachlan, 2007); detectable levels have been observed in the culture medium of primary thyrocytes (Couet et al., 1996) however detectable levels of shed A-subunit have not been found in murine serum (Pichurin et al., 2006). In humans, two single nucleotide polymorphisms (SNPs) in intron 1 of the TSHR gene lead to the generation of truncated soluble variants of the TSHR which may be secreted, increasing the immunogenicity of the receptor in genetically susceptible individuals (Brand and Gough, 2010; Płoski et al., 2010).
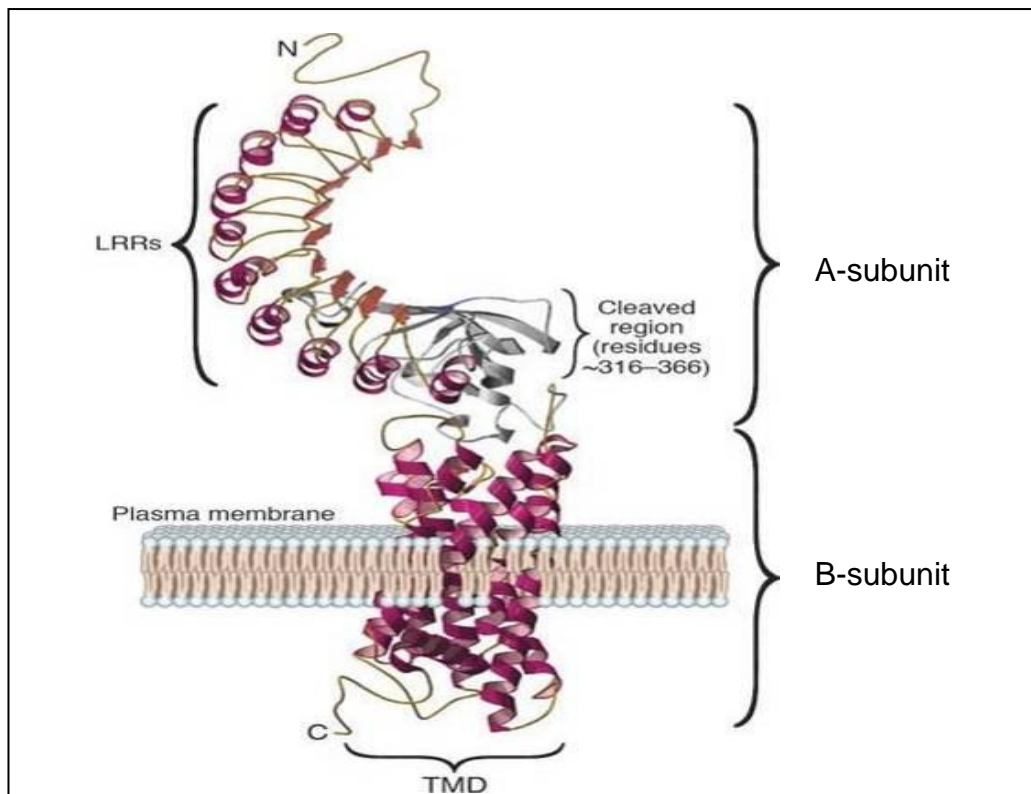
Figure 9: Computer-modelled structure of the TSHR.

In common with other glycoprotein hormone receptors, the TSHR comprises an ectodomain (A subunit) linked to 7 transmembrane domains (TMD, or B subunit). The ectodomain is composed of 9 leucine-rich repeats (LRRs) and may be shed following proteolytic cleavage. The cleavage region is unique to the TSHR amongst other similar receptors. Figure is adapted from (Davies et al., 2005).

1.6.3.1 TSHR activation and signalling

TSHR activation by TSH results in thyroid hormone synthesis, iodide uptake and cellular growth. The transmembrane region of the TSHR is involved in transmitting the activating signal across the membrane following TSH ligation. The receptor is coupled to $G_{s\alpha}$ and adenylyl cyclase is activated and cyclic adenosine monophosphate (cAMP) levels are increased. The rise in cAMP gives rise to phosphorylation of protein kinase A and the subsequent activation of factors in the cytosol and nucleus (Dremier et al., 2002; Kopp, 2001). Higher doses of TSH couple

the TSHR to $G_{q/11}$, activating phospholipase C-dependent diacylglycerol/inositol 1,4,5 triphosphate pathway which results in H_2O_2 generation and iodination (Laurent et al., 1987). Following TSH binding the receptor is internalised and accumulates in endosomes before being recycled to the cell surface again (Singh et al., 2004).

Many G protein-coupled receptors are constitutively active and some may signal without ligand interactions (Farid and Szkudlinski, 2004). The TSHR transmembrane domain displays a high level of constitutive activity, with a truncated form displaying constitutive activity, despite lacking 98% of the A-subunit. This constitutive activity was suppressed in part by rejoining the truncated receptor with the A-subunit, suggesting that the A-subunit inhibits the constitutive activity of the transmembrane domain. (Zhang et al., 2000). Zhang *et al* proposed a 'two-state' model of receptor activation, whereby the two subunits of the receptor are in equilibrium between an inactive "closed" state and a constitutively active "opened" state that can associate with G_s in the absence of TSH and trigger downstream signalling pathways. Furthermore, TSH preferentially binds "open" receptors and stabilises them, switching the A-subunit from an inverse agonist to a full agonist of the transmembrane domain (Zhang et al., 2000).

1.7 Graves' disease

1.7.1 History, pathogenesis and aetiology

Caleb Hillier Parry first described GD in 1825 after noticing patients with goitres, palpitations and exophthalmos (Larner, 2005). The clinical

features were further elucidated and defined independently by Karl Adolf Von Basedow and Dr Robert Graves in 1835, the latter after whom the disease was named (Weetman, 2000). Evidence for the autoimmune nature of GD was provided by the discovery that long-acting thyroid stimulation in GD patient sera was associated with serum Ig (Adams and Purves, 1956). It is now accepted that the hyperthyroidism associated with GD is a result of IgG autoantibodies directed against the TSHR.

GD is characterised by agonistic thyroid stimulating antibodies (TSAbs) binding and stimulating the TSHR in a manner similar to TSH, preventing TSH binding and stimulating the receptor. An excess of T_4 and T_3 hormone production and release results in hyperthyroidism (Smith et al., 1988). The hypothalamus detects the rise in T_4 and T_3 levels in the blood, reduces thyroid releasing hormone secretion and, consequently, the pituitary gland reduces TSH secretion. However as stimulation of the thyroid gland in GD patients is being caused TSAbs by rather than TSH, there is no change in thyroid hormone synthesis and release, causing an excess of T_4 and T_3 within the body (Brent, 2008; McIver and Morris, 1998). Clinical features caused by the excess of T_4 and T_3 include goitre and the features of hyperthyroidism, namely palpitations and increased cardiovascular risk (Nyirenda et al., 2005), nervousness, heat intolerance, weight loss and excess sweating (Brent, 2008; Simmonds and Gough, 2004a).

GD typically develops in the 4th through 6th decades of life (Manji et al., 2006), although can occur at any age, and exhibits a female predominance, affecting women and men in a 7-10:1 ratio (Brent, 2008),

however men undergo a more severe disease pathogenesis (Manji et al., 2006). The Whickham survey has shown there to be an annual incidence of GD of 50 in every 100,000 women and 10 in every 100,000 men (Tunbridge et al., 1977).

1.7.2 Antibody repertoire in GD

Anti-TSHR autoantibodies are present in very low levels in the serum (<1 µg/mL) (de Forteza et al., 1994; Nakatake et al., 2006; Zakarija, 1983) yet are still able to induce hyperthyroidism and thus are biologically powerful stimulants. The autoantibody repertoire in GD is diverse, with three varieties of antibody TSAbs inhibit TSH stimulation, induce cAMP production and bind discontinuous epitopes; Thyroid stimulating blocking antibodies (TSBAbs) block TSH binding but may also act as weak agonists and recognise discontinuous and linear epitopes and are typically polyclonal (Kim et al., 2000; Smith et al., 1988); neutral antibodies bind to linear epitopes in the hinge region between 316-366 aa. They neither block TSH binding nor induce cAMP production, but may be involved in thyrocyte apoptosis (Morshed et al., 2010a). It is the sum activity of these antibodies which contributes to clinical presentation of the disease (de Forteza et al., 1994). It is thought that differing epitope recognition is the key for the differing biological activities.

Crystallisation studies of the TSHR A-subunit in complex with the Fabs of a human TSAb and a TSBAb have demonstrated that there are several aa residues along the leucine rich repeats that are important for TSHR binding. Furthermore such studies have shown the differing epitope

binding of the two types of antibody. The TSAb, M22, bound towards the N-terminus of the receptor whilst the TSBAb, K1-70, bound towards the TSHR C-terminus; the epitopes of both antibodies overlapped in the middle (Sanders et al., 2007; Sanders et al., 2011) (discussed further in Section 1.7.9).

Antibodies to Tg and TPO are also found in GD patients. They are found in high titres in HT patients, are polyclonal and recognise conformational epitopes. Their presence correlates with the degree of lymphocytic infiltration into the thyroid gland.

It is not known whether the antibodies arise from rogue individual B cells that have escaped tolerance or from a limited number of B cell clones. Evidence suggests an oligoclonal response with IgG_1 and $λ$ L-chain restriction (Weetman et al., 1990; Williams et al., 1988; Zakarija, 1983). Thus defects in B cell development or in the GC reaction could contribute to the generation and expansion of autoreactive B cells.

1.7.3 Extrathyroidal complications

A subset of patients develop extrathyroidal complications, including GO (also known as Graves' ophthalmopathy, thyroid-associated ophthalmopathy, thyroid eye disease) and localised thyroid dermopathy, particularly on the shins (pretibial myxoedema) (Ai et al., 2003) (Figure 10).

GO is a potentially sight-threatening complication affecting 16 women and 3 men in 100,000 (Bartley, 1994). Some degree of GO manifestation may

be observed in almost all GD patients but is clinically relevant in approximately 50%, with 3-5% of patients developing severe disease (Wiersinga and Bartalena, 2002). GO is a result of increased orbital fat and extraocular muscle volume in the orbit displacing the eye. Disease hallmarks include expansion of orbital muscle and adipose tissue, mononuclear cell infiltrates in the muscle and adipose tissue and tissue remodelling, including fibrosis.

GO is poorly understood although progress has been made in recent years in understanding the underlying molecular pathogenesis. Orbital fibroblasts are believed to be the key targets and protagonists in disease pathogenesis (Sisson et al., 1973). They represent a unique subtype of fibrocyte with distinct phenotypic and functional characteristics, including elevated pro-inflammatory responses in responses to IL-1β and CD40L treatment (Smith et al., 2008). Following stimulation with anti-TSHR antibody or the T_H1-type cytokines, IFN-γ and TNF, orbital fibroblasts secrete hyaluronan, IL-16 and RANTES (Pritchard et al., 2002), and a subset (Thy-1⁻) may differentiate into pre-adipocytes (Sorisky et al., 1996), leading to expansion of ocular muscle and adipose tissues. A second autoantigen, in addition to TSHR, insulin growth factor 1-receptor (IGF1-R), has been proposed to contribute to GO pathogenesis. It is known that IGF1-R can co-localise with TSHR (Tsui et al., 2008) and its stimulation on orbital fibroblasts results in chemokine and hyaluronan secretion (Pritchard et al., 2003). It is unknown whether there are two distinct antibody populations, each recognising a distinct antigen, one

population that recognises both, or whether the co-localised antigens form a neo-antigen (Wiersinga, 2011).

Figure 10: Extrathyroidal complications.

A subset of patients develop extrathyroidal complications such as GO and thyroid dermopathy. Axial images of computer tomography scans display (A) a normal orbit and (B) enlarged extraocular muscles in a GO patient. (C) Photograph of patient with GO. (D) Photograph of a patient's pretibial myxoedema. Panels A-C taken from (Bahn, 2010) and Panel D taken from (Ai et al., 2003).

Little is known about the pathogenesis of thyroid dermopathy (Rapoport et al., 2000). It is characterised by a localised thickening of the skin and may be due to autoantibody stimulation of TSHR expressed by dermal fibroblasts. Indeed thyroid dermopathy patients have increased levels of TSHR expression by pretibial fibroblasts (Daumerie et al., 2002). As in

the case of GO, dermal fibroblasts may subsequently secrete glycosaminoglycans in response to TSHR stimulation, causing local oedema (Ai et al., 2003; Rapoport et al., 2000).

1.7.4 Genetics

GD is a multi-factorial disease with both genetic and environmental factors contributing to its onset and pathogenesis (Hasham and Tomer, 2012). There is certainly a genetic component to GD as shown by the observed clustering of autoimmune diseases in families, and 40-50% of AITD patients report another family member with a thyroid disorder (Boelaert et al., 2010; Brix et al., 1998a; Brix et al., 1998b). A Danish twin study found a concordance rate of 35% in monozygotic twins and 3% in dizygotic twins (Brix et al., 1998a) and a Californian twin study found concordance rates of 17% and 1.9% in monozygotic and dizygotic twins, respectively (Ringold et al., 2002).

There is marked phenotypic variation amongst GD patients including disease severity, goitre size and the presence and severity of GO (Manji et al., 2006) which is likely the result of the complex gene-environment combinations and interactions. HLA genes were the first candidate genes to be analysed for a role in AITD. Initial studies found a significant association between HLA-DR3 and GD (Baldet et al., 1974; Zamani et al., 2000). The susceptibility haplotype has been further delineated as DRB1*03-DQB1*02-DQA1*0501 (Gough and Simmonds, 2007). Molecular studies analysed the reasons behind this association as hypotheses suggest that certain HLA alleles may allow binding and

presentation of autoantigens. An arginine residue at position 74 of the HLA-DRβ1 chain was shown to be the key aa in conferring GD susceptibility (Ban et al., 2002; Menconi et al., 2008; Simmonds et al., 2005).

The first report of CTLA4's association with autoimmunity came from a GD candidate gene study (Yanagawa et al., 1995). CTLA4 has subsequently been confirmed as a susceptibility gene in many other autoimmune conditions (Jacobson and Tomer, 2007). The CTLA4 gene is highly polymorphic and the three SNPs most commonly associated with autoimmunity are an AT-repeat in the 3` untranslated region microsatellite, an A/G SNP named CT60 downstream of the AT-repeat and an A/G SNP in the signal peptide (Ueda et al., 2003).

PTPN22 is located on chromosome 1p13 and encodes the lymphoid tyrosine phosphatase protein, a cell signalling molecule which inhibits T cell activation (Cohen et al., 1999). The R620W SNP encodes a loss of function mutation (Zhang et al., 2011).

The TSHR has been confirmed as the first thyroid-specific gene to be associated with GD. Japanese studies have found a consistent association, including SNPs in introns 1, 7 and 8 (Akamizu et al., 2000; Hiratani et al., 2005; Sale et al., 1997). In a multinational Caucasian study of subjects with GD, an association was found with a SNP in intron 1, and was independently confirmed in a large (>2,000 GD patients) UK Caucasian case-control cohort (Dechairo et al., 2005), and a Caucasian cohort of three European nations (Płoski et al., 2010).

1.7.5 Non-genetic factors

The concordance rate amongst twins is not 100% and statistical modelling as revealed a contribution of 21% from non-genetic factors (Brix et al., 1998a; Brix and Hegedüs, 2012). Non-genetic susceptibility factors may be constitutional or environmental.

1.7.5.1 Constitutional factors

The peak ages for diagnosis of GD are between the 4th and 6th decades of life (Manji et al., 2006). Women have a 7-10 times greater risk of developing GD than men (Vanderpump et al., 1995) however men are more likely to develop more severe disease (Manji et al., 2006). Proposed constitutional mechanisms to explain this divide include sex hormones, foetal microchimerism and X chromosome inactivation.

The reported contribution of foetal microchimerism to AITD has been inconsistent. An increased incidence of foetal microchimerism was observed in two independent reports comparing thyroid sections from AITD patients and normal controls by detecting the sex determining region of the Y chromosome by ELISA-PCR or fluorescence in situ hybridisation (Ando et al., 2002; Renne et al., 2004). Two studies which state no correlation between foetal microchimerism and HT did not directly evaluate the presence of foetal cells in the thyroid, but rather tried to correlate the number of previous pregnancies (parity) with the presence of anti-TPO and anti-Tg antibodies (Pedersen et al., 2006; Walsh et al., 2005). A twin study analysed the effect of *in utero* transfer of cells between dizygotic twins (cases) and the presence of anti-TPO, -Tg

and –TSHR antibodies. Whilst this study showed an increased prevalence of anti-thyroid antibodies in dizygotic twins, it did not examine thyroid biopsies for the presence of microchimerism, and did not establish a correlation between microchimerism and the development of an AITD (Brix et al., 2009).

Skewed and extremely skewed X chromosome inactivation has been found in numerous autoimmune diseases such as SLE (Huang et al., 1997), scleroderma (Özbalkan et al., 2005) and juvenile idiopathic arthritis (Uz et al., 2009). In AITD skewed inactivation was found in 37% of GD patients and 34% of HT patients, which was statistically significantly higher than external controls, in a small Danish twin study of n=32 concordant female twin pairs with AITD (Brix et al., 2005). A Turkish study of similar size (n=29 GD patients and n=83 HT patients) found 31% of GD patients and 34% of HT patients with skewed X chromosome inactivation. This skewing was statistically significant (Ozcelik et al., 2006).

1.7.5.2 Exogenous factors

Exogenous environmental factors have been implicated in predisposition to and the pathogenesis of GD.

Iodine deficiency results in an increased risk of GD in the elderly whereas iodine excess may result in GD manifesting at a younger age (Camargo et al., 2008; Laurberg et al., 1991). The trace element selenium is an essential micronutrient, and selenoproteins are involved in thyroid hormone metabolism. Smoking activates B and T cells and enhances IL-2

production and results in an increased risk of GO in current and ex-smokers with GD (Brix et al., 1998a; Manji et al., 2006; Vestergaard et al., 2002). Stress drives the antibody-producing immune response. Retrospective studies on the role of stress in GD have suggested that GD is often preceded by stressful life events which promote a pro-inflammatory cytokine response (Tsatsoulis, 2006; Vos et al., 2008; Winsa et al., 1991). However a recent prospective study of euthyroid female relatives of an AITD patient found that stressful life events did not predispose to AITD (Effraimidis et al., 2012).

The concept that infections may trigger autoimmune conditions has become increasingly relevant (Ercolini and Miller, 2009). Microbial agents have long been implicated in various autoimmune conditions (Chervonsky, 2010). In the case of GD, *Yersinia enterocolitica* infection has been reported as a potential environmental agent for many decades (Bech et al., 1974). Whilst it remains a controversial topic with inconsistent findings (Effraimidis et al., 2011), recent bioinformatics data has reported significant amino acid similarity between *Y. enterocolitica* proteins and the TSHR (Guarneri et al., 2011; Wang et al., 2010). GD patient sera and a neutral anti-TSHR mAb were shown to display binding to a *Y. enterocolitica* protein identified as outer membrane porin F (OmpF) (Wang et al., 2010). Bioinformatics data has also reported on amino acid similarity between the TSHR and *Borellia burgdorferi* proteins. However there is no biological data to support this (Benvenga et al., 2004).

The role of infectious agents and *Y. enterocolitica* in particular are discussed in greater detail in Chapter 5. The contribution of genetic and environmental factors to GD susceptibility are summarised in Figure 11.

Figure 11: Genetic and environmental contributions to GD susceptibility and pathogenesis.

Twin studies and biometric statistical modelling has shown that 75% of the phenotypic variation in GD is due to genetics, and the remaining 25% due to non-genetics factors. Non-genetic factors may include constitutional and exogenous factors. It is the combination of these factors which will contribute to disease susceptibility and pathogenesis.

1.7.6 Current treatment options

Treatment options for patients with GD have not changed for the past 60 years and include anti-thyroid drugs, radioiodine ablation of the thyroid

gland and thyroidectomy (Banga et al., 2008). Anti-thyroid drugs interfere with thyroid hormone synthesis and form the first-line treatment in the majority of countries outside the US, where radioiodine is the most common therapy. Thyroidectomy represents the least common treatment, but can be used for patients who have declined radioiodine treatment or for whom anti-thyroid drugs are unsuitable (Bahn, 2012; Brent, 2008). However, current treatment options only target the symptoms of GD rather than the underlying pathological condition. Thyroidectomy and radioiodine therapy render the patients hypothyroid necessitating life-long thyroid hormone replacement and anti-thyroid drugs, at the correct dosage, promote euthyroidism but are associated with serious side-effects.

1.7.6.1 Emerging therapies

TSBAbs isolated from patients undergoing thyroid disease (Evans et al., 2010; Sanders, 2008) are capable of blocking TSAb-mediated stimulation of the thyroid and could be developed for specific blocking therapy (Bahn, 2012; Furmaniak et al., 2012a). Indeed injection of K1-70, into rats following a dose of M22, completely inhibited any stimulatory effects (Furmaniak et al., 2012b). Recently small molecule therapy has been proposed as a new therapeutic intervention. Advantages of small-molecules are that they can be administered orally and produced in high quantities at low cost. Antagonist and inverse agonist molecules have been developed that bind to an allosteric site in the TSHR transmembrane domain without interfering with TSH binding (Neumann et

al., 2010a; Neumann et al., 2010b; Neumann et al., 2009; Neumann et al., 2008).

Rituximab is a humanised chimeric anti-CD20 biological agent (Reff et al., 1994) that is an effective therapy in other autoimmune conditions (Nielsen et al., 2007). There have been 3 non-randomised control trials thus far assessing rituximab in GD (El Fassi et al., 2009; El Fassi et al., 2007; Salvi et al., 2007). These studies suggest that rituximab may prolong the remission rates of patients with mild hyperthyroidism and low anti-TSHR antibody levels prior to treatment (El Fassi et al., 2007). There was no effect on total IgG levels and only a moderate reduction in the level of anti-TSHR antibodies with a specific decrease in the stimulatory capacity of anti-TSHR antibodies (El Fassi et al., 2009). Two randomised control trials are currently underway (Bahn, 2010).

1.7.7 Mouse models

The difficulties in isolating anti-TSHR mAbs from patients have necessitated the use of experimental models of disease, such as mice. However GD is a human-only condition and does not occur spontaneously in animals, including great apes (Dağdelen et al., 2009; McLachlan et al., 2011b). Whilst studies have included hamsters (Ando, 2003), the mouse remains the most popular induced disease model. Methods of induction have included injection of syngeneic cells, plasmids or adenoviruses encoding TSHR cDNA and electroporation and have resulted in varying degrees of success. Success of the animal model can also depend on the strain of mice used. C57BL/6 mice are normally

resistant to GD induction except in the case of T_{reg} depletion followed by immunisation with an adenovirus construct expressing aa 22-289 of the TSHR A-subunit (Ad-TSHR289) (Saitoh et al., 2007; Saitoh and Nagayama, 2006), however the disease-susceptible strain, BALB/c, do not develop more severe disease on T_{reg} depletion (Saitoh and Nagayama, 2006).

There have been many stumbling blocks on the path to developing murine models of GD and in trying to isolate mAbs from both mice and humans (Banga, 2007; McLachlan and Rapoport, 2004). These mAbs needed to inhibit TSH binding, stimulate cAMP production in TSHR-expressing cells or block stimulation of TSH and TSAbs. Murine mAbs to the TSHR were developed with varying degrees of success (Dağdelen et al., 2009). Disadvantages of experimental models to date include a lack of extrathyroidal complications such as dermopathy and GO. Anatomical differences between the human and mouse orbit could explain the lack of GO observed in experimental models. Isolated murine mAbs are described in Table 1.

1.7.8 Early models

The first murine model of hyperthyroid GD, termed the Shimojo model, was described in 1996 (Shimojo et al., 1996) and was successfully replicated by other groups (Dağdelen et al., 2009). AKR/N mice were immunised with fibroblasts co-expressing TSHR and MHC class II and although a small proportion of mice became hyperthyroid, no mAbs were

isolated and several months are required for development of the model (Rao et al., 2003).

1.7.8.1 Plasmid cDNA injection delivery model

Costagliola *et al* injected BALB/c mice with naked plasmid encoding TSHR cDNA and despite the animals remaining euthyroid, stimulating autoantibodies were induced (Costagliola et al., 1998). Another group, using the same procedure in NIMR mice, generated three TSAbs, TSmAbs 1-3, derived from the same mouse with identical germline V-region gene usage (Sanders et al., 2002).

1.7.8.2 Adenovirus-DNA injection delivery model

The use of adenovirus as a method of TSHR holoreceptor gene delivery was shown to result in a 50% disease incidence in female BALB/c mice (Nagayama et al., 2002). This method was further improved by the serendipitous discovery that TSAbs preferentially recognise the TSHR A-subunit (aa 1-289; TSHR289) over the holoreceptor (Chazenbalk, 2002). Immunisation of BALB/c mice with Ad-TSHR289 increases the disease incidence to 80% (Chen et al., 2004).

This method of gene delivery facilitated the isolation of two TSAbs with powerful agonist properties, KSAb1 (IgG_{2b}/κ) and KSAb2 (IgG_{2a}/κ), from a single mouse undergoing experimental GD (Gilbert et al., 2006a). Both mAbs are full agonists with activity in a nanomolar range, display TSH binding inhibiting Ig properties and have a high affinity for TSHR but KSAb1 is the more powerful of the two mAbs. Injecting non-immunised

mice with μg doses of KSAb1 and KSAb2 caused the mice to become hyperthyroid within 7 hs. Histological analysis of recipient mice showed no thyroidal lymphocytic infiltrate and no ocular pathogenesis. However these features may require chronic disease activity to develop (Flynn et al., 2007).

1.7.8.3 Electroporation of plasmid cDNA injection delivery model

In vivo electroporation was recently described as an improved method of plasmid cDNA gene delivery, with disease incidence improving from 12% to 32% using the TSHR holoreceptor, and from 80% to 95% using the TSHR A-subunit (Kaneda et al., 2007). Another advantage of this model compared to the adenovirus delivery model is the long-lasting antibody response. This model was replicated by this laboratory and importantly, mice also developed signs of orbital fibrosis (Zhao et al., 2011).

1.7.8.4 Adoptive transfer of splenocytes

Immunisation of mice with murine TSHR (mTSHR) is not sufficient to break tolerance and anti-mTSHR antibodies are not induced, and neither is hyperthyroidism (Nakahara et al., 2010). However, as described above, immunisation with human TSHR (hTSHR) can induce potent TSAbs and GD-like symptoms. This is because hTSHR has high sequence similarity with mTSHR, but it is not a true murine autoantigen as the aa sequence similarity is not 100%.

A recent mouse model has been proposed to counter-act this issue of the inauthentic autoantigen, hTSHR, and create an authentic autoimmune

model with mTSHR as the autoantigen. In this case, spleens from TSHR knockout mice immunised twice with Ad-TSHR289 are adoptively transferred into TSHR-sufficient immune-deficient athymic nude BALB/c mice. Transfer efficiency was improved by prior depletion of T_{regs} in recipient mice. Whilst 70% of donor mice were anti-TmSHR antibody positive, only 46% of recipient mice were antibody positive and only 21% developed hyperthyroidism. More than half of the mice eventually became hypothyroid. Hyperthyroid glands were diffusely enlarged, hypertrophied and some developed small lympocytic infiltrations. (Nakahara et al., 2012).

Table 1: Summary of isolated murine anti-TSHR monoclonal antibodies.

	mAb	V_H	D_H	J_H	V_L	J_L	Subclass	Activity
Gilbert, 2006a	KSAb1	1S135	4-1*02	2	6-13	2	IgG$_{2b}$/κ	Agonist
	KSAb2	1S135	4-1*02	2	6-13	2	IgG$_{2a}$/κ	Agonist
Costagliola, 2004	IRI-SAb2	1S135	3-2*01	2	6-13	5	IgG$_{2a}$/κ	Agonist
	IRI-SAb3	1S135	4-1*02	2	6-13	5	IgG$_1$/κ	Partial agonist
Sanders, 2002	TSmAbs 1-3	1S135	4-1*02	4	23-48	5	IgG/κ	

A summary of the monoclonal antibodies with varying stimulatory capacity isolated from mice undergoing experimental GD. The V-region gene usage, L-chain and subclass are described. There is considerable V-region gene restriction amongst murine anti-TSHR antibodies.

1.7.9 Human anti-TSHR monoclonal antibodies

As described previously in Section 1.7.2, anti-TSHR antibodies are found in GD patients at very low serum concentrations and have thus been notoriously difficult to isolate (McLachlan and Rapoport, 2004).

The landmark first report of a human monoclonal TSAb came in 2003 (Sanders et al., 2003) and the group of Rees Smith have subsequently isolated a monoclonal TSBAb from a patient with post-partum thyroiditis (Sanders et al., 2005) and both a TSAb and a TSBAb from the same GD patient (Evans et al., 2010). The isolation of such mAbs has allowed for their genetic and physiological analysis. As with previous studies using total Ig (Weetman et al., 1990; Williams et al., 1988), isolated mAbs were restricted to the IgG_1 isotype although there is no obvious restriction of κ or λ L-chain usage. There is some degree of V-region gene usage restriction, with 3 of 4 mAbs using the V_H5 family and 3 of 4 using the V_L1 family. Interestingly both TSBAbs, 5C9 and K1-18, use J_H4 genes (Table 2). However it is difficult to draw definitive conclusions on gene usage from such a small repertoire of isolated mAbs.

Table 2: Isolated human monoclonal antibodies to the TSHR.

mAb	V_H	D_H	J_H	V_L	J_L	Subclass	Agonist activity	Reference
M22	5	6-13	5	1-11	3b	IgG$_1$/λ	TSAb	(Sanders et al., 2003)
5C9	3-53	2-2	4	1-39	2	IgG$_1$/κ	TSBAb	(Sanders et al., 2005)
K1-18	5-51*01	3-16*02	3*02 or *01	3-20*01	1*01	IgG$_1$/κ	TSAb	(Evans et al., 2010)
K1-70	5-51*01	1-7*01	4*02	1-51*01	7*1	IgG$_1$/λ	TSBAb	

A summary of the monoclonal antibodies isolated from GD patients. The V-region gene usage, L-chain and subclass are described. There is less V-region gene restriction than that observed for murine anti-TSHR antibodies but there is some restriction amongst V_H genes.

1.7.9.1 Atomic structure of human mAbs and the TSHR

As FSHR is the closest G protein-coupled receptor homologue to the TSHR, modelling of TSH interacting with TSHR was based on the interactions of FSH and FSHR (Fan and Hendrickson, 2005; Núñez Miguel et al., 2008). However the atomic structure of the TSHR A-subunit in complex with M22 has been resolved (Sanders et al., 2007). The atomic structure of M22 Fab and part of the TSHR A-subunit (aa 22-260; TSHR260) was analysed by X-ray diffraction at a resolution of 2.5 Å.

TSHR260 is a curved helical tube made of leucine-rich repeats. The inner surface of the tube is lined with hydrophobic residues and the concave surface is formed of an 11-stranded untwisted β sheet. The convex surface contains eight small strands that form two 3-stranded β sheets and one 2-stranded β sheet. The convex surface also contains five glycosylation sites distant from the TSH binding site so there is no interference. There are no α-helices in the structure (Sanders et al., 2007), see Figure 12, page 77.

Crystallisation of a TSAb in complex with the TSHR

M22 Fab binds the concave surface of the TSHR260 at 90˚ to the helical tube axis (Figure 12, page 77). The interaction between the receptor and M22 is formed of an extensive network of polar, hydrophobic bonds with the M22 H-chain having more residues interacting with TSHR260 than the L-chain. The majority of the residues interacting with TSHR260 are in the H- and L-chain CDRs. There was very little movement in atoms of bound M22 residues compared to unbound M22 suggesting 'lock and

key' binding (Sanders et al., 2007). The M22 L-chain mimics the binding of TSHα whilst the H-chain mimics the binding of TSHβ, based on comparative modelling (Nunez Miguel et al., 2009).

Mutation of the TSHR residues R80A, E107A, R109A, K129A, K183A, Y185A and R225A had a significantly detrimental effect on M22 Fab-TSHR260 interactions. Mutation of R28D in the M22 H-chain affected its stimulatory activity. The manipulation of these mutations opens up an opportunity to develop small molecules that block them, thereby preventing M22 and other TSAbs with similar surface structures binding to, and activating, the receptor (Sanders et al., 2007).

Crystallisation of a TSBAb in complex with the TSHR

The atomic structure of K1-70 Fab has been resolved in complex with TSHR260 at a resolution of 1.9 Å (Figure 12). The structure of TSHR260 is very similar in both crystallisations studies, although there is improved resolution of the crystal in the more recent study.

The antigen-binding site of K1-70 is irregular in that acidic residues lie on one side whilst basic residues are on the other side. There are 12 L-chain and 15 H-chain residues in direct contact with TSHR260, and 24 TSHR residues in total in direct contact with K1-70 Fab. K1-70, like M22, binds to the concave surface of TSHR260 but differs in that it binds towards the N-terminus; whilst M22 bound towards the C-terminus, there is however overlap of the two mAbs' epitopes in the middle of the concave surface.

TSHR mutations K58A, I60A, E61A, Y82A, R109A and K183A all interact with K1-70 Fab and their mutation resulted in a loss of or decrease in K1-70's antagonist function. Mutation of K1-70 H-chain residues W97A and N100A markedly decreased the antagonism of TSH stimulation of cAMP production in TSHR-transfected cells. The mutation of L-chain residue R94D and H-chain residues Y99A and N32A also affected K1-70 function but to a lesser extent. The combination of all 5 mutations resulted in a complete loss of K1-70 function (Sanders et al., 2011).

Comparison of TSAb and TSBAb binding to TSHR A-subunit

The resolution of the atomic structures of stimulating and blocking antibodies has allowed for the comparison of how the differing types of antibody interact with the TSHR. The TSBAb, K1-70 does not interact with the extreme N-terminus of TSHR260, but has more contact with the N-terminus than the TSAb, M22. M22 is directed more towards the C-terminus; however both antibodies, as well as TSH, have extensive overlap of interactions with TSHR residues. The functional differences of the antibodies are likely a result of the precise TSHR amino acid residues bound by antibodies (Figure 12, page 77).
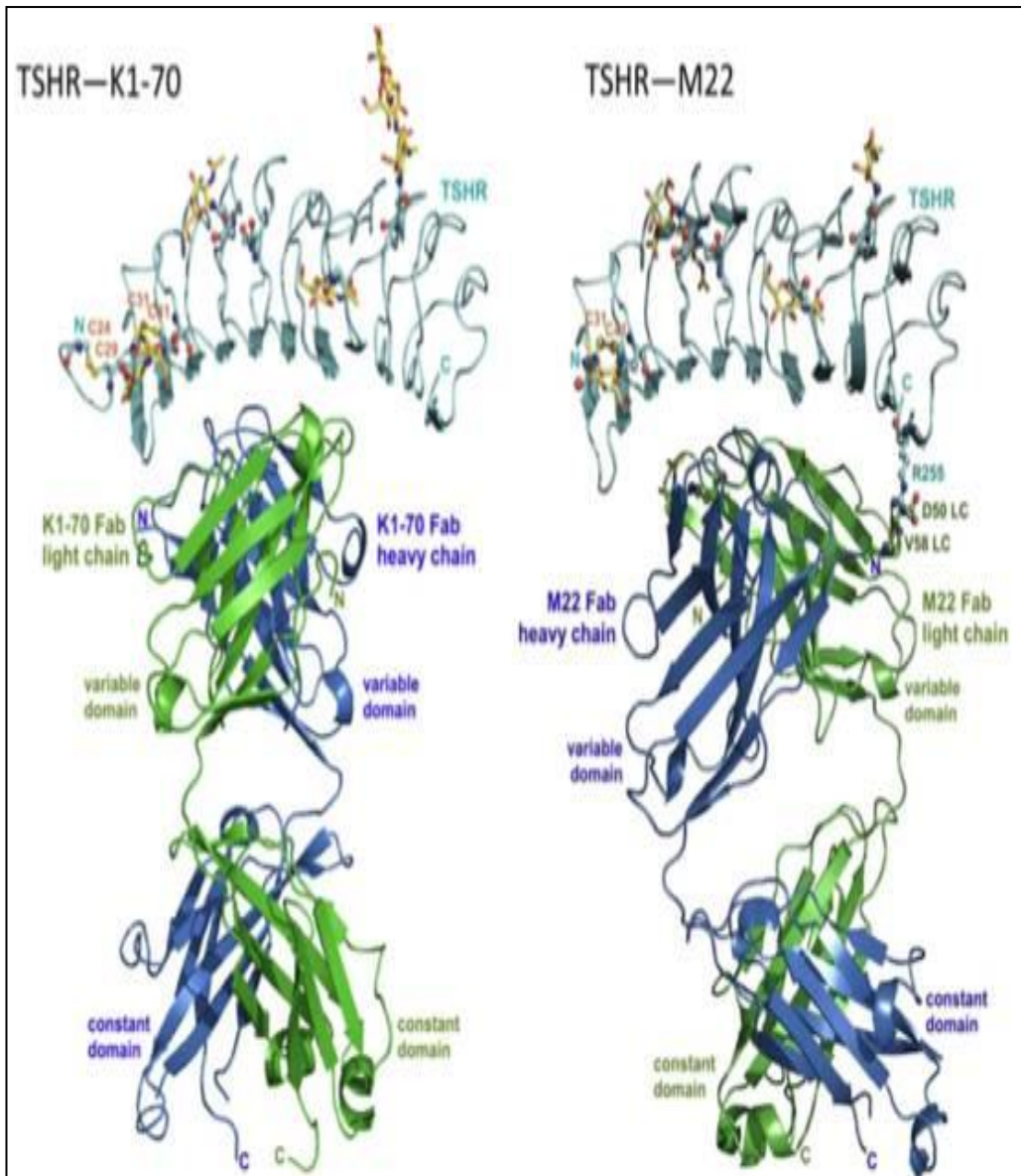
Figure 12: Comparison of the atomic structure of TSHR ectodomain in complex with M22 Fab and K1-70 Fab.

The atomic structure of the Fab regions of K1-70, a TSBAb, and M22, a TSAb, in complex with the TSHR ectodomain, aa residues 22-260 was resolved. These studies have shed important light on the 'lock and key' binding interactions of mAbs and the TSHR. M22 binds to the entire leucine rich repeat region whilst K1-70 is positioned towards the N-terminus. Residues essential for antibody binding have been identified and may lead to targeted therapeutic intervention. Figure is taken from (Furmaniak et al., 2012a).

1.8   Aims of thesis

The isolation of murine and human mAbs has provided new insights into the pathogenic antibodies in GD allowing greater understanding of their mechanism of action. Despite the data indicating a restricted usage of germline Ig genes in the TSAb repertoire, the germline Ig genes encoding anti TSHR antibodies have not been previously investigated. Furthermore, recent genetic linkage analyses in inbred strains of mice have highlighted a role for the IGHV genes in predisposing to the development of TSAbs. Therefore new knowledge on germline genes and their rearrangements is greatly needed. As both KSAb1 and KSAb2 are disease-associated and derived from the same precursor B cell clone, it was important to establish the antigen specificity of the primary B cell clone which through SHM events, develops reactivity with TSHR. This antigen specificity could either be the target autoantigen, (TSHR) or an infectious agent.

The aims of thesis were to evaluate the antigen specificity of the germline genes predisposing to two potent TSAbs, by expressing them as recombinant Fab. We aimed to identify where in the chain of SHM events pathogenicity arose and whether or not an infectious agent contributed to the break in tolerance allowing disease to occur.

CHAPTER TWO

MATERIALS AND METHODS

2 CHAPTER TWO: Materials and methods

2.1 Materials

2.1.1 Medium and growth supplements

Ham's F12 and foetal calf serum (FCS) were purchased from Invitrogen, UK. FCS was heat inactivated at 56°C for 30 minutes prior to use in all experiments.

2.1.2 Chemicals

Chemicals were purchased from the following companies:

Sigma-Aldrich, Dorset, UK: Ammonium molybdate, ampicillin, benzamidine, boric acid, Bovine Heart Infusion medium, bovine serum albumin (BSA), cell dissociation solution, CaCl2.2H2O, chloramphenicol, $CoCl_2.6H_2O$, Coomassie blue R250, CuSO4, dimethyl sulphoxide (DMSO), DNase I, ethidium bromide, $FeSO_4$, glucose, hen egg lysozyme, H_2O_2, imidazole, KCl, $MgCl_2$, molecular biology water, $MnCl_2$, MOPS, NaOx, PMSF, TEMED, tetracycline, thiamine, trichloroacetic acid, Trypsin EDTA, Triton-X-100, Tween-20, $ZnSO_4$.

Invitrogen, Paisley, UK: Novex® Sharp Pre-stained Protein Standard, Phosphate buffer solution (PBS), Geneticin G418, fungizone (PSF).

VWR International, UK: Ethanol, glycine, HEPES, isopropanol, KH2PO4, $MgSO_4.7H_2O$, NaAc, NaCl, $NaHCO_3$, Na_2HPO_4, NaOH, NH4Cl, $(NH4)_2S_2O8$, SDS, sucrose, Tris base.

New England Biolabs Ltd, Herts, UK: BsrGI, ColorPlus prestained protein marker, EcoRI, HindIII, Protein Ladder (10-250 kDa), Quick-Load® 1 kB DNA Ladder, T4 DNA Ligase, 10X T4 DNA Ligase Reaction Buffer.

Protogel was purchased from National Diagnostics, UK.

Novagen: DNA ladder

2.1.3 Sterile tissue culture plastic ware

Cells were cultured in sterile tissue culture flasks and 96-well plates (CELLSTAR®, Greiner Bio-One, GmbH, Germany) as described below.

2.1.4 Cells

2.1.4.1 Chinese hamster ovary (CHO) cells

Chinese hamster ovary (CHO) cells expressing the full-length TSHR at an approximate density of 90,000 TSHR/cell and called JP09 cells, were donated by Professor G Vassart, Brussels (Perret et al., 1990). CHO cells expressing the TSHR A-subunit anchored by a glycosylphosphatidylinositol (GPI) moiety, and expressing the TSHR A-subunit at an approximate density of 500,000/cell (Metcalfe et al., 2002) were donated by Dr Phillip Watson, University of Sheffield, and called GPI9-5 cells.

The JP09 cells were used for cAMP stimulating bioassays and the GPI9-5 cells were used in flow cytometry assays. Cells were cultured in Ham's F12 medium containing 10% FCS and 0.01% PSF. The cells in culture

were supplemented with Geneticin G418 to a final concentration of 200 µg/mL.

2.1.5 Bacterial serotypes

Y. enterocolitica serotype O:3 was kindly provided as serotype Ye58/O3 by Professor Brendan Wren (London School of Hygiene and Tropical Medicine, UK) and serotype O:8 was provided as serotype 8081 was kindly provided by Dr. Steve Atkinson (University of Nottingham, UK).

Both serotypes were cultured in a category two laboratory in the School of Molecular and Medical Sciences, University of Nottingham with the assistance and guidance of Mr Marco Grasso and Dr Steve Atkinson.

2.2 Methods

2.2.1 DNA preparation

2.2.1.1 Isolation of KSAb1 and KSAb2 from BALB/c mice

A mouse model of GD was established and KSAb1 and KSAb2 isolated according to published protocols (Gilbert et al., 2006a). Briefly, female BALB/c mice were immunised with Ad-TSHR289 and hybridomas created from their splenocytes

The H- and L-chains of KSAb1 and KSAb2 were prepared and cloned in pAK19 vector (Carter P, 1992; Padoa et al., 2003; Padoa et al., 2010). The vector pAK19 synthesises the H- and L-chains as an rFab protein using a phoA promoter and heat stable enterotoxin II leader sequence following removal of phosphate in the growth medium. rFabs are secreted

into the periplasm of the bacterial cell where disulphide bonds are created by disulphide isomerase to link the H- and L-chains (Knappik and Pluckthun, 1995).

2.2.1.2 Design and synthesis of germline gene construct

The rearranged germline gene construct was designed based on the germline gene matches identified by the IMGT® database of Ig (and TCR) germline genes (Lefranc et al., 1999). The H-chain is formed of IGHV1S135, IGHD2*01 and IGHJ4*02 and the L-chain is formed of IGKV6-3*01 and IGKJ4*01. The vector used for expression, pAK19, requires the L-chain sequence to precede the H-chain, thus in the construct, the L-chain sequence is first and is separated from the H-chain by a pAK19 linker sequence. An *Eco*RI restriction enzyme site precedes the L-chain; the H-chain sequence is followed by 5 histidine residues (penta His tag), pAK19 sequence and a *Hind*III restriction enzyme site. The construct is 1680 bp in length and was synthesised by Genscript (USA) cloned in a pUC57 vector. The lyophilised germline-pUC57 DNA construct was reconstituted with 100 µL molecular biology water.

GAATTCGAGCTCGGTACCCGGGGATCCTCTAGAGGTTGAGGTGATTATGAAAAAGAATATCG
CATTTCTTCTTGCATCTATGTTCGTTTTTTCTATTGCTACAAACGCGTATGCTGACATTGTGATG
ACCCAGTCTCAAAAAATTCATGTCCACATCAGTAGGAGACAGGGTCAGCATCACCTGCAAGG
CCAGTCAGAATGTGGGTACTGCTGTAGCCTGGTATCAACAGAAACCAGGACAATCTCCTAA
ACTACTGATTTACTCGGCATCCAATCGGTACACTGGAGTCCCTGATCGCTTCACAGGCAGTG
GATCTGGGACAGATTTCACTCTCACCATCAGCAATATGCAGTCTGAAGACCTGGCAGATTA
TTTCTGCCAGCAATATAGCAGCTATCCTTACACGTTCGGAGGGGGGACCAAGCTGGAAATA
AAACGGGCTGATGCTGCACCAACTGTATCCATCTTCCCACCATCCAGTGAGCAGTTAACATC
TGGAGGTGCCTCAGTCGTGTGCTTCTTGAACAACTTCTACCCCAAAGACATCAATGTCAAGT
GGAAGATTGTTGGCAGTGAACGACAAAATGGCGTCCTGAACAGTTGGACTGATCAGGACA
GCAAAGACAGCACCTACAGCATGAGCAGCACCCTCACGTTGACCAAGGACGAGTATGAAC
GACATAACAGCTATACCTGTGAGGCCACTCACAAGACATCAACTTCACCCATTGTCAAGAG
CTTCAACAGGAATGAGACGTAAGCTGATCCTCTACGCCGGACGCATCGTGGCCCTTGTACAC
AAGTTCACGTAAAAAGGGTATCTAGAGGTTGAGGTGATTTTATGAAAAAGAATATCGCATTTC
TTCTTGCATCTATGTTCGTTTTTTCTATTGCTACAAACGCGTACGCTGAGATCCAGCTGCAGCA
GTCTGGACCTGAGCTGGTGAAGCCTGGGGCTTCAGTGAAGGTATCCTGCAAGGCTTCTGG
TTACTCATTCACTGACTACAACATGTACTGGGTGAAGCAGAGCCATGGAAAGAGCCTTGA
GTGGATTGGATATATTGATCCTTACAATGGTGGTACTAGCTACAACCAGAAGTTCAAGGGC
AAGGCCACATTGACTGTTGACAAGTCCTCCAGCACAGCCTTCATGCATCTCAACAGCCTGAC
ATCTGAGGACTCTGCAGTCTATTACTGTGCAAGAAGGGACTGGGACTACTTTGACTACTGG
GGCCAAGGCACCACTCTCACAGTCTCCTCAGCCAAAACAACAACCCCATCAGTCTATCCACT
GGCCCCTGGGTGTGGAGATACAACTGGTTCCTCCGTGACTCTGGGATGCCTGGTCAAGGGC
TACTTCCCTGAGTCAGTGACTGTGACTTGGAACTCTGGATCCCTGTCCAGCAGTGTGCACAC
CTTCCCAGCTCTCCTGCAGTCTGGACTCTACACTATGAGCAGCTCAGTGACTGTCCCCTCCA
GCACCTGGCCAAGTCAGACCGTCACCTGCAGCGTTGCTCACCCAGCCAGCAGCACCAAGGT
GGACAAGAAAATTGAGACCCGTCACCACCACCACCACCACTAACGCGGCATGCGACGGCCCT
AGAGTCCCTAACGCTCGGTTGCCGCCGGGCGTTTTTTATTGTTAACTCATGTTTGACAGCTTAT
CATCGATAAGCTT

Figure 13: Germline gene cassette nucleotide sequence for synthesis.

The nucleotide sequence of the germline gene cassette was optimised for protein expression and synthesised. The L-chain nucleotide sequence is coloured in blue and the H-chain nucleotide sequence is coloured in green. Restriction enzyme sites are in red and the penta his tag is in purple. Intervening plasmid sequence is in black.

2.2.1.3 Transformation of XL10 Gold Ultracompetent cells

For each competent cell transformation with plasmid:

i. A 15 mL polypropylene centrifuge tube (VWR International, UK) was pre-chilled on ice.

ii. 50 µL of XL10 Gold Ultracompetent cells (Stratagene, Stockport, UK) were thawed on ice and incubated with 2 µL β-mercaptoethanol in the tube for 10 minutes on ice.

iii. 50 ng of plasmid DNA was added and incubated on ice for 30 minutes.

iv. The tubes were heat-pulsed at 42°C for 30 seconds and then incubated on ice for two minutes.

v. 450 µL of preheated SOC medium (Appendix 1) was added and incubated for 1 h at 37°C with shaking at 250 rpm.

vi. 50 µL of transformation mixture was grown on LB-ampicillin (Appendices 1 and 3) agar plates. The plate was incubated for 18 h at 37°C.

2.2.1.4 Overnight bacterial cultures

i. A single colony was picked from agar plates and grown for 16 h at 37°C in 5 mL Luria Bertani (LB) medium (Appendix 1) containing 100 µg/mL ampicillin (Appendix 3) in an orbital shaker at 300 rpm.

2.2.1.5 Glycerol stocks of bacterial cultures

A glycerol stock of each colony grown in LB was prepared by adding 600 µL bacterial culture to 400 µL 50% glycerol (Appendix 1) and stored at -70°C.

2.2.1.6 Mini-prep purification of bacterial cultures

Plasmid DNA was purified from bacterial cultures using Mini-Prep Spin Columns (Qiagen, West Sussex, UK) according to the supplier's protocol:

i. 5 mL bacterial culture was added to a microcentrifuge tube (Fisher Brand, Fisher Scientific, UK) and spun in a microcentrifuge

(Biofuge Fresco, Heraeus Instruments) at 13,000 g for 1 minute at 4°C.

ii.   The supernatant was discarded and the pellet dried and resuspended in 250 µL buffer P1.

iii. 250 µL of buffer P2 was added followed by 350 µL of buffer N3. The microcentrifuge tube was spun for 10 minutes at 13,000 g.

iv.   The supernatant was added to a spin column and incubated for one minute at room temperature.

v.   The flow through was discarded and 0.75 mL of buffer EB added before centrifuging at 13,000 g for one minute.

vi.   The flow through was discarded and 0.5 mL of buffer added and the tube was centrifuged for 5 minutes at 13,000 g.

vii. Flow through was discarded and the tube was centrifuged again for one minute to remove any excess EtOH.

viii. The spin column was applied to a fresh microcentrifuge tube and 30 µL of dH_2O was added directly to the filter and incubated for one minute at room temperature before centrifuging at 13,000 g.

ix.   The flow through contains purified plasmid DNA.

2.2.1.7 DNA quantification by nanodrop

The 'Nucleic Acid' program of nd-1000-v3.7 Spectrophotometer (Thermo Fisher Scientific) was used to quantify the amount of purified plasmid DNA. Adding 1.2 µL of dH_2O first cleaned the pedestals and was then used as a blank. DNA was measured by applying 1.2 µL of purified

plasmid to the pedestal and the absorbance read at 260 nm. DNA concentration was measured in ng/mL.

2.2.1.8 Sequencing

The DNA sequencing of germline, KSAb1 and KSAb2 V-region genes cloned in pAK19 was performed by Geneservice (Cambridge, UK) using Sanger sequencing. Primers (Sigma-Aldrich, Dorset, UK) were designed in conjunction with Dr. Shuang-xia Zhao, KCL. The sequence analysis was performed using SeqMan software (DNAStar, Inc, Madison, WI, USA).

Table 3: Sequencing primers.

Primer	Primer sequence	Length (bp)
F1	5' AGCTGTCATAAAGTTGTCACG 3'	21
R1	5' GGGTATCTAGAGGTTGAGGTG 3'	21
F2	5' AAACGCGTACGCTGAGAT 3'	18
R2	5' CAGTTAAATTGCTAACGCAG 3'	20

2.2.1.9 Restriction enzyme digest

For restriction enzyme digests, 1 µg of purified DNA was digested with 1U of enzyme and 10X reaction buffer for 1.5 h at 37°C in a water bath.

To create constructs of L-mature and H-mature in pAK19, 2 µg of each of germline and KSAb1 V-region gene constructs in pAK19 were digested with 2 U *Eco*RI and 2 U *Bsr*GI and 10X reaction buffer for 3 h at 37°C.

2.2.1.10   DNA electrophoresis

To analyse restriction enzyme digests and isolate separated DNA bands, digested DNA samples were resolved by agarose gel electrophoresis alongside 1 kB DNA ladder. DNA digested with *Eco*RI and *Hind*III were analysed by 0.8% agarose gels containing 10 µg/mL ethidium bromide whilst DNA digested with *Eco*RI and *Bsr*GI were analysed by 1.2% agarose gels (Appendix 2). Gels were run in 1X TAE buffer (Appendix 2) at 110 V for approximately 45 minutes, or until the bromophenol blue loading dye had reached the end of the gel.

2.2.1.11   Gel visualisation

The agarose gels were viewed under UV light, for as brief a time as possible, and a photograph was taken (Gene Flash, Syngene Bio Imaging).

2.2.1.12   Gel extraction

To excise the bands of DNA from the agarose gel, the gel was placed in a UV light box (UV Transilluminator, UVP inc) and the required DNA bands were excised with a scalpel and stored in microcentrifuge tubes.

i.   The samples were purified using Wizard® SV Gel and PCR Clean-Up System (Promega, UK).

ii.   The excised agarose slices were weighed and 10 µL of membrane binding buffer was added for every 10 µg of agarose. The slices in membrane binding buffer were heated to 60°C or until the agarose had completely melted.

iii. This mixture was applied to the filter membrane of a spin column and incubated for one minute at room temperature before centrifuging at 13,000 g for one minute.

iv. The supernatant was discarded, 0.5 mL of elution buffer was added and the tube centrifuged for one minute at 13,000 g.

v. The supernatant was discarded and 0.75 mL of elution buffer was added and tube centrifuged at 13,000 g for five minutes.

vi. The supernatant was discarded and the tube was centrifuged again for one minute at 13,000 g to remove any remaining ethanol.

vii. 15 µL of dH$_2$O was applied directly to the membrane and incubated for one minute at room temperature.

viii. The tube was then centrifuged as before and the DNA concentration measured by nanodrop.

2.2.1.13   Ligation

The concentrations of plasmid and insert DNA were calculated using the following formula to give a 3:1 ratio of insert to vector:

$$\text{Insert (ng)} = \frac{3 \times 50\text{ng}/}{\text{Vector (Kb)}}$$

The insert and plasmid were ligated with 1 µL T4 ligase and 10X ligase buffer and incubated overnight at 4°C.

2.2.2 Protein expression

2.2.2.1 Constructs for rFab expression

Purified DNA constructs were transfected in optimised competent cells for expression as rFab proteins. Germline, L-mature, H-mature and L-irrelevant constructs were expressed as rFab, alongside KSAb1 as positive control. For use as an irrelevant control antigen, Dr Michael Christie (KCL) donated the Fab construct of a human anti-islet cell antigen 2 (IA-2) mAb, 96/3, cloned in pAK19. To create the L-irrelevant construct, Dr Christiane Hampe (University of Washington, USA) donated the Ti-401 rFab which recognises a bacterial antigen.

Table 4: Constructs used for rFab expression in this thesis.

Construct	H-chain	L-chain
KSAb1	Mature	Mature
Germline	Germline	Germline
L-mature	Germline	Mature
H-mature	Mature	Germline
L-irrelevant	Mature (KSAb1)	Mature (Ti-401)
96/3 (anti-IA2)	Mature	Mature

2.2.2.2 Transformation of Rosetta2 cells

Purified DNA was transformed into Rosetta2 competent cells (Merck-chemicals, Darmstadt, Germany). Rosetta2 cells encode tRNAs for rare codons which are not normally expressed in *E. coli*. Thus Rosetta2 cells allow for the expression of proteins whose translation might be inhibited by the codon usage of *E. coli*.

i. 1 µL of purified DNA was incubated on ice with 20 µL of Rosetta2 cells for 5 minutes.

ii. The cells were then heat-shocked for 30 seconds at 42°C.

iii. The cells and plasmid were incubated on ice for 2 minutes.

iv. The transformed cells were incubated with 0.8 mL SOC medium (supplied in kit) in an orbital shaker for 1 h at 37°C with 250 rpm shaking.

v. The transformation mix was spread on agar plates containing 100 µg/mL ampicillin and 3.4 µg/mL chloramphenicol (Appendix 3), and incubated overnight at 37°C.

2.2.2.3 rFab expression method 1 (2 day)

It was necessary to establish suitable methods for optimal rFab expression. Three methods were studied.

i. A fresh single colony was selected and grown in 10 mL LB with 20 µL 5 mg/mL tetracycline (Appendix 3) for 6-8 h, or until the medium became cloudy, at 37°C with 300 rpm shaking.

ii. The LB culture was split between two 2 L flasks of 500 mL 1X 4-morpholinepropanesulphonic (MOPS) acid medium with phosphate (Appendix 4) and grown overnight under the same conditions.

iii. Cultures were centrifuged at 8,000 g for 5 minutes at 4°C and the supernatants discarded. 25 mL samples were taken to test for rFab expression in non-induced cultures.

iv. Each pellet was resuspended in 500 mL 1X MOPS without phosphate (Appendix 4) and grown for 4 h at 30°C with 300 rpm shaking.

v. Cultures were centrifuged at 8,000 g for 10 min and the supernatants discarded. 25 mL samples were taken to use as an expression check for induced samples.

vi. Pellets were frozen at -20°C.

vii. This expression protocol was adapted by Dr Kerry McLaughlin, KCL from published methods (Padoa et al., 2003; Padoa et al., 2010).

2.2.2.4 rFab expression method 2 (4 day)

i. A fresh single colony was selected and grown in 5 mL LB with 10 µL 5 mg/mL tetracycline overnight at 37°C with 300 rpm shaking.

ii. This was inoculated in 100 mL 1X MOPS with phosphate and grown overnight at 37°C with 300 rpm shaking.

iii. This was then split between two 2 L flasks each containing 450 mL 1X MOPS with phosphate and grown at 37°C with 300 rpm shaking until an OD_{600} of 0.6 was reached.

iv. The cultures were centrifuged at 8,000 g for 5 minutes at 4°C and the supernatants discarded. 25 mL samples were taken to test for rFab expression in non-induced cultures.

v. Each pellet was resuspended in 500 mL 1X MOPS without phosphate and grown overnight at 30°C with 300 rpm shaking.

vi. Cultures were centrifuged at 8,000 g for 10 minutes and the supernatants discarded. 25 mL samples were taken to use as an expression check for induced samples.

vii. Pellets were frozen at -20°C.

2.2.2.5 rFab expression method 3 (LB broth)

i. A fresh single colony was selected and grown for 6-8 h in 5 mL SB medium with 10 µL 5 mg/mL tetracycline overnight at 37°C with 300 rpm shaking.

ii. This was then split between two 2 L flasks each containing 450 mL LB medium and grown at 37°C with 300 rpm shaking overnight.

iii. The cultures were centrifuged at 8,000 g for 5 minutes at 4°C and the supernatants discarded. 25 mL samples were taken to test for rFab expression in non-induced cultures.

iv. Each pellet was resuspended in 500 mL 1X MOPS without phosphate and grown overnight at 30°C with 300 rpm shaking.

v.   Cultures were centrifuged at 8,000 g for 10 minutes and the supernatants discarded. 25 mL samples were taken to use as an expression check for induced samples.

vi. Pellets were frozen at -20°C.

2.2.2.6 Measuring OD_{600} of bacterial cultures

To measure the OD_{600} of bacterial cultures, 1 mL samples were analysed every h in cuvettes in a spectrophotometer (Ultrospec 2000, UV/Visible Spectrophotometer, Pharmacia Biotech) at 600 nm. Once the OD_{600} had reached 0.5 it was measured every 15 minutes until the OD_{600} reached 0.6.

2.2.2.7 Purification of rFab proteins

i.   Pellets from 500 mL cultures were thawed on ice and re-suspended in 12.5 mL extraction buffer (Appendix 4).

ii. 50 mg/mL hen egg lysozyme was prepared in extraction buffer and added to a final concentration of 1 mg/mL and left to stir gently at 4°C for 30 minutes.

iii. 1% Triton-X-100 made in dH_2O was added to a final concentration of 0.1% and left to stir for 5 minutes.

iv. 200 U DNase I was added and the solution left to stir for an additional 10 minutes.

v.   The solution was centrifuged at 10,000 g for 15 minutes at 4°C.

vi. The supernatant (periplasmic extract) was filtered through a 0.22 µm filter.

vii. Purification by metal chelation chromatography

viii. Purification was performed 1 mL polypropylene columns (Qiagen, West Sussex, UK).

ix. 1 mL of 50% slurry was equilibrated in wash buffer.

x. The resin was incubated for 30 minutes at room temperature with the filtered supernatant with agitation.

xi. The supernatant and resin were applied to a column and the supernatant was allowed to pass through the column.

xii. The resin was washed in the column three times with 5 mL wash buffer (Appendix 4); the buffer was allowed to completely enter the resin bed each time.

xiii. Purified fractions were eluted with 1 mL elution buffer (Appendix 4) into microcentrifuge tubes.

xiv. Purified rFab samples were dialysed overnight against 1X phosphate buffered saline (PBS) (Appendix 4) at 4°C with gentle stirring to remove imidazole and any proteins <10 kDa. Dialysis membrane tubing was prepared by boiling twice in each of sodium bicarbonate, EDTA and dH$_2$O and stored in 70% ethanol at 4°C. The samples were pipetted into the dialysis tubing and separated with plastic clips.

2.2.2.8 Protein quantification of purified rFab samples

i. The protein quantification of dialysed purified rFab samples was measured using the Bradford Concentration Assay (Novagen).

ii. 25 µL of each standard and each protein sample was pipetted into individual wells of a 96-well plate in duplicate.

iii.   BCA working reagent was prepared (4 mL BCA solution and 80 µl 4% cupric sulphate for every 20 wells)

iv.   200 µL of BCA working reagent was added to each sample.

v.   The plate was mixed on a plate shaker for 30 seconds and then incubated for 30 minutes at 37°C.

vi.   The protein quantification was measured by colour densitometry with a plate reader at 504 nm wavelength using the Revelation program.

2.2.3 SDS-PAGE

The apparatus was set up according to the manufacturer's protocol:

i.   Two glass plates were placed one in front of the other, with the smaller plate at the front. Two separators were placed between the plates with one on either the side.

ii.   The glass plates and separators were aligned on the alignment stage and clicked firmly into place.

iii.   Buffers were prepared as described in Appendix 5.

iv.   The 12% separating gel (Appendix 5) was poured immediately after adding TEMED, covered in a layer of 50% isopropanol solution and left to set.

v.   Once set, the isopropanol solution was washed off with dH_2O and the 10% stacking gel (Appendix 5) was poured on top of the separating gel. A comb was inserted and the gel left to set.

vi.   The comb was removed and the wells were washed with dH_2O and the wells were marked on the glass with marker.

vii. The gels were placed in the tank with 1X SDS-PAGE running buffer (Appendix 5).

viii. 2X loading buffer (Appendix 5) was added to the samples in an equal volume, which were then heated to 100°C for 5 minutes.

ix. The samples and protein markers were loaded.

x. Gels were run at 70 V for 30 minutes, or until the samples have passed through the stacking gel, and 200 V until the loading dye reaches the bottom of the gel.

2.2.3.1 Coomassie blue staining

The gels were prised from between the plates and left in Coomassie blue stain for 1 h. The Coomassie blue stain was then removed and the gels were incubated in destain solution (Appendix 5) overnight. To prevent the gel from cracking during the process, the gels were incubated in 3% glycerol overnight at room temperature. The gel was placed on wet filter paper, covered in cling film and dried (Model 583 Gel Drier and HydroTech Vacuum Pump, Bio-Rad) at 80°C for 2 h.

2.2.3.2 Western blotting

Dialysed samples were assessed for the presence of rFab using a penta-His HRP-Conjugate (Qiagen, West Sussex, UK) and Western blotting. Samples were run on SDS-PAGE gels (as described in 2.6) with coloured markers (Fisher Scientific UK Ltd).

i. The gel was placed on three sheets of wet 3 mm filter paper on the top leaf of the Western blotting cassette (Trans-Blot Electrophoretic Transfer Cell, BioRad).

ii. The gel was covered with a wet Protan Nitrocellulose membrane (Scheiler and Schuell, Dassel, Germany), ensuring no air bubbles were present by rolling with a pastette.

iii. Three further sheets of filter paper were placed over the membrane and the cassette was closed.

iv. The cassette was placed in the tank such that the gel-side of the sandwich was facing the cathode, and the nitrocellulose membrane was facing the anode.

v. The tank was filled with 1X transfer buffer (Appendix 5), connected to the power pack, placed in a polystyrene box containing ice and run for 1 h at 100 V, or until the prestained MW ladder had fully transferred to the blot.

vi. Following transfer, the nitrocellulose membrane was blocked for 1 h at room temperature with PBST/5% marvel milk protein/0.05% Tween-20.

vii. The blocked membrane was incubated with anti-penta His HRP Conjugate (Qiagen; 1:1000 dilution), for 1 h at room temperature.

viii. The membrane was then washed 3 times for 5 minutes each in PBST, incubated with AEC developer (Appendix 5) for 5 minutes, and rinsed with dH$_2$O to stop the reaction.

2.2.4 Assays for measuring binding to TSHR

2.2.4.1 Radiobinding (TRAK) assay.

The ability of purified rFabs to displace radiolabelled ^{125}I-TSH from binding immobilised TSHR was assayed using commercial kits (Brahms TRAK Human RIA, Thermo Fisher Scientific, Germany). Varying concentrations of 10–100,000 ng/mL dialysed purified rFabs were diluted in normal human serum, as the kits are optimised for performance in human serum. All samples were diluted in normal human serum (that did not interfere with the assay) from the same donor (JPB). A maximum dilution of human serum to 66% was used to ensure kit performance was maintained. The experiment was performed on at least three independent occasions with independently prepared samples.

i.   200 µL of Buffer D was added to TSHR-coated tubes, except the first two tubes.

ii.   100 µL of each of standards were added to the appropriate tubes.

iii.   Test samples were prepared by adding 30 µL rFab or IgG to 75 µL normal human serum. 100 µL of this was added to the appropriate tube.

iv.   If less than 30 µL of sample was added, the sample was made up to 105 µL with sterile PBS.

v.   The tubes were incubated for 2 h with shaking at room temperature.

vi. After washing twice with 2 mL wash buffer, 200 µL of ^{125}I-TSH was added to each tube and incubated for 1 h with shaking at room temperature.

vii. The tubes were washed three times with wash buffer and counted in a gamma counter (DSLaboratories).

viii. The inhibition of binding of rFab samples was expressed as percentage inhibition of ^{125}I-TSH binding to TSHR.

2.2.4.2 Flow cytometry

Flow cytometry analysis was used to detect any weak but measurable binding between the rFabs and the TSHR, as expressed on GPI9-5 and JP09 cells. Flow cytometry provides a more sensitive method for detecting binding than radioimmunoassay.

i. GPI9-5 cells were used following at least one passage following thawing from liquid nitrogen. Low passage cells are preferred as TSHR expression may be down-regulated at high passage number.

ii. Cell culture medium was removed and the cells were washed twice in sterile PBS. Cells were detached from the tissue culture flask using 3 mL warm cell dissociation medium and resuspended in 7 mL complete Ham's F12 medium.

iii. The cells were counted using a haemocytometer before being centrifuged at 1500 g for 8 minutes.

iv. The cell pellet was resuspended in PBS containing 1% BSA, 0.05% sodium azide to a cell concentration of 1 x 10^6 cells/mL.

v. 1 mL of cells were transferred to microcentrifuge tubes and spun at 4000 g for 1 minute.

vi. The cell supernatant was removed and the cells were resuspended in 100 µL of the appropriate primary antibody:

vii. Cells were incubated with primary antibodies for 1 h, on ice and in the dark. 4C1 (IgG$_{2a}$, Santa Cruz Biotechnology) was used as a gold-standard anti-TSHR positive control.

viii. The cells were centrifuged and washed twice with cold PBS/1% BSA/0.05% sodium azide and resuspended in 100 µL of the secondary antibody, goat anti-mouse conjugated to phycoerythrin (PE) (AbCam) before incubating on ice for 30 minutes in the dark.

ix. Samples were centrifuged and washed three times with cold PBS/1% BSA/0.05% sodium azide. Samples were analysed immediately and resuspended in 300 µL PBS.

x. Samples were analysed on the same day using a FACS Canto II machine (BD Biosciences).

2.2.4.3 cAMP stimulation bioassay

The potencies of purified rFab and their ability to stimulate the TSHR was assessed using TSHR stably transfected CHO cells (JP09 cells). The intracellular cAMP released into the culture medium was assessed using commercial radioimmunoassay kits (R&D Systems or Enzo Life Sciences). rFab samples were tested at differing concentrations of 10–100,000 ng/mL and tested on independent occasions with independently

prepared samples. Controls included KSAb1 IgG and IgG$_{2b}$ as an isotype-matched control. In addition, forskolin, a direct activator of adenyl cyclase, was used to determine the total cAMP stimulation in culture.

i. JP09 cells, which had been in culture for a minimum of 7 days following thawing from liquid nitrogen, were plated in a 96-well plate at a density of 30,000 cells/well and incubated overnight at 37°C with 5% CO2.

ii. The following day, samples were prepared in complete HBSS (Appendix 6).

iii. The cell culture medium was removed and the cells were washed once in warm sterile PBS.

iv. Samples and controls were added to the cells in complete HBSS: 56.25 µL of each dilution and 93.75 µL of complete HBSS per well and 15 µL of 100 µM forskolin and 135 µL complete HBSS was added, such that the total volume for each well was 150 µL.

v. The stimulated cells were incubated for 4 h at 37°C with 5% CO$_2$.

vi. Assay Buffer was prepared by first diluting 1:2 with dH$_2$0 and by mixing 3:1 with complete HBSS.

vii. Standards were prepared and diluted in Assay Buffer/complete HBSS.

viii. Standards and samples were added to a plate containing wells coated with goat anti-rabbit wells.

ix. The plate was sealed with a plastic wrap and incubated with 500 g shaking for 2 h at room temperature.

x.   The plate was washed three times with wash buffer diluted 1:20 with dH_2O and 200 µL pNpp substrate was added to each well and incubated, covered in foil, for 1 h at room temperature.

xi. 50 µL Stop solution was added to each well and the colour densitometry of the plate was read immediately at 405 nm using the Revelation program.

2.2.4.4 Growth of *Y. enterocolitica* serotypes 8081 and Ye58/03 on Congo Red-Magnesium Oxalate plates

Glycerol stocks of *Y. enterocolitica* serotypes 8081 and Ye58/03 were streaked on Congo Red-Magnesium Oxalate plates (Riley and Toma, 1989) prepared by Mr Marco Grasso. Colonies that express pYVe are dependent on calcium for growth and also absorb Congo Red from the agar medium. The streaked plates were incubated overnight at 37°C in Yersinia Luria Bertani broth (YLB; Appendix 7). pYVe-positive colonies grew and were red in colour; pYVe-negative colonies were white in colour. Plasmid expression is unstable so there was a mix of both plasmid-positive and –negative colonies. Isolated single red colonies were easily obtained for *Y. enterocolitica* serotype 8081, however it was not possible to isolate single colonies for Ye58/O3.

2.2.4.5 Checking for presence of pYVe plasmid in *Y. enterocolitica* serotypes 8081 and Ye58/03 by PCR

For *Y. enterocolitica* serotype 8081, one half of three single isolated red colonies were taken using a toothpick for PCR analysis, to confirm the presence of pYVe. The remaining half of each colony was taken for

overnight growth under conditions described in section 2.2.4.5. For serotype Ye58/O3, no easily identifiable single colonies were obtained on the streaked plate. Three small streaks of densely packed Ye58/O3 colonies were taken for PCR analysis.

Table 5: Primers used for amplification of yscU gene of pYVe plasmid.

Primer	Sequence
Forward	5' TCTGTACTGTTGGCTTTGTGG 3'
Reverse	5' TTGCGCACAGACTGAACTTGG 3'

Table 6: PCR cycling conditions for amplification of yscU gene in pYVe plasmid.

Temperature (°C)	Time	
95	5 minutes	
95	30 seconds	
54	30 seconds	x30
72	1 minute	
72	10 minutes	
10	Hold	

2.2.4.6 Growth of *Y. enterocolitica* serotypes 8081 and Ye58/O3 for the isolation of Yops

As described in section 2.2.4.5, half of three single isolated red 8081 colonies were taken for PCR analysis and the other half of the same

colony was grown overnight in YLB broth. No isolated single colonies of Ye58/03 formed so three small streaks of Ye58/03 grown overnight instead. The Yop isolation protocol is adapted from a published protocol (Trulzsch et al., 2004).

i. The 8081 colony or Ye58/03 streak was inoculated in 10 mL YLB media and grown overnight in an orbital shaker (Gallenkamp Cooled Orbital Incubator) at 30°C with 200 rpm shaking.

ii. The following morning this was diluted 1:40 in 10 mL Bovine Heart Infusion and grown for 2 h at 37°C.

iii. 20 mM sodium oxalate and 20 mM $MgCl_2$ were added to induce Yop secretion and the cultures were grown for a further 3 h at 37°C.

iv. The cultures were centrifuged at 5000 g for 10 minutes at room temperature (Beckman Avanti 30).

v. 10 mL of supernatant was filtered through a 2 μm filter and incubated on ice with 1 mL 100% TCA for 30 minutes.

vi. The mixture was centrifuged at 10,000 g for 10 minutes at 4°C and the supernatant discarded.

vii. The pellet was resuspended in 500 μL 10% SDS and 1 mL of ice-cold acetone was added to the resuspension add incubated for 30 minutes on ice.

viii. The mixture was centrifuged at 14,000 g for 30 minutes at 4°C and the supernatant discarded.

ix.   The acetone was allowed to evaporate, heating to 37°C aided this evaporation and the pellet resuspended in 60 µL PBS.

2.2.4.7 Preparation of whole cell lysates from *Y. enterocolitica* serotypes 8081 and Ye58/03

Preparation of whole cell lysates:

i.   *Y. enterocolitica* serotype 8081 and Ye58/03 were grown overnight in 10 mL YLB at 30°C with 250 rpm shaking.

ii.   1 mL of cultures was centrifuged at 13,000 g for 1 minute at room temperature.

iii. Pellets were resuspended in 100 µL PBS and 100 µL 2X SDS-PAGE loading buffer.

iv.   The resuspended pellets were sonicated for 1 pulse every two seconds for 1 minute.

v.   Pellets were discarded and 5 µL supernatant were analysed by SDS-PAGE.

Preparation of envelope proteins from *Y. enterocolitica* serotypes 8081 and Ye58/O3:

vi.   The protocol for the preparation of envelope proteins was adapted from a previous publication (Luo et al., 1993).

vii. 40 mL overnight cultures of 8081 and Ye58/03 serotypes were centrifuged at 5,000 g for 10 minutes.

viii. The supernatant was discarded and the pellets were resuspended in 2 mL PBS.

ix. Sonication was performed in ice-water slurry. The first sonication involved a one second pulse every two seconds for 1 minute.

x. Large cellular debris was removed by centrifuging at 7,000 g for 10 minutes.

xi. The envelope proteins were isolated by ultracentrifugation of the supernatant at 38,500 g for 1 h.

xii. Pellets were resuspended in 100 µL PBS and 100 µL 2X SDS-PAGE loading buffer.

2.2.4.8 *Y. enterocolitica* protein extract for affinity enrichment

i. *Y. enterocolitica* cultures were grown overnight by Mr Marco Grasso until an OD_{600} of 2.5-3 was reached. Cells were then collected by centrifugation, frozen and sent to our laboratory.

ii. Centrifuged cells were thawed on ice and resuspended in 2 mL lysis buffer (Appendix 7).

iii. 40 µL of hen egg lysozyme (50 mg/mL) was added and incubated at 37°C for 30 minutes with gentle agitation.

iv. The solution was sonicated on ice for 20-second pulse followed by a 20 second pause for a total of 5 minutes.

v. Cells were centrifuged at 10,000 g for 10 minutes at 4°C.

vi. The supernatant was removed and 20 µL of 100 mM phenylmethylsulfonyl fluoride was added.

vii. The protein extract was incubated with KSAb1 IgG coupled to Cyanogen Bromide-activated Sepharose immediately.

2.2.4.9 Affinity-enrichment of *Y. enterocolitica* with affinity matrix-coupled antibody

i.   Dried Cyanogen Bromide-activated Sepharose 4B (Sigma-Aldrich) was swelled and activated in 200 mL cold 1 mM HCl for 30 minutes.

ii. The swelled gel was washed with dH$_2$O followed by coupling buffer (Appendix 7) in a sintered glass funnel.

iii. The washed resin was incubated with either KSAb1 IgG or BSA in coupling buffer at a concentration of 10 mg/mL overnight at 4°C.

iv. The following day the incubated mix was washed in coupling buffer and resuspended in 0.2 M glycine-NaOH pH 8 for 2 h at room temperature.

v.   The resin was washed with alternate washes of coupling buffer and acetate buffer (Appendix 7) five times.

vi. The resin was then incubated with *Y. enterocolitica* protein extract (protocol described below in section 2.2.4.10) overnight at 4°C.

vii. The resin was centrifuged and the supernatant removed. The resin was washed twice with 1X PBS.

viii. The resin was incubated with 50 µL 0.1 M glycine-HCl pH 2.5 for 5 minutes at room temperature.

ix. 5 µL Tris-HCl pH 8 was added to neutralise the 0.1 M glycine pH 2.5, the resin was centrifuged and the supernatant collected and measured for protein concentration.

2.2.4.10 Western blotting of prepared *Y. enterocolitica* proteins

i. SDS-PAGE was run as described in section 2.2.3 and transferred to a nitrocellulose membrane as described in section 2.2.3.2.

ii. Following transfer, the blot was incubated for 1 h at room temperature in PBST with 5% Marvel non-fat milk.

iii. The blots were then incubated overnight at 4°C with gentle agitation with primary antibody.

iv. Blots were washed three times for 10 minutes each in PBST.

v. The blots with transferred Yops were then incubated for 2 h at room temperature with goat anti-mouse polyclonal IgG conjugated to alkaline phosphatase (Sigma-Aldrich) at a 1:1000 dilution. Blots with transferred whole cell lysates, envelope proteins or outer membrane proteins were incubated with sheep anti-mouse IgG HRP-linked species-specific whole antibody (GE Healthcare) at a 1:5000 dilution.

vi. Blots were washed again as in step (v).

vii. The Yop blots were then incubated for 3-5 minutes with BCIP/NBT conjugate. Rinsing the blots with dH_2O stopped the reaction.

viii. The other blots were incubated with a 1:1 ratio of Amersham Prime Western Blotting Detection Reagents, Solution A and Solution B, for 5 minutes. Excess reagent was drained from the blot and the blot was wrapped in cling film.

ix. Blots were exposed to Amersham Hyperfilm.

2.2.4.11   MALDI-TOF sequencing analysis

Bands excised from polyacrylamide gels underwent MALDI-TOF sequencing analysis at the University of Leicester Protein Nucleic Acid Chemistry Laboratory, using a 4000 Q-TRAP® LC/MS/MS System. The band was excised using clean gloves and scalpel, stained with fresh Coomassie blue solution and destained in a clean box to prevent contamination of the gel with keratin.

2.2.4.12   Outer membrane porin A synthesis

The nucleotide sequence of OmpA (*Y. enterocolitica* 8081) was obtained from PubMed using the 'Protein' accession number provided by the MALDI-TOF analysis (A1JMT3). The nucleotide accession number of ompA is nc 008800. The nucleotide sequence of *ompA* (1,080 bp) was optimised for protein expression and subsequently synthesised as a synthetic gene by GenScript, USA. The first 21 aa (63 nucleotides) of OmpA is a signal sequence which is cleaved by a peptidase(s), underlined in Figure 14, page 111.

```
at gaaaaagacagct at cgcat t agcagt ggcact ggct ggt t t cgct acagt agcgcaa
  M   K   K   T   A   I   A   L   A   V   A   L   A   G   F   A   T   V   A   Q
gccgcaccgaaagat aacacct ggt acaccggt ggt aaact gggct ggt ct cagt at caa
  A   A   P   K   D   N   T   W   Y   T   G   G   K   L   G   W   S   Q   Y   Q
aat act ggcact ggcggt at ct at ggcgaccaaggcaat gacggt ccaact cat aaagac
  N   T   G   T   G   G   I   Y   G   D   Q   G   N   D   G   P   T   H   K   D
caat t aggt gct ggt gcgt t ct t gggt t accaagcaaaccaat acct gggct t t gaaat g
  Q   L   G   A   G   A   F   L   G   Y   Q   A   N   Q   Y   L   G   F   E   M
ggat acgact ggct t ggccgt at gcct t acaaaggcgacgt t cgt aacggcgact t t aaa
  G   Y   D   W   L   G   R   M   P   Y   K   G   D   V   R   N   G   D   F   K
gcacaaggcgt t caact ggct gcaaaact gagct acccaat t gct caggat t t ggacct g
  A   Q   G   V   Q   L   A   A   K   L   S   Y   P   I   A   Q   D   L   D   L
t acaccgt t t aggt ggt at ggt t t ggcgt gcagact caagcgcgt t t gacgcagct act
  Y   T   R   L   G   G   M   V   W   R   A   D   S   S   A   F   D   A   A   T
ggcgaccgt caaaacaaccat gat accggt gt t t ct ccact ggt agcact gggt gct gaa
  G   D   R   Q   N   N   H   D   T   G   V   S   P   L   V   A   L   G   A   E
t acgcat ggaccaaaaact gggcaacccgt at ggaat accaat gggt t agcaacat cggt
  Y   A   W   T   K   N   W   A   T   R   M   E   Y   Q   W   V   S   N   I   G
gat aaagct accgt t ggt gct cgt ccagacaacggcat gct aagcgt aggt gt t t ct t ac
  D   K   A   T   V   G   A   R   P   D   N   G   M   L   S   V   G   V   S   Y
cgt t t cggt caggaagat gcagt agct ccaat t gct ccggct ccagct ccagct ccagt t
  R   F   G   Q   E   D   A   V   A   P   I   A   P   A   P   A   P   A   P   V
gt t gat accaagcgt t t cacact gaaat ct gacgt gct gt t t gct t t caacaaat caacg
  V   D   T   K   R   F   T   L   K   S   D   V   L   F   A   F   N   K   S   T
t t gaaaccagaaggccagcaagct ct ggaccaact gt at gcacaact gagct ct at cgat
  L   K   P   E   G   Q   Q   A   L   D   Q   L   Y   A   Q   L   S   S   I   D
cct aaagat ggt t ct gt agt ggt t ct gggct t cgct gaccgt at cggccaaccagct cct
  P   K   D   G   S   V   V   V   L   G   F   A   D   R   I   G   Q   P   A   P
aact t agct ct gt ct cagcgt cgt gct gacagcgt gcgt gat t acct ggt t t ct aaaggt
  N   L   A   L   S   Q   R   R   A   D   S   V   R   D   Y   L   V   S   K   G
at ccct gct gacaaaat caccgct cgcggt gaaggccaagct aacccagt t acaggcaac
  I   P   A   D   K   I   T   A   R   G   E   G   Q   A   N   P   V   T   G   N
acct gt gacaacgt gaaaccacgt gct gct ct gat t gagt gcct ggcaccagat cgt cgc
  T   C   D   N   V   K   P   R   A   A   L   I   E   C   L   A   P   D   R   R
gt agagat cgaagt t aaaggct acaaagaagt t gt aact cagccacaggct t aa
  V   E   I   E   V   K   G   Y   K   E   V   V   T   Q   P   Q   A   -
```

Figure 14: Nucleotide and amino acid sequence of OmpA for gene synthesis.

The nucleotide and amino acid sequence of OmpA was found using a PubMed search. The 21 aa signal sequence is underlined. The nucleotide construct was synthesised by GenScript, USA.

2.2.4.13   Cloning of *ompA* gene cassette

The *ompA* gene insert was digested from pUC57 vector by restriction digest with *Nde*I and *Xho*I and sub-cloned into pET22b vector (Novagen) and One Shot® TOP10 Chemically Competent *E. coli* cells (Invitrogen). pET22b vector and competent cells were kindly donated by Dr Kevin Ford

and Dr Joop Gaken, KCL. DNA preparation and cloning protocols used were as described in Chapter 2, section 2.2.1, page 82.

2.2.4.14   Cloning of *ompC* and *ompF* genes

The cDNA of *ompC* (*Y. enterocolitica* 8081*)* and *ompF* (*Y. enterocolitica* 8081*)* genes were kindly donated by Dr Anna Stenkova, Pacific Institute of Bioorganic Chemistry, Russia, cloned in pET32b vector (Novagen) using *Nde*I and *Bam*HI restriction sites. The nucleotide and amino acid sequences of OmpC and OmpF are detailed in Figure 15, page 113, and Figure 16, page 114, respectively.

The first 21 aa (63 nucleotides) of OmpC and OmpF are a signal sequence which is cleaved by a peptidase(s), underlined in Figure 15 and Figure 16. The gene constructs donated by Dr Anna Stenkova do not include the signal sequence.

```
at gaaact gcgcgt gct gagcct gct ggt gccggcgct gct ggt ggcgggcagcgcgggc
 M   K   L   R   V   L   S   L   L   V   P   A   L   L   V   A   G   S   A   G
gcggcggaaat t t at aacaaagat ggcaacaaact ggat ct gt at ggcaaagt ggat ggc
 A   A   E   I   Y   N   K   D   G   N   K   L   D   L   Y   G   K   V   D   G
ct gcat t at t t t agcgat gat aaaagcaaagat ggcgat cagagct at at gcgct t t ggc
 L   H   Y   F   S   D   D   K   S   K   D   G   D   Q   S   Y   M   R   F   G
ct gaaaggcgaaacccagat t agcgat cagct gaccggct at ggccagt gggaat at cag
 L   K   G   E   T   Q   I   S   D   Q   L   T   G   Y   G   Q   W   E   Y   Q
gcgaacct gaacaaagcggaagat caggat cagggcaact t t acccgcat t ggct t t gcg
 A   N   L   N   K   A   E   D   Q   D   Q   G   N   F   T   R   I   G   F   A
ggcct gaaat t t gcggat t at ggcagct t t gat t at ggccgcaact at ggcgt gct gt at
 G   L   K   F   A   D   Y   G   S   F   D   Y   G   R   N   Y   G   V   L   Y
gat gt gaccagct ggaccgat gt gct gccggaat t t ggcggcgat acct at ggcgcggat
 D   V   T   S   W   T   D   V   L   P   E   F   G   G   D   T   Y   G   A   D
aact t t ct gagccagcgcggcaacggcat ggcgacct at cgcaacaccaact t t t t t ggc
 N   F   L   S   Q   R   G   N   G   M   A   T   Y   R   N   T   N   F   F   G
ct ggt ggat ggcct gaact t t gcgct gcagt at cagggcaaaaacggcagcggcaccgaa
 L   V   D   G   L   N   F   A   L   Q   Y   Q   G   K   N   G   S   G   T   E
accgat aacggccgcgat gt gcagggccagaacggcgat ggct at ggcat gagcct gagc
 T   D   N   G   R   D   V   Q   G   Q   N   G   D   G   Y   G   M   S   L   S
t at gat ct gggct ggggcgt gagcgcgagcgcggcgat ggcgagcagcaaacgcaccgat
 Y   D   L   G   W   G   V   S   A   S   A   A   M   A   S   S   K   R   T   D
gaacagaacaacct ggcgt t ggccat ggcgat cgcgcggat gcgt at agcggcggcct g
 E   Q   N   N   L   A   F   G   H   G   D   R   A   D   A   Y   S   G   G   L
aaat at gat gcgaacaacgt gt at ct ggcggcgacct at gcgcagacct at aacct gacc
 K   Y   D   A   N   N   V   Y   L   A   A   T   Y   A   Q   T   Y   N   L   T
cgct t t ggcaact t t aaaaacaacaccgat agcggct t t gcgaacaaagcgcagaacat t
 R   F   G   N   F   K   N   N   T   D   S   G   F   A   N   K   A   Q   N   I
gaact ggt ggcgcagt at cagt t t gat t t t ggcct gcgcccgagcgt ggcgt at ct gcag
 E   L   V   A   Q   Y   Q   F   D   F   G   L   R   P   S   V   A   Y   L   Q
agcaaaggcaaagat ct gggcaacggct at agcgat caggat ct ggt gaaat at gt ggat
 S   K   G   K   D   L   G   N   G   Y   S   D   Q   D   L   V   K   Y   V   D
gt gggcgcgacct at t at t t t aacaaaaacat gagcacct at gt ggat t at aaaat t aac
 V   G   A   T   Y   Y   F   N   K   N   M   S   T   Y   V   D   Y   K   I   N
ct gct ggat gaaaacgaat t t accaaaaacgcgggcat t aacaccgat gat at t gt ggcg
 L   L   D   E   N   E   F   T   K   N   A   G   I   N   T   D   D   I   V   A
gt gggcct ggt gt at cagt t t
 V   G   L   V   Y   Q   F
```

Figure 15: Nucleotide and amino acid sequence of OmpC.

The nucleotide and amino acid sequence of OmpC. The 21 aa signal sequence is underlined. The gene construct donated by Dr Anna Stenkova does not include this signal sequence.

```
at gaagcgcaat at t ct t gcagt agt aat cccagcat t gt t agt agct ggt gcagct aat
 M   K   R   N   I   L   A   V   V   I   P   A   L   L   V   A   G   A   A   N
gcagcagaaat ct acaacaaagacggcaacaaact t gacct gt acggt aaagt t gacgca
 A   A   E   I   Y   N   K   D   G   N   K   L   D   L   Y   G   K   V   D   A
cgt caccagt t ct ct gacaacgct ggccaagacggcgacgaat ct t at gt t cgt t t cggc
 R   H   Q   F   S   D   N   A   G   Q   D   G   D   E   S   Y   V   R   F   G
t t caaaggt gaaacccaaat t act gaccagct gaccggt t acggccagt gggaat acaac
 F   K   G   E   T   Q   I   T   D   Q   L   T   G   Y   G   Q   W   E   Y   N
gt t caggct aaccacgct gaat ct caaggcgat aaaggcaacaaaacccgt ct gggct t t
 V   Q   A   N   H   A   E   S   Q   G   D   K   G   N   K   T   R   L   G   F
gct ggt ct gaaat t t gct gaat t cggt t cat t cgact at ggccgt aact acggcgt aat c
 A   G   L   K   F   A   E   F   G   S   F   D   Y   G   R   N   Y   G   V   I
t at gat gt caacgcat ggact gacat gct gccagt gt t cggt ggt gat t caat ct ccaac
 Y   D   V   N   A   W   T   D   M   L   P   V   F   G   G   D   S   I   S   N
t ct gacaact acat gact ggccgt t ct act ggcct ggct act t accgt aacaccaact t c
 S   D   N   Y   M   T   G   R   S   T   G   L   A   T   Y   R   N   T   N   F
t t cggt ct ggt t gat ggcct gaact t t gct ct gcaat at caaggcaaaaacgaaaacgat
 F   G   L   V   D   G   L   N   F   A   L   Q   Y   Q   G   K   N   E   N   D
cgcagcgct gt t gcaaacggt gt t t acact ggt gacaacct gaaagat cagaacggcgac
 R   S   A   V   A   N   G   V   Y   T   G   D   N   L   K   D   Q   N   G   D
ggct t cggt at ct ct t ct act t at gat at cggt t at ggccgt gaact t t ggt gct ggt t t c
 G   F   G   I   S   S   T   Y   D   I   G   Y   G   V   N   F   G   A   G   F
t ct t ct t ccaaccgt accaaccaacaaaaagcat t cagcact gct gaaggcgat aaagct
 S   S   S   N   R   T   N   Q   Q   K   A   F   S   T   A   E   G   D   K   A
caggcat ggaacgt t ggt gct aaat acgacgcaaacaat gt at acct agct gt aat gt at
 Q   A   W   N   V   G   A   K   Y   D   A   N   N   V   L   A   V   M   Y
gct gaaact caaaacat gact ccat at ggcgat gct t ct aat act at cgct aacaagact
 A   E   T   Q   N   M   T   P   Y   G   D   A   S   N   I   A   N   K   T
cgt gacat t gaaat cact gcacaat accagt t cgact t cggt ct acgt ccat ct t t aggc
 R   D   I   E   I   T   A   Q   Y   Q   F   D   F   G   L   R   P   S   L   G
t acgt t cagt ct aaagggaaagat ct t aacgcgaat ggcgat aaccaagat ct gt t gaaa
 Y   V   Q   S   K   G   K   D   L   N   A   N   G   D   N   Q   D   L   L   K
t at gt t t ct gt aggt t ct t act act act t caacaaaaacat gt ct acct at gt t gat t ac
 Y   V   S   V   G   S   Y   Y   Y   F   N   K   N   M   S   T   Y   V   D   Y
aaaat caact t gct ggacgaaaat gact t cact cgt gcaacggt ct gaacacagacgac
 K   I   N   L   L   D   E   N   D   F   T   R   A   N   G   L   N   T   D   D
gt t gt aggt gt t ggct t ggt t t accagt t ct aa
 V   V   G   V   G   L   V   Y   Q   F   -
```

Figure 16: Nucleotide and amino acid sequence of OmpF.

The nucleotide and amino acid sequence of OmpF. The 21 aa signal sequence is underlined. The gene construct donated by Dr Anna Stenkova does not include this signal sequence.

2.2.4.15 Expression of *ompA, ompC* and *ompF* gene constructs as recombinant protein

The *ompA* gene cloned in pET22b vector, and *ompC* and *ompF* cloned in pET32b vector were transformed in BL21 (DE3) cells for recombinant protein expression. The transformation protocol was the same as that

used for Rosetta2 cells (see Chapter 2, section 2.2.2.2, page 91) and agar plates with ampicillin as a selection marker were used.

For expression as recombinant protein:

i. A single colony was inoculated in LB broth containing 100 μg/mL ampicillin (Appendix 3) and grown at 37°C overnight with shaking at 250 rpm.

ii. The next morning, overnight culture was diluted 1:100 in fresh LB containing 100 μg/mL ampicillin and grown for 3 h at 37°C with shaking at 250 rpm.

iii. Isopropyl β-D-1-thiogalactopyranoside (IPTG) was added to a final concentration of 0.5 mM or 1 mM to induce protein expression and grown for 4 h at 37°C.

iv. Protein expression was confirmed by SDS-PAGE analysis with Coomassie blue staining (Chapter 2, section 2.2.3, page 96) and Western blotting (Chapter 2, section 2.2.3, page 96 and Chapter 5, section 2.2.4.10, page 109).

CHAPTER THREE

RECOMBINANT FAB EXPRESSION AND

EVALUATION OF GERMLINE PRECURSOR OF

THYROID STIMULATING ANTIBODIES

3 CHAPTER THREE: Recombinant Fab expression and evaluation of germline genes of thyroid stimulating antibodies.

3.1 Introduction

3.1.1 KSAb1 and KSAb2 monoclonal antibodies

As has been previously described in Chapter 1, section 1.7.2, page 55, the antibody repertoire of a GD patient can be very diverse, including stimulating, antagonist and neutral antibody populations (Evans et al., 2010; Morshed et al., 2010b). It is therefore important to evaluate and understand these antibodies at a molecular level to appreciate how they arise in pathogenesis and how they may be targeted as a specific therapy. The paucity of such antibodies in patient serum (de Forteza et al., 1994; Nakatake et al., 2006) and the notorious difficulties involved in their isolation from human serum (Martin et al., 1997; Pichurin et al., 2002; Soliman et al., 1995) has made animal models of induced experimental disease a necessity (Dagdelen et al., 2009).

One such model established in this laboratory using Ad-TSHR289 resulted in the isolation of two potent monoclonal TSAbs with powerful agonist properties, KSAb1 (IgG_{2b}/κ) and KSAb2 (IgG_{2a}/κ) (Gilbert et al., 2006a). The isolation of these antibodies allows for important studies to characterise the pathogenic antibody response in the mouse. The stimulatory properties of these antibodies in the nanomolar range, their strong affinity for TSHR and their *in vivo* pathogenicity make these antibodies comparable to the human mAbs and relevant for study (see Chapter 1, Sections 1.7.7 and 1.7.9 for details).

The DNA sequence of the V-region genes of KSAb1 and KSAb2 revealed the germline gene rearrangements of both mAbs, and their pattern of SHM (Padoa et al., 2010). Comparison of the V-region sequences with the IMGT® database of Ig (and TCR) germline genes (Lefranc et al., 1999) revealed that both KSAb1 and KSAb2 shared the same germline IGHV and IGLV genes and are high likely to be derived from the same original B cell clone. The two antibodies share 21 SHM in their H-chains, with 8 additional unique mutations in KSAb1 and 5 additional unique mutations in KSAb2 suggesting that following 21 SHM events, the original B cell clone diverged into two separate clones, each expressing a sequentially different H-chain following additional unique mutations. The L-chains of both mAbs do not share any common SHM and thus diverged independently, with 8 mutations in KSAb1 and 11 mutations in KSAb2 (Padoa et al., 2010) as shown in Figure 17.

Figure 17: lineage tree illustrating the clonal relationship between KSAb1 and KSAb2.

Both mAbs are derived from the same germline VDJ rearrangement and have undergone significant SHM in their H- and L-chains. In the H-chain (A) there are 21 common mutations before divergence with 8 unique mutations in KSAb1 and 5 in KSAb2, whilst the L-chain (B) diverged immediately with 5 mutations in KSAb1 and 11 mutations in KSAb2. Figure taken from (Padoa et al., 2010).

The sequencing of KSAb1 and KSAb2 provided us with an opportunity to investigate the stage in their development when TSHR recognition and pathogenic activity was acquired, beginning with their original germline gene rearrangement. Determining whether the germline revertant of the two mAbs could recognise TSHR would reveal whether KSAb1 and KSAb2 developed from an already autoreactive precursor antibody, which

119

would point to a defect in central tolerance allowing autoreactive B cell clones to exit the bone marrow, or whether KSAb1 and KSAb2 developed from a non-autoreactive precursor which acquired pathogenic activity through SHM in the periphery.

3.1.2 Previous germline revertant studies in other autoimmune conditions

Germline revertant studies in autoantibodies have been evaluated in only one other autoimmune condition, SLE, where antibodies to DNA antigens have been studied. Such studies have also discussed the contribution of SHM to autoreactivity development.

Radic *et al* reverted a murine anti-DNA antibody to the germline sequence and found low but measurable binding to double-stranded DNA (dsDNA) (Radic et al., 1993). A recent study in a murine SLE model, also found evidence for SHM-driven autoreactivity, demonstrating that a single non-autoreactive B cell clone can give rise to 15 pathogenic autoantibodies through SHM. The same loss of autoreactivity was found in the germline revertants of a further 8 autoreactive B cells descended from different original B cell clones. However the germline revertant of one autoreactive clone displayed only a 50-fold decrease in autoreactivity (Guo et al., 2010). Most interestingly, Guo *et al* postulate that a non-autoreactive B cell leaving the bone marrow may be more dangerous than one leaving with an autoreactive specificity, as the latter may be subjected to deleterious or anergic tolerance mechanisms sooner than the former.

Reversion of two anti-dsDNA mAbs isolated from SLE patientsto the germline sequence resulted in a complete loss of anti-DNA recognition, clearly demonstrating the roles of SHM and affinity maturation in driving autoreactivity. Furthermore, introduction of selected mutations in the germline sequence in one of the mAbs revealed three replacement mutations essential for dsDNA binding, 1 mutation in the H-chain, and two in the L-chain. Re-introduction of these three mutations alone in the germline sequence was sufficient to generate dsDNA binding comparable to that of the original antibody (Wellmann et al., 2005). In a later paper, 6 polyreactive anti-Ro and anti-La autoantibodies and 21 IgG memory B cells isolated from a single patient undergoing SLE were reverted to the germline sequence. The majority of these antibodies lost reactivity to a variety of SLE autoantigens, with only a few antibodies retaining autoreactivity (Mietzner et al., 2008).

To accurately assess the contribution of SHM in the autoantibody response in GD, a large database of antibodies and their sequences are required both from the same individual and others for comparison to detect patterns of mutation, their effects on affinity and to rule out any polymorphisms. In the case of GD, four anti-TSHR mAbs have been isolated from three patients (Evans et al., 2010; Sanders et al., 2003; Sanders, 2008). Whilst there is some restricted usage of V_H genes, with three of the four mAbs using the V_H5 family of genes, this is too small a number to examine for trends in mutation and gene usage. It has been reported that these antibodies have undergone SHM events, although details of the precise mutations have not been published so it is not

possible at this stage to comment in any great detail on the role of certain somatic mutations, if any, in the human GD antibody response.

3.1.3 Monoclonal antibody fragment technology

Recombinant Fab (rFab) fragments consist of the full L-chain ($V_L C_L$) and the Fd portion of the H-chain ($V_H C_H 1$) linked by a disulphide bond. rFabs are easily produced in prokaryotic expression systems at high levels and prove to be a more stable antibody fragment than scFv due to cooperation between the variable and constant regions (Röthlisberger et al., 2005). Both the IGHV and IGKV genes must be cloned in the expression vector and expressed in the same cell which may be bacterial, yeast, insect or mammalian (Rahman et al., 1998). In the expression system used in this thesis, using the pAK19 vector (Carter et al., 1992), each antibody chain is produced as a separate peptide in the bacterial cell and a signal sequence in the vector will direct them to the bacterial periplasm, where a disulphide isomerase will link the chains with disulphide bonds (Knappik and Pluckthun, 1995). Bacterial expression systems do not alter or affect the peptide sequence or structure with any post-translational modifications (Rahman et al., 1998). However, a major setback of antibody fragments is their monovalency; resulting in fast dissociation times from their antigenic target due to lower avidity for antigen than their IgG counterparts (Holliger and Hudson, 2005).

Figure 18: Antibody engineering.

Monoclonal antibodies and their derivations have been used for therapeutic and diagnostic purposes. Adapted from (Holliger and Hudson, 2005).
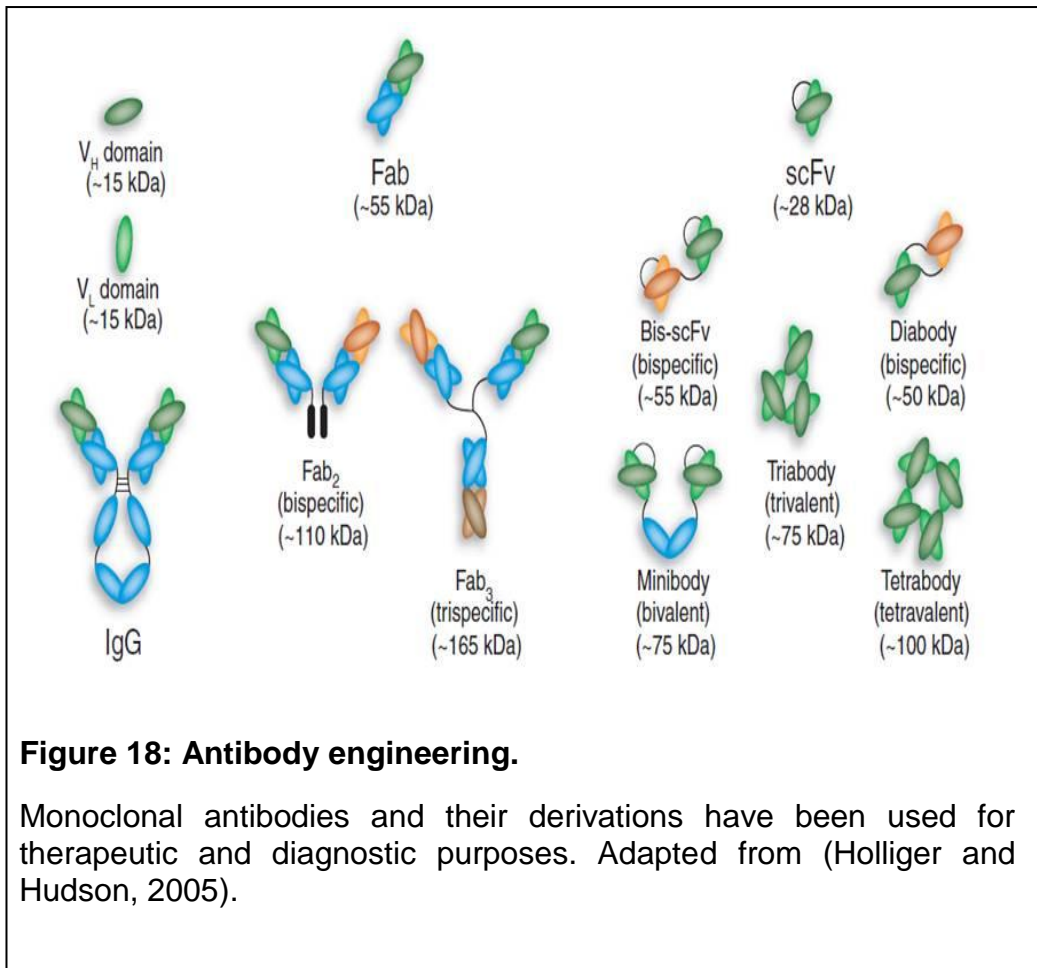
The rFab expression system was thus chosen for this thesis on the basis of ease of expression, relative stability compared to other engineered small fragments. It has proven to be successful in producing rFab molecules capable of binding antigens involved in T1D: the 65 kDa isoform of glutamate decarboxylase (GAD65) (Padoa et al., 2003), IA-2 (Dr Michael Christie and Dr Kerry McLaughlin, KCL, unpubished) and the TSHR (Padoa et al., 2010).

3.2 Aims

The aims of this chapter were to evaluate the antigen specificity of the shared germline precursor antibody of two TSAbs, KSAb1 and KSAb2:

i.   The germline genes were expressed and purified as rFab for evaluation of antigen-specific binding.

ii. Once available in purified form, rFab germline was evaluated in the following assays:

   a. Radioreceptor (TRAK) assay: binding of the receptor is determined by the rFab's ability to displace radiolabelled TSH from binding immobilised TSHR.

   b. Flow cytometry: binding of the receptor is determined by rFab binding to CHO cells expressing high levels of TSHR A-subunit.

   c. cAMP stimulation bioassay: production of cAMP by CHO cells expressing full length TSHR following stimulation by rFab preparations. cAMP stimulation signifies not only binding of the TSHR, but also pathogenic activity.

3.3 Results

3.3.1 Cloning of synthetic germline construct in pAK19 vector

The germline construct, comprising the germline IGHV and IGLV gene sequence of KSAb1 and KSAb2 was cloned in pUC57 and was received with verification of its full nucleotide sequence (not shown). The insert was excised by restriction digestion with *Eco*RI/*Hind*III followed by agarose gel electrophoresis to verify its size as migrating at 1.7 kB (Figure 19A). The purified insert was sub-cloned into pAK19 and confirmed by agarose gel electrophoresis to ensure that the construct and digested pAK19 plasmid were running at the expected sizes of 1.6 kB and 6 kB, respectively (Figure 19B) The sub-cloned insert in pAK19 plasmid was re-sequenced to confirm faithful cloning into pAK19 (Appendix 8).

Figure 19: Cloning of germline in plasmid pAK19.

(A) The germline construct in pUC57 was digested with *Eco*RI and *Hind*III to give a germline construct digest product of 1.6 kB (B) KSAb1 and germline construct cloned in pAK19 were digested with *Eco*RI and *Hind*III. The digested products were analysed by 0.8% agarose gel to confirm they were of the expected sizes. The insert was 1.6 kB and the plasmid was 6 kB.

3.3.2 rFab expression

Following successful cloning of the germline gene cassette in pAK19 vector, expression of the germline construct as rFab alongside positive and negative controls was initiated using the expression protocol described by Padoa *et al* (Padoa et al., 2010). Although the expression method described by that study was successful in expressing adequate yield of purified rFab KSAb1, the expression method would need to be optimised for other rFab constructs used in this thesis, or new expression methods developed to ensure optimum rFab expression.

rFab germline was to be expressed alongside positive and negative controls also expressed as rFab. Purified rFab of mAb 96/3 (Dromey et al., 2004) to pancreatic islet cell antigen IA-2 (rFab 96/3) (Dr Michael Christie, KCL, unpublished), was used as a negative control. Due to the number of constructs to be expressed, the large volumes of each expression culture and the difficulties involved with the expression of constructs (described in detail below), it was decided to express only KSAb1, (the more potent of the two TSAbs), for a positive control. For this reason KSAb2 was not expressed as rFab for studies in this thesis. The methods of rFab expression are summarised in Table 7, page 127 and described in detail in Chapter 2, pages 91-93.

Table 7: Description of rFab expression methods.

Expression method	*Brief description*
Expression method 1 (2 days)	An LB broth starter culture is inoculated in 1 L of complete MOPs medium before induction in phosphate-deficient MOPs medium.
Expression method 2 (4 days)	An LB broth starter culture is inoculated into a 100 mL starter culture of complete MOPs medium before inoculation of 1 L MOPs and induction in phosphate-deficient MOPs medium.
Expression method 3 (LB broth)	A superbroth starter culture is inoculated in 1 L LB broth before induction in phosphate-deficient MOPs medium.

3.3.2.1 Expression method 1 (2 days)

In expression method 1, a single colony was grown in MOPs medium (Neidhardt et al., 1974) before sub-culturing in phosphate-deficient medium to induce rFab expression (see Chapter 2, section 2.2.2.3) (Padoa et al., 2003; Padoa et al., 2005; Padoa et al., 2010). A sample of culture was taken both before and after induction to test for rFab presence in non-induced and induced cultures to evaluate the efficacy of the expression method on the individual constructs. Evaluations were

performed by SDS-PAGE analysis with both Coomassie blue staining and Western blotting using an anti-penta His tag antibody. The penta His-tagged H-chain has a MW of approximately 25 kDa and the L-chain has a slightly smaller MW. Thus two bands migrating close together at ~ 25 kDa are anticipated in Coomassie blue stained gels, and a single band of ~25 kDa is expected in Western blot analysis.

rFab KSAb1 was detected in the induced expression sample with two clear bands migrating at 25 kDa following Coomassie blue staining (Figure 20, panel A i), and a single band observed at the appropriate MW by Western blotting (Figure 20, panel A ii). No rFab band was observed in the non-induced sample.

For rFab germline, positive expression levels were detected in the induced sample with two closely spaced bands migrating at ~25 kDa following Coomassie blue staining (Figure 20, panel B i) and a single ~25 kDa band observed by Western blotting (Figure 20, panel B ii). There was faint rFab presence observed in the non-induced sample as well due to background or 'leaky' expression, more clearly observed by Western blotting analysis. Leaky expression of rFab through the outer bacterial cell membrane in to the culture medium may occur as a result of the bacterial strain chosen, expression and induction conditions and also the unique amino acid sequence of the individual rFab (Verma et al., 1998). This explains why the leaky expression may be seen in some rFab cultures and not others, and why leaky expression of some rFabs is higher than that seen in others.

The presence of rFab 96/3 was confirmed in induced samples as observed for rFab KSAb1 and rFab germline. Leaky rFab expression was not observed in the case of rFab 96/3 (Figure 20, panel C ii, page 130).

Although presence of rFab germline, rFab KSAb1 and rFab 96/3 was confirmed in induced samples, the rFab levels were not over-expressed compared to host cell proteins. It was thought that expression levels could be improved over what was obtained using this method of rFab expression using an extended method of expression.

Figure 20: SDS-PAGE analysis of rFab expression levels in total bacterial lysate.

rFab expression of (A) rFab KSAb1, (B) rFab germline and (C) rFab 96/3 was analysed in non-induced and induced samples under reducing conditions. Expression levels were analysed by (i) Coomassie blue staining and (ii) Western blotting using an anti-penta His tag antibody. The rFab band is highlighted by a red box and the His-tagged H-chain runs at approximately 25 kDa. MWs are in kDa and different MW markers were used for Western blotting.

3.3.2.2 Expression method 2 (4 days)

In an attempt to improve levels of expression and yields of purified rFab, two longer starter cultures, measuring the OD_{600} of the culture growing with phosphate, and a longer induction phase were evaluated (Figure 21, page 132). This method of expression was devised by Dr Kerry McLaughlin, KCL. An expression check of the induced cultures was performed prior to purification (see Chapter 2, section 2.2.2.4).

In this method of expression, a sample of expression culture was taken only after induction hence no information was available on the 'leakiness' of this expression method in non-induced cultures. The expression levels of rFab germline, rFab KSAb1 and rFab 96/3 were analysed by SDS-PAGE using Coomassie blue staining (Figure 21A) and Western blotting using an anti-penta His tagged antibody (Figure 21B). Levels of expressed rFab KSAb1, rFab germline and rFab 96/3 were greater than those achieved with expression method 1 as more intensely-staining bands are observed following Coomassie blue staining. The highest level of expression is observed for rFab 96/3 (Figure 21A). The presence of rFab was also confirmed by Western blotting with bands observed at 25 kDa in the induced samples of all three constructs (Figure 21B). This data would indicate that expression method 2 is the optimum method of expressing rFab germline, rFab KSAb1 and rFab 96/3.
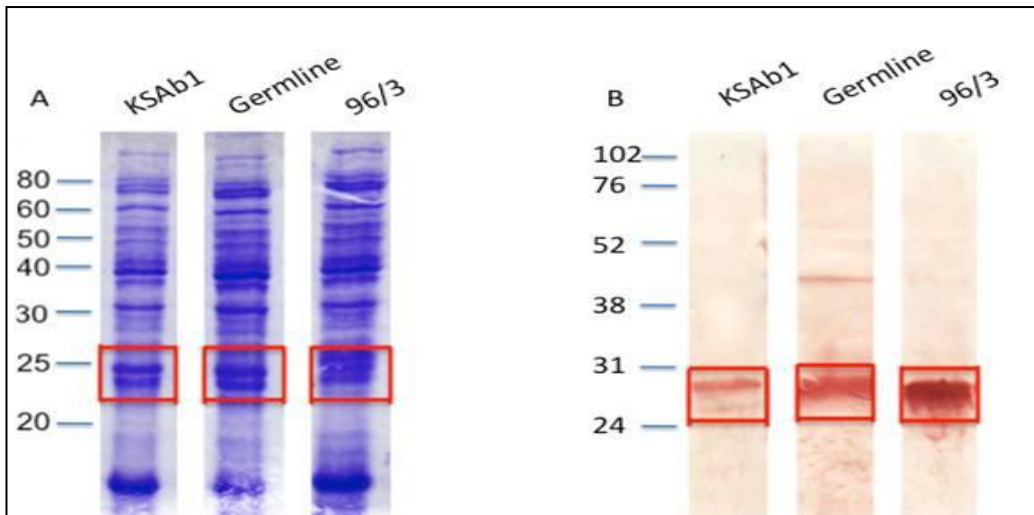
Figure 21: Expression check of rFab KSAb1, rFab germline and rFab 96/3 following expression method 2 (4 days) in total bacterial lysate.

SDS-PAGE analysis of rFab germline, rFab KSAb1 and rFab 96/3 under reducing conditions following expression method 2. The levels of rFab expression were determined in induced samples by (A) Coomassie blue staining and (B) Western blot using an anti- penta His tag antibody. The expressed rFab is highlighted by a red box at 25 kDa.

3.3.3 Purification of rFabs germline, KSAb1 and 96/3

3.3.3.1 Purification following expression method 1

The purification protocol following expression method 1 involved 1 L culture volume and 0.5 mL purification resin. This was based on the premise that a large culture volume will provide more available rFab for purification, whilst a low volume of resin should decrease the surface area for non-specific binding. This method of expression and purification resulted in an acceptable purity of eluted fractions, although 100% purity was not achieved for any rFab preparation. Purified expressed yields remained low at 100-150 µg from a litre culture for each rFab.

Figure 22: Purified rFab preparations following expression method 1 analysed by SDS-PAGE and Western blot.

The degree of purity after purification of (A) rFab KSAb1, (B) rFab germline and (C) rFab 96/3 was analysed by (i) Coomassie Blue-stained gel and (ii) Western blot using an anti-penta His tag antibody. The expressed rFab is highlighted by a red box at 25 kDa.
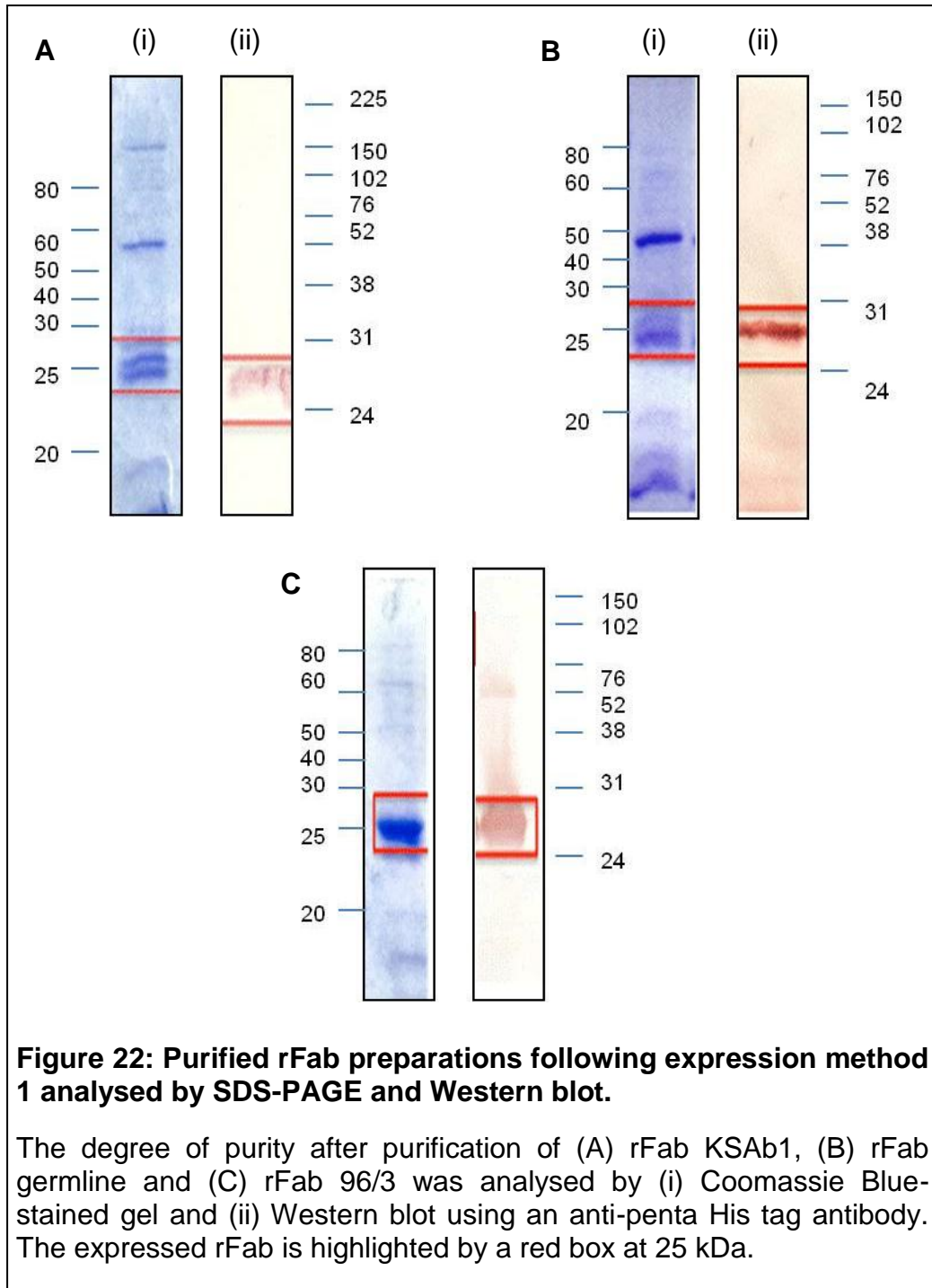
3.3.3.2 Purification following expression method 2

Expression method 2 had produced high levels of expressed rFab germline, rFab KSAb1 and rFab 96/3. Purification resulted in bands of rFab at 25 kDa as analysed by Coomassie blue staining (Figure 23A) and

Western blotting using an antibody to the penta His tag of the H-chain (Figure 23B). High levels of purified rFab 96/3 were obtained (1 mg/mL) which obscures the presence of the second band of the rFab. This combination of expression and purification methods is the optimum for expressing and purifying high amounts of rFab 96/3, despite the presence of other contaminating *E. coli* bands. For rFab germline and rFab KSAb1 there was clear expression of both constructs, although not to the same degree as rFab 96/3. There was a high amount of contaminating *E. coli* bands compared to the level of purified rFabs. Of the three constructs, rFab germline had the lowest expression levels as seen in the expression check suggesting that rFab germline may have lower expression levels overall, regardless of the expression method used
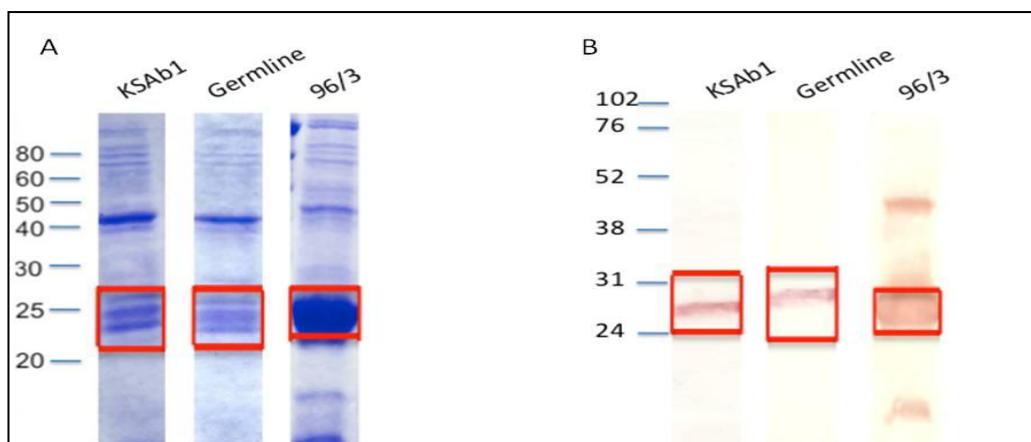
Figure 23: Analysis of purified rFab preparations following expression method 2.

SDS-PAGE analysis of purified rFab germline, rFab KSAb1 and rFab 96/3 under reducing conditions following expression method 2. The purity of rFab expression was determined after purification in by (A) Coomassie blue staining and (B) Western blot using an anti-penta His tag antibody. The expressed rFab is highlighted by a red box at 25 kDa.

The level of purified rFab KSAb1 and rFab germline following expression method 1 was comparable to that of the levels of purified rFab KSAb1

obtained following expression method 2. However there was a purer rFab preparations following expression method 1, despite the presence of some high and low MW contaminating bands (Figure 22, page 133). Therefore expression method 1 and purification was considered the optimum conditions for expressing rFab KSAb1 and rFab germline. Although the observed yield following the expression method 2 was sufficient for testing in functional assays at high concentration, it was not taken further as it took longer than expression method 1 without any improved results. Purification of rFab 96/3 following expression method 1 resulted in high purity but did not produce as high a yield of purified rFab as expression method 2 (Figure 23). Expression method 2 was chosen as the optimum expression method for rFab 96/3.

3.3.4 Evaluation of integrity of rFab 96/3 preparation

The ability of purified rFab 96/3 to bind its natural ligand, IA-2, was evaluated to ensure that this was a functional rFab capable of binding its ligand (Figure 24, page 136). The purified rFab 96/3 was prepared by me and the functional assay was performed and analysed by Dr Kerry McLaughlin, KCL. This assay was necessary to ensure that if the rFab 96/3 does not display binding to the TSHR in subsequent assays, it is because rFab 96/3 cannot recognise the TSHR, rather than it has not folded correctly and cannot recognise any antigen.

Dr McLaughlin incubated the purified mAb 96/3 (Dromey et al., 2004) with radiolabelled IA-2 intracellular region protein alone or with rFab 96/3 at varying concentrations. This was incubated with protein A Sepharose,

which can bind the mAb 96/3 Fc region and whatever is bound to the mAb 96/3 Fab region. Scintillant was added and the counts of radioactivity measured on a beta-counter in counts per million (cpm). Normal human serum, which should not contain any anti-IA-2 antibodies, was used as a negative control. When mAb 96/3 antibody was incubated with IA-2 alone, there were radioactivity counts of over 10,000 cpm. In the presence of rFab 96/3, even at a 1/100 dilution, the binding of 96/3 antibody to IA-2 was outcompeted and the radioactivity counts decrease. This assay demonstrated that rFab 96/3 is functionally active and can bind IA-2 by out-competing its IgG form.
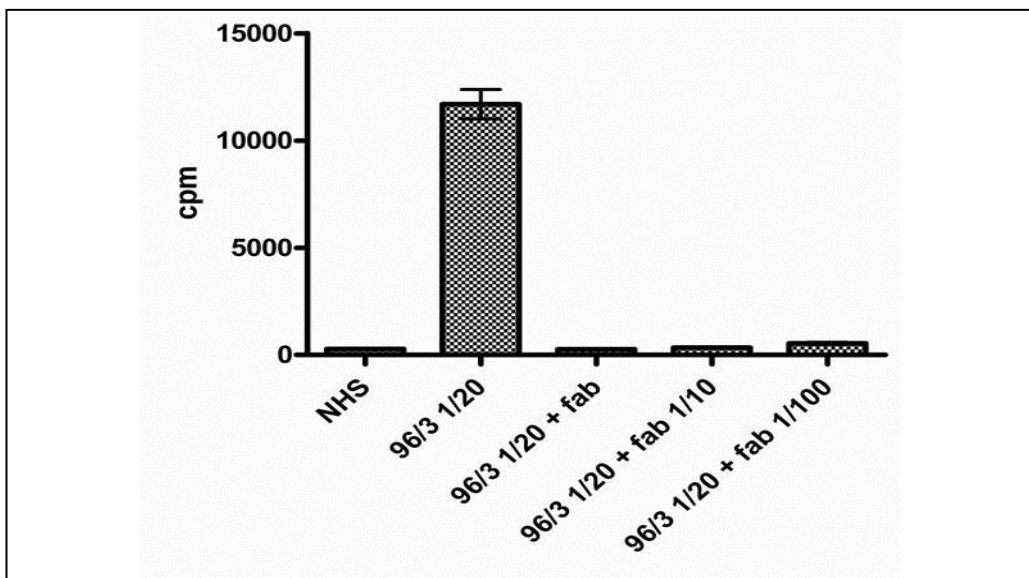
Figure 24: Evaluation of antigen-specificity of rFab 96/3.

The ability of rFab 96/3 to bind its natural ligand, IA-2 intracellular region was first tested to ensure this was a functional rFab. In the absence of rFab 96/3, mAb 96/3 IgG is capable of binding radiolabelled IA-2. This binding is decreased in the presence of varying concentrations of rFab 96/3 as it outcompetes the mAb 96/3 IgG for binding to IA-2. Dr Kerry McLaughlin, KCL, performed this assay. NHS, normal human serum.

3.3.5 Evaluation of antigen specificity of rFab germline

Three different assay systems of varying sensitivity were used to evaluate rFab germline for measurable binding to TSHR to ensure that robust conclusions could be made of its functional activity, if any.

3.3.5.1 Interference of *E. coli* proteins in radioreceptor assay

The ability of rFab germline to bind the TSHR was evaluated by radioreceptor (TRAK) assay, an *in vitro* assay that can measure the inhibition of binding of ^{125}I-TSH to detergent-solubilised TSHR by rFab preparations in a commercial kit (Ajjan and Weetman, 2008). The binding of the rFab to TSHR is measured by the percentage of ^{125}I-TSH inhibited from binding immobilised TSHR coated on tubes.

As 100% purity was not achieved in any of the purified rFab fractions, we first sought to ensure that any contaminating *E. coli* bands would not interfere with any functional assays by measuring the inhibitory capacity of rFab in crude bacterial lysates. As it was not possible to determine the exact concentration of rFab present in the induced expression culture lysates, four volumes of lysate were chosen for testing: 30 µl, 20 µl, 10 µl and 3 µl. At a volume of 30 µl, rFab KSAb1 inhibited ≥90% of radiolabelled TSH from binding TSHR. This inhibition decreased with decreasing volumes of rFab KSAb1. rFab germline did not display any ability to compete with radiolabelled TSH for binding to TSHR.

The results from this preliminary experiment suggest that the presence of *E. coli* bands from the bacterial cell lysate do not interfere with the

radioreceptor assay by preventing rFab KSAb1 from binding the TSHR, as observed by the ≥90% inhibition of radiolabelled TSH binding. Nor is there any non-specific inhibition of TSH as rFab 96/3, the irrelevant control, does not display any radiolabelled TSH inhibition. Thus it is likely that any contaminating *E. coli* bands present in the purified rFab samples do not interfere with the assay results.

This experiment was performed on three independent occasions, each time with independent rFab preparations. Figure 25 is a representative example of these experiments.

Figure 25: Measurement of inhibition of ^{125}I-TSH by rFab total bacterial lysates.

Radioreceptor (TRAK) assay measuring inhibition of ^{125}I-TSH binding to immobilised TSHR by rFab lysates. The results are expressed as % inhibition of ^{125}I-TSH binding. The cut off for the assay is 15%, shown as a dotted line and values above this are considered positive in the commercial assay. The assay was performed on single samples on three occasions, a representative experiment is shown.

3.3.5.2 Evaluation of antigen binding specificity of purified rFab

The preliminary results with rFab bacterial lysates were confirmed using purified rFab material of known concentration (Figure 26). At high concentrations, purified rFab KSAb1 displays ^{125}I-TSH inhibition comparable to that of full-length purified, KSAb1 IgG. At concentrations below 30 μg/mL KSAb1 IgG displays a slightly higher level of inhibition. At high concentration of purified rFab germline no inhibition of radiolabelled TSH is displayed, suggesting that rFab germline does not recognise TSHR. However, this radioreceptor assay is insensitive for detection of low levels of antibody binding at low levels of inhibition. Inhibition of 10-15% of ^{125}I-TSH in the radioreceptor assay kit is considered to be in the 'grey zone' and hence not amenable to accurate measurement. It is possible that rFab germline binds weakly to the TSHR but this binding is not detectible using this assay. Flow cytometry and cAMP stimulation bioassay were performed as a more sensitive means of determining measurable binding of rFab germline to TSHR.

Figure 26: Measurement of inhibition of ^{125}I-TSH by purified rFab preparations.

Radioreceptor (TRAK) assay measuring inhibition of ^{125}I-TSH binding to immobilised TSHR by purified rFab. The results are expressed as % inhibition of ^{125}I-TSH binding. The cut off for the assay is 15%, shown as a dotted line and values above this are considered positive in the commercial assay. The assay was performed on single samples and the bars represent SEM of data from three independent experiments.

3.3.5.3 Evaluation of rFab antigen specificity by flow cytometry

Flow cytometry was used as a more sensitive method of detecting measurable binding of rFab preparations to the TSHR. Flow cytometry experiments were performed using GPI9-5 cells, a cell line expressing high levels of TSHR A-subunit (500,000 receptors/cell) (Metcalfe et al., 2002). The GPI9-5 cells already in culture in the laboratory were at a high

passage number and were observed to be losing their TSHR expression (data not shown). Another primary clone of cells at low passage number was kindly donated by Dr Philip Watson (University of Sheffield, UK) which in flow cytometry experiments showed dramatic improvement in the signal of detection.

The mAb 4C1 (IgG$_{2a}$) is considered a gold-standard, anti-TSHR mAb and was thus selected as the optimum positive control. 1 µg/mL of 4C1 was chosen as per the manufacturer's instructions and titrated with the goat anti-mouse IgG secondary antibody conjugated with PE at dilutions of 1/50, 1,100 and 1/200, as recommended by the manufacturer's specifications. A dilution of 1/100 was shown to be optimal for use with IgG preparations whilst a dilution of 1/50 of secondary antibody was shown to be optimal for rFab preparations (data not shown). rFab germline and other rFab and IgG preparations was tested for measurable binding to TSHR at concentrations of 10 µg/mL and 1 µg/mL, based on radioreceptor (TRAK) assay data (Figure 26, page 140). Results are displayed as percentage of cells bound by antibody (Figure 27A), mean fluorescence intensity (MFI) (Figure 27B) and histograms (Figure 27C).

In Figure 27A, the percentage of cells bound by KSAb1 IgG is higher than that for rFab KSAb1 (Figure 27A) at the same concentration. This is not surprising as the IgG preparation is divalent and rFab preparations are monovalent hence a reduction in avidity is responsible. This response is also observed when represented as MFI (Figure 27B). There is a shift to the right of the axis away from the negative control peaks for 4C1, KSAb1 IgG and rFab KSAb1 when displayed as a histogram (Figure 27C). In

histogram figures the negative control's peak is shaded in grey and the histogram of the preparations of interest is shown as a blue line. The x-axis is a log-scale of the fluorescence intensity of the PE fluorochrome and the y-axis measures the number of events. No measurable binding of rFab germline was observed at either of the tested concentrations. There is no shift to the right of the axis or shift away from the negative control's (rFab 96/3) peak (Figure 27C), the number of cells bound by rFab germline is 0% (Figure 27A), and the MFI value is not above the MFI observed for rFab 96/3 (Figure 27B)
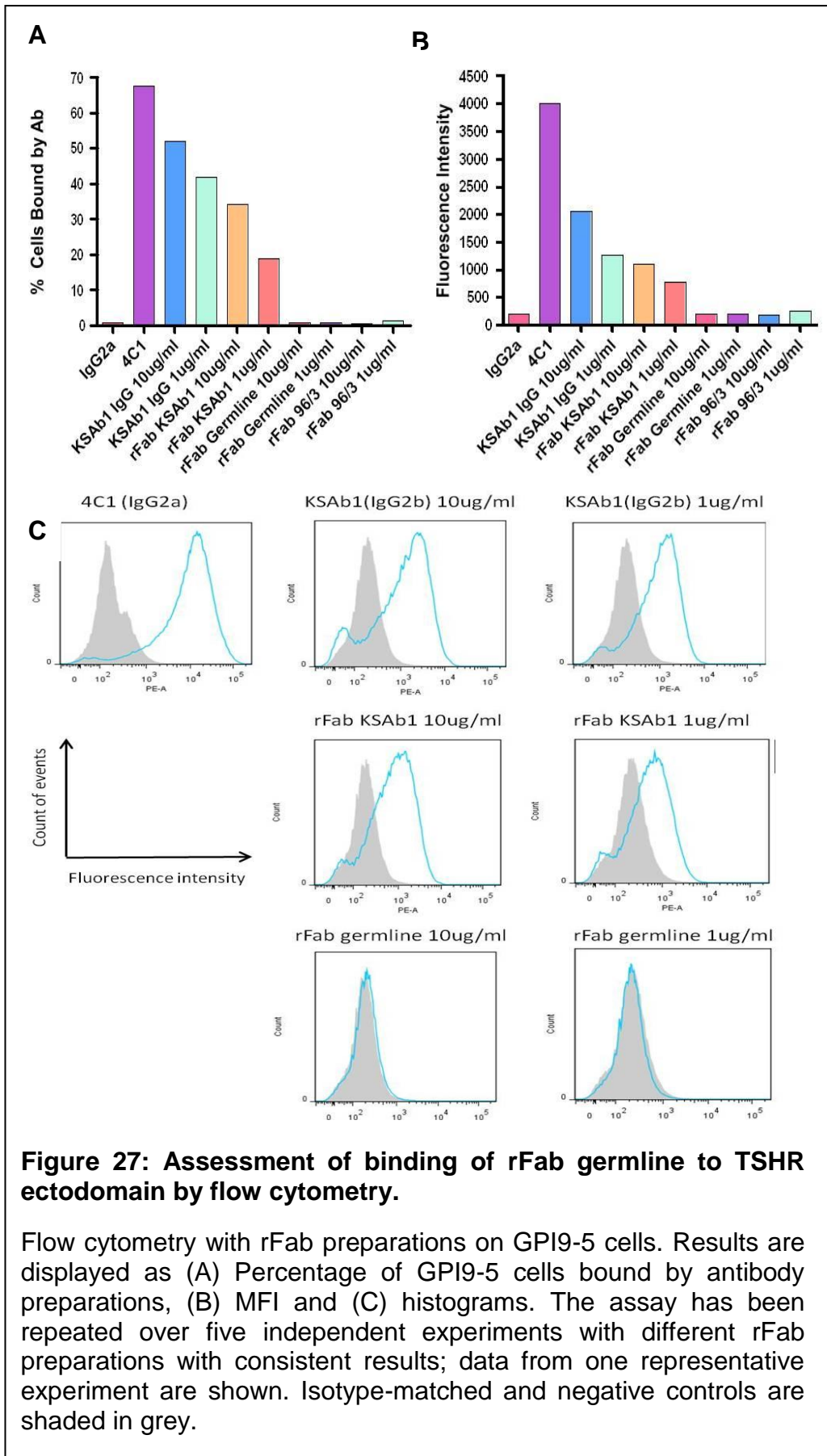
Figure 27: Assessment of binding of rFab germline to TSHR ectodomain by flow cytometry.

Flow cytometry with rFab preparations on GPI9-5 cells. Results are displayed as (A) Percentage of GPI9-5 cells bound by antibody preparations, (B) MFI and (C) histograms. The assay has been repeated over five independent experiments with different rFab preparations with consistent results; data from one representative experiment are shown. Isotype-matched and negative controls are shaded in grey.

3.3.5.4 Flow cytometric analysis of rFab germline binding to full-length TSHR expressed by JP09 cells

Following analysis of rFab germline to the TSHR A-subunit by flow cytometry, rFab germline was tested for binding to the full-length receptor using JP09 cells. JP09 cells express 90-100,000 receptors per cells (Metcalfe et al., 2002; Perret et al., 1990). Due to a shortage of cells, KSAb1 IgG was not evaluated in this assay. However following the results of Figure 27, it could be predicted that KSAb1 IgG would display a weaker binding signal than that of 4C1.

In Figure 28, rFab KSAb1, rFab germline and rFab 96/3 are evaluated for measurable binding. 4C1 displays approximately 30% binding to JP09 cells, compared to the 90% binding observed with GPI9-5 cells (Figure 27). No measurable binding to JP09 cells is observed for rFab KSAb1; this is most likely due to the level of receptor expression being too low for detection of binding. Thus it is impossible to say whether the lack of binding observed for rFab germline is due to a genuine lack of binding to TSHR, or because the receptor expression is too low to detect measurable binding. This experiment was performed on one occasion.

Figure 28: Flow cytometric analysis of rFab germline binding to full-length TSHR expressed by JP09 cells.

Flow cytometry with rFab preparations on JP09 cells. The assay has been performed on one occasion. Isotype-matched and negative controls are shaded in grey.
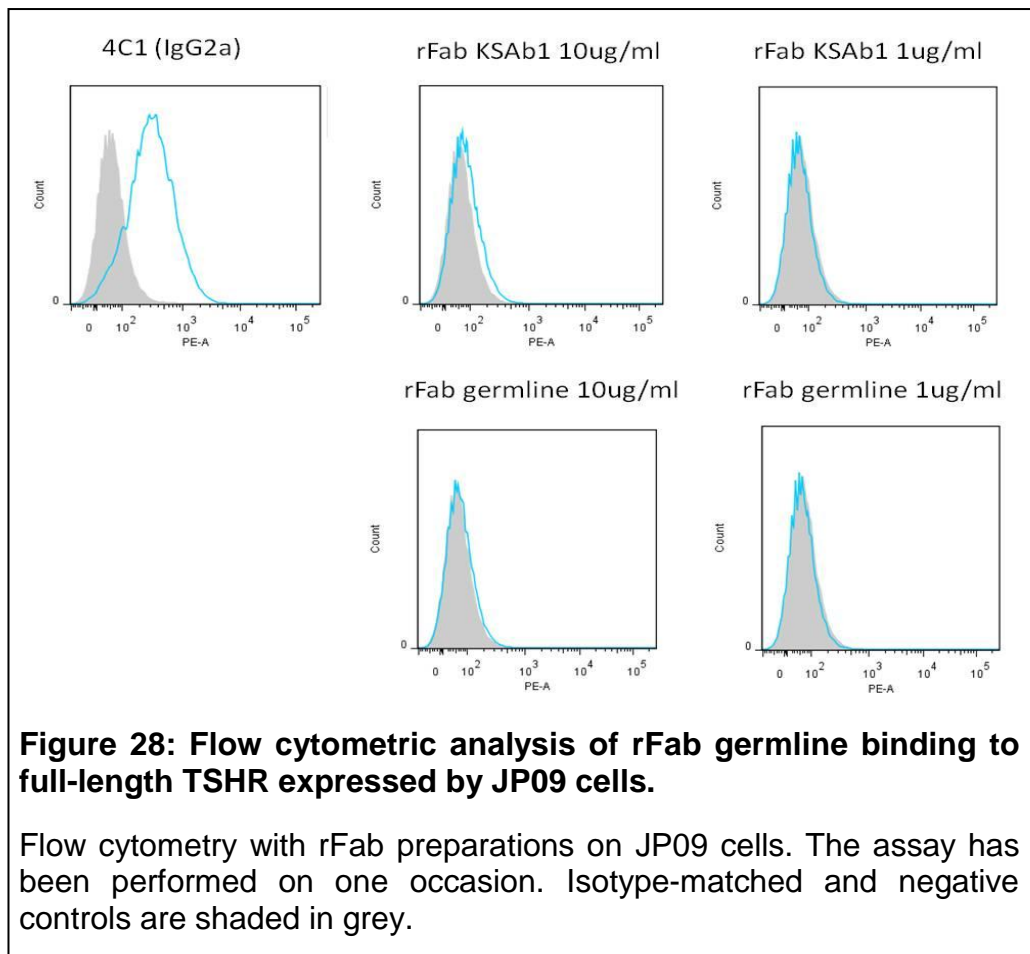
3.3.5.5 cAMP stimulation bioassay

cAMP is the second messenger of the TSHR, and its production is indicative of receptor binding and stimulation, and thus pathogenic agonist activity (Dremier et al., 2002; Kopp, 2001). The ability of rFab germline to bind and stimulate the receptor was determined by incubating the relevant controls and rFab preparations with JP09 cells (Metcalfe et al., 2002), and analysing the supernatants for presence of cAMP (Ajjan and Weetman, 2008). This is a more sensitive assay than the radioreceptor (TRAK) assay, so any weak cAMP stimulation observed as a result of rFab germline stimulation would indicate binding and

recognition of the TSHR. The assay was performed in duplicate as described previously (Gilbert et al., 2006a).

In this cAMP stimulation bioassay, positive controls included forskolin, a direct stimulator of intracellular adenyl cyclase, bTSH, a natural ligand of TSHR and KSAb1 IgG. Negative controls included IgG_{2b}, an isotype-matched control of KSAb1 IgG, and HBSS buffer. Forskolin, bTSH and 100 µg/mL KSAb1 IgG provided the maximal cAMP response for this assay of 500-600 pmol/mL, no cAMP was observed for the negative controls. At 100 µg/mL, rFab KSAb1 produced 250 pmol/mL of cAMP, approximately half that seen for KSAb1 IgG at the same concentration, as has been described before, this is to be expected for monovalent rFab fragments produced in bacteria. Although only 2 doses of KSAb1 IgG were used, there is a dose-response that confirms the findings of Gilbert *et al*, 2006a who performed a dose-response over a wider range. Padoa *et al*, 2010 performed a dose-response with rFab KSAb1 and rFab KSAb2. At high concentration, no cAMP stimulation was observed for rFab 96/3 and rFab germline, at either concentration tested, and was repeated on three independent occasions wih independently prepared rFab.

Taken together, data from the three assays, including radioreceptor assay (Figure 26), flow cytometric analysis (Figure 27) and cAMP stimulation (Figure 29), indicates that rFab germline is not capable of binding and stimulating the TSHR, providing compelling evidence that KSAb1 and KSAb2 are derived from a non-autoreactive germline antibody rearrangement.
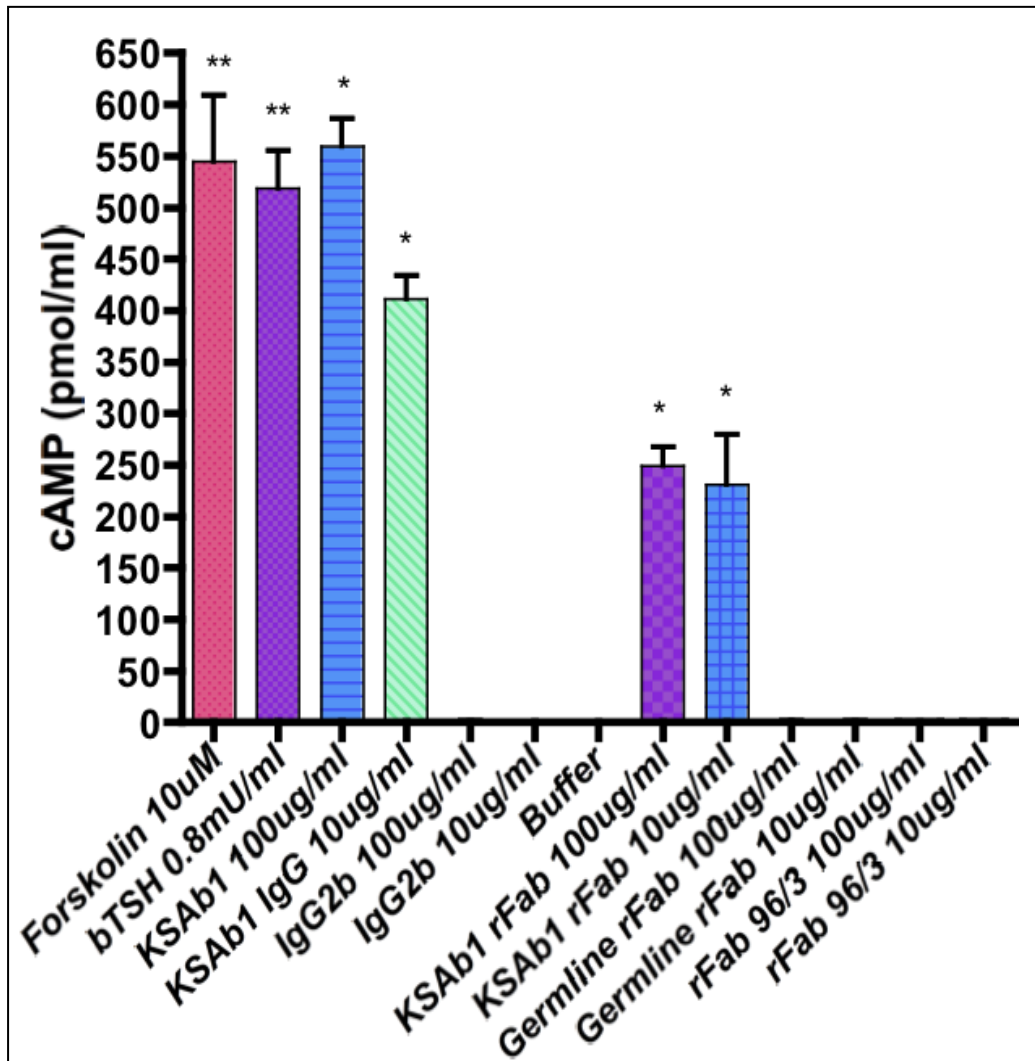
Figure 29: cAMP stimulation by purified rFab germline.

Stimulation of TSHR in bioassay by measuring induction of intracellular cAMP (pmol/mL) following incubation with purified rFab preparations. Statistical significance determined using Mann-Whitney test. The p value ranges are indicated in figures as follows: * $p > 0.05$, ** $p > 0.01$. Error bars = SEM.

3.4 Discussion

Our objective was to study the antigen binding properties of the germline precursor of KSAb1 and KSAb2, expressed as rFab to provide information on recognition of a thyroid or non-thyroid self-antigen by immature B cells, before the antibodies undergo affinity maturation.

The germline V-region genes were synthesised and cloned in a specialised vector for rFab expression in *E. coli*, named rFab germline. It was necessary to optimise the conditions of expression for each of the relevant rFab constructs due to high expression variability between. The initial method of expression already established in the laboratory (Padoa et al., 2010) produced reasonable levels of expression for rFab germline, rFab KSAb1 and rFab 96/3 (Figure 22, page 133) but a further extended method of expression was evaluated in an attempt to improve expression levels (Figure 23, page 134). This extended method of expression did produce visibly higher levels of rFab expression, particularly for rFab 96/3.

The possibility remains that rFab germline may not fold correctly during the expression step to give a functional protein, resulting in no measurable binding to the TSHR, or that there was loss of structure upon purification. However it is unlikely as the rFab expression protocols described here produced active rFab KSAb1 and rFab 96/3, on no occasion was inactive rFab produced for either of these constructs. This has been the consistent experience in my hands and in the laboratories of Dr Michael Christie (KCL) and Dr Christiane Hampe (University of

Washington, USA) Thus there is no reason to believe that the lack of measurable binding observed for rFab germline is due to inactive rFab being produced. It is unlikely that purification has had any negative effect on rFab germline's structure as bacterial lysates showed there was no binding observed by radioreceptor assay prior to purification. It is possible to analyse rFab germline for correct folding by circular dichroism (CD spectra), however, a large amount of highly pure protein is needed for such analysis which we have not been able to achieve by any of the tested expression methods. Further testing for rFab germline's binding capabilities to an infectious agent are discussed in Chapter 5.

No measurable binding was observed for rFab germline in any of the three methods tested: radioreceptor assay, flow cytometry or cAMP bioassay. There are weaknesses to the range of assays used here to detect any measurable binding of rFab germline to the TSHR. The radioreceptor assay will only display a positive result if the rFab or antibody can prevent TSH from binding its active site; similarly, cAMP is only produced if the rFab binds the TSH binding site to trigger the receptor. GPI9-5 cells, used in flow cytometric experiments, only express the TSHR A-subunit (aa 22-289) thus it is possible that the potential TSHR epitopes to which rFab germline binds have not been appropriately displayed by the three assay systems tested. However as the mice used to generate KSAb1 and KSAb2 were immunised with Ad-TSHR289 (Chazenbalk et al., 2002; Gilbert et al., 2006b) and evidence has shown that it is the A-subunit which drives the immune response towards TSHR (Mizutori et al., 2008), it is most likely that the relevant TSHR epitopes are

expressed by the GPI9-5 cells. Furthermore, the epitope(s) recognised by TSAbs are not fully exposed in the full-length TSHR but are revealed when the A-subunit is tethered to the cell-surface by a GPI-linker (Chazenbalk et al., 2002) thus GPI9-5 cells present the optimum cell line for evaluating measurable binding by flow cytometry. Nevertheless, JP09 cells, which express full-length receptor, were used to evaluate rFab germline for binding to the holoreceptor by flow cytometry. However the receptor expression of these cells, whilst optimum for cAMP bioassay, is too low for detection of rFab KSAb1 binding, therefore it is not a sensitive enough method for measuring the weak binding that may occur with rFab germline.

Another method for testing for measurable binding to TSHR would be using human and/or murine primary thyrocytes for flow cytometric analysis. Advantages of this method would be testing for binding with native receptor that would be the closest match to the *in vivo* receptor confirmation and high level of glycosylation (Rapoport et al., 1998). TSHR expression *in vivo* is low and as there is no detection of rFab KSAb1 binding with JP09 cells, there would certainly be no detection with primary cells that express even fewer numbers of receptors. Previous experience in this laboratory has found difficulty with loss of receptor expression from primary thyrocytes when exposed to tissue culture flasks and thus we decided not to pursue this as an experimental method.

This data indicates that the TSAbs, KSAb1 and KSAb2, arise from non-autoreactive germline V-region genes, which through extensive SHM develop TSAb activity. These findings are in agreement with studies in

SLE as in both mouse and human germline reversion studies, most pathogenic anti-DNA antibodies, when reverted to their germline sequences, lost all or most of their DNA reactivity (Guo et al., 2010; Mietzner et al., 2008; Tiller et al., 2007; Wellmann et al., 2005). These studies serve to strengthen the evidence that SHM is a driver of autoimmune pathogenesis and antibodies can acquire pathogenic properties in the periphery.

It is as yet unknown what defects in central and/or peripheral tolerances may allow autoreactivity to TSHR to develop to cause GD in humans. In T cell tolerance, both central and peripheral tolerance have been implicated in pathogenesis, with a SNP in intron 1 of the TSHR in Caucasian populations (Colobran et al., 2011; Płoski et al., 2010) and intron 7 in Japanese populations (Hiratani et al., 2005). These SNPs alter the level of TSHR expressed in the thymus and thus affect the presentation of TSHR to developing thymocytes by mTECs (Colobran et al., 2011). Additionally such SNPs also lead to truncated mRNA isoform variants of TSHR A-subunit to be expressed, which if immunogenic, could lead to GD (Brand and Gough, 2010). With respect to peripheral T cell tolerance, there has been conflicting evidence on the presence of either defective T_{reg} function or numbers in patients (Mao et al., 2011; Pan et al., 2009) and mice (Zhou et al., 2012) whilst depletion of T_{regs} in mice prior to immunisation with TSHR A-subunit did not affect the subsequent anti-TSHR antibody response compared to non-T_{reg} depleted mice (McLachlan et al., 2007).

Whilst the data presented here may indicate a defect in peripheral tolerance and intact central tolerance, it is unlikely that there would be a defect in central tolerance in these mice as this is a not a spontaneous form of GD and spontaneous disease would be more likely if there were abnormalities in early B cell development. Furthermore, it is unsurprising that antibodies acquired TSHR reactivity in the periphery as the mice have been immunised with high doses of a foreign antigen, hTSHR, which precipitates autoimmunity due to the high degree of sequence similarity (87%) with mTSHR (Patibandla et al., 1999). However, peripheral tolerance mechanisms such as anergy, receptor editing or deletion should have been initiated when the antibodies to the hTSHR began cross-reacting with mouse mTSHR to cause GD.

3.5   Conclusions

In conclusion, the germline V-region genes of two highly potent TSAbs have been synthesised in a gene cassette for expression as rFab, and termed rFab germline. Measurable binding to the TSHR was determined using three gold-standard assays: radioreceptor, flow cytometry and cAMP stimulation. No measurable binding to TSHR was observed for rFab germline. This demonstrates that the two TSAbs, KSAb1 and KSAb2, are derived from a non-autoreactive precursor antibody, and pathogenicity developed in the periphery through SHM. Subsequent chapters in this thesis will investigate further the role of SHM in the H- and L-chains of KSAb1 to TSHR recognition, and whether an infectious agent played a role in the expansion of an autoreactive B cell clone.

CHAPTER FOUR

ASSESSING THE CONTRIBUTION OF HEAVY AND LIGHT CHAINS OF THYROID STIMULATING ANTIBODIES TO TSHR RECOGNITION

4 CHAPTER FOUR: Assessing the contribution of heavy and light chains of thyroid stimulating antibodies to TSHR binding and stimulation

4.1 Introduction

A role for the IGHV genes in the development of TSAbs in inbred mice has been reported in recent genetic analysis studies (McLachlan et al., 2011a; Rapoport et al., 2010). Studies in SLE have further delineated the individual roles of the H- and L-chains in determining their binding to DNA antigens, dividing their contributions as the H-chain being the dominant chain in determining binding to various forms of DNA, whilst the L-chain is important, not for binding, but for additional specificities (Ibrahim et al., 1995; Radic et al., 1991). However the presence of SHM in the L-chain, particularly replacement mutations, would suggest that there is antigen-driven mutation of the L-chain which must be affecting antigen-binding, and is thus not a redundant partner to the H-chain. The larger number of SHM in the IGHV genes of KSAb1 and KSAb2 compared to the L-chain indicates that the IGHV may play a critical role in the strong TSAb function of the antibodies.

This chapter describes various chimeric constructs and their expression as rFab molecules to study the individual contribution of the mature H- and L-chains of KSAb1 to TSHR binding.

4.2 Aims

Following the results of Chapter 3 demonstrating that two TSAbs developed from a non-autoreactive germline precursor, and the published literature in other autoimmune diseases demonstrating a dominant role for the H-chain in autoantibody activity, the aims of this chapter were as follows:

i. To evaluate chimeric constructs expressed as rFab to characterise the individual effects of the H- and L-chain of KSAb1, on binding to TSHR, by radioreceptor assay, flow cytometry and cAMP bioassay.

ii. To further assess the dominance of the role of the mature H-chain in TSHR recognition, by pairing the mature KSAb1 H-chain with the L-chain of another antibody, Ti-401, which recognises a bacterial antigen.

4.3   Results

4.3.1   Cloning L-chain chimeric constructs in pAK19

Two L-chain swap constructs were constructed by excising the L-chains from each of the KSAb1 and germline constructs by restriction enzyme digest (Figure 30). The excised L-chain from one construct was ligated upstream of the H-chain in the other construct (summarised in Table 8). In this manner, the mutated mature L-chain of KSAb1 was paired with the non-mutated H-chain of the germline construct to form the swap construct L-mature, and the non-mutated L-chain of the germline construct was paired with the mutated mature H-chain of KSAb1 to form the swap construct H-mature. Analysis by restriction digestion showed the L-chains migrate at ~0.7 kB and the plasmids containing the H-chain at ~7 kB. Both constructs were cloned in pAK19 for expression as rFabs.

Table 8: Summary of L-chain swap constructs.

Construct	H-chain	L-chain
H-mature	Mature (KSAb1)	Germline
L-mature	Germline	Mature (KSAb1)

Figure 30: Cloning of swap constructs in pAK19.

The H- and L-chain genes of the KSAb1 and germline constructs were digested and analysed on a 1.2% agarose gel such that their L-chains could be isolated and chimeric constructs made. M denotes the MW ladder in kB. The pAK19 plasmid containing the H-chain migrates at 7 kB and the L-chain migrates at 0.7 kB. The plasmid constructs were isolated from competent cells expressing a second plasmid, pRARE, observed running at 5 kB below the pAK19 band.

4.3.2 Expression of swap constructs as rFabs using MOPs protocol

The two swap constructs were cloned in pAK19 for expression as rFabs. The first protocol attempted for this expression was expression method 1 (described in Chapter 2, section 2.2.2.3, page 91). SDS-PAGE analysis of expression was first performed to verify presence of rFab in the bacterial culture. In Figure 31A, the rFab L-mature SDS-PAGE analysis of expression shows two bands are clearly visible in the induced lane migrating at ~25 kDa when stained with Coomassie blue and with an anti-penta His tag antibody for Western blotting. The higher MW band is the H-chain and the smaller MW band is the L-chain. The rFab expression with this construct was 'leaky' since in the non-induced lane there is a faint H-chain band observed by Coomassie blue staining (Figure 31A, panel i) and Western blotting (Figure 31A, panel ii). The L-chain is the

strongest band of the two as the pAK19 plasmid over-expresses the L-chain to a higher degree than the H-chain. There is stronger rFab expression in the induced sample.

However, SDS-PAGE analysis of expression for rFab H-mature (Figure 31B, panel i) shows only one band when stained with Coomassie blue, the smaller MW L-chain, suggesting little to no expression of the H-chain peptide. This lack of expression was confirmed by Western blotting with no bands observed (Figure 31B, panel ii). The pellet size of rFab H-mature cultures before and after induction were also much smaller than that of other rFab cultures, suggesting that the low expression levels of rFab H-mature may be due to a lack of competent cell growth, rather than a failure of the induction step. One possible reason may be the rFab H-mature may be toxic to the competent cells grown in MOPS medium, preventing their replication and the amount of cells available to secrete rFab.

Figure 31: SDS-PAGE and Western blot analysis of expression of rFab L-mature and rFab H-mature using MOPs protocol.

SDS-PAGE analysis of rFab expression levels prior to purification. (A) rFab L-mature expression analysed by (i) Coomassie blue staining and (ii) Western blot using an anti-His tag antibody and (B) rFab H-mature expression analysed by (i) Coomassie blue staining and (ii) Western blot using an anti-His tag antibody. MWs are in kDa. rFab is observed at approximately 25 kDa, a red box highlights the rFab bands.

Whilst another expression method was needed for optimal expression of rFab H-mature, expression method 1 was seen as optimal for rFab L-mature expression and this culture was used for purification (Figure 32). From 1 L expression culture, 1 mg/mL of rFab L-mature was obtained. It appears that the higher the level of rFab expressed in the preparation, the higher the purity of the eluted fractions. This may be because there is more rFab present to out-compete any non-specific binding from any potentially contaminating *E. coli* proteins.

Figure 32: SDS-PAGE and Western blot analysis of Purified rFab L-mature.

SDS-PAGE analysis of purified rFab L-mature measured by (i) Coomassie blue staining and (ii) Western blotting using an anti-His tag antibody. High yields of purified material were obtained using the MOPs expression protocol (>1mg/mL culture). The rFab band is observed at approximately 25 kDa and is highlighted by a red band.

4.3.3 Expression of swap constructs as rFabs using expression method 3 (LB broth)

Dr Christiane Hampe (University of Washington, Seattle, USA) suggested an alternative method (expression method 3, Chapter 2, section 2.2.2.5, page 93) to improve the levels of rFab H-mature expression. A single colony was grown in the modified nutrient-rich superbroth medium during the day and overnight in LB broth before inducing in phosphate-deficient MOPs medium.

Compared to the previous expression protocol, the pellets of H-mature culture before and after induction were much larger, suggesting the competent cells were proliferating without inhibition, or with less inhibition. The expression of rFab H-mature under this expression protocol was verified before purification (Figure 33).

Figure 33: SDS-PAGE and Western blot analysis of rFab H-mature expression level before purification following expression method 3 (LB broth).

SDS-PAGE analysis of expression levels of rFab H-mature measured by (i) Coomassie blue staining and (ii) Western blotting using an anti-His tag antibody. The rFab band is observed at approximately 25 kDa and is highlighted by a red band.

This SDS-PAGE (Figure 34, panel i) and Western blot (Figure 34, panel ii) analysis shows expression method 3 to be the optimum expression protocol for rFab H-mature as there are visible bands of approximately 25 kDa in the induced samples. There are no visible rFab bands in the Western blot analysis of non-induced samples showing that there is no leaky expression before induction, like that seen in rFab L-mature (Figure 32). The rFab H-mature culture was purified and 100 µg/mL was obtained from a 1 L culture. The purified material was thus of a lower yield than that obtained for rFab L-mature, but comparable to those of rFab KSAb1 and rFab germline. The purified preparation was also of high purity, demonstrating that expression method 3 is the optimum method of expressing rFab H-mature (Figure 34).

Figure 34: SDS-PAGE and Western blotting analysis of purified rFab H-mature following expression method 3 (LB broth).

SDS-PAGE analysis of purified rFab H-mature by (i) Coomassie blue staining and (ii) Western blotting using an anti-His tag antibody. Purification yield was improved using the LB expression protocol, over the MOPs expression protocol. The rFab is observed at approximately 25 kDa and is highlighted

4.3.4 Measurement of inhibition of radiolabelled TSH by chimeric constructs expressed as rFab

rFab L-mature and rFab H-mature cultures were purified and a dose-response of known concentrations of purified materials was evaluated for their ability to inhibit radiolabelled TSH binding to TSHR. As before (Chapter 3, Figure 26, page 140) KSAb1 IgG and rFab KSAb1 inhibited >90% of radiolabelled TSH which decreased with lower concentrations, and no inhibition was observed for the negative control, rFab 96/3. rFab L-mature did not display any measurable binding at any of the concentrations tested, whilst high concentration (100 µg/mL) of rFab H-mature inhibited approximately 35% of radiolabelled TSH from binding TSHR. This degree of inhibition was only apparent at high concentrations since lower concentrations did not show any measurable inhibition (Figure 35).
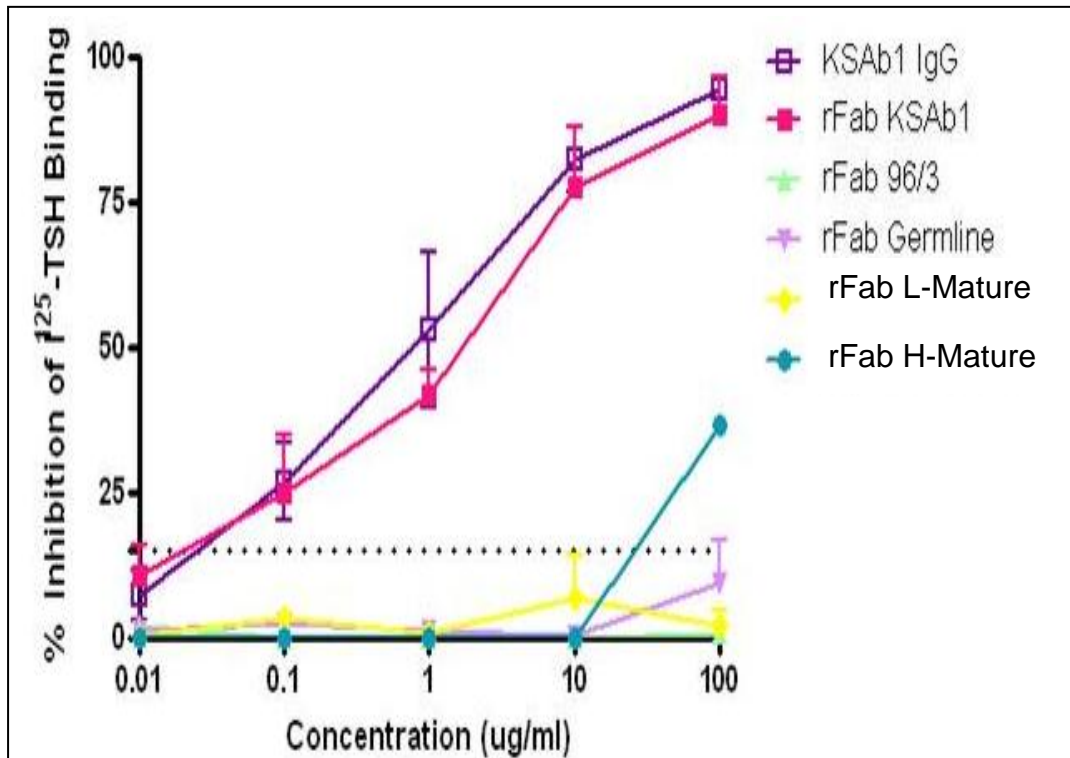
Figure 35: Measurement of inhibition of ^{125}I-TSH by purified rFab preparations.

Radioreceptor (TRAK) assay measuring inhibition of ^{125}I-TSH binding to immobilised TSHR by purified rFab preparations. The results are expressed as % inhibition of ^{125}I-TSH binding. The 'grey zone' of the assay is 10-15%, shown as a dotted line and values above this are considered positive in the commercial assay. The assay was performed on single samples and the bars represent SEM of data from three independent experiments, except purified rFab H-mature which was tested once.

4.3.5 Characterisation of the role of the H-chain by pairing with an irrelevant L-chain

To further characterise the role of the H-chain in TSHR binding, a third chimeric construct was generated by using an L-chain from a non-TSHR specific antibody. rFab L-irrelevant is formed of the mature H-chain of KSAb1 paired with the mature L-chain of rFab Ti-401 (gift from Dr Hampe, Seattle, USA). rFab Ti-401 is a murine antibody that recognises

163

a bacterial antigen, *Chlamydophila pneumoniae.* The L-irrelevant cDNA construct was cloned in pAK19 vector for expression as rFab (Figure 36).

Figure 36: Digestion of Ti-401 for L-irrelevant cloning.

Constructs of Ti-401 and KSAb1 were digested with *Eco*RI/*Bsr*GI for excision of digested L-chains for ligation as the L-irrelevant construct. Digested gene products were analysed by 1.2% agarose gel electrophoresis; the pAK19 plasmid containing the H-chain migrates at 7 kB and the L-chain migrates at 0.7 kB
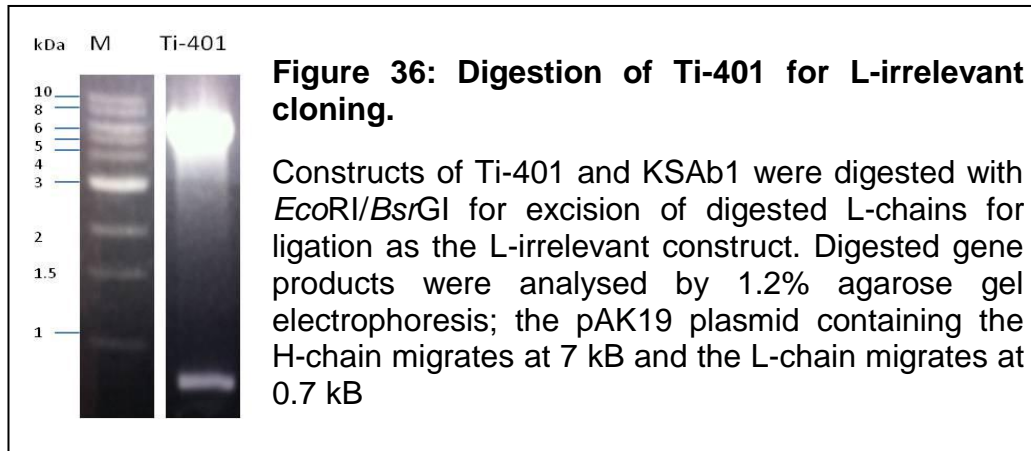
rFab L-irrelevant was expressed using expression method 3 and purified to homogeneity by metal chelation. Purified rFab material was analysed by SDS-PAGE and the presence of rFab was confirmed by Western blotting (Figure 37, page 164). A relatively low concentration of rFab L-irrelevant was obtained, and there are some high and low MW contaminating bands.

Figure 37: SDS-PAGE and Western blot analysis of purified rFab L-irrelevant.

SDS-PAGE analysis of purified L-irrelevant construct by (i) Coomassie blue staining and (ii) Western blot using an anti-His tag antibody. The rFab is observed migrating at 25 kDa and is highlighted by a red box.
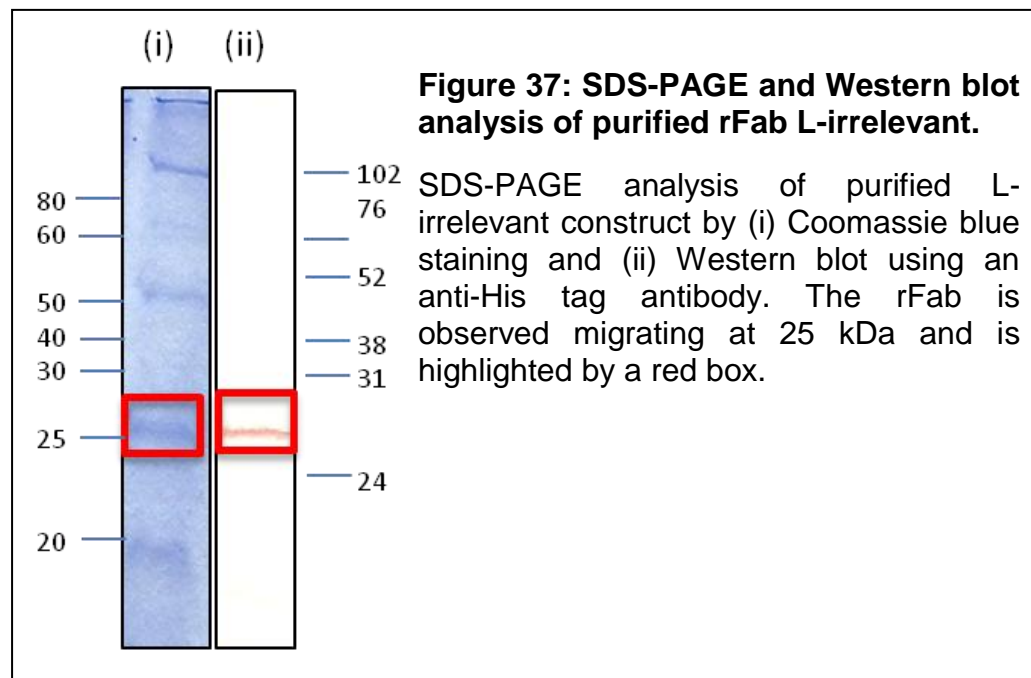
4.3.6 Measurement of inhibition of radiolabelled TSH by purified chimeric constructs expressed as rFab

Purified rFab L-irrelevant, alongside purified rFab L-mature and rFab H-mature were evaluated in radioreceptor assay for their ability to inhibit radiolabelled TSH from binding TSHR (Figure 38, page 166). Furthermore, rFab preparations were tested on a semi-log scale following the sharp decline in inhibition observed for rFab H-mature after 100 µg/mL (Figure 35, page 163). rFab H-mature displays inhibition only at high concentration of 100 µg/mL, with 30 µg/mL displaying inhibition slightly below the cut-off for positive inhibition. The radioreceptor assay was repeated three times with independently expressed rFab preparations each time, except rFab L-irrelevant was tested on one occasion.
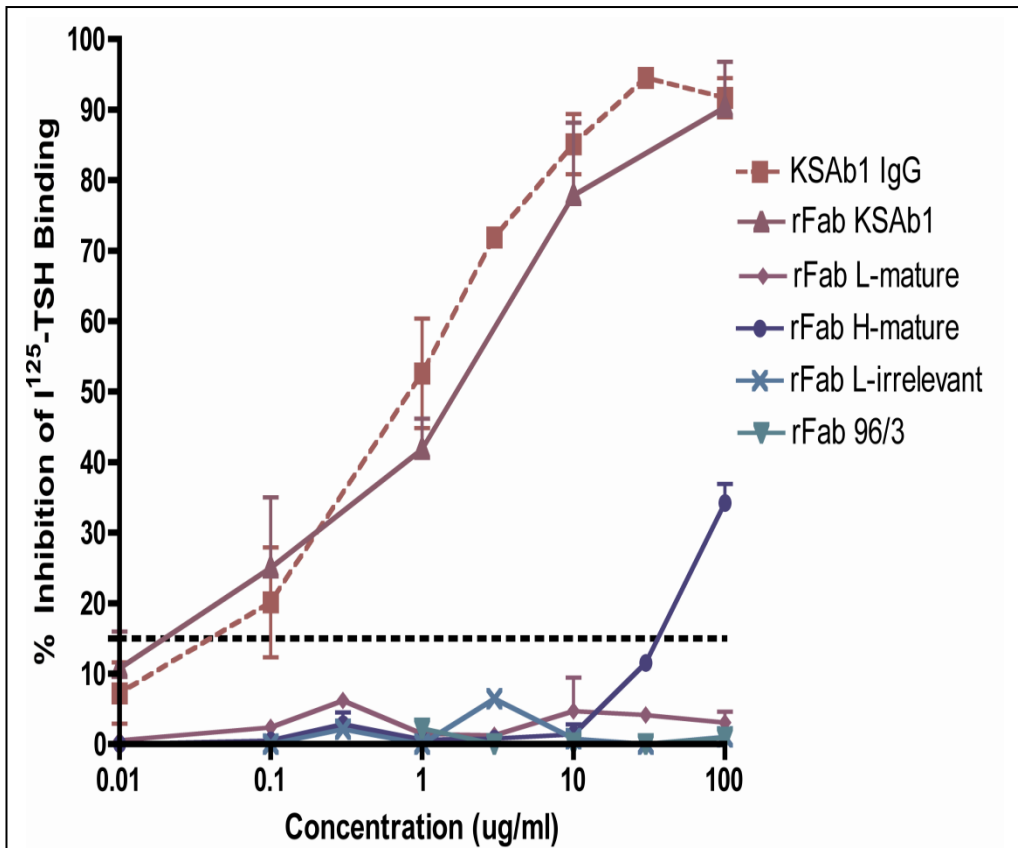
Figure 38: Measurement of inhibition of radiolabelled TSH by purified rFab preparations.

Radioreceptor (TRAK) assay measuring inhibition of ^{125}I-TSH binding to immobilised TSHR by purified rFab preparations. The results are expressed as % inhibition of ^{125}I-TSH binding. The 'grey zone' of the assay is 10-15%, shown as a dotted line and values above this are considered positive in the commercial assay. The assay was performed on single samples and the bars represent SEM of data from three independent experiments, except purified rFab L-Irrelevant which was tested once.

4.3.7 Flow cytometric analysis

Purified chimeric constructs were further tested for measurable binding to TSHR by flow cytometry. The gold standard anti-TSHR mAb, 4C1, was used as positive control, and concentrations of 10 µg/mL and 1 µg/mL were used for all other mAbs and rFab preparations, as in Chapter 3, Figure 27, page 145. Isotype-matched controls were used as negative

controls for anti-TSHR antibodies and rFab 96/3 served as a negative rFab control. Results were expressed as the number of cells bound by the test mAb or rFab (Figure 39A, page 169), by MFI (Figure 39B) and histograms (Figure 39C). In Figure 39C, there are a slightly higher proportion of cells not bound by antibody in panels for positive controls such as 4C1 and KSAb1 IgG, seen as small peaks in the bottom left corner of the panel. Almost 70% of cells were bound by 1 µg/mL 4C1 and 50% of cells bound by 10 µg/mL of KSAb1 IgG. It has been observed in this laboratory that the longer the GPI9-5 cells are kept growing in culture, i.e. the higher the number of cell passages, the lower the percentage of cells bound by 4C1 when analysed by flow cytometry.

Dose-dependent decreases in the percentage of cells bound by antibody and in the MFI were observed for positive controls KSAb1 IgG and rFab KSAb1. No measurable binding was observed with any of the negative controls. The lack of measurable binding observed for rFab L-mature in the radioreceptor assay (Figure 38, page 166) was repeated by flow cytometry, as no cells were bound and there was negligible MFI observed. No measurable binding was also observed for rFab L-irrelevant. Interestingly, no measurable binding was observed for rFab H-mature. It could be that the high concentration of 100 µg/mL is necessary for measurable binding when analysing by flow cytometry, as was the case for the radioreceptor assay. It is unlikely that binding observed in the radioreceptor assay is an artefact as it was repeated on three separate occasions, with an independently prepared rFab sample on each occasion with consistent results. There is precedence for various anti-

TSHR antibodies showing differing binding to TSHR in flow cytometry as observed with 4C1 and KSAb1. However, as rFab H-mature is capable of displacing ^{125}I-TSH, this would indicate its epitopes are located within the TSH binding region of the TSHR, which is expressed by GPI9-5 cells.

The flow cytometry was repeated three times with independently expressed rFab preparations each time, except rFab L-irrelevant was tested twice. The data shown is a representative experiment.
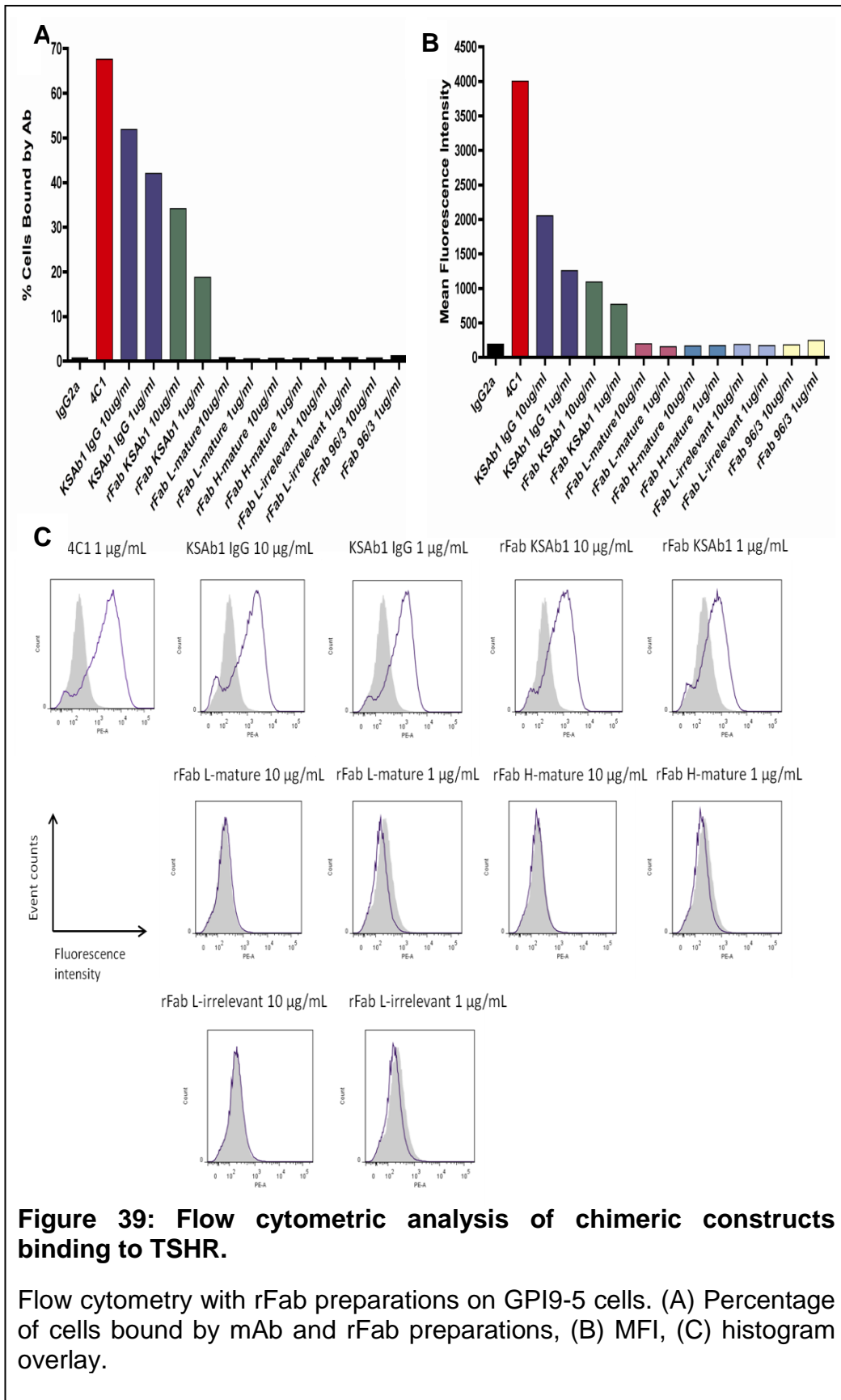
Figure 39: Flow cytometric analysis of chimeric constructs binding to TSHR.

Flow cytometry with rFab preparations on GPI9-5 cells. (A) Percentage of cells bound by mAb and rFab preparations, (B) MFI, (C) histogram overlay.

4.3.8 Stimulation of cAMP by purified rFab chimeric construct preparations

Following the positive response in radioreceptor assay, but negative response in flow cytometry, it was necessary to confirm this result with cAMP stimulation of the receptor would signify binding (Ajjan and Weetman, 2008). However, it is possible that rFab H-mature may be capable of binding TSHR but not of stimulating, in that case another method of confirming binding would be needed.

As before, forskolin, bTSH and KSAb1 IgG are positive controls and provide guidance on the maximal cAMP response possible for the assay; buffer and IgG_{2b} are negative controls. rFab KSAb1 stimulated 250-300 pmol/mL cAMP, approximately half that observed for KSAb1 IgG. rFab L-mature did not stimulate any cAMP production, consistent with the findings in the other two assays that rFab L-mature does not display any measurable binding of the TSHR. rFab H-mature, however, did produce statistically significant cAMP responses of 25-80 pmol/mL at both 100 and 10 µg/mL, with a higher response at 10 µg/mL (Figure 40, page 171). This data confirms the binding observed in the radioreceptor assay, and suggests that flow cytometry is not an optimum assay for assessing rFab H-mature's functional activity. This data demonstrates the superiority of the cAMP bioassay over the radioreceptor assay and flow cytometry in detecting weak but measurable binding to TSHR. However, it can only detect this measurable binding if the antibodies possess agonist activity. It is possible that rFab L-mature and rFab L-irrelevant display weak

binding that radioreceptor and flow cytometry are too insensitive to detect, but do not stimulate cAMP production, similar to the results for rFab germline.

The cAMP assay was performed in duplicate as described previously (Gilbert et al., 2006a), and repeated on three separate occasions with independently expressed rFab preparations, except rFab L-irrelevant which was tested once.
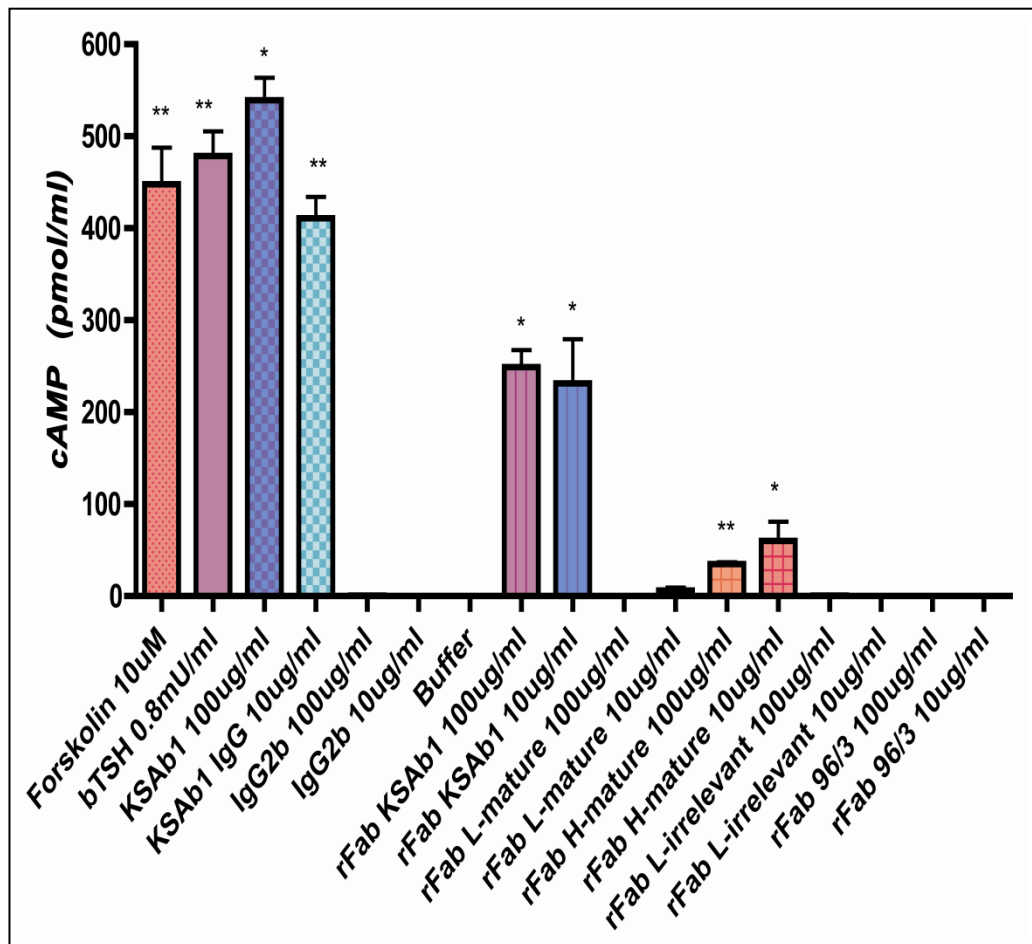
Figure 40: cAMP stimulation by purified rFab preparations.

Stimulation of TSHR in bioassay by measuring induction of intracellular cAMP (pmol/ml) following incubation of JP09 cells with purified rFab preparations. Statistical significance determined using Mann-Whitney test. The p value ranges are indicated in figures as follows: * p>0.05, ** p>0.01. Error bars = SEM.

4.4 Discussion

The role of SHM in autoimmunity has previously been established in SLE by reverting antibodies to the germline sequence and their resulting loss of autoreactivity. Chapter 3 of this thesis has directly implicated SHM in GD and the development of TSAbs from a non-autoreactive precursor.

This chapter sought to distinguish whether the mature H- and L-chains of KSAb1 play a dominant or contributory role in TSHR recognition. Due to the time constraints of this thesis and the number of potential mutations to choose from, 29 in the KSAb1 H-chain and 8 in the L-chain, we decided to investigate the total contribution of SHM in each chain to binding the TSHR rather than selecting individual mutations for evaluation. Three constructs were created (i) rFab L-mature, (ii) rFab H-mature and finally, following the data of rFab H-mature, we created a third construct (iii) rFab L-irrelevant (Chapter 2, Table 4, page 90). These constructs were cloned and expressed as rFab and tested for binding to TSHR in the three assays described in Chapter 3: radioreceptor assay, flow cytometry and cAMP bioassay.

Our results demonstrate a dominant role for the mature H-chain in TSHR binding. This is the first time this has been shown for TSAbs at a molecular level. Recent genetic studies using linkage analysis in inbred mice strains have highlighted the importance of the IGHV in the development of TSAbs (McLachlan et al., 2011a; Rapoport et al., 2010). Furthermore, our data with rFab H-mature and rFab L-mature supports observations in studies of SLE anti-DNA antibodies. When pairing the

3H9 H-chain with the majority of random L-chains, DNA binding was unaffected; however certain L-chains blocked DNA binding altogether. 3H9 was paired with mature L-chains rather than the germline revertant of its original L-chain, and the mature L-chains were derived from other anti-DNA antibodies (Ibrahim et al., 1995). Thus it is of interest to pair the KSAb1 H-chain with both the mature L-chain from another TSAb that uses different germline genes. Pairing the H-chain of KSAb1 with the mature L-chain of KSAb2 resulted in altered activity compared to the parent antibodies (Padoa et al., 2010). Additionally, it may be of interest to pair the KSAb1 H-chain with the germline revertant of another non anti-TSHR irrelevant L-chain. The germline revertant IGLV genes of Ti-401 were not available for our studies. This may help ascertain whether KSAb1 H-chain may be paired with any combination of germline L-chain genes and still maintain binding to TSHR as rFab L-irrelevant is the pairing of two chains which have both undergone affinity maturation for two separate antigens. Whilst rFab H-mature was able to overcome the lack of binding conferred by the germline L-chain, it could not overcome the lack of TSHR binding, and affinity for another antigen, conferred by Ti-401's L-chain.

Interestingly, in studies of anti-idiotypic antibodies for autoantibodies isolated from Pemphigus Vulgaris patients, it was demonstrated that when rabbits were immunised with scFv forms of pathogenic mAbs to generate anti-idiotypic antibodies, the H-chain was the key antigenic target. When the L-chains of the various scFv were swapped, the sera could still bind to the scFv provided that the H-chain remained the same

as that of the immunising scFv (Payne et al., 2007). It would thus be off interest to further delineate the mutation(s) of interest in the H- change that are most involved with TSHR binding, as well as investigating the feasibility of generating anti-idiotypic antibodies to KSAb1 and KSAb2. If anti-idiotypic antibodies are generated, it could be of biologic relevance if the H-chain was the key antigenic target as this would reinforce the data described here highlighting the dominant role of the H-chain and present a potential therapeutic option.

4.5 Conclusions

In conclusion, this data demonstrates for the first time to our knowledge, the dominant role at a molecular level of the H-chain in determining binding to TSHR. Although the L-chain does not have a dominant role in TSHR binding, it is critical for antigen binding as replacement with an irrelevant L-chain leads to loss of all binding. Further work may centre on investigating the individual SHMs in the H-chain that are most important for conferring TSHR binding.

CHAPTER FIVE

DETERMINING BINDING OF THYROID STIMULATING ANTIBODIES AND ʀFAB GERMLINE TO *Y. ENTEROCOLITICA* ANTIGENS

5 CHAPTER FIVE: Evaluating binding of thyroid stimulating antibodies and rFab germline to *Y. enterocolitica* antigens

5.1 Introduction

5.1.1 Role of infectious agents in autoimmune disease

Microorganisms including bacteria and viruses may trigger autoimmunity in genetically susceptible individuals or accelerate disease progression. As has been previously discussed in section 1.7.4 (page 59) on genetics and GD, the concordance rate of disease amongst monozygotic twins is not 100% (Brix et al., 1998a) implicating a role for environmental factors. In the case of autoimmune disease where there the concordance rate amongst twins is not 100%, the scenario may be that the affected siblings contracted an infection that increased susceptibility to disease or the non-affected siblings may be protected from disease by microbial agents (Chervonsky, 2010). Infectious agents may have a role to play in autoimmune disease, either in disease susceptibility or protection; however there is little conclusive evidence for the exact mechanism of action of the reported infectious agents and no pathogens have been compellingly isolated from an autoimmune-affected organ (Ruiz-Riol et al., 2011). The infectious agent may have been eliminated long before the disease's clinical phenotype becomes apparent making it difficult to associate a particular infection with disease susceptibility (Albert and Inman, 1999).

5.1.2 Yersinia enterocolitica

Y. enterocolitica is an infectious agent which has been implicated as a susceptibility factor for GD. *Y.* enterocolitica is a gram-negative enterobacterium that uses a Type III secretion system (Cornelis, 2002; Wren, 2003). There are six biotypes of *Y. enterocolitica*: 1A, 1B, 2, 3, 4, and 5 which include numerous serotypes that are defined by their expression of a specific O-antigen (lipopolysaccharide). The prevalence of certain serotypes varies geographically. Serotypes O:3 and O:9 are more prevalent in Europe, O:3 in Japan and O:8 in North America. The main symptom of *Y. enterocolitica* infection in humans is diarrhoea but can lead to appendicitis and acute mesenteric lymphadenitis and it is thought to be a food- or water-borne pathogen (Fredriksson-Ahomaa et al., 2006). It has also been implicated in reactive arthritis in HLA-B27-positive individuals (Schiellerup et al., 2008).

Biotypes 1B and 2-5 are considered pathogenic whilst biotype 1A is considered non-pathogenic (Huovinen, 2010). The virulence of the *Y. enterocolitica* biotypes is dependent on the expression of the pYVe virulence plasmid. pYVe encodes the type III secretion system which the bacterium uses to transport its effector proteins, Yersinia outer proteins (Yops), into the target cell (Viboud and Bliska, 2005), Figure 41, page 179.

Outer membrane porin proteins

As a gram negative bacterium, *Y. enterocolitica* has an outer and an inner membrane (Figure 41). Outer membrane proteins and porins (Omps) may

be divided into non-specific (or classical) porins, for example of OmpC and OmpF, and specific porins, for example, OmpA. The two groups of porins differ in terms of their structure and function (Nikaido, 2003). Omps are located in the outer membrane of *Y. enterocolitica* and are thus exposed to the immune system (Białas et al., 2012).

OmpA functions as a membrane stabiliser by interacting through its C-terminus with peptidoglycan (Nikaido, 2003). It is thought that OmpA is formed of two-domains, although its exact confirmation remains controversial. At the N-terminus 8 β-sheets create a small pore in the outer membrane whilst the C-terminus is located in the periplasm where it interacts with the peptidoglycan layer (Reusch, 2012). The crystal structure of its N-terminal domain has been resolved (Pascal et al., 2010) (Figure 41B). OmpC and OmpF are trimeric proteins with each monomeric subunit formed of 16-stranded anti-parallel β-sheets (Figure 41C). They function to allow the passage of small nutrients across the outer membrane, with some preference over cations over anions and OmpF preferentially transporting slightly larger molecules than OmpC does (Nikaido, 2003).

Figure 41: *Y. enterocolitica*: **Type III secretion system and inner and outer membranes.**

(A) The bacterial cell surface of *Y.* enterocolitica including porins (Omps). Figure taken from (Białas et al., 2012). CW, cell wall; ECA, enterobacterial common antigen; IM, inner membrane; LPS, lipopolysaccharide; OM, outer membrane; OMP, outer membrane protein; PS, periplasmic space. (B) crystal structure of OmpA at 2.5 Å resolution (Pascal et al., 2010). (C) crystal structure of trimeric OmpF at a 1.6 Å resolution (Yamashita et al., 2008).

5.1.2.1 Implications with GD

Patient studies

A link between GD and *Y. enterocolitica* was first proposed four decades ago (Bech et al., 1974) yet to date it remains a controversial and inconsistent subject with no definitive answer on the role of *Y. enterocolitica* in GD susceptibility and pathogenesis. The initial link between *Y. enterocolitica* was first established following the discovery of agglutinating antibodies to the O-antigen of serotype O:3 in patients with GD and thyrotoxicosis using the tube agglutination method. This study showed the presence of such antibodies was statistically significant when compared to a control group of patients with non-toxic goitre (Bech et al., 1974). Similarly, sera from patients infected with *Y. enterocolitica* O:3 displayed binding to a cytoplasmic antigen of thyroid epithelial cells as measured by immunoflourescence. This binding disappeared following absorption of the sera with sonicated *Y. enterocolitica*, suggesting cross-reactivity between thyroid and bacterial antigens. No yersiniosis patient showed signs of thyroid disease (Lidman et al., 1976). A significant finding came from the discovery of a saturable binding site for TSH in *Y. enterocolitica* under non-physiological conditions. TSH binding sites have also been demonstrated in strains of *E. coli* (Weiss et al., 1983). Another study confirmed the presence of such a binding site in a study where total Ig from 5 of 7 GD patients significantly inhibited ^{125}I-TSH binding to thyroid membranes and 4 of those 5 to *Y. enterocolitica* under physiological conditions. Control immunoglobulins did not display any

inhibition of ^{125}I-TSH binding to either thyroid membranes or *Y. enterocolitica*, however only 2 control samples were evaluated (Heyma et al., 1986). In another study, varying concentrations of IgG from patients recovering from *Y. enterocolitica* infection were shown to inhibit TSH binding and stimulate cAMP activity in thyroid membranes, despite no sign of thyroid dysfunction in any of the patients. IgG from normal controls did not display any TSHR stimulation (Wolf et al., 1991). A Danish case-control study and a Danish discordant twin study found that the GD-affected individual had a higher prevalence of anti-Yop IgA and IgG compared to controls. The authors speculate that the class-switched anti-Yop antibodies suggest chronic *Y. enterocolitica* infection (Brix et al., 2008).

However not all studies have confirmed a link between GD and *Y. enterocolitica* infection. A Canadian study did not find any significant differences between sera from 44 GD patients and controls as measured by Western blotting, ELISA or the test agglutination method (Resetkova et al., 1994). A recent prospective study did not find a link between the development of GD and *Y. enterocolitica.* This study only looked for the presence of anti-Yop antibodies in the patient sera, and not for antibodies to the total bacterium (Effraimidis et al., 2011).

Mouse studies

Experimental studies have immunised CBA/J and C57BL6/J mice with total *Y. enterocolitica* bacteria and analysed the serum for anti-TSHR antibodies (Luo et al., 1993; Luo et al., 1994). Antibodies to TSHR

developed which cross-reacted with antigen(s) from an envelope protein preparation of *Y. enterocolitica*. The mice remained euthyroid and thyroid histology remained normal but it is possible that histological changes are a symptom of chronic disease (Flynn et al., 2007) and were studied too early to detect changes (Luo et al., 1993; Luo et al., 1994). No attempt to reproduce the findings of Luo *et al* has been published and thus the findings remain uncorroborated. It has since been shown that BALB/c mice are a better model of studying GD than CBA/J and C57BL6/J mice, which are resistant to induced hyperthyroidism, and this could explain the euthyroid status of the immunised mice (Nagayama et al., 2002). Additionally total bacterium may provide antigenic competition and so a robust immune response capable of generating TSAbs was not generated.

Outer membrane porin proteins

Bioinformatic modelling has demonstrated homology between the TSHR A-subunit and proteins from *Y. enterocolitica* (Benvenga et al., 2004; Benvenga et al., 2006). OmpM was reported to have a high degree of sequence homology with the TSHR (Guarneri et al., 2011). However this report featured inconsistencies between the sequence alignments, with TSHR and OmpM sequences being mislabelled. In another study, a biological association between GD and OmpF was demonstrated using GD patient sera in combination with mass spectrometry, which identified OmpF of *Y. enterocolitica* as the cross-reactive antigen with TSHR (Wang et al., 2010). OmpF antiserum was also shown to induce weak but statistically significant cAMP responses in CHO cells transfected with

TSHR holoreceptor and in thyroid follicular cells. The data was further substantiated using a neutral anti-TSHR mAb, mAb A9, to identify aa homology between TSHR and OmpF, where 5 residues from a sequence of 8 were shown to be identical between TSHR (residues 198-205) and OmpF (residues 190-197), as shown below, with common residues highlighted in bold:

TSHR: 198 **DA**F**G**G**V**Y**S** 205

OmpF: 190 **DA**L**G**N**VTS** 197

Discrepancies between published studies

Inconsistencies between patient studies may stem from using serum or total IgG from patients that will contain a mix of anti-thyroid IgG amongst other specificities, rather than using purified anti-TSHR mAbs. As has been previously discussed, anti-TSHR antibodies are present in very low concentrations in patient serum and thus would make a very small proportion of the total IgG used in studies. Furthermore, of the small proportion of anti-TSHR antibodies, there is heterogeneity amongst this population with stimulating, blocking and neutral antibodies with varying epitopes. This heterogeneity amongst the anti-TSHR antibodies could be affected by the treatment undergone by the patient. It is also unknown which subtype of anti-TSHR antibody (TSAb, TSBAb, neutral) is cross-reacting with a *Y. enterocolitica* protein, if at all. Thus it could be that a particular patient's serum or the pooled sera from a group of patients could have an over-representation of a particular antibody subtype that does not cross-react with a *Y. enterocolitica* protein. It is also possible

that the antibodies have a low-affinity for the bacterial antigen and this binding may not be measurable when serum is diluted for evaluation.

Variation between studies may come from differences in patient exposure to *Y. enterocolitica* and the genetic and environmental background of the patients and the diagnostic criteria. Additionally, differences in the methods used to culture and measure *Y. enterocolitica* may impact, particularly as the temperature the *Y. enterocolitica* are cultured in can have a dramatic effect on the expression of various genes proteins (Rohde et al., 1994).

5.2 Aims

No studies have been conducted to evaluate whether or not there is cross-reactivity between monoclonal TSAbs and *Y. enterocolitica*. The aims of this chapter were therefore to investigate the cross-reactivity of KSAb1, KSAb2 and rFab germline to *Y. enterocolitica* proteins using whole cell lysates, envelope proteins and isolated effector Yops from two serotypes previously studied in the GD literature, O:3 and O:8. The aims of this chapter were:

i. To evaluate whether TSAbs KSAb1 and KSAb2 cross react with *Y. enterocolitica* proteins, which may indicate a role for microbial infection and molecular mimicry in the pathogenesis of GD. These would be the first studies to examine monoclonal TSAbs in the context of molecular homology between TSHR and *Y. enterocolitica*

ii. To evaluate the binding of rFab germline to *Y. enterocolitica*. These experiments would be the first studies to examine the role of infection in potentially expanding precursor B cells to mature TSAbs.

iii. To evaluate cross-reactivity between the neutral anti-TSHR mAb, mAb A9, and other porins such as to OmpC and Omp A to ascertain if other porins may also be involved in the pathogeneses of GD, following the report of Wang *et al*, 2010.

5.3 Results

5.3.1 Confirming presence of pYVe plasmid in Ye58/03 and 8081 serotype colonies

We first sought to evaluate whether rFab germline, KSAb1 and KSAb2 recognised Yops, as binding of Yops has been reported in the literature for GD patient serum samples (Brix et al., 2008). Expression of Yops is dependent on expression of the pYVe plasmid. PCR was thus performed to confirm that each red colony expressed the pYVe plasmid. A 300 bp yscU gene product encoded by the pYVe plasmid was amplified as proof of plasmid expression.

For 8081, half of a single colony was chosen for PCR, and the remaining half was grown overnight. As there were no easily identifiable single colonies for Ye58/03, a small streak was taken for PCR analysis. Strong expression of the pYVe plasmid was observed in the O:8 colony, with weaker expression observed for O:3, this is to be expected as single colonies could not be obtained from culture plates (Figure 42).

Figure 42: Confirmation of pYVe expression by *Y. enterocolitica* serotypes 8081 and Ye58/03 by PCR.

The yscU gene of the pYVe plasmid was amplified by PCR to confirm expression of the plasmid which is necessary for Yop production.
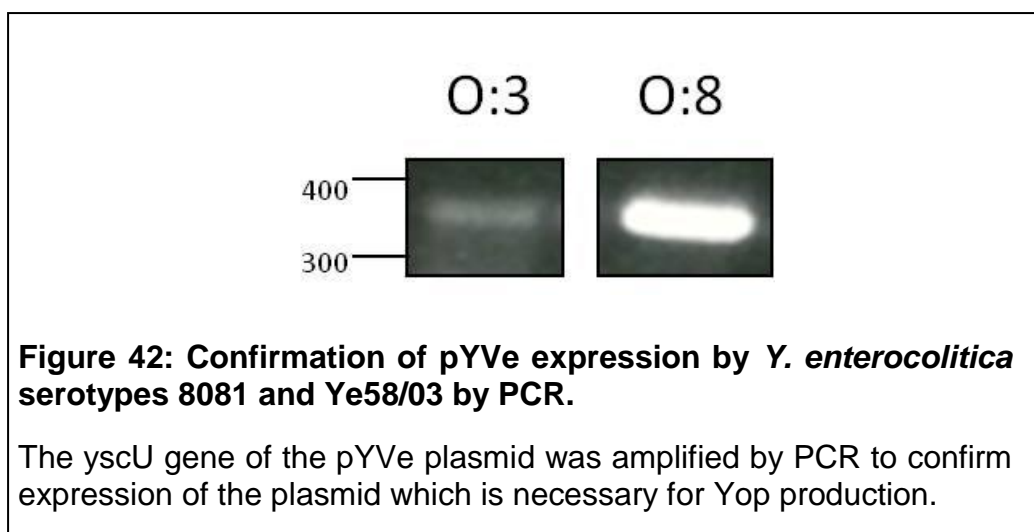
5.3.2 Isolation of effector Yop proteins from *Y. enterocolitica* serotypes 8081 and Ye58/03

Both serotypes of *Y. enterocolitica* were cultured for Yop expression and analysed by SDS-PAGE with Coomassie blue staining (data not shown). Neither serotype produced visible Yops, despite the confirmed presence of pYVe in serotype O:8. Our collaborators, Mr Marco Grasso and Dr Steve Atkinson (University of Nottingham, UK) had experienced previously difficulty in expressing Yops in the O:8 serotype.

It was therefore decided to use frozen samples of Yops isolated from serotype O:8 from a previous successful experiment of Mr Marco Grasso (Figure 43, page 187). Thus, serotype O:3 was not used for further Yop isolation experiments for this thesis.

Figure 43: Isolated Yops from serotype O:8.

Mr Marco Grasso donated expressed Yops from a previous experiment using the O:8 serotype.
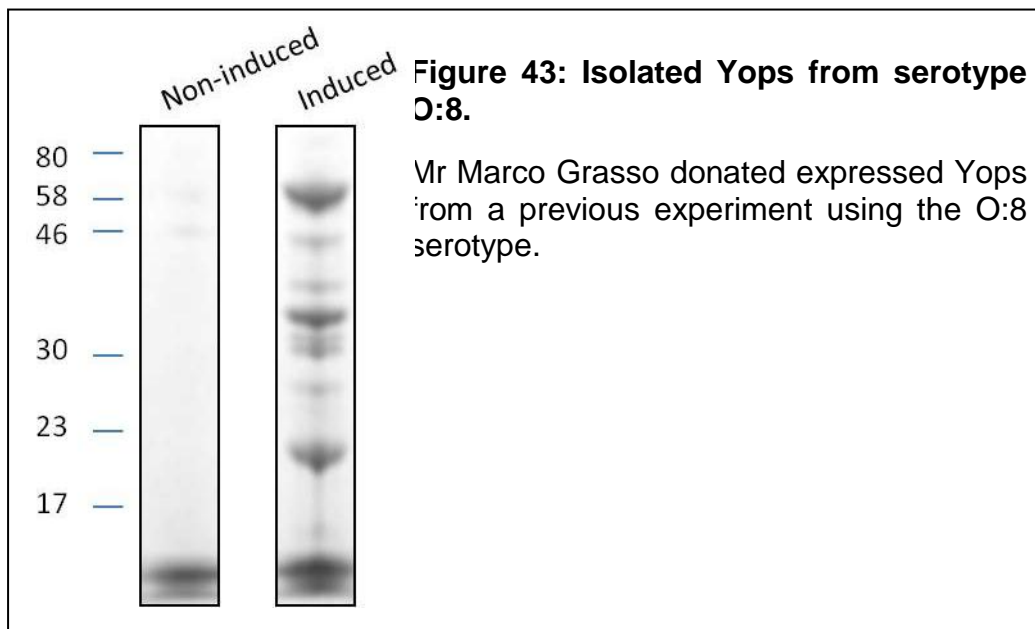
5.3.3 Determining measurable binding of TSAbs and rFab germline to Yops

At the time of performing the experiment, no anti-Yop antibodies were available to us to use as positive control for Western blotting experiments. Instead, whole mouse cell lysate containing vinculin antigen and mouse anti-vinculin primary antibody (both kindly donated by Dr Yolanda Calle, KCL) were used as positive control for the alkaline phosphatase-conjugated secondary anti-mouse antibody and the BCIP/NBT secondary conjugate. A band was observed migrating at approximately 120 kDa (Figure 44, page 188), which is to be expected for the 116 kDa vinculin protein.

Figure 44: Positive control: Vinculin.

To confirm the activity of the alkaline-phosphatase antibody and conjugate system, a mixed cell lysate containing vinculin protein was incubated with a murine anti-vinculin primary antibody, followed by the alkaline phosphatase reagents. A band was found at the expected MW, at ~120 kDa (highlighted by a box). Vinculin is known to be 116 kDa.

Binding to the isolated Yops was evaluated with KSAb1 IgG, KSAb2 IgG and rFab germline, all at 10 µg/mL. Due to the paucity of purified Yops available to us, and the difficulty involved in their isolation, no Yop samples were available for evaluation with isotype controls. No visible bands were observed with any of the antibodies (Figure 45, page 189),

and the experiment was performed on two independent occasions as it was considered important to confirm the lack of binding observed.

Figure 45: Western blot testing binding of mAb and rFab binding to Yops.

Yops were incubated with 10 µg/mL concentrations of KSAb1 IgG, KSAb2 IgG or rFab Germline and tested for binding by Western blot. No binding was observed for any of the preparations. This experiment was performed on two independent occasions.
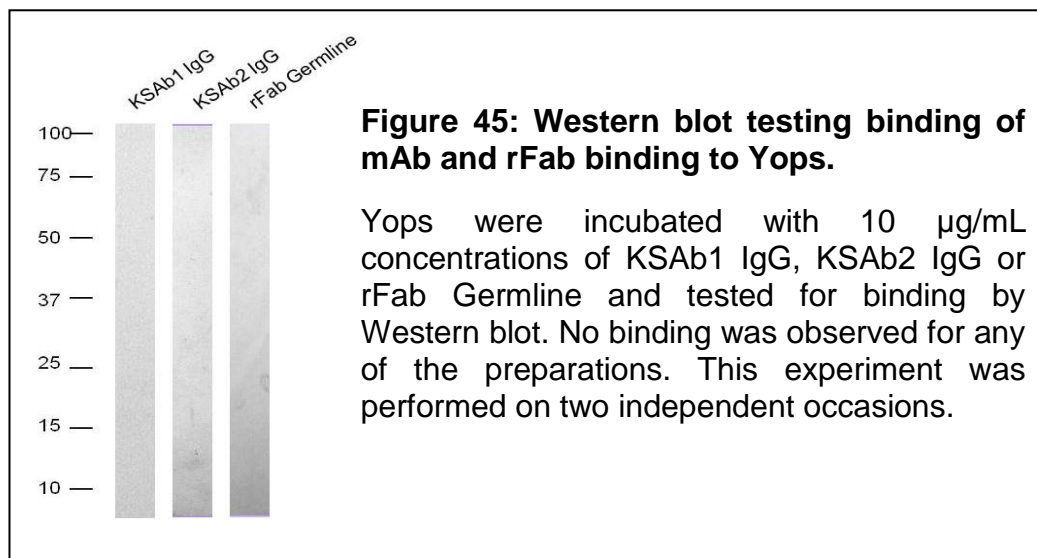
However the Western blotting system based upon enzyme development using secondary antibody conjugated with alkaline phosphatase is a relatively insensitive system. It is possible that the enzyme development system used here was too insensitive to detect measurable binding to Yops. Thus to summarise, my preliminary data indicate that rFab germline, KSAb1 and KSAb2 do not recognise Yops of *Y. enterocolitica* serotype O:8.

5.3.4 Preparation of *Y. enterocolitica* 8081 and Ye58/O3 whole cell lysates and envelope proteins

Following previous studies analysing binding to *Y. enterocolitica* (Luo et al., 1994), both whole cell lysate and envelope proteins were prepared for each serotype. Preparations were analysed by SDS-PAGE and showed over-expressed proteins and subtle differences in protein expression (Figure 46).

Figure 46: Preparation of whole cell lysate and envelope protein preparations.

Whole cell lysate and envelope proteins were prepared for both serotypes and analysed by SDS-PAGE and Coomassie blue staining.
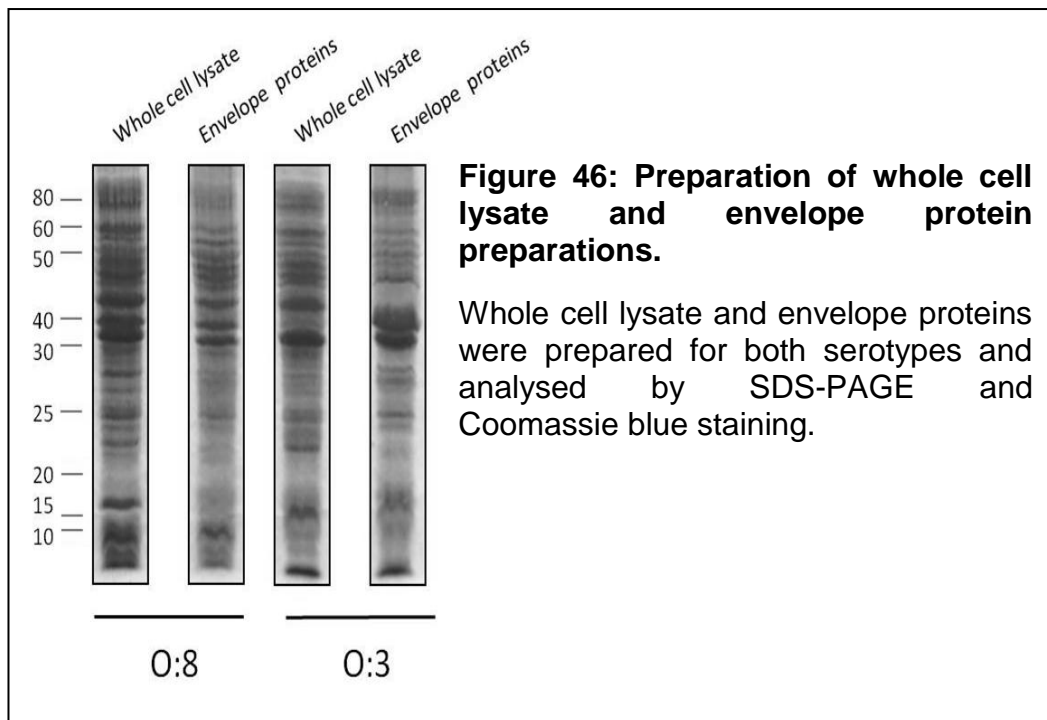
5.3.5 Binding of anti-TSHR mAbs and rFab germline to whole cell lysate and envelope protein preparations of *Y. enterocolitica*

Evaluation of KSAb1 IgG binding to Y. enterocolitica

Y. enterocolitica protein preparations were evaluated for binding with KSAb1 IgG and binding was observed with a band migrating below the MW marker band of 37 kDa. However whilst it is important to note that Western blotting represents an approximate method of MW determination, this band has an apparent MW of 37 kDa. This band was observed in both serotypes and in both protein preparations, indicating that the protein is in the outer envelope of the bacterium. No binding was observed for the isotype control (IgG_{2b}) indicating that the binding observed for KSAb1 IgG was specific (Figure 47).

Figure 47: Evaluating KSAb1 IgG and its isotype control binding to whole cell lysate and envelope protein preparations.

(A) KSAb1 IgG was incubated with whole cell lysate (W) and envelope protein (Env) preparations from both serotypes and tested for binding by Western blotting. A band was observed running just under 37 kDa, in all preparations. (B) No bands were observed for its isotype control, IgG$_{2b}$.

Evaluation of KSAb2 IgG binding to Y. enterocolitica

Y. enterocolitica protein preparations were evaluated for binding with KSAb2 IgG and binding was observed with a band of an apparent MW of 37 kDa, similar to that observed for KSAb1 IgG (Figure 47). The 37 kDa band was observed in both serotypes and in both protein preparations, indicating that the protein is in the outer envelope of the bacterium. No binding was observed for the isotype control (IgG$_{2a}$) indicating that the binding observed for KSAb2 IgG was specific (Figure 48). The *Y. enterocolitica* binding data for KSAb1 and KSAb2 IgG indicates that both mAbs re cross-reactive as they recognise TSHR (Gilbert et al., 2006a) as well as a *Y. enterocolitica* protein.

Figure 48: Evaluating KSAb2 IgG and its isotype control binding to whole cell lysate and envelope protein preparations.

(A) KSAb2 IgG was incubated with W and Env preparations from both serotypes and tested for binding by Western blotting. A band was observed running just under 37 kDa, in all preparations. (B) No bands were observed for IgG_{2a}.
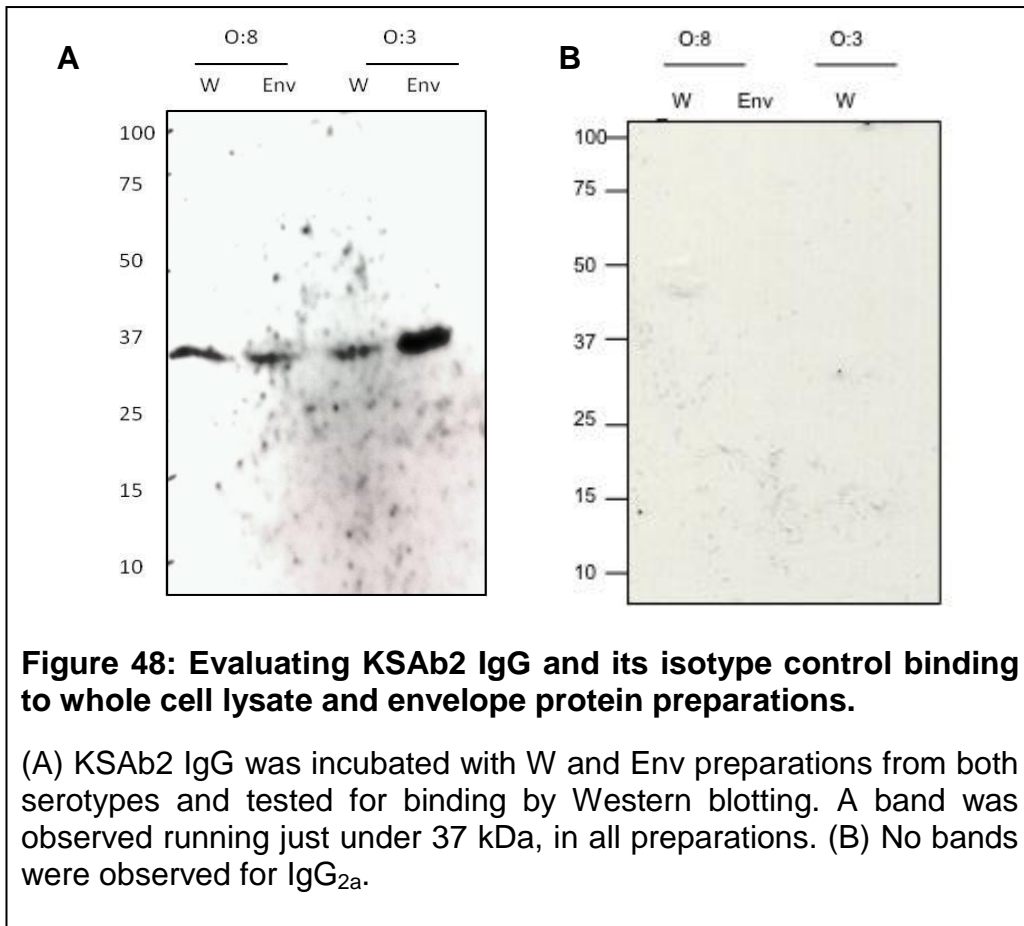
Evaluation of rFab germline binding to Y. enterocolitica

Y. enterocolitica protein preparations were evaluated for binding with rFab germline and as in the cases of both KSAb1 and KSAb2 IgG, binding was observed with a band migrating with an apparent MW of 37 kDa (Figure 49).This band was observed for both protein preparations in serotype O:8, and to envelope proteins in serotype O:3, Weaker binding was observed in the whole cell lysate preparation of serotype O:3. This may be due to the particular preparation of O:3 whole cell lysate not expressing high enough levels of the particular protein, or the protein may be obscured by others of similar MW as a large loading volume was necessary to measure binding. No binding was observed with the

negative control, rFab96/3, indicating that the binding observed for rFab germline was specific.

Figure 49: Evaluating rFab germline binding to whole cell lysate and envelope protein preparations.

(A) rFab germline was incubated with W and Env preparations, and binding was determined by Western blotting. A band was observed running just under 37 kDa, in all preparations. (B) No binding was observed for rFab 96/3.
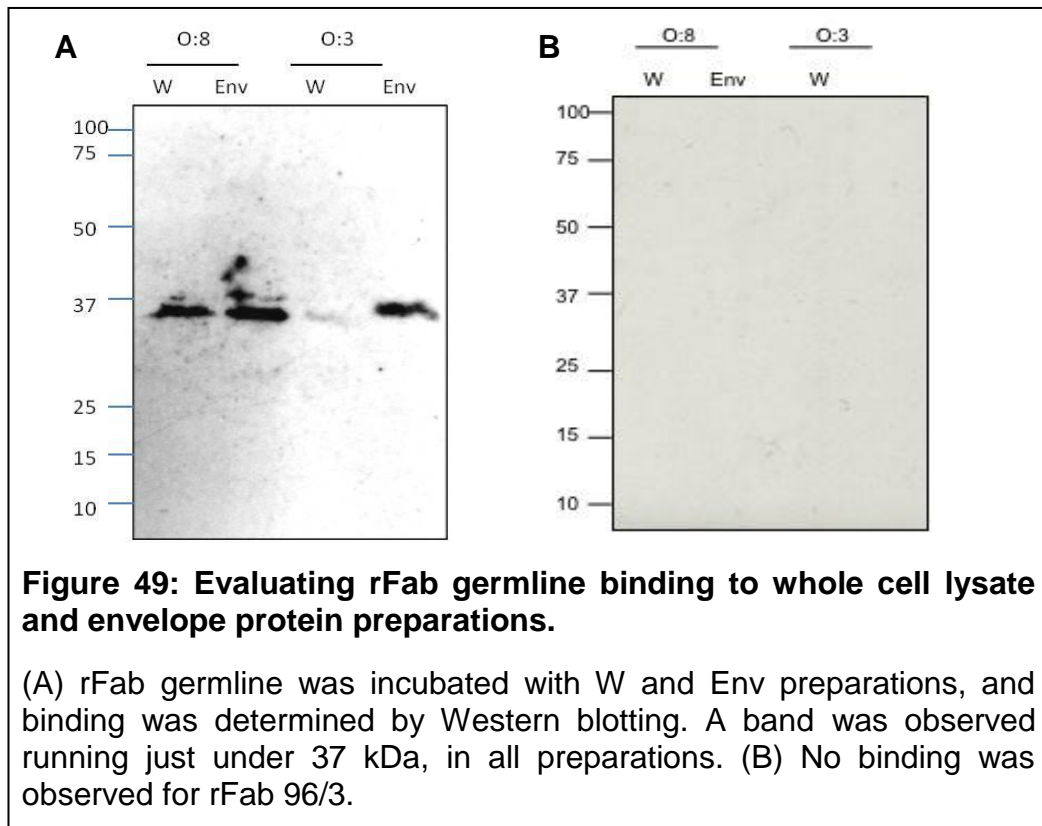
Evaluation of mAb A9 IgG binding to Y. enterocolitica

mAb A9 (Nicholson et al., 1996) is a neutral anti-TSHR mAb that has been epitope-matched to aa 214-222 of the TSHR (Andresen et al., 2006), or residues 193-201 using the aa numbering system without the signal sequence. Recently it has also been shown to react with OmpF, a 40 kDa outer membrane porin protein, from *Y. enterocolitica* serotype O:3 (Wang et al., 2010). In this thesis mAb A9 IgG was evaluated for binding to the *Y. enterocolitica* serotypes and preparations already described. Binding to a band at approximately 37 kDa was observed O:8 whole cell lysate and both preparations of serotype O:3 (Figure 50), suggesting that

mAb A9 is binding a similar antigen(s) to KSAb1 IgG, KSAb2 IgG and rFab germline. The lack of binding to O:8 envelope proteins may be due to the particular preparation of O:8 envelope proteins not expressing high enough levels of the particular protein, or the protein may be obscured by others of similar MW as a large loading volume was necessary to measure binding.

Figure 50: Evaluating mAb A9 binding to whole cell lysate and envelope protein preparations.

(A) mAb A9 is an epitope-mapped anti-TSHR mAb and was tested for binding to W and Env preparations by Western blotting. Binding was observed at just under 37 kDa in all preparations, except O:8 Env. (B) No binding was observed with IgG_1 isotype control.
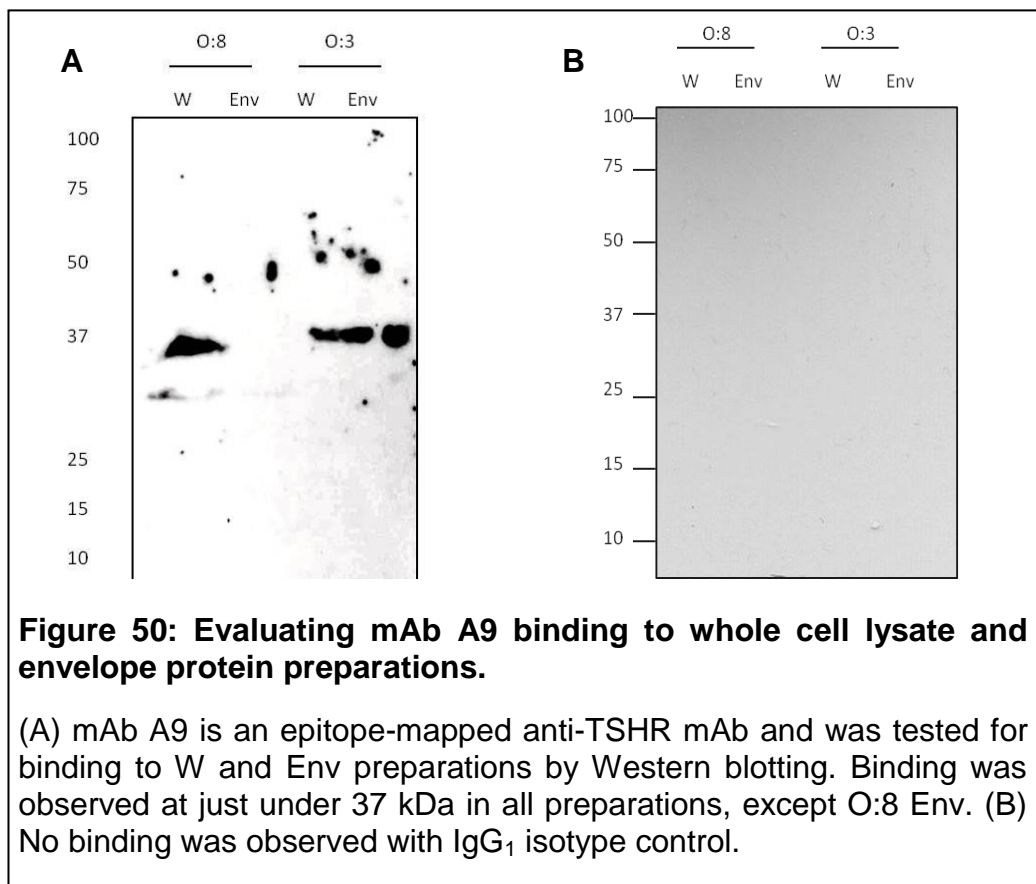
5.3.6 Identification of *Y. enterocolitica* protein displaying binding to anti-TSHR mAbs by MALDI-TOF

We attempted to identify the *Y. enterocolitica* 37 kDa band by MALDI-TOF. To narrow the potential proteins within a sample, we enriched for the *Y. enterocolitica* protein of interest by antibody capture analysis using

immobilised KSAb1 IgG (conjugated to Cyanogen Bromide-activated Sepharose 4B beads). As a negative control, coupled BSA was prepared.

Y. enterocolitica lysate was incubated with either KSAb1 IgG-Sepharose 4B or BSA-Sepharose 4B and bound protein was eluted and analysed by SDS-PAGE and Western blotting. Coomassie blue staining revealed two faint bands in close proximity migrating just below 37 kDa (data not shown due to photography software being too insensitive to visualise the bands). The eluted sample was also analysed by Western blotting and probed with KSAb1 IgG (primary antibody) and HRP-conjugated sheep anti-mouse IgG secondary antibody. A single band is observed migrating below 37 kDa in both the lysate and eluted fractions. In the eluted fraction there are also two bands at above 50 kDa and approximately 25 kDa. It is likely that these bands are KSAb1 IgG H-chain (55 kDa) and L-chain (25 kDa) that were eluted during the purification process and have been detected by the polyclonal anti-mouse IgG secondary antibody. This experiment confirms that a protein of approximately 37 kDa has been eluted following affinity enrichment with KSAb1 IgG-Sepharose 4B and this protein was further confirmed by Western blotting with KSAb1 IgG. A band of an apparent MW of 37 kDa is visible in the lysate lane of BSA-coupled matrix following probing with KSAb1 IgG, but not in the eluted lane (Figure 51).

Figure 51: Affinity enrichment of *Y. enterocolitica* with affinity matrix-coupled antibody.

(A) Purification of *Y. enterocolitica* following incubation with KSAb1 IgG-Sepharose 4B. A band below 37 kDa is observed in both the lysate and elution lanes. IgG H-chain (55 kDa) and L-chain (25 kDa) bands are also observed in the elution suggesting that some KSAb1 IgG may have been cleaved during the elution process. (B) Purification of *Y. enterocolitica* following incubation with BSA-Sepharose 4B. A band below 37 kDa is observed in the lysate lane but not in the eluted lane.

As both eluted bands in the SDS-PAGE sample were too close together to accurately separate them, a gel slice containing both bands was excised and sent for MALDI-TOF analysis. This analysis revealed 38 proteins contained in the analysed sample, along with their expected MW (in kDa) and their relative abundance within the sample. The majority of proteins identified within the sample are enzymes involved in processes such as metabolism. The two most abundant proteins within the sample are OmpA and OmpC. OmpC had also been identified by MALDI-TOF attempt 1. OmpF (Wang et al., 2010) was not found in either of our MALDI-TOF analyses. This is likely due to the reciprocal regulation of OmpC and OmpF, and because OmpF is typically expressed at temperatures of 2-24°C, whilst the *Y. enterocolitica* cultures described

here were grown at 30°C (Ozawa and Mizushima, 1983). Wang *et al* do not describe the *Y. enterocolitica* growth conditions used in their study.

5.3.7 Expression of recombinant OmpC and OmpF protein

The gene constructs of *ompC* and *ompF*, cloned in pET32b, were provided by our collaborator Dr Anna Stenkova, Russia, as plasmid spots which were subsequently transformed into competent cells for recombinant protein expression. Dr Stenkova recommended that the cultures be grown at 37°C and induced with 1 mM IPTG for 4 h. Expression of the recombinant proteins was analysed by SDS-PAGE (Figure 52, page 197). No protein expression is observed in the non-induced lane of OmpC but there is a strong band migrating just below 37 kDa in the induced lane. There is strong expression of OmpF in both the non-induced and induced samples migrating slightly above 37 kDa.

Figure 52: Analysis of recombinant OmpC and OmpF expression by SDS-PAGE.

Recombinant OmpC and OmpF expression was induced following addition of IPTG. There was no induction of OmpC before IPTG (NI; non-induced) but clear induction after induction (highlighted by a box). There is leaky expression of OmpF as there is a band in both the non-induced and induced lanes.
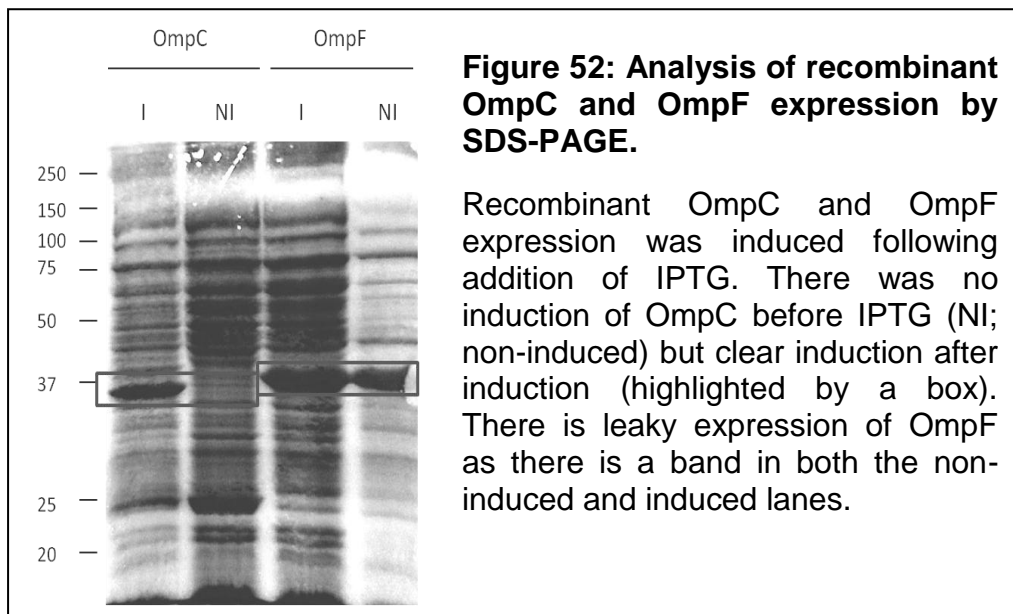
5.3.8 Cloning of *omp* genes and expression as recombinant protein

Based on the MALDI-TOF data, the 1,080 bp nucleotide sequence of *ompA* was obtained from PubMed (accession number nc 008800) and synthesised as a gene construct. The gene arrived cloned in a pUC57 vector and was subsequently sub-cloned in pET22b (Figure 53).

Figure 53: Cloning of OmpA.

Agarose gel electrophoresis of OmpA synthetic construct: Lane 1 is purified pET22b vector, lane 2 is the MW ladder in kB, lane 3 is purified OmpA digested with *Nde*I and *Xho*I restriction enzymes. The OmpA construct is 1,080 bp and migrates between 1-1.5 kB.
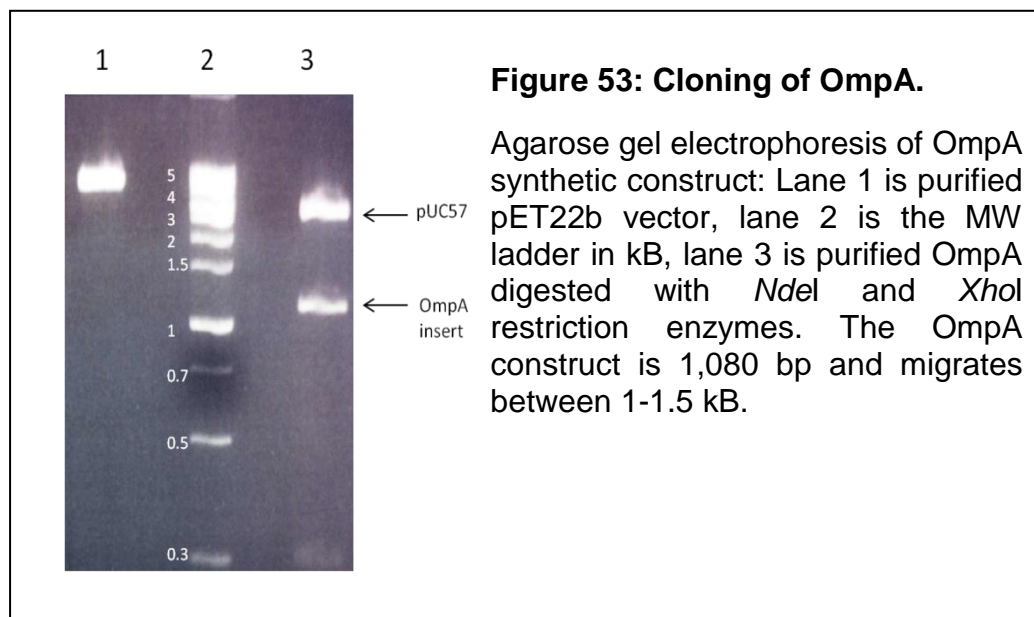
The same expression conditions that were used for OmpC and OmpF protein expression were used for recombinant OmpA protein expression. There is a clear induction of a band, migrating at approximately 37 kDa, which is not observed in the non-induced lane see Figure 54.

Figure 54: Analysis of recombinant OmpA expression by SDS-PAGE.

Recombinant OmpA expression was induced following addition of IPTG. There was no induction of OmpA before IPTG (NI; non-induced) but clear induction after induction (highlighted by a box).
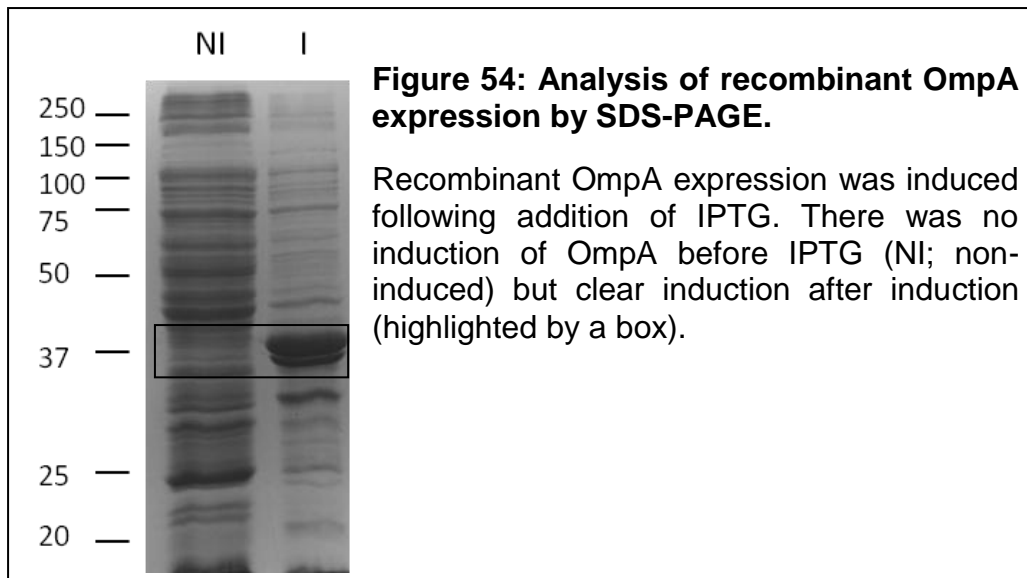
5.3.9 Evaluation of binding of anti-TSHR mAbs and rFab germline to purified OmpA, OmpC and OmpF

Western blotting was performed to assess binding of the anti-TSHR mAbs and rFab germline to recombinant OmpA, OmpC and OmpF in total *E. coli* lysate (Figure 55, page 200). rFab germline displayed binding to OmpC and OmpF, with weak binding to OmpA. KSAb1 and KSAb2 both showed binding to all three recombinant porins. The previously reported binding of mAb A9 to OmpF (Wang et al., 2010) was confirmed, and it also displayed binding to the other non-specific porin, OmpC, but not OmpA (Figure 55, page 200).

Figure 55: Evaluation of mAbs and rFab germline binding to OmpA, OmpC and OmpF.

Anti-TSHR mAbs and rFab germline were evaluated for binding to recombinant OmpA, OmpC and OmpF. Isotype controls did not display any binding to the recombinant Omps.
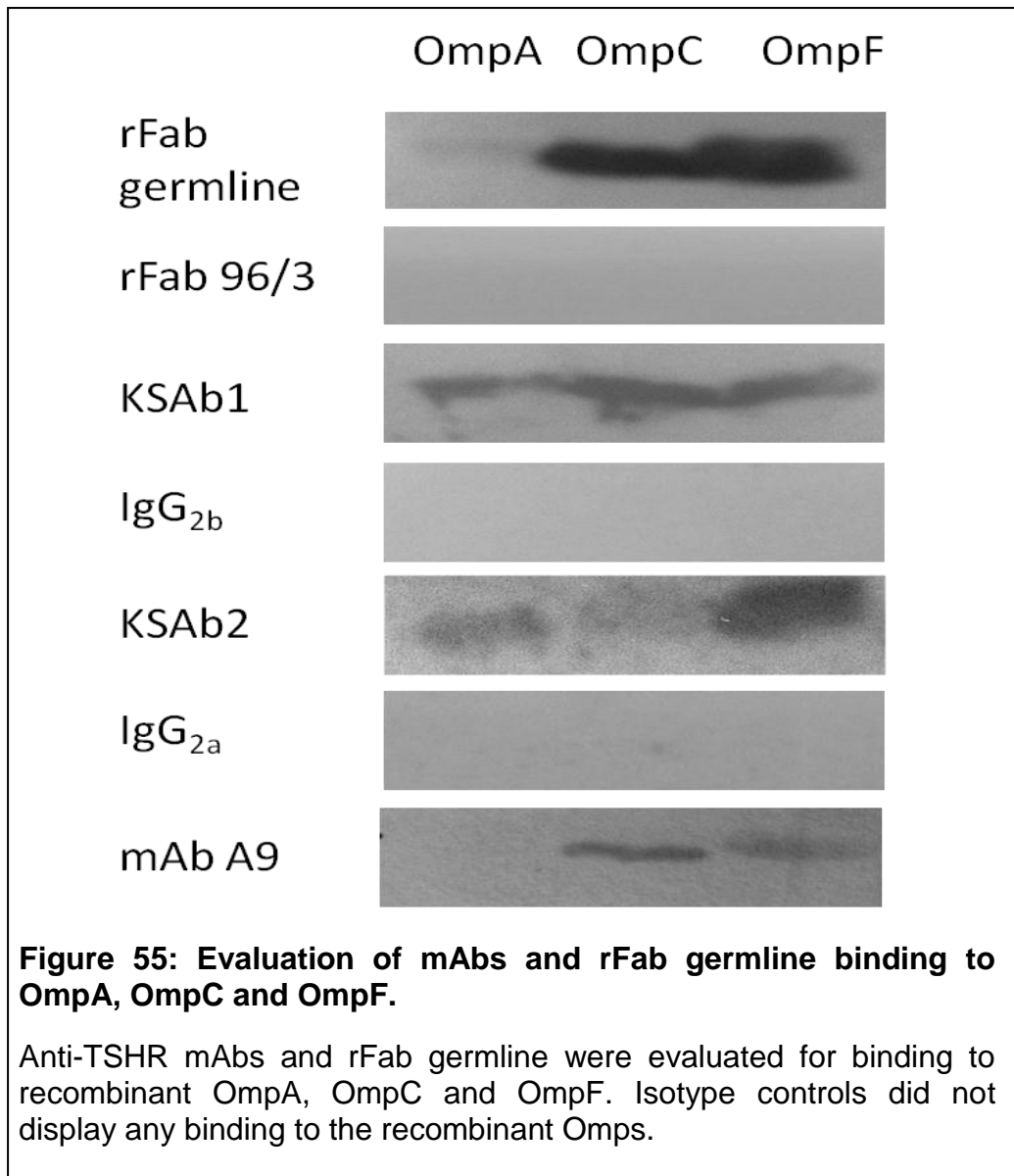
5.3.10 Amino acid sequence homology of OmpA, OmpC and OmpF with TSHR

Sequence alignments were performed to evaluate whether there is any aa sequence homology between the Omps and the TSHR. As the TSHR epitopes of KSAb1 and KSAb2 are discontinuous rather than linear (Gilbert et al., 2006a) and have not been determined, it is difficult to know which region of the TSHR is most important for homology to the OmpA, OmpC amd OmpF.

200

Sequence homology between OmpF and TSHR

As shown by Wang *et al*, 2010, when TSHR residues 198 DAFGGVYS 205 and OmpF residues 190 DALGNVTS 197 are deleted, mAb A9 binding is lost (Wang et al., 2010), but as the mAb A9 TSHR epitope is actually mapped to 193 TVIDKDAFG 201 (Andresen et al., 2006), then the key OmpF residues for mAb A9 binding are 190 DALG 193 (Figure 56) which has a high degree of homology with TSHR with 3 out 4 identical residues (shown in bold):

OmpF   190 **DA**L**G** 193

TSHR   198 **DA**F**G** 201

```
OMPF    -MMKRNILAVVIPALLVAGAANAAEIYNKDG-----NKLDLYGKVDARHQFSDNAGQDGD 54
TSHR    MGCSSPPCECHQEEDFRVTCKDIQRIPSLPPSTQTLKLIETHLRTIPSHAFSNLPNISRI 60
                      :..:. .*. .    : :: : :,. * **: ... .

OMPF    ESYVRFGFKG-ETQITDQLTGYGQWEYNVQANHAESQGDKGNKTRLG------FAGLKFA 107
TSHR    YVSIDVTLQQLESHSFYNLSKVTHIEIRNTRNLTYIDPDALKELPLLKFLGIFNTGLKMF 120
             : .:: *:: :*:  : *,  * :  : *  ::  *      :***:

OMPF    EFGSLDYGRNYGVIYDVN--AWTDMLPVFGGDSISNSDNYMTGRSTGLATYRNTNFFGLV 165
TSHR    PDLTKVYSTDIFFILEITDNPYMTSIPVNAFQGLCNETLTLKLYNNGFTSVQGYAFN--- 177
            :  *,: ,* ::,  ,:  :** .:,:.*,  :.  ..*::: :,  *

OMPF    DGLNFALQYQGKNEDGRNGVVETTDALGNVTSTTYSNLKDQNGDGFGISSTYDIGYGVNF 225
TSHR    -GTKLDAVYLNKN---KYLTVIDKDAFGGVYSG--PSLLDVSQTSVTALPSKGLEHLKEL 231
          * ::  * ,**   :  .*  **:,* * *   ..* *. ..  .: .: :  ::

OMPF    GAG-FSSSNRTDQQKRFS- 242
TSHR    IARNTWTLKKLPLSLSFLHL 251
          *    : ::   . *
```

Figure 56: Amino acid sequence alignment of OmpF and TSHR.

A sequence alignment was performed to assess whether there is any aa sequence homology between OmpF and TSHR. The epitope of mAb A9 is highlighted in red, and its OmpF epitope as proposed by Wang et al, 2010 is highlighted in green. The more accurate OmpF epitope of mAb A9, 193 VVETTDALG 201, is highlighted by a purple box.

Sequence homology between OmpA and TSHR

There are two aa sequence homology regions of interest between OmpA and the TSHR (Figure 57), identical aa residues are in bold:

Region 1 (highlighted in Figure 57 by a purple box):

OmpA   190 D**NG**ML**SV**GVS**Y**R**F** 202

TSHR   165 N**NG**FT**SV**QG-**YA**F** 177

Region 2 (highlighted in Figure 57 by a blue box):

OmpA   257 **S**SI**D**PKDG**SV**VV**L** 269

TSHR   208 **S**LL**D**VSQT**SV**TA**L** 221

Thus there are 6 out of 13 identical residues in region 1 and 6 out of 13 identical residues in region 2. Further experiments to confirm whether these epitopes are necessary for KSAb1, KSAb2 and rFab germline's binding to OmpA could include selectively deleting these aa regions and testing whether there is still measurable binding by Western blotting (Wang et al., 2010) or by using peptide library of truncated OmpA peptides.

```
OMPA          MKKTAIALAVALAGFATVAQAAPKDNTWYTGGKLGWSQYQNTGTGGIYGDQGNDGPTHKD 60
TSHR          -----------MGCSSPPCECHQEEDFRVTCKDIQRIPSLPPSTQTLKLIETHLRTIPSH 49
                    :.   :. .:. :::    *  .:        ..*  :  : :  .  ..

OMPA          QLGAGAFLGYQANQYLGFEMGYDWLGRMPYKGDVRNGDFKAQGVQLAAKLSYPIAQDLDL 120
TSHR          AFSN---LPNISRIYVSIDVTLQQLESHSFYNLSKVTHIEIRNTRNLTYIDPDALKELPL 106
               :.    *   :. *:.::  : *    .: .  :  .:: :..:  : :.    ::* *

OMPA          YTRLGGMVWRADSSAFDAATGDRQNNHDTGVSPLVALGAEYAWTKNWATRMEYQWVSNIG 180
TSHR          LKFLG--IFNTGLKMFPDLT----KVYSTDIFFILEITDN-----PYMTSIPVNAFQGLC 155
                . **  ::.:. . *   *      : :.*.:  ::  :  :     : * :   : ...:

OMPA          DKATVGARP┌DNGMLSVGVSYRF┐GQEDAVAPIAPAPAPAPVVDTKRFTLKSDVLFAFNKST 240
TSHR          NETLTLKLY│NNGFTSVQG-YAF│NG---------------------TKLDAVYLNKNKY 191
              :::  .   └.**: ** * *┘              * *.::  ::.

OMPA          LKPEGQQALDQLYAQL┌SSIDPKDGSVVVL┐GFADRIGQPAPNLALSQRRADSVRDYLVSKG 300
TSHR          L TVIDKDAFGGVYSGP│SLLDVSQTSVTAL│----------PSKGLEHLKELIARNTWTLKK 241
              *. .::*:. :*:    │ * :* .: **..*│         *. .*.: :   .*:  . *

OMPA          IPADKITARGEGQANPVTGNTCDNVKPRAALIECLAPDRRVEIEVKGYKEVVTQPQA 357
TSHR          LPLSLSFLHL------------------------------------------ 251
              :* .    :
```

Figure 57: Amino acid sequence alignment of OmpA and TSHR.

A sequence alignment was performed to assess whether there is any aa sequence homology between OmpA and TSHR. The epitope of mAb A9 is highlighted in red, region of sequence homology 1 is highlighted in a purple box and region of sequence homology 2 in a blue box. There is little homology between OmpA and the mAb A9 TSHR epitope which is to be expected as mAb A9 does not show any binding to OmpA.

Sequence homology between OmpC and TSHR

As previously discussed OmpC and OmpF are part of the same family of non-specific, classical porins (Nikaido, 2003) and have a high degree of aa sequence homology, which is most apparent at the N-terminus. This homology may explain why all of the mAbs evaluated have displayed binding to both OmpC and OmpF, including mAb A9. In Figure 58 the finely-mapped TSHR epitope of mAb A9 is highlighted in red. As mAb A9 binds both OmpC and OmpF, its epitopes in TSHR and OmpF are important predictors of its epitope in OmpC. The stretch of 4 key TSHR

aa residues is homologous in OmpC, as shown below with identical residues in bold:

OmpC   286 YQ**FG** 289

TSHR   198 DA**FG** 201

Although not identical, the OmpC glutamine residue (Y286) and the TSHR aspartic acid residue (D198) are both hydrophilic with structural similarity (below), and thus could also be involved as part of mAb A9's OmpC epitope.

Aspartate   Glutamate
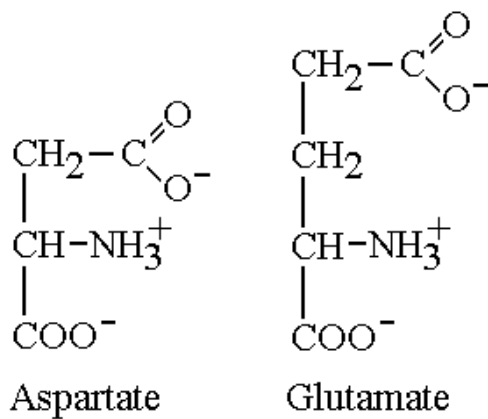
This data also shows how antibody binding may be mediated by as little as 2-3 aa residues.

```
OMPC        MKLRVLSLLVPALLVAGSAGAAEIYNKDGNKLDLYGKVDGLHYFSDDKSKDGDQSYMRFG 60
TSHR        --------------MGCSSPPCECHQEE----DFRVTCKDIQRIPSLPPSTQTLKLIETH 42
                          :. *: ..* ::::    *:  . ..:: :..  ..    . :.
OMPC        LKGETQISDQLTGYGQWEYQANLNKAEDQDQGNFTRIGFAGLKFADYGSFDYGRNYGVLY 120
TSHR        LR-----TIPSHAFSNLPNISRIYVSIDVTLQQLESHSFYNLSKVTHIEIRNTRNLTYID 97
            *:       :    .:.:    :.: : *    ::   .* .*. . : .:   **   :
OMPC        DVTSWTDVLPEFGGDTYGADNFLSQRGNGMATYRNTNFFGLVDGLNFALQYQGKNGSGTE 180
TSHR        -----PDALKELP-----LLKFLGIFNTGLKMFPDLTKVYSTD-IFFILEITDN------ 140
                 .*.* *:         :**. ..*: : : . .  .* : * *:  .:
OMPC        TDNGRDVQGQNGDGYGMSLSYDLGWGVSASAAMASSKRTDEQNNLAFGHGDRADAYSGGL 240
TSHR        ------------------PYMTSIPVNAFQGLCNETLTLKLYNNGFTS-VQGYAFNG-- 178
                              .*  .  *.*  .:.... * :  * .*    :. *:.*
OMPC        KYDANNVYLAATYAQTYNLTRFGNFKNNTDSGFANKAQNIELVA YQF DFGLRPSVAYLQ 300
TSHR        ------------------------TKLDAVYLNKNKYLTVIDK DAF ----------- 200
                                    .: *: : ** : : :: : *
OMPC        SKGKDL G NGYSDQDLVKYVDVGATYYFNKNMSTYVDYKINLLDENEFTKNAGINTDDIVA 360
TSHR        ------ G VYSGPSLLDVSQTSVTALPSK----GLEHLKELIARNTWTLKKLPLSLSFLH 250
            *  **. .*:. :...*  .*      ::: :*: .* :* :    : .::
OMPC        VGLVYQF 367
TSHR        L------ 251
            :
```
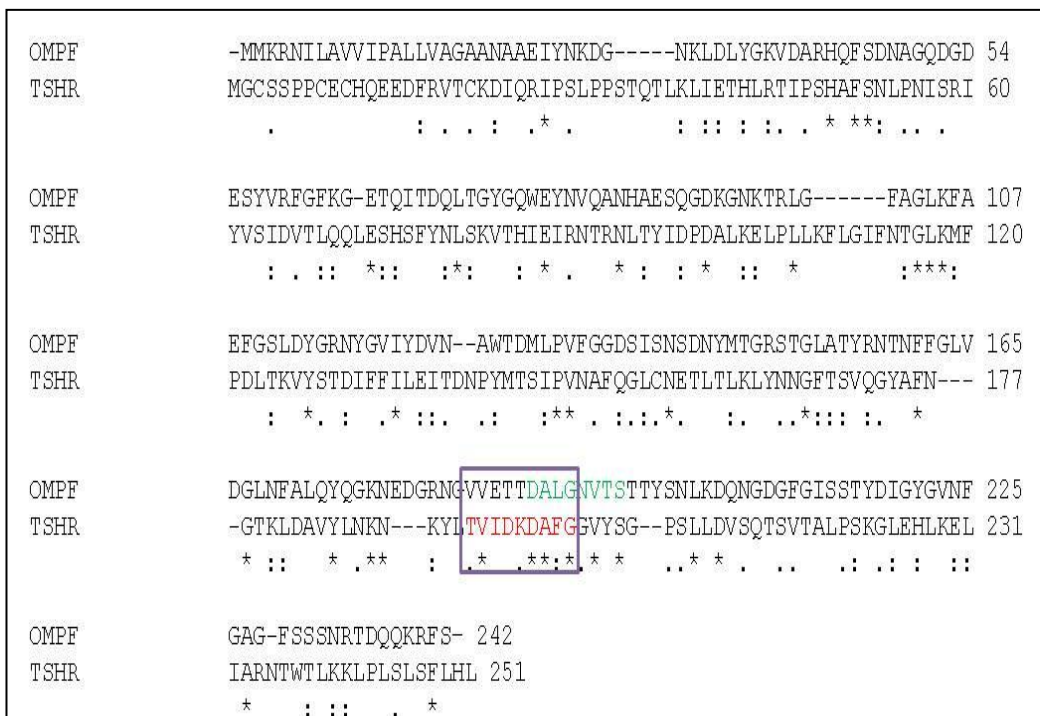
Figure 58: Amino acid sequence alignment of OmpC and TSHR.

A sequence alignment was performed to assess whether there is any aa sequence homology between OmpC and TSHR. The epitope of mAb A9 is highlighted in red. The four TSHR aa residues highlighted by a purple box, 198 DAFG 201, were shown by deletion to be essential for mAb A9 binding to TSHR and OmpF by Wang *et al*, 2010. Two of these four residues, 201 FG 202, are identical between OmpC and TSHR, whilst the aa residue at position 198 differs between the two proteins, they are both hydrophilic and structurally similar.

5.4 Discussion

Despite an initial link being made with GD and *Y. enterocolitica* in the late 1970s, consistent findings are lacking and the potential role of *Y. enterocolitica* remains controversial (Bech et al., 1974; Brix et al., 2008; Resetkova et al., 1994). One definitive way to examine the role of *Y. enterocolitica proteins* in the pathogenesis of GD is to use pathogenic TSAbs, rather than whole serum samples as have been used in all previous studies over the past three decades. Thus, my studies reported here with KSAb1 and KSAb2 are novel in their approach as the first use of TSAbs to tackle this question. At the same time, this also gave us the opportunity to examine the relationship of rFab germline with *Y. enterocolitica,* which may potentially give an insight into the role of microbial proteins in expanding early precursor B cells by SHM into pathogenic antibodies.

In order to attempt to ascertain the antigen specificity of rFab germline, a number of different possible avenues were considered, including screening commercially available autoantigen arrays, pathogen-associated peptide microarrays and random peptide screens (Maier et al., 2010; Prechl et al., 2010). In a rational approach, we decided to focus our efforts on *Y. enterocolitica* and Western blotting due to the precedence in the literature. We used two serotypes, O:3 and O:8, both of which have been widely used by various studies investigating a potential link between GD and *Y. enterocolitica* (Luo et al., 1993; Wang et al., 2010). No consistent *Y. enterocolitica* protein from either serotype has been

implicated with GD. We attempted to use all of the various protein preparations that have been previously reported in the literature: Yops, whole cell lysates and envelope proteins. Due to difficulties in their isolation, Yops were prepared solely from serotype O:8.

No binding of Yops was observed with KSAb1 IgG, KSAb2 IgG or rFab germline when assessed by Western blotting using alkaline phosphatase development system. Binding to whole cell lysate and envelope preparations was observed for KSAb1 IgG, KSAb2 IgG, rFab germline and the neutral mAb A9. A consistent band was observed in the whole cell lysate and envelope protein preparations of both serotypes migrating with an apparent MW of 37 kDa for rFab germline, KSAb1 IgG, KSAb2 IgG and mAb A9. No binding was observed with the relevant isotype controls. Binding to envelope protein preparations suggest that these proteins are on the outer surface of the bacterium where it may be easily accessed by the immune system (Białas et al., 2012). Interestingly, KSAb1 IgG and KSAb2 IgG show bimodal reactivity by recognising TSHR and continuing to recognise a *Y. enterocolitica* protein. There is precedence in the literature for autoreactive antibodies to bind both an autoantigen and a bacterial antigen, as myocarditis antibodies have been shown to cross-react with Streptococcus polysaccharide (Malkiel et al., 2000).

Immobilised matrix-coupled KSAb1 IgG was incubated with *Y. enterocolitica* and the eluted proteins with an approximate MW of 37 kDa were analysed by MALDI-TOF for identification. The two most abundant proteins were identified as OmpA and OmpC. A synthetic gene construct

of *ompA* was synthesised for cloning and expression as recombinant protein whilst *ompC* was provided as cDNA by Dr Anna Stenkova, as well as *ompF* as mAb A9 has previously been shown to bind to this porin (Wang et al., 2010).

Recombinant OmpA, OmpC and OmpF were evaluated for binding with rFab germline, KSAb1 IgG, KSAb2 IgG, mAb A9 IgG and their relevant isotype-matched and negative controls. rFab germline displayed binding to OmpC and OmpF, the binding to both porins may be a result of the high degree of N-terminal sequence homology between the two porins, as well as weak binding to OmpA. KSAb1 and KSAb2 IgG surprisingly displayed binding to all three porins and the previously published binding of mAb A9 to OmpF (Wang et al., 2010) was confirmed as well as the novel finding of mAb A9 showing reactivity to OmpC. This data suggests that two TSAbs developed from a germline precursor antibody that recognised Omp proteins and that through SHM, TSHR reactivity was acquired and reactivity to porin proteins was maintained.

KSAb1 and KSAb2 were established from BALB/c mice, housed under specific pathogen-free conditions and thus unlikely to have been exposed to *Y. enterocolitica*. Porins are ubiquitously expressed by gram-negative bacteria (Nikaido, 2003) and it is possible that the precursor B cell clone expressing the germline antibody that would give rise to KSAb1 and KSAb2 was expanded by a pathogen of the microbiota expressing OmpC and/or OmpF. Through SHM and molecular mimicry this precursor clone then began to develop TSHR reactivity. However as this is an induced model of disease, it is most likely that the clone was expanded by the

immunogen, the TSHR A-subunit, as a result of immunisation. Thus it is likely that Omp-specific precursor was expanded by TSHR A-subunit antigen as a result of cross-reactivity.

The studies described here have been limited to *Y. enterocolitica* but future work could include the screening of porins from other bacterial species, as for example, there is a high degree of sequence homology between the Omps expressed by *Y. enterocolitica* and Omps expressed by *E. coli* K12. Immunisation of female BALB/c mice independently with purified recombinant OmpA, OmpC or OmpF and analysing serum for measurable anti-TSHR antibodies or hyperthyroidism would indicate whether there is a casual relationship between *Y. enterocolitica* Omps or whether priming of susceptible B cells with these proteins can precipitate an anti-thyroid immune response. Previous studies that have immunised mice with total *Y. enterocolitica* proteins lead to anti-TSHR antibodies but did not precipitate hyperthyroidism, therefore the anti-TSHR antibodies produced were not pathogenic (Luo et al., 1993). This may have been due to antigenic competition as whole *Y. enterocolitica* was used and this may have weakened the induced immune response, or because the mouse strain used was not the most suited for induced hyperthyroidism (Nagayama, 2007).

This data raises the interesting implication that two TSAbs have developed from a non-autoreactive pathogen-specific precursor, and whilst TSHR reactivity was acquired through numerous SHM, pathogen binding was maintained.

5.5   Conclusions

In conclusion, the results reported are novel and indicate recognition of *Y. enterocolitica* porins, OmpA, OmpC and OmpF by TSAbs, KSAb1 and KSAb2 and their precursor, expressed as rFab germline. With the available data, it is presently difficult to either support or dismiss a causal relationship between the development of TSHR reactivity and recognition of the porins and how they may be related to the development of TSAbs resulting in hyperthyroidism. However my work sets a precedent for future *in vivo* experiments to explore this further. Importantly, as reported by Wang and colleagues (Wang et al., 2010) the binding of mAb A9 to OmpF was confirmed, in addition this mAb shows binding to the related porin, OmpC. Future work can also include studies on evaluation on the structural basis of the porins and their homology to the TSHR A-subunit to begin to understand cross-reactivity at a molecular level.

CHAPTER SIX

CONCLUDING REMARKS

6   CHAPTER SIX: Concluding remarks

There are a number of novel research findings reported in this thesis:

- The germline antibody committed to producing two TSAbs through SHM does not recognise the TSHR, the target autoantigen of GD.

- The antigens recognised by the germline revertant, when expressed as rFab, has been identified by MALDI-TOF analysis as OmpA, OmpC and OmpF of *Y. enterocolitica*, thereby providing additional supporting evidence for the role on infection in GD

- The unexpected discovery of the bimodal reactivity of the two TSAbs, recognising TSHR and OmpA, OmpC and OmpF of *Y. enterocolitica*. This potentially provides a model for (i) activation of the early precursor B cell clones by the microbial antigen to expand by SHM to form pathogenic TSAbs and (ii) the chronic nature of GD where the B cells secreting pathogenic TSAbs in the secondary lymphoid organs are constantly activated by the microbial antigen to maintain the hyperthyroidism.

- Unequivocal demonstration of the dominant role of the H-chain in conferring binding to the TSHR, demonstrated for the first time at the molecular level.

The finding that the shared immature antibody encoded by the germline genes of two TSAbs does not recognise the TSHR is a novel finding and has not been reported previously for GD. This suggests that the precursor B cells are not deleted by central tolerance as they do not recognise the autoantigen, TSHR, and thus exit the bone marrow as immature B cells to

enter the secondary lymphoid organs. In the periphery, these precursor B cells are activated to undergo SHM to become autoreactive and produce TSAbs. The only other autoimmune condition where the autoantigen-specificity of the germline revertant has been studied in detail is SLE. Importantly, both mouse and human mAbs have been investigated in detail, where many of the germline revertants do not recognise the autoantigens, DNA and nucleoproteins. (Guo et al., 2010; Wellmann et al., 2005), been investigated. Thus our findings that germline revertant in an experimental model of GD does not recognise the target autoantigen are comparable to the findings in SLE. As the antigen-specificity of germline forms of pathogenic antibodies has previously only been described in the non-organ specific SLE, it is difficult to draw firm conclusions on the contribution of precursor antibodies in autoimmunity in general. It is therefore of interest for such germline revertant studies to be repeated in other antibody-mediated autoimmune conditions, and importantly, for this study to be replicated with human thyroid antibodies to validate the findings described here for mouse-derived thyroid antibodies.

GD is known to have a complex aetiology, with both genetic and environmental factors (Brix and Hegedüs, 2012), however how they interact to cause disease is currently unknown. Previous studies whereby mice have been immunised with *Y. enterocolitica* serotype O:8 have generated anti-TSHR antibodies without pathogenic activity that cross-react with lipoprotein (Luo et al., 1993; Zhang et al., 1997). A recent study showed cross-reactivity of a non-pathogenic neutral mAb, mAb A9, with

OmpF of *Y. enterocolitica,* serotype O:3 (Wang et al., 2010). The novelty of the study described here relies on the evaluation of two highly potent TSAbs, whose pathogenicity is without doubt (Flynn et al., 2007; Gilbert et al., 2006b), for cross-reactivity with *Y. enterocolitica* serotypes O:3 and O:8. KSAb1 and KSAb2 have been shown to cross-react with OmpA, OmpC and OmpF of *Y. enterocolitica*.

Further studies are warranted to immunise BALB/c mice with individual purified Omps in adjuvant and to evaluate the serum for anti-TSHR antibodies, as well as examining thyroid and orbital tissues for histological changes. It is of particular interest to evaluate whether the isolated human TSAbs, M22 and K1-18, also cross react with OmpA, OmpC and/or OmpF, or other *Y. enterocolitica* proteins. Considering that TSHR agonism is a special antibody property and that KSAb1 is a comparable stimulator to M22 (Mizutori et al., 2009), it may be assumed that KSAb1 and M22 have over-lapping TSHR epitopes and thus may have overlapping Omp epitopes. Evaluation of the isolated human TSBAbs, 5C9 and K1-70, for cross-reactivity with *Y. enterocolitica* porins would also be of interest, particularly as we have shown that a neutral mAb recognises OmpC and OmpF, but not OmpA, whilst TSAbs and their germline precursor recognise all three. Potentially any differences in TSHR binding and stimulating activity may be reflected in the porins recognised.

Genetic studies in various strains of inbred mice have shown that loci in the IGHV gene locus are responsible for the major contribution towards the recognition of TSHR (Rapoport et al., 2010). The data in this thesis

based upon L-chain swaps between KSAb1 and its germline revertant show unequivocally that the somatically mutated H-chain of the TSAb, KSAb1, dominates in contributing to the binding of TSHR. However the pairing of the H-chain with the germline L-chain originally used by the TSAbs was essential for the binding to TSHR, since when the mature H-chain was paired with an irrelevant L-chain, all measurable TSHR binding was lost. For future studies, it would be interesting to investigate in greater detail the role of SHM towards recognition of TSHR and hence the development of autoreactivity. A pressing example would be the role of the n=21 SHM common to the H-chains of both KSAb1 and KSAb2 prior to their diversification (Padoa et al., 2010), see Chapter 3, Figure 17, page 119, paired with the mature L-chains of KSAb1 and KSAb2 to recognise the TSHR.

The novel finding that the germline precursor antibody of two TSAbs recognises a microbial antigen of *Y. enterocolitica*, rather than TSHR, raises interesting possibilities for the development of autoimmunity in humans. DCs in the gastrointestinal tract could process antigens derived from *Y. enterocolitica* or other Omp-expressing commensal bacteria and present this antigen to T cells and B cells in secondary lymphoid organs. In a genetically predisposed individual, with the convergence of certain genetic and environmental factors, an Omp-specific B cell may develop thyroid reactivity through SHM and may not be deleted by peripheral tolerance mechanisms, allowing autoimmunity to develop.

Appendices

Appendix 1

<u>LURIA BERTANI (LB) AGAR</u>   <u>600 mL</u>

Tryptone   6 g

Yeast   3 g

NaCl   6 g

Agar   9 g

<u>LURIA BERTANI (LB) BROTH</u>   <u>1 L</u>

Tryptone   10 g

Yeast   5 g

NaCl   10 g

<u>SOC MEDIUM</u>   <u>100 mL</u>

Tryptone   0.2 g

Yeast   0.05 g

5 M NaCl   0.02 mL

1 M KCl   0.025 mL

1 M $MgCl_2$ 0.1 mL

1 M $MgSO_4$ 0.1 mL

1 M glucose (added after autoclaving)   0.2 mL

<u>50% GLYCEROL</u>

100% glycerol	50 mL
dH$_2$O	50 mL

Appendix 2

<u>50 X TAE BUFFER</u>	<u>1 L</u>
Tris	242 g
Glacial acetic acid	57.1 mL
EDTA	18.6 g

Dilute 20 mL 50 X TAE with 980 mL dH$_2$O for 1 X solution

<u>AGAROSE GEL</u>

<u>0.8%:</u>

Agarose	0.8 g
1 X TAE	100 mL

<u>1.2%</u>

Agarose	1.2 g
1 X TAE	100 mL

Appendix 3

<u>ANTIBIOTICS</u>

AMPICILLIN (100 mg/mL)

Ampicillin	1 g
dH$_2$O	10 mL

CHLORAMPHENICOL (34 mg/mL)

| Chloramphenicol | 3.4 g |
| Ethanol | 10 mL |

TETRACYCLINE (5 mg/mL)

Tetracycline	50 mg
dH$_2$O	5 mL
Ethanol	5 mL

Stored at -20°C away from light

Appendix 4

10 X MOPS BUFFER	1 L
MOPS	83.72 g
Tricine	7.17 g

Volume made up to 300 mL with dH$_2$O and pH adjusted to pH 7.4 with 10 M

KOH

0.1 M FeSO$_4$	10 mL
1.9 M NH$_4$Cl	50 mL
0.296 M K$_2$SO$_4$	10 mL
0.02 M CaCl$_2$.2H$_2$O	250 µl
2.5 M MgCl$_2$	2.1 mL
5 M NaCl	100 mL
Micronutrient broth	0.2 mL
dH$_2$O	387 mL

Filter sterilised with a 0.22 µm filter

MICRONUTRIENT BROTH	50 mL
Ammonium molybdate	0.009 g
Boric acid	0.062 g
Cobalt chloride	0.018 g
Cupric sulphate	0.006 g
Manganese chloride	0.04 g
Zinc sulphate	0.007 g

Volume made up to 50mL with dH_2O

1 X MOPS WITH PHOSPHATE	1 L
10 X MOPS medium	100 mL
0.132 M K_2HPO_4	10 mL
1 mg/mL thiamine	0.1 mL
dH_2O	990 mL

The pH was adjusted to pH 7.2 with 10 M NaOH and the buffer filter sterilised

with a 0.22 µm filter

Just before use:

10% filter-sterilised glucose	10 mL
5 mg/mL tetracycline	2 mL

1 X MOPS WITHOUT PHOSPHATE	1L

As above for 1 X MOPS with phosphate, but no K_2HPO_4 was added. The

pH was not adjusted.

EXTRACTION BUFFER	100 mL
100 mM Hepes pH 7.5	10 mL
5 M NaCl	10 mL
1 M Imidazole	100 µl
100 mM Benzamidine	10 mL
10 mM PMSF	10 mL

WASH BUFFER	100 mL
100 mM Hepes pH 7.5	10 mL
5 M NaCl	10 mL
1 M Imidazole	100 µl
dH_2O	90.9 mL

ELUTION BUFFER	100 mL
100 mM Hepes pH 7.5	10 mL
5 M NaCl	10 mL
1 M Imidazole	30 mL
dH_2O	50 mL

10 X PBS	1 L
NaCl	8 g
KCL	0.2 g
Na_2HPO_4	1.44 g
KH_2PO_4	0.24 g

Diluted 1/10 to make 1 X solution and both were autoclaved before use

Appendix 5

SEPARATING GEL (12%)	30 mL
30% acrylamide (Protogel)	12 mL
1 M Tris pH 8.8	11.25 mL
1.5% ammonium persulphate	1 mL
10% SDS	0.5 mL
dH$_2$O	5.75 mL
TEMED	10 µl

STACKING GEL	10 mL
30% acrylamide (Protogel)	1 mL
1 M Tris pH 8.8	1.25 mL
1.5% ammonium persulphate	0.5 mL
10% SDS	0.3 mL
dH$_2$O	6.95 mL
TEMED	10 ul

1 M TRIS BASE pH 8.8	1 L
Tris base	121.8 g
dH$_2$O	700 mL

Volume made up to 1 L with dH$_2$O adjusting pH to 8.8 with 5 M HCl

1 M TRIS BASE pH 6.8	500 mL
Tris base	60.5 g
dH$_2$O	250 mL

Volume made up to 1 L with dH$_2$O adjusting pH to 6.8 with 5 M HCl

RUNNING BUFFER (10 X)	1 L
Glycine	144.13 g
Tris base	30.28 g
SDS	10 g

Dilute 1/10 with dH$_2$O for 1 X solution

LOADING GEL BUFFER (2 X)	5 mL
1 M Tris pH 6.8	1.25 mL
10% SDS	1 mL
50% Sucrose, 0.1% Bromophenol blue	2 mL
dH$_2$O	0.75 mL

Dilute 1:2 with sample

COOMASSIE BLUE	
Coomassie R250	0.5 g
Methanol	250 mL
Stir for 30 minutes, and then add:	
dH$_2$O	250 mL
Acetic acid	50 mL

DESTAIN   1 L

Methanol   300 mL

Acetic acid   100 mL

dH$_2$O   600 mL

WESTERN TRANSFER BUFFER (1 X)   2 L

10 X SDS running buffer   200 mL

Methanol   200 mL

dH$_2$O   1600 mL

Appendix 6

HANK'S BUFFERED SALT SOLUTION 1 L
(HBSS)

CaCl$_2$.2H$_2$O	0.185 g
KCl	5.33 g
KH$_2$PO$_4$	0.06 g
MgCl$_2$	0.048 g
MgSO$_4$.7H$_2$O	0.101 g
NaHCO$_3$	0.336 g
Na$_2$HPO$_4$	0.043 g
Glucose	1.008 g
Hepes	4.776 g
Sucrose	75.991 g

Appendix 7

YERSINIA LURIA BERTANI (LB) BROTH	1 L
Tryptone	10 g
Yeast	5 g
NaCl	5 g

COUPLING BUFFER	1 L
NaHCO$_3$	8.3 g
NaCl	29 g

Adjusted to pH 8.5 with 1 M NaOH

ACETATE BUFFER (0.1 M)	1 L
NaOAc	13.6 g
NaCL	29.22 g

Adjusted to pH 4 with concentrated acetic acid

LYSIS BUFFER	50 mL
5 M NaCl	1 mL
1 M Tris-HCl pH 8	500 µL
0.5 M EDTA	80 µL
10% Triton-X 100	200 µL
dH$_2$O	48.25 mL

Appendix 8: Sequence confirmation of germline construct compared to the expected, reference, sequence

```
REFERENCE        ------------------------------------------GAATTCGAGCTCGGTAC
L CHAIN          NNNNNNNNNNCNNNTNNTTTTATTTTTTATGTATTTGTAACTAGAATTCGAGCTCGGTAC
                                                           ****************


REFERENCE        CCGGGGATCCTCTAGAGGTTGAGGTGATTTTATGAAAAAGAATATCGCATTTCTTCTTGC
L CHAIN          CCGGGGATCCTCTAGAGGTTGAGGTGATTTTATGAAAAAGAATATCGCATTTCTTCTTGC
                 ************************************************************


REFERENCE        ATCTATGTTCGTTTTTTCTATTGCTACAAACGCGTATGCTGACATTGTGATGACCCAGTC
L CHAIN          ATCTATGTTCGTTTTTTCTATTGCTACAAACGCGTATGCTGACATTGTGATGACCCAGTC
                 ************************************************************


REFERENCE        TCAAAAATTCATGTCCACATCAGTAGGAGACAGGGTCAGCATCACCTGCAAGGCCAGTCA
L CHAIN          TCAAAAATTCATGTCCACATCAGTAGGAGACAGGGTCAGCATCACCTGCAAGGCCAGTCA
                 ************************************************************


REFERENCE        GAATGTGGGTACTGCTGTAGCCTGGTATCAACAGAAACCAGGACAATCTCCTAAACTACT
L CHAIN          GAATGTGGGTACTGCTGTAGCCTGGTATCAACAGAAACCAGGACAATCTCCTAAACTACT
                 ************************************************************


REFERENCE        GATTTACTCGGCATCCAATCGGTACACTGGAGTCCCTGATCGCTTCACAGGCAGTGGATC
L CHAIN          GATTTACTCGGCATCCAATCGGTACACTGGAGTCCCTGATCGCTTCACAGGCAGTGGATC
                 ************************************************************


REFERENCE        TGGGACAGATTTCACTCTCACCATCAGCAATATGCAGTCTGAAGACCTGGCAGATTATTT
L CHAIN          TGGGACAGATTTCACTCTCACCATCAGCAATATGCAGTCTGAAGACCTGGCAGATTATTT
                 ************************************************************


REFERENCE        CTGCCAGCAATATAGCAGCTATCCTTACACGTTCGGAGGGGGGACCAAGCTGGAAATAAA
L CHAIN          CTGCCAGCAATATAGCAGCTATCCTTACACGTTCGGAGGGGGGACCAAGCTGGAAATAAA
                 ************************************************************
```

```
REFERENCE     ACGGGCTGATGCTGCACCAACTGTATCCATCTTCCCACCATCCAGTGAGCAGTTAACATC
L CHAIN       ACGGGCTGATGCTGCACCAACTGTATCCATCTTCCCACCATCCAGTGAGCAGTTAACATC
              ************************************************************


REFERENCE     TGGAGGTGCCTCAGTCGTGTGCTTCTTGAACAACTTCTACCCCAAAGACATCAATGTCAA
L CHAIN       TGGAGGTGCCTCAGTCGTGTGCTTCTTGAACAACTTCTACCCCAAAGACATCAATGTCAA
              ************************************************************


REFERENCE     GTGGAAGATTGTTGGCAGTGAACGACAAAATGGCGTCCTGAACAGTTGGACTGATCAGGA
L CHAIN       GTGGAAGATTGTTGGCAGTGAACGACAAAATGGCGTCCTGAACAGTTGGACTGATCAGGA
              ************************************************************


REFERENCE     CAGCAAAGACAGCACCTACAGCATGAGCAGCACCCTCACGTTGACCAAGGACGAGTATGA
L CHAIN       CAGCAAAGACAGCACCTACAGCATGAGCAGCACCCTCACGTTGACCAAGGACGAGTATGA
              ************************************************************


REFERENCE     ACGACATAACAGCTATACCTGTGAGGCCACTCACAAGACATCAACTTCACCCATTGTCAA
L CHAIN       ACGACATAACAGCTATACCTGTGAGGCCACTCACAAGACATCAACTTCACCCATTGTCAA
              ************************************************************
REFERENCE     TGTACACAAGTTCACGTAAAAAGGGTATCTAGAGGTTGAGGTGAT
H CHAIN       TGTACACAAGTTCACGTAAAAAGGGTATCTAGAGGTTGAGGTGAT
              *********************************************


REFERENCE     TTTATGAAAAAGAATATCGCATTTCTTCTTGCATCTATGTTCGTTTTTTCTATTGCTACA
H CHAIN       TTTATGAAAAAGAATATCGCATTTCTTCTTGCATCTATGTTCGTTTTTTCTATTGCTACA
              ************************************************************


REFERENCE     AACGCGTACGCTGAGATCCAGCTGCAGCAGTCTGGACCTGAGCTGGTGAAGCCTGGGGCT
H CHAIN       AACGCGTACGCTGAGATCCAGCTGCAGCAGTCTGGACCTGAGCTGGTGAAGCCTGGGGCT
              ************************************************************


REFERENCE     TCAGTGAAGGTATCCTGCAAGGCTTCTGGTTACTCATTCACTGACTACAACATGTACTGG
H CHAIN       TCAGTGAAGGTATCCTGCAAGGCTTCTGGTTACTCATTCACTGACTACAACATGTACTGG
```

```
              ************************************************************

REFERENCE     GTGAAGCAGAGCCATGGAAAGAGCCTTGAGTGGATTGGATATATTGATCCTTACAATGGT
H CHAIN       GTGAAGCAGAGCCATGGAAAGAGCCTTGAGTGGATTGGATATATTGATCCTTACAATGGT
              ************************************************************

REFERENCE     GGTACTAGCTACAACCAGAAGTTCAAGGGCAAGGCCACATTGACTGTTGACAAGTCCTCC
H CHAIN       GGTACTAGCTACAACCAGAAGTTCAAGGGCAAGGCCACATTGACTGTTGACAAGTCCTCC
              ************************************************************

REFERENCE     AGCACAGCCTTCATGCATCTCAACAGCCTGACATCTGAGGACTCTGCAGTCTATTACTGT
H CHAIN       AGCACAGCCTTCATGCATCTCAACAGCCTGACATCTGAGGACTCTGCAGTCTATTACTGT
              ************************************************************

REFERENCE     GCAAGAAGGGACTGGGACTACTTTGACTACTGGGGCCAAGGCACCACTCTCACAGTCTCC
H CHAIN       GCAAGAAGGGACTGGGACTACTTTGACTACTGGGGCCAAGGCACCACTCTCACAGTCTCC
              ************************************************************

REFERENCE     TCAGCCAAAACAACAACCCCATCAGTCTATCCACTGGCCCCTGGGTGTGGAGATACAACT
H CHAIN       TCAGCCAAAACAACAACCCCATCAGTCTATCCACTGGCCCCTGGGTGTGGAGATACAACT
              ************************************************************

REFERENCE     GGTTCCTCCGTGACTCTGGGATGCCTGGTCAAGGGCTACTTCCCTGAGTCAGTGACTGTG
H CHAIN       GGTTCCTCCGTGACTCTGGGATGCCTGGTCAAGGGCTACTTCCCTGAGTCAGTGACTGTG
              ************************************************************

REFERENCE     ACTTGGAACTCTGGATCCCTGTCCAGCAGTGTGCACACCTTCCCAGCTCTCCTGCAGTCT
H CHAIN       ACTTGGAACTCTGGATCCCTGTCCAGCAGTGTGCACACCTTCCCAGCTCTCCTGCAGTCT
              ************************************************************

REFERENCE     GGACTCTACACTATGAGCAGCTCAGTGACTGTCCCCTCCAGCACCTGGCCAAGTCAGACC
H CHAIN       GGACTCTACACTATGAGCAGCTCAGTGACTGTCCCCTCCAGCACCTGGCCAAGTCAGACC
              ************************************************************
```

227

```
REFERENCE      GTCACCTGCAGCGTTGCTCACCCAGCCAGCAGCACCAAGGTGGACAAGAAAATTGAGACC
H CHAIN        GTCACCTGCAGCGTTGCTCACCCAGCCAGCAGCACCAAGGTGGACAAGAAAATTGAGACC
               ************************************************************


REFERENCE      CGTCACCACCACCACCACCACTAACGCGGCATGCGACGGCCCTAGAGTCCCTAACGCTCG
H CHAIN        CGTCACCACCACCACCACCACTAACGCGGCATGCGACGGCCCTAGAGTCCCTAACGCTCG
               ************************************************************
```

228

References

Adams, D.D., and H.D. Purves. 1956. The assessment of thyroid function by tracer tests with radioactive iodine. *N Z Med J* 55:36-41.

Ai, J., J.M. Leonhardt, and a.W.R. Heymann. 2003. Autoimmune thyroid diseases: Etiology, pathogenesis, and dermatologic manifestations. *Journal of the American Academy of Dermatology* 48:641-659.

Ajjan, R., and A. Weetman. 2008. Techniques to quantify TSH receptor antibodies. *Nature Clinical Practice Endocrinology & Metabolism* 4:461-468.

Akamizu, T., M.M. Sale, S.S. Rich, H. Hiratani, J.Y. Noh, N. Kanamoto, M. Saijo, Y. Miyamoto, Y. Saito, K. Nakao, and D.W. Bowden. 2000. Association of autoimmune thyroid disease with microsatellite markers for the thyrotropin receptor gene and CTLA-4 in Japanese patients. *Thyroid : official journal of the American Thyroid Association* 10:851-858.

Akirav, E.M., N.H. Ruddle, and K.C. Herold. 2011. The role of AIRE in human autoimmune disease. *Nat Rev Endocrinol* 7:25-33.

Albert, L.J., and R.D. Inman. 1999. Molecular mimicry and autoimmunity. *N Engl J Med* 341:2068-2074.

Alegre, M.-L., K.A. Frauwirth, and C.B. Thompson. 2001. T-cell regulation by CD28 and CTLA-4. *Nat Rev Immunol* 1:220-228.

Ando, T. 2003. Induction of Thyroid-Stimulating Hormone Receptor Autoimmunity in Hamsters. *Endocrinology* 144:671-680.

Ando, T., M. Imaizumi, P.N. Graves, P. Unger, and T.F. Davies. 2002. Intrathyroidal fetal microchimerism in Graves' disease. *J Clin Endocrinol Metab* 87:3315-3320.

Andresen, H., K. Zarse, C. Grotzinger, J. Hollidt, E. Ehrentreichforster, F. Bier, and O. Kreuzer. 2006. Development of peptide microarrays for epitope mapping of antibodies against the human TSH receptor. *Journal of Immunological Methods* 315:11-18.

Armengol, M.P., M. Juan, A. Lucas-Martín, M.T. Fernández-Figueras, D. Jaraquemada, T. Gallart, and R. Pujol-Borrell. 2001. Thyroid Autoimmune Disease: Demonstration of Thyroid Antigen-Specific B Cells and Recombination-Activating Gene Expression in Chemokine-Containing Active Intrathyroidal Germinal Centers. *The American Journal of Pathology* 159:861-873.

Bahn, R.S. 2010. Graves' Ophthalmopathy. *New England Journal of Medicine* 362:726-738.

Bahn, R.S. 2012. Autoimmunity and Graves/' Disease. *Clin Pharmacol Ther* 91:577-579.

Baldet, L., M. Robin, and H. Lapinski. 1974. [HL-A and Basedow's disease]. *Revue francaise de transfusion* 17:305-321.

Ban, Y., D.A. Greenberg, E.S. Concepcion, and Y. Tomer. 2002. A Germline Single Nucleotide Polymorphism at the Intracellular Domain of the Human Thyrotropin Receptor Does Not Have a Major Effect on the Development of Graves' Disease. *Thyroid* 12:1079-1083.

Banga, J.P., editor. 2007. The long and winding road for an experimental model of hyperthyroid Graves' disease. Georg Thieme Verlag, Stuttgart. 118-125 pp.

Banga, J.P., R. Mirakian, L. Hammond, G. Pryce, S. Bidey, F. Bottazzo, A.P. Weetman, A.M. McGregor, and I.M. Roitt. 1986. Characterization of monoclonal antibodies directed towards the microsomal/microvillar thyroid autoantigen recognized by Hashimoto autoantibodies. *Clinical and Experimental Immunology* 64:544-554.

Banga, J.P., C.H. Nielsen, J.A. Gilbert, D. El Fassi, and L. Hegedus. 2008. Application of New Therapies in Graves' Disease and Thyroid-Associated Ophthalmopathy: Animal Models and Translation to Human Clinical Trials. *Thyroid* 18:973-981.

Barin, J.G., M.V. Talor, R.B. Sharma, N.R. Rose, and C.L. Burek. 2005. Iodination of murine thyroglobulin enhances autoimmune reactivity in the NOD.H2h4 mouse. *Clinical & Experimental Immunology* 142:251-259.

Bartley, G.B. 1994. The epidemiologic characteristics and clinical course of ophthalmopathy associated with autoimmune thyroid disease in Olmsted County, Minnesota. *Trans Am Ophthalmol Soc* 92:477-588.

Bassett, J.H.D., and G.R. Williams. 2008. Critical role of the hypothalamic–pituitary–thyroid axis in bone. *Bone* 43:418-426.

Basten, A., and P.A. Silveira. 2010. B-cell tolerance: mechanisms and implications. *Current Opinion in Immunology* 22:566-574.

Bech, K., J. Larsen, J. Hansen, and J. Nerup. 1974. Letter: Yersinia enterocolitica infection and thyroid disorders. *Lancet* 7886:951-952.

Benvenga, S., F. Guarneri, M. Vaccaro, L. Santarpia, and F. Trimarchi. 2004. Homologies between proteins of Borrelia burgdorferi and thyroid autoantigens. *Thyroid* 14:964-966.

Benvenga, S., L. Santarpia, F. Trimarchi, and F. Guarneri. 2006. Human thyroid autoantigens and proteins of Yersinia and Borrelia share amino acid sequence homology that includes binding motifs to HLA-DR molecules and T-cell receptor. *Thyroid* 16:225-236.

Białas, N., K. Kasperkiewicz, J. Radziejewska-Lebrecht, and M. Skurnik. 2012. Bacterial Cell Surface Structures in <i>Yersinia enterocolitica</i>. *Archivum Immunologiae et Therapiae Experimentalis* 60:199-209.

Bianco, A.C., and B.W. Kim. 2006. Deiodinases: implications of the local control of thyroid hormone action. *The Journal of Clinical Investigation* 116:2571-2579.

Blair, P.A., L.Y. Norena, F. Flores-Borja, D.J. Rawlings, D.A. Isenberg, M.R. Ehrenstein, and C. Mauri. 2010. CD19(+)CD24(hi)CD38(hi) B cells exhibit regulatory capacity in healthy individuals but are functionally impaired in systemic Lupus Erythematosus patients. *Immunity* 32:129-140.

Blanchin, S., V. Estienne, J.M. Durand-Gorde, P. Carayon, and J. Ruf. 2003. Complement activation by direct C4 binding to thyroperoxidase in Hashimoto's thyroiditis. *Endocrinology* 144:5422-5429.

Boehm, T. 2011. Design principles of adaptive immune systems. *Nat Rev Immunol* 11:307-317.

Boelaert, K., P.R. Newby, M.J. Simmonds, R.L. Holder, J.D. Carr-Smith, J.M. Heward, N. Manji, A. Allahabadia, M. Armitage, K.V. Chatterjee, J.H. Lazarus, S.H. Pearce, B. Vaidya, S.C. Gough, and J.A. Franklyn. 2010. Prevalence and Relative Risk of Other Autoimmune Diseases in Subjects with Autoimmune Thyroid Disease. *The American Journal of Medicine* 123:183.e181-183.e189.

Brand, O.J., and S.C.L. Gough. 2010. Genetics of thyroid autoimmunity and the role of the TSHR. *Molecular and Cellular Endocrinology* 322:135-143.

Brent, G.A. 2008. Clinical practice. Graves' disease. *N Engl J Med* 358:2594-2605.

Brix, T.H., K. Christensen, N.V. Holm, B. Harvald, and L. Hegedus. 1998a. A population-based study of Graves' disease in Danish twins. *Clinical Endocrinology* 48:397-400.

Brix, T.H., P.S. Hansen, L. Hegedüs, and B.E. Wenzel. 2008. Too early to dismiss Yersinia enterocolitica infection in the aetiology of Graves' disease: evidence from a twin case-control study. *Clinical Endocrinology* 69:491-496.

Brix, T.H., P.S. Hansen, K.O. Kyvik, and L. Hegedus. 2009. Aggregation of Thyroid Autoantibodies in Twins from Opposite-Sex Pairs Suggests that Microchimerism May Play a Role in the Early Stages of Thyroid Autoimmunity. *Journal of Clinical Endocrinology & Metabolism* 94:4439-4443.

Brix, T.H., and L. Hegedüs. 2012. Twin studies as a model for exploring the aetiology of autoimmune thyroid disease. *Clinical Endocrinology* 76:457-464.

Brix, T.H., G.P.S. Knudsen, M. Kristiansen, K.O. Kyvik, K.H. Ørstavik, and L. Hegedüs. 2005. High Frequency of Skewed X-Chromosome Inactivation in Females with Autoimmune Thyroid Disease: A Possible Explanation for the Female Predisposition to Thyroid Autoimmunity. *Journal of Clinical Endocrinology & Metabolism* 90:5949-5953.

Brix, T.H., K.O. Kyvik, and L. Hegedus. 1998b. What is the evidence of genetic factors in the etiology of Graves' disease? A brief review. *Thyroid : official journal of the American Thyroid Association* 8:727-734.

Buckner, J.H. 2010. Mechanisms of impaired regulation by CD4+CD25+FOXP3+ regulatory T cells in human autoimmune diseases. *Nat Rev Immunol* 10:849-859.

Camargo, R.Y.A., E.K. Tomimori, S.C. Neves, I. G S Rubio, A.L. Galrao, M. Knobel, and G. Medeiros-Neto. 2008. Thyroid and the environment: exposure to excessive nutritional iodine increases the prevalence of thyroid disorders in Sao Paulo, Brazil. *European Journal of Endocrinology* 159:293-299.

Campbell, P.N., D. Doniach, R.V. Hudson, and I.M. Roitt. 1956. Auto-antibodies in Hashimoto's disease (lymphadenoid goitre). *Lancet* 271:820-821.

Carter, N.A., E.C. Rosser, and C. Mauri. 2012. Interleukin-10 produced by B cells is crucial for the suppression of Th17/Th1 responses,

induction of T regulatory type 1 cells and reduction of collagen-induced arthritis. *Arthritis Res Ther* 14:R32.

Carter, N.A., R. Vasconcellos, E.C. Rosser, C. Tulone, A. Mu√±oz-Suano, M. Kamanaka, M.R. Ehrenstein, R.A. Flavell, and C. Mauri. 2011. Mice Lacking Endogenous IL-10‚ÄìProducing Regulatory B Cells Develop Exacerbated Disease and Present with an Increased Frequency of Th1/Th17 but a Decrease in Regulatory T Cells. *The Journal of Immunology* 186:5569-5579.

Carter, P., R.F. Kelley, M.L. Rodrigues, B. Snedecor, M. Covarrubias, M.D. Velligan, W.L. Wong, A.M. Rowland, C.E. Kotts, M.E. Carver, and et al. 1992. High level Escherichia coli expression and production of a bivalent humanized antibody fragment. *Biotechnology (N Y)* 10:163-167.

Carter P, K.R., Rodrigues ML, Snedecor B, Covarrubias M, Velligan MD, Wong WL, Rowland AM, Kotts CE, Carver ME, et al. 1992. High level Escherichia coli expression and production of a bivalent humanized antibody fragment. *Biotechnology (N Y)* 10:163-167.

Chaplin, D.D. 2010. Overview of the immune response. *Journal of Allergy and Clinical Immunology* 125:S3-S23.

Chazenbalk, G.D. 2002. Thyroid-stimulating autoantibodies in Graves disease preferentially recognize the free A subunit, not the thyrotropin holoreceptor. *Journal of Clinical Investigation* 110:209-217.

Chazenbalk, G.D., P. Pichurin, C.R. Chen, F. Latrofa, A.P. Johnstone, S.M. McLachlan, and B. Rapoport. 2002. Thyroid-stimulating autoantibodies in Graves disease preferentially recognize the free

A subunit, not the thyrotropin holoreceptor. *The Journal of Clinical Investigation* 110:209-217.

Chen, C.R., P. Pichurin, G.D. Chazenbalk, H. Aliesky, Y. Nagayama, S.M. McLachlan, and B. Rapoport. 2004. Low-dose immunization with adenovirus expressing the thyroid-stimulating hormone receptor A-subunit deviates the antibody response toward that of autoantibodies in human Graves' disease. *Endocrinology* 145:228-233.

Chen, C.R., P. Pichurin, Y. Nagayama, F. Latrofa, B. Rapoport, and S.M. McLachlan. 2003. The thyrotropin receptor autoantigen in Graves disease is the culprit as well as the victim. *The Journal of Clinical Investigation* 111:1897-1904.

Chen, K., and A. Cerutti. 2011. The function and regulation of immunoglobulin D. *Current Opinion in Immunology* 23:345-352.

Chervonsky, A.V. 2010. Influence of microbial environment on autoimmunity. *Nature Immunology* 11:28-35.

Ciofani, M., and J.C. Zúñiga-Pflücker. 2010. Determining γδ versus αβ T cell development. *Nat Rev Immunol* 10:657-663.

Cohen, S., H. Dadi, E. Shaoul, N. Sharfe, and C.M. Roifman. 1999. Cloning and characterization of a lymphoid-specific, inducible human protein tyrosine phosphatase, Lyp. *Blood* 93:2013-2024.

Collins, A.V., D.W. Brodie, R.J. Gilbert, A. Iaboni, R. Manso-Sancho, B. Walse, D.I. Stuart, P.A. van der Merwe, and S.J. Davis. 2002. The interaction properties of costimulatory molecules revisited. *Immunity* 17:201-210.

Colobran, R., M.d.P. Armengol, R. Faner, M. Gärtner, L.-O. Tykocinski, A. Lucas, M. Ruiz, M. Juan, B. Kyewski, and R. Pujol-Borrell. 2011. Association of an SNP with intrathymic transcription of TSHR and Graves' disease: a role for defective thymic tolerance. *Human Molecular Genetics* 20:3415-3423.

Cornelis, G.R. 2002. Yersinia type III secretion. *J Cell Biol* 158:401-408.

Costagliola, S., P. Rodien, M.-C. Many, M. Ludgate, and G. Vassart. 1998. Genetic Immunization Against the Human Thyrotropin Receptor Causes Thyroiditis and Allows Production of Monoclonal Antibodies Recognizing the Native Receptor. *The Journal of Immunology* 160:1458-1465.

Couet, J., S. Sar, A. Jolivet, M.-T.V. Hai, E. Milgrom, and M. Misrahi. 1996. Shedding of Human Thyrotropin Receptor Ectodomain. *Journal of Biological Chemistry* 271:4545-4552.

Crotty, S., R.J. Johnston, and S.P. Schoenberger. 2010. Effectors and memories: Bcl-6 and Blimp-1 in T and B lymphocyte differentiation. *Nat Immunol* 11:114-120.

Czarnocka, B., J. Ruf, M. Ferrand, P. Carayon, and S. Lissitzky. 1985. Purification of the human thyroid peroxidase and its identification as the microsomal antigen involved in autoimmune thyroid diseases. *FEBS Lett* 190:147-152.

Dagdelen, S., Y.C. Kong, and J.P. Banga. 2009. Toward better models of hyperthyroid Graves' disease. *Endocrinol Metab Clin North Am* 38:343-354, viii.

Dağdelen, S.u., Y.-c.M. Kong, and J.P. Banga. 2009. Toward Better Models of Hyperthyroid Graves' Disease. *Endocrinology & Metabolism Clinics of North America* 38:343-354.

Daumerie, C., M. Ludgate, S. Costagliola, and M.C. Many. 2002. Evidence for thyrotropin receptor immunoreactivity in pretibial connective tissue from patients with thyroid-associated dermopathy. *Eur J Endocrinol* 146:35-38.

Davies, T.F., T. Ando, R.-Y. Lin, Y. Tomer, and R. Latif. 2005. Thyrotropin receptor–associated diseases: from adenomata to Graves disease. *The Journal of Clinical Investigation* 115:1972-1983.

de Forteza, R., C.U. Smith, J. Amin, J.M. McKenzie, and M. Zakarija. 1994. Visualization of the thyrotropin receptor on the cell surface by potent autoantibodies. *The Journal of Clinical Cndocrinology and Metabolism* 78:1271-1273.

Dechairo, B.M., D. Zabaneh, J. Collins, O. Brand, G.J. Dawson, A.P. Green, I. Mackay, J.A. Franklyn, J.M. Connell, J.A.H. Wass, W.M. Wiersinga, L. Hegedus, T. Brix, B.G. Robinson, P.J. Hunt, A.P. Weetman, A.H. Carey, and S.C. Gough. 2005. Association of the TSHR gene with Graves' disease: the first disease specific locus. *Eur J Hum Genet* 13:1223-1230.

Derbinski, J., A. Schulte, B. Kyewski, and L. Klein. 2001. Promiscuous gene expression in medullary thymic epithelial cells mirrors the peripheral self. *Nat Immunol* 2:1032-1039.

Dremier, S., K. Coulonval, S. Perpete, F. Vandeput, N. Fortemaison, A. Van Keymeulen, S. Deleu, C. Ledent, S. ClÉMent, S. Schurmans, J.E. Dumont, F. Lamy, P.P. Roger, and C. Maenhaut. 2002. The Role of Cyclic AMP and Its Effect on Protein Kinase A in the

Mitogenic Action of Thyrotropin on the Thyroid Cell. *Annals of the New York Academy of Sciences* 968:106-121.

Dromey, J.A., S.M. Weenink, G.H. Peters, J. Endl, P.J. Tighe, I. Todd, and M.R. Christie. 2004. Mapping of Epitopes for Autoantibodies to the Type 1 Diabetes Autoantigen IA-2 by Peptide Phage Display and Molecular Modeling: Overlap of Antibody and T Cell Determinants. *The Journal of Immunology* 172:4084-4090.

Duhen, T., R. Duhen, A. Lanzavecchia, F. Sallusto, and D.J. Campbell. 2012. Functionally distinct subsets of human FOXP3+ Treg cells that phenotypically mirror effector Th cells. *Blood* 119:4430-4440.

Dunn, J.T., and A.D. Dunn. 2001. Update on Intrathyroidal Iodine Metabolism. *Thyroid* 11:407-414.

Effraimidis, G., J.G. Tijssen, J.F. Brosschot, and W.M. Wiersinga. 2012. Involvement of stress in the pathogenesis of autoimmune thyroid disease: a prospective study. *Psychoneuroendocrinology* 37:1191-1198.

Effraimidis, G., J.G.P. Tijssen, T.G.A. Strieder, and W.M. Wiersinga. 2011. No causal relationship between Yersinia enterocolitica infection and autoimmune thyroid disease: evidence from a prospective study. *Clinical & Experimental Immunology* 165:38-43.

El Fassi, D., J.P. Banga, J.A. Gilbert, C. Padoa, L. Hegedüs, and C.H. Nielsen. 2009. Treatment of Graves' disease with rituximab specifically reduces the production of thyroid stimulating autoantibodies. *Clinical Immunology* 130:252-258.

El Fassi, D., C.H. Nielsen, S.J. Bonnema, H.C. Hasselbalch, and L. Hegedus. 2007. B lymphocyte depletion with the monoclonal antibody rituximab in Graves' disease: a controlled pilot study. *J Clin Endocrinol Metab* 92:1769-1772.

Ercolini, A.M., and S.D. Miller. 2009. The role of infections in autoimmune disease. *Clinical & Experimental Immunology* 155:1-15.

Evans, M., J. Sanders, T. Tagami, P. Sanders, S. Young, E. Roberts, J. Wilmot, X. Hu, K. Kabelis, J. Clark, S. Holl, T. Richards, A. Collyer, J. Furmaniak, and B.R. Smith. 2010. Monoclonal autoantibodies to the TSH receptor, one with stimulating activity and one with blocking activity, obtained from the same blood sample. *Clinical Endocrinology* 73:404-412.

Fan, Q.R., and W.A. Hendrickson. 2005. Structure of human follicle-stimulating hormone in complex with its receptor. *Nature* 433:269-277.

Farid, N.R., and M.W. Szkudlinski. 2004. Minireview: Structural and Functional Evolution of the Thyrotropin Receptor. *Endocrinology* 145:4048-4057.

Fernando, R., S. Atkins, N. Raychaudhuri, Y. Lu, B. Li, R.S. Douglas, and T.J. Smith. 2012. Human fibrocytes coexpress thyroglobulin and thyrotropin receptor. *Proceedings of the National Academy of Sciences of the United States of America* 109:7427-7432.

Feuerer, M., J.A. Hill, D. Mathis, and C. Benoist. 2009. Foxp3+ regulatory T cells: differentiation, specification, subphenotypes. *Nat Immunol* 10:689-695.

Flynn, J.C., J.A. Gilbert, C. Meroueh, D.P. Snower, C.S. David, Y.-c.M. Kong, and J. Paul Banga. 2007. Chronic exposure in vivo to thyrotropin receptor stimulating monoclonal antibodies sustains high thyroxine levels and thyroid hyperplasia in thyroid autoimmunity-prone HLA-DRB1*0301 transgenic mice. *Immunology* 122:261-267.

Frazier, A.L., L.S. Robbins, P.J. Stork, R. Sprengel, D.L. Segaloff, and R.D. Cone. 1990. Isolation of TSH and LH/CG receptor cDNAs from human thyroid: regulation by tissue specific splicing. *Molecular Endocrinology* 4:1264-1276.

Fredriksson-Ahomaa, M., A. Stolle, and H. Korkeala. 2006. Molecular epidemiology of Yersinia enterocolitica infections. *FEMS Immunology & Medical Microbiology* 47:315-329.

Furmaniak, J., J. Sanders, and B. Rees Smith. 2012a. Blocking type TSH receptor antibodies. *Autoimmunity Highlights* 1-16.

Furmaniak, J., J. Sanders, S. Young, K. Kabelis, P. Sanders, M. Evans, J. Clark, J. Wilmot, and B. Rees Smith. 2012b. In vivo effects of a human thyroid-stimulating monoclonal autoantibody (M22) and a human thyroid-blocking autoantibody (K1-70). *Autoimmunity Highlights* 3:19-25.

Gatto, D., and R. Brink. 2010. The germinal center reaction. *Journal of Allergy and Clinical Immunology* 126:898-907.

Gilbert, J.A., A.G. Gianoukakis, S. Salehi, J. Moorhead, P.V. Rao, M.Z. Khan, A.M. McGregor, T.J. Smith, and J.P. Banga. 2006a. Monoclonal Pathogenic Antibodies to the Thyroid-Stimulating Hormone Receptor in Graves' Disease with Potent Thyroid-Stimulating Activity but Differential Blocking Activity Activate

Multiple Signaling Pathways. *The Journal of Immunology* 176:5084-5092.

Gilbert, J.A., A.G. Gianoukakis, S. Salehi, J. Moorhead, P.V. Rao, M.Z. Khan, A.M. McGregor, T.J. Smith, and J.P. Banga. 2006b. Monoclonal Pathogenic Antibodies to the Thyroid-Stimulating Hormone Receptor in Graves' Disease with Potent Thyroid-Stimulating Activity but Differential Blocking Activity Activate Multiple Signaling Pathways. *The Journal of Immunology* 176:5084-5092.

Gilbert, J.A., S.L. Kalled, J. Moorhead, D.M. Hess, P. Rennert, Z. Li, M.Z. Khan, and J.P. Banga. 2006c. Treatment of Autoimmune Hyperthyroidism in a Murine Model of Graves' Disease with Tumor Necrosis Factor-Family Ligand Inhibitors Suggests a Key Role for B Cell Activating Factor in Disease Pathology. *Endocrinology* 147:4561-4568.

Gillam, M.P., A.R. Sidhaye, E.J. Lee, J. Rutishauser, C.W. Stephan, and P. Kopp. 2004. Functional characterization of pendrin in a polarized cell system. Evidence for pendrin-mediated apical iodide efflux. *J Biol Chem* 279:13004-13010.

Godfrey, V.L., Wilkinson, J. E., Russell, L. B. 1991. X-linked lymphoreticular disease in the scurfy (sf) mutant mouse. *Am J Pathol* 138:1379-1387.

Gonzalez, D., M. van der Burg, R.n. Garcia-Sanz, J.A. Fenton, A.W. Langerak, M. Gonzalez, J.J.M. van Dongen, J.F. San Miguel, and G.J. Morgan. 2007. Immunoglobulin gene rearrangements and the pathogenesis of multiple myeloma. *Blood* 110:3112-3121.

Gough, S.C.L., and M.J. Simmonds. 2007. The HLA Region and Autoimmune Disease: Associations and Mechanisms of Action. *Curr Genomics* 8:453-465.

Guarneri, F., D. Carlotta, G. Saraceno, F. Trimarchi, and S. Benvenga. 2011. Bioinformatics Support the Possible Triggering of Autoimmune Thyroid Diseases by Yersinia enterocolitica Outer Membrane Proteins Homologous to the Human Thyrotropin Receptor. *Thyroid : official journal of the American Thyroid Association* 21:1283-1284.

Guo, W., D. Smith, K. Aviszus, T. Detanico, R.A. Heiser, and L.J. Wysocki. 2010. Somatic hypermutation as a generator of antinuclear antibodies in a murine model of systemic autoimmunity. *The Journal of Experimental Medicine* 207:2225-2237.

Hadj-Kacem, H., S. Rebuffat, M. Mnif-Féki, S. Belguith-Maalej, H. Ayadi, and S. Péraldi-Roux. 2009. Autoimmune thyroid diseases: genetic susceptibility of thyroid-specific genes and thyroid autoantigens contributions. *International Journal of Immunogenetics* 36:85-96.

Halverson, R., R.M. Torres, and R. Pelanda. 2004. Receptor editing is the main mechanism of B cell tolerance toward membrane antigens. *Nature Immunology* 5:645-650.

Hasham, A., and Y. Tomer. 2012. Genetic and epigenetic mechanisms in thyroid autoimmunity. *Immunologic Research* 1-10.

Heyma, P., L.C. Harrison, and R. Robins-Browne. 1986. Thyrotrophin (TSH) binding sites on Yersinia enterocolitica recognized by immunoglobulins from humans with Graves' disease. *Clinical and Experimental Immunology* 64:249-254.

Hiratani, H., D.W. Bowden, S. Ikegami, S. Shirasawa, A. Shimizu, Y. Iwatani, and T. Akamizu. 2005. Multiple SNPs in Intron 7 of Thyrotropin Receptor Are Associated with Graves' Disease. *Journal of Clinical Endocrinology & Metabolism* 90:2898-2903.

Holliger, P., and P.J. Hudson. 2005. Engineered antibody fragments and the rise of single domains. *Nat Biotech* 23:1126-1136.

Hu, D., X. Liu, W. Zeng, H.L. Weiner, and J. Ritz. 2011. A clonal model for human CD8+ regulatory T cells: Unrestricted contact-dependent killing of activated CD4+ T cells. *European Journal of Immunology* n/a-n/a.

Huang, Q., A. Parfitt, D.M. Grennan, and N. Manolios. 1997. X-Chromosome Inactivation in Monozygotic Twins with Systemic Lupus Erythematosus. *Autoimmunity* 26:85-93.

Huizinga, T., F. Humby, M. Bombardieri, A. Manzo, S. Kelly, M.C. Blades, B. Kirkham, J. Spencer, and C. Pitzalis. 2009. Ectopic Lymphoid Structures Support Ongoing Production of Class-Switched Autoantibodies in Rheumatoid Synovium. *PLoS Medicine* 6:e1.

Huovinen, E., Sihvonen, L.M., Virtanen, M.J., Haukka, K., Siitonen, A., Kuusi, M. 2010. Symptoms and sources of Yersinia enterocolitica-infection: a case-control study. *BMC Infect Dis* 10:

Ibrahim, S., M. Weigert, C. Basu, J. Erikson, and M. Radic. 1995. Light chain contribution to specificity in anti-DNA antibodies. *The Journal of Immunology* 155:3223-3233.

Iezzi, G., K. Karjalainen, and A. Lanzavecchia. 1998. The Duration of Antigenic Stimulation Determines the Fate of Naive and Effector T Cells. *Immunity* 8:89-95.

Jacobson, E.M., and Y. Tomer. 2007. The CD40, CTLA-4, thyroglobulin, TSH receptor, and PTPN22 gene quintet and its contribution to thyroid autoimmunity: Back to the future. *Journal of Autoimmunity* 28:85-98.

Janeway, C. 1989. Approaching the asymptote? Evolution and revolution in immunology. *Cold Spring Harb Symp Quant Bio* 54:1-3.

Jung, D., C. Giallourakis, R. Mostoslavsky, and F.W. Alt. 2006. Mechanism and Control of V(D)J Recombination at the Immunoglobulin Heavy Chain Locus. *Annual Review of Immunology* 24:541-570.

Kakinuma, A., and Y. Nagayama. 2002. Multiple messenger ribonucleic acid transcripts and revised gene organization of the human TSH receptor. *Endocr J* 49:175-180.

Kalinski, P., C.M. Hilkens, E.A. Wierenga, and M.L. Kapsenberg. 1999. T-cell priming by type-1 and type-2 polarized dendritic cells: the concept of a third signal. *Immunol Today* 20:561-567.

Kaneda, T., A. Honda, A. Hakozaki, T. Fuse, A. Muto, and T. Yoshida. 2007. An improved Graves' disease model established by using in vivo electroporation exhibited long-term immunity to hyperthyroidism in BALB/c mice. *Endocrinology* 148:2335-2344.

Karumuthil-Melethil, S., N. Perez, R. Li, B.S. Prabhakar, M.J. Holterman, and C. Vasu. 2010. Dendritic Cell-Directed CTLA-4 Engagement

during Pancreatic Cell Antigen Presentation Delays Type 1 Diabetes. *The Journal of Immunology* 184:6695-6708.

Kim, W.B., H.K. Chung, Y.J. Park, D.J. Park, K. Tahara, L.D. Kohn, and B.Y. Cho. 2000. The prevalence and clinical significance of blocking thyrotropin receptor antibodies in untreated hyperthyroid Graves' disease. *Thyroid : official journal of the American Thyroid Association* 10:579-586.

Klein, L., M. Hinterberger, G. Wirnsberger, and B. Kyewski. 2009. Antigen presentation in the thymus for positive selection and central tolerance induction. *Nat Rev Immunol* 9:833-844.

Knappik, A., and A. Pluckthun. 1995. Engineered turns of a recombinant antibody improve its in vivo folding. *Protein Eng.* 8:81-89.

Koble, C., and B. Kyewski. 2009. The thymic medulla: a unique microenvironment for intercellular self-antigen transfer. *Journal of Experimental Medicine* 206:1505-1513.

Kohler, F., E. Hug, C. Eschbach, S. Meixlsperger, E. Hobeika, J. Kofer, H. Wardemann, and H. Jumaa. 2008. Autoreactive B cell receptors mimic autonomous pre-B cell receptor signaling and induce proliferation of early B cells. *Immunity* 29:912-921.

Kopp, P. 2001. Human Genome and Diseases: Review¶The TSH receptor and its role in thyroid disease. *Cellular and Molecular Life Sciences* 58:1301-1322.

Kriss, J.P., V. Pleshakov, A.L. Rosenblum, M. Holderness, G. Sharp, and R. Utiger. 1967. Studies on the pathogenesis of the

ophthalmopathy of Graves' disease. *J Clin Endocrinol Metab* 27:582-593.

Kushwah, R., and J. Hu. 2011. Role of dendritic cells in the induction of regulatory T cells. *Cell Biosci* 1:20.

Ladi, E., X. Yin, T. Chtanova, and E.A. Robey. 2006. Thymic microenvironments for T cell differentiation and selection. *Nat Immunol* 7:338-343.

Larner, A.J. 2005. Caleb Hillier Parry (1755–1822): clinician, scientist, friend of Edward Jenner (1749–1823). *Journal of Medical Biography* 13:189-194.

Laurberg, P., K.M. Pedersen, H. Vestergaard, and G. Sigurdsson. 1991. High incidence of multinodular toxic goitre in the elderly population in a low iodine intake area vs. high incidence of Graves' disease in the young in a high iodine intake area: comparative surveys of thyrotoxicosis epidemiology in East-Jutland Denmark and Iceland. *J Intern Med* 229:415-420.

Laurent, E., J. Mockel, J. Van Sande, I. Graff, and J.E. Dumont. 1987. Dual activation by thyrotropin of the phospholipase C and cyclic AMP cascades in human thyroid. *Molecular and Cellular Endocrinology* 52:273-278.

Lefranc, M.-P., V. Giudicelli, C. Ginestoux, J. Bodmer, W. Müller, R. Bontrop, M. Lemaitre, A. Malik, V. Barbié, and D. Chaume. 1999. IMGT, the international ImMunoGeneTics database. *Nucleic Acids Research* 27:209-212.

Li, H.S., and G. Carayanniotis. 2006. Iodination of tyrosyls in thyroglobulin generates neoantigenic determinants that cause thyroiditis. *Journal of Immunology* 176:4479-4483.

Li, J., J. Park, D. Foss, and I. Goldschneider. 2009. Thymus-homing peripheral dendritic cells constitute two of the three major subsets of dendritic cells in the steady-state thymus. *The Journal of Experimental Medicine* 206:607-622.

Lidman, K., U. Eriksson, R. Norberg, and A. Fagraeus. 1976. Indirect immunofluorescence staining of human thyroid by antibodies occurring in Yersinia enterocolitica infections. *Clinical and Experimental Immunology* 23:429-435.

Linsley, P.S., J.L. Greene, P. Tan, J. Bradshaw, J.A. Ledbetter, C. Anasetti, and N.K. Damle. 1992. Coexpression and functional cooperation of CTLA-4 and CD28 on activated T lymphocytes. *The Journal of Experimental Medicine* 176:1595-1604.

Liu, S.M., A.P.R. Sutherland, Z. Zhang, D.B. Rainbow, F.J. Quintana, A.M. Paterson, A.H. Sharpe, M. Oukka, L.S. Wicker, and V.K. Kuchroo. 2011. Overexpression of the CTLA-4 Isoform Lacking Exons 2 and 3 Causes Autoimmunity. *The Journal of Immunology*

Liu, Z., and A. Davidson. 2011. BAFF and selection of autoreactive B cells. *Trends in Immunology* 32:388-394.

Loosfelt, H., C. Pichon, A. Jolivet, M. Misrahi, B. Caillou, M. Jamous, B. Vannier, and E. Milgrom. 1992. Two-subunit structure of the human thyrotropin receptor. *Proceedings of the National Academy of Sciences of the United States of America* 89:3765-3769.

Luo, G., J. Fan, G. Seetharamaiah, R. Desai, J. Dallas, N. Wagle, R. Doan, D. Niesel, G. Klimpel, and B. Prabhakar. 1993. Immunization of mice with Yersinia enterocolitica leads to the induction of antithyrotropin receptor antibodies. *The Journal of Immunology* 151:922-928.

Luo, G., G. Seetharamaiah, D. Niesel, H. Zhang, J. Peterson, B. Prabhakar, and G. Klimpel. 1994. Purification and Characterization of Yersinia enterocolitica Envelope Proteins Which Induce Antibodies That React with Human Thyrotropin Receptor. *J. Immunol* 152:2555-2561.

Mackay, M., A. Stanevsky, T. Wang, C. Aranow, M. Li, S. Koenig, J.V. Ravetch, and B. Diamond. 2006. Selective dysregulation of the FcgammaIIB receptor on memory B cells in SLE. *The Journal of Experimental Medicine* 203:2157-2164.

Maier, R.H., C.J. Maier, R. Rid, H. Hintner, J.W. Bauer, and K. Onder. 2010. Epitope Mapping of Antibodies Using a Cell Array-Based Polypeptide Library. *Journal of Biomolecular Screening* 15:418-426.

Malkiel, S., L. Liao, M.W. Cunningham, and B. Diamond. 2000. T-Cell-dependent antibody response to the dominant epitope of streptococcal polysaccharide, N-acetyl-glucosamine, is cross-reactive with cardiac myosin. *Infection and Immunity* 68:5803-5808.

Manji, N., J.D. Carr-Smith, K. Boelaert, A. Allahabadia, M. Armitage, V.K. Chatterjee, J.H. Lazarus, S.H.S. Pearce, B. Vaidya, S.C. Gough, and J.A. Franklyn. 2006. Influences of Age, Gender, Smoking, and Family History on Autoimmune Thyroid Disease Phenotype. *Journal of Clinical Endocrinology & Metabolism* 91:4873-4880.

Mao, C., S. Wang, Y. Xiao, J. Xu, Q. Jiang, M. Jin, X. Jiang, H. Guo, G. Ning, and Y. Zhang. 2011. Impairment of Regulatory Capacity of CD4+CD25+ Regulatory T Cells Mediated by Dendritic Cell Polarization and Hyperthyroidism in Graves' Disease. *The Journal of Immunology* 186:4734-4743.

Martin, A., M. Nakashima, A. Zhou, D. Aronson, A.J. Werner, and T.F. Davies. 1997. Detection of major T cell epitopes on human thyroid stimulating hormone receptor by overriding immune heterogeneity in patients with Graves' disease. *J Clin Endocrinol Metab* 82:3361-3366.

Mathis, D., and C. Benoist. 2009. Aire. *Annual Review of Immunology* 27:287-312.

Mauri, C., and A. Bosma. 2012. Immune Regulatory Function of B Cells. *Annual Review of Immunology* 30:null.

McIver, B., and J.C. Morris. 1998. The pathogenesis of Graves' disease. *Endocrinol Metab Clin North Am* 27:73-89.

McLachlan, S., A. Dickinson, A. Malcolm, J. Farndon, E. Young, S. Proctor, and B. Smith. 1983. Thyroid autoantibody synthesis by cultures of thyroid and peripheral blood lymphocytes. I. Lymphocyte markers and response to pokeweed mitogen. *Clin Exp Immunol* 52:45-53.

McLachlan, S.M., H.A. Aliesky, C.-R. Chen, R.W. Williams, and B. Rapoport. 2011a. Exceptional Hyperthyroidism and a Role for both Major Histocompatibility Class I and Class II Genes in a Murine Model of Graves' Disease. *PLoS ONE* 6:e21378.

McLachlan, S.M., K. Alpi, and B. Rapoport. 2011b. Review and Hypothesis: Does Graves' Disease Develop in Non-Human Great Apes? *Thyroid* 21:1359-1366.

McLachlan, S.M., Y. Nagayama, P.N. Pichurin, Y. Mizutori, C.R. Chen, A. Misharin, H.A. Aliesky, and B. Rapoport. 2007. The Link between Graves' Disease and Hashimoto's Thyroiditis: A Role for Regulatory T Cells. *Endocrinology* 148:5724-5733.

McLachlan, S.M., and B. Rapoport. 2004. Thyroid stimulating monoclonal antibodies: overcoming the road blocks and the way forward. *Clinical Endocrinology* 61:10-18.

McLachlan, S.M., and B. Rapoport. 2007. Thyroid peroxidase as an autoantigen. *Thyroid : official journal of the American Thyroid Association* 17:939-948.

Menconi, F., M.C. Monti, D.A. Greenberg, T. Oashi, R. Osman, T.F. Davies, Y. Ban, E.M. Jacobson, E.S. Concepcion, C.W. Li, and Y. Tomer. 2008. Molecular amino acid signatures in the MHC class II peptide-binding pocket predispose to autoimmune thyroiditis in humans and in mice. *Proceedings of the National Academy of Sciences* 105:14034-14039.

Metcalfe, R., N. Jordan, P. Watson, S. Gullu, M. Wiltshire, M. Crisp, C. Evans, A. Weetman, and M. Ludgate. 2002. Demonstration of Immunoglobulin G, A, and E Autoantibodies to the Human Thyrotropin Receptor Using Flow Cytometry. *Journal of Clinical Endocrinology & Metabolism* 87:1754-1761.

Mietzner, B., M. Tsuiji, J. Scheid, K. Velinzon, T. Tiller, K. Abraham, J.B. Gonzalez, V. Pascual, D. Stichweh, H. Wardemann, and M.C. Nussenzweig. 2008. Autoreactive IgG memory antibodies in

patients with systemic lupus erythematosus arise from nonreactive and polyreactive precursors. *Proceedings of the National Academy of Sciences* 105:9727-9732.

Miller, J.F.A.P. 2011. The golden anniversary of the thymus. *Nat Rev Immunol* 11:489-495.

Misrahi, M., N. Ghinea, S. Sar, B. Saunier, A. Jolivet, H. Loosfelt, M. Cerutti, G. Devauchelle, and E. Milgrom. 1994. Processing of the precursors of the human thyroid-stimulating hormone receptor in various eukaryotic cells (human thyrocytes, transfected L cells and baculovirus-infected insect cells). *Eur J Biochem* 222:711-719.

Misrahi, M., H. Loosfelt, M. Atger, S. Sar, A. Guiochon-Mantel, and E. Milgrom. 1990. Cloning, sequencing and expression of human TSH receptor. *Biochemical and Biophysical Research Communications* 166:394-403.

Mix, E., R. Goertsches, and U.K. Zett. 2006. Immunoglobulins—Basic considerations. *Journal of Neurology* 253:v9-v17.

Mizutori, Y., C.R. Chen, F. Latrofa, S.M. McLachlan, and B. Rapoport. 2008. Evidence that Shed Thyrotropin Receptor A Subunits Drive Affinity Maturation of Autoantibodies Causing Graves' Disease. *Journal of Clinical Endocrinology & Metabolism* 94:927-935.

Mizutori, Y., C.R. Chen, F. Latrofa, S.M. McLachlan, and B. Rapoport. 2009. Evidence that shed thyrotropin receptor A subunits drive affinity maturation of autoantibodies causing Graves' disease. *J Clin Endocrinol Metab* 94:927-935.

Morlacchi, S., C. Soldani, A. Viola, and A. Sarukhan. 2011. Self-antigen presentation by mouse B cells results in regulatory T-cell induction rather than anergy or clonal deletion. *Blood* 118:984-991.

Morshed, S.A., T. Ando, R. Latif, and T.F. Davies. 2010a. Neutral antibodies to the TSH receptor are present in Graves' disease and regulate selective signaling cascades. *Endocrinology* 151:5537-5549.

Morshed, S.A., T. Ando, R. Latif, and T.F. Davies. 2010b. Neutral Antibodies to the TSH Receptor Are Present in Graves‚Äô Disease and Regulate Selective Signaling Cascades. *Endocrinology* 151:5537-5549.

Muramatsu, M., K. Kinoshita, S. Fagarasan, S. Yamada, Y. Shinkai, and T. Honjo. 2000. Class Switch Recombination and Hypermutation Require Activation-Induced Cytidine Deaminase (AID), a Potential RNA Editing Enzyme. *Cell* 102:553-563.

Nacionales, D.C., J.S. Weinstein, X.J. Yan, E. Albesiano, P.Y. Lee, K.M. Kelly-Scumpia, R. Lyons, M. Satoh, N. Chiorazzi, and W.H. Reeves. 2009. B Cell Proliferation, Somatic Hypermutation, Class Switch Recombination, and Autoantibody Production in Ectopic Lymphoid Tissue in Murine Lupus. *The Journal of Immunology* 182:4226-4236.

Nagayama, Y. 2007. Animal Models of Graves' Hyperthyroidism. *Thyroid* 17:981-988.

Nagayama, Y., K.D. Kaufman, P. Seto, and B. Rapoport. 1989. Molecular cloning, sequence and functional expression of the cDNA for the human thyrotropin receptor. *Biochemical and Biophysical Research Communications* 165:1184-1190.

Nagayama, Y., M. Kita-Furuyama, T. Ando, K. Nakao, H. Mizuguchi, T. Hayakawa, K. Eguchi, and M. Niwa. 2002. A novel murine model of Graves' hyperthyroidism with intramuscular injection of adenovirus expressing the thyrotropin receptor. *Journal of Immunology* 168:2789-2794.

Nakahara, M., K. Johnson, A. Eckstein, R. Taguchi, M. Yamada, N. Abiru, and Y. Nagayama. 2012. Adoptive Transfer of Antithyrotropin Receptor (TSHR) Autoimmunity from TSHR Knockout Mice to Athymic Nude Mice. *Endocrinology*

Nakahara, M., N. Mitsutake, H. Sakamoto, C.-R. Chen, B. Rapoport, S.M. McLachlan, and Y. Nagayama. 2010. Enhanced Response to Mouse Thyroid-Stimulating Hormone (TSH) Receptor Immunization in TSH Receptor-Knockout Mice. *Endocrinology* 151:4047-4054.

Nakatake, N., J. Sanders, T. Richards, P. Burne, C. Barrett, C.D. Pra, F. Presotto, C. Betterle, J. Furmaniak, and B.R. Smith. 2006. Estimation of serum TSH receptor autoantibody concentration and affinity. *Thyroid : official journal of the American Thyroid Association* 16:1077-1084.

Neefjes, J., M.L.M. Jongsma, P. Paul, and O. Bakke. 2011. Towards a systems understanding of MHC class I and MHC class II antigen presentation. *Nat Rev Immunol* 11:823-836.

Neidhardt, F.C., P.L. Bloch, and D.F. Smith. 1974. Culture Medium for Enterobacteria. *J Bacteriol* 119:736-747.

Neumann, S., E. Eliseeva, J.G. McCoy, G. Napolitano, C. Giuliani, F. Monaco, W. Huang, and M.C. Gershengorn. 2010a. A New Small-Molecule Antagonist Inhibits Graves' Disease Antibody Activation

of the TSH Receptor. *Journal of Clinical Endocrinology & Metabolism* 96:548-554.

Neumann, S., W. Huang, E. Eliseeva, S. Titus, C.J. Thomas, and M.C. Gershengorn. 2010b. A small molecule inverse agonist for the human thyroid-stimulating hormone receptor. *Endocrinology* 151:3454-3459.

Neumann, S., W. Huang, S. Titus, G. Krause, G. Kleinau, A.T. Alberobello, W. Zheng, N.T. Southall, J. Inglese, C.P. Austin, F.S. Celi, O. Gavrilova, C.J. Thomas, B.M. Raaka, and M.C. Gershengorn. 2009. Small-molecule agonists for the thyrotropin receptor stimulate thyroid function in human thyrocytes and mice. *Proceedings of the National Academy of Sciences* 106:12471-12476.

Neumann, S., G. Kleinau, S. Costanzi, S. Moore, J.K. Jiang, B.M. Raaka, C.J. Thomas, G. Krause, and M.C. Gershengorn. 2008. A low-molecular-weight antagonist for the human thyrotropin receptor with therapeutic potential for hyperthyroidism. *Endocrinology* 149:5945-5950.

Nicholson, L.B., H. Vlase, P. Graves, M. Nilsson, J. Molne, G.C. Huang, N.G. Morgenthaler, T.F. Davies, A.M. McGregor, and J.P. Banga. 1996. Monoclonal antibodies to the human TSH receptor: epitope mapping and binding to the native receptor on the basolateral plasma membrane of thyroid follicular cells. *Journal of Molecular Endocrinology* 16:159-170.

Nielsen, C.H., D. El Fassi, H.C. Hasselbalch, K. Bendtzen, and L. Hegedus. 2007. B-cell depletion with rituximab in the treatment of autoimmune diseases. Graves' ophthalmopathy the latest addition to an expanding family. *Expert Opin Biol Ther* 7:1061-1078.

Nikaido, H. 2003. Molecular basis of bacterial outer membrane permeability revisited. *Microbiol Mol Biol Rev* 67:593-656.

Núñez Miguel, R., J. Sanders, D.Y. Chirgadze, T.L. Blundell, J. Furmaniak, and B. Rees Smith. 2008. FSH and TSH binding to their respective receptors: similarities, differences and implication for glycoprotein hormone specificity. *Journal of Molecular Endocrinology* 41:145-164.

Nunez Miguel, R., J. Sanders, D.Y. Chirgadze, J. Furmaniak, and B. Rees Smith. 2009. Thyroid stimulating autoantibody M22 mimics TSH binding to the TSH receptor leucine rich domain: a comparative structural study of protein-protein interactions. *Journal of Molecular Endocrinology* 42:381-395.

Nyirenda, M.J., D.N. Clark, A.R. Finlayson, J. Read, A. Elders, M. Bain, K.A. Fox, and A.D. Toft. 2005. Thyroid disease and increased cardiovascular risk. *Thyroid : official journal of the American Thyroid Association* 15:718-724.

Oda, Y., J. Sanders, S. Roberts, M. Maruyama, A. Kiddie, J. Furmaniak, and B. Rees Smith. 1999. Analysis of Carbohydrate Residues on Recombinant Human Thyrotropin Receptor. *Journal of Clinical Endocrinology & Metabolism* 84:2119-2125.

Ozawa, Y., and S. Mizushima. 1983. Regulation of outer membrane porin protein synthesis in Escherichia coli K-12: ompF regulates the expression of ompC. *J Bacteriol* 154:669-675.

Özbalkan, Z., S. Bağışlar, S. Kiraz, C.B. Akyerli, H.T.E. Özer, Ş. Yavuz, A.M. Birlik, M. Çalgüneri, and T. Özçelik. 2005. Skewed X chromosome inactivation in blood cells of women with scleroderma. *Arthritis & Rheumatism* 52:1564-1570.

Ozcelik, T., E. Uz, C.B. Akyerli, S. Bagislar, C.A. Mustafa, A. Gursoy, N. Akarsu, G. Toruner, N. Kamel, and S. Gullu. 2006. Evidence from autoimmune thyroiditis of skewed X-chromosome inactivation in female predisposition to autoimmunity. *Eur J Hum Genet* 14:791-797.

Padoa, C.J., J.P. Banga, A.-M. Madec, M. Ziegler, M. Schlosser, E. Ortqvist, I. Kockum, J. Palmer, O. Rolandsson, K.A. Binder, J. Foote, D. Luo, and C.S. Hampe. 2003. Recombinant Fabs of Human Monoclonal Antibodies Specific to the Middle Epitope of GAD65 Inhibit Type 1 Diabetes–Specific GAD65Abs. *Diabetes* 52:2689-2695.

Padoa, C.J., N.J. Crowther, J.W. Thomas, T.R. Hall, L.M. Bekris, C. Torn, M. Landin-Olsson, E. Ortqvist, J.P. Palmer, A. Lernmark, and C.S. Hampe. 2005. Epitope analysis of insulin autoantibodies using recombinant Fab. *Clinical and Experimental Immunology* 140:564-571.

Padoa, C.J., S.L. Larsen, C.S. Hampe, J.A. Gilbert, E. Dagdan, L. Hegedus, D. Dunn-Walters, and J.P. Banga. 2010. Clonal relationships between thyroid-stimulating hormone receptor-stimulating antibodies illustrate the effect of hypermutation on antibody function. *Immunology* 129:300-308.

Pan, D., Y.-H. Shin, G. Gopalakrishnan, J. Hennessey, and L.J. De Groot. 2009. Regulatory T cells in Graves' disease. *Clinical Endocrinology* 71:587-593.

Pancer, Z., and M.D. Cooper. 2006. The evolution of adaptive immunity. *Annual review of immunology* 24:497-518.

Panigrahi, A.K., N.G. Goodman, R.A. Eisenberg, M.R. Rickels, A. Naji, and E.T. Luning Prak. 2008. RS rearrangement frequency as a marker of receptor editing in lupus and type 1 diabetes. *The Journal of Experimental Medicine* 205:2985-2994.

Parmentier, M., F. Libert, C. Maenhaut, A. Lefort, C. Gerard, J. Perret, J. Van Sande, J. Dumont, and G. Vassart. 1989. Molecular cloning of the thyrotropin receptor. *Science* 246:1620-1622.

Pascal, T.A., R. Abrol, R. Mittal, Y. Wang, N.V. Prasadarao, and W.A. Goddard. 2010. Experimental Validation of the Predicted Binding Site of Escherichia coli K1 Outer Membrane Protein A to Human Brain Microvascular Endothelial Cells. *Journal of Biological Chemistry* 285:37753-37761.

Patibandla, S.A., J.L. Fan, B.S. Prabhakar, and G.S. Seetharamaiah. 1999. Comparison of immune responses to extracellular domains of mouse and human thyrotropin receptor. *Journal of Autoimmunity* 13:205-213.

Payne, A.S., D.L. Siegel, and J.R. Stanley. 2007. Targeting Pemphigus Autoantibodies through their Heavy-Chain Variable Region Genes. *Journal of Investigative Dermatology*

Pedersen, I.B., P. Laurberg, N. Knudsen, T. Jørgensen, H. Perrild, L. Ovesen, and L.B. Rasmussen. 2006. Lack of association between thyroid autoantibodies and parity in a population study argues against microchimerism as a trigger of thyroid autoimmunity. *European Journal of Endocrinology* 154:39-45.

Pelanda, R., S. Schwers, E. Sonoda, R.M. Torres, D. Nemazee, and K. Rajewsky. 1997. Receptor editing in a transgenic mouse model:

site, efficiency, and role in B cell tolerance and antibody diversification. *Immunity* 7:765-775.

Perret, J., M. Ludgate, F. Libert, C. Gerard, J.E. Dumont, G. Vassart, and M. Parmentier. 1990. Stable expression of the human TSH receptor in CHO cells and characterization of differentially expressing clones. *Biochemical and Biophysical Research Communications* 171:1044-1050.

Pichurin, P., L. Schwarz-Lauer, H. Braley-Mullen, C. Paras, O. Pichurina, J.C. Morris, B. Rapoport, and S.M. McLachlan. 2002. Peptide scanning for thyrotropin receptor T-cell epitopes in mice vaccinated with naked DNA. *Thyroid : official journal of the American Thyroid Association* 12:755-764.

Pichurin, P.N., C.R. Chen, G.D. Chazenbalk, H. Aliesky, N. Pham, B. Rapoport, and S.M. McLachlan. 2006. Targeted expression of the human thyrotropin receptor A-subunit to the mouse thyroid: insight into overcoming the lack of response to A-subunit adenovirus immunization. *Journal of Immunology* 176:668-676.

Pillai, S., H. Mattoo, and A. Cariappa. 2011. B cells and autoimmunity. *Current Opinion in Immunology* 23:721-731.

Płoski, R., O.J. Brand, B. Jurecka-Lubieniecka, M. Franaszczyk, D. Kula, P. Krajewski, M.A. Karamat, M.J. Simmonds, J.A. Franklyn, S.C.L. Gough, B. Jarząb, and T. Bednarczuk. 2010. Thyroid Stimulating Hormone Receptor (TSHR) Intron 1 Variants Are Major Risk Factors for Graves' Disease in Three European Caucasian Cohorts. *PLoS ONE* 5:e15512.

Prechl, J., K. Papp, and A. Erdei. 2010. Antigen microarrays: descriptive chemistry or functional immunomics? *Trends in Immunology* 31:133-137.

Pritchard, J., R. Han, N. Horst, W.W. Cruikshank, and T.J. Smith. 2003. Immunoglobulin activation of T cell chemoattractant expression in fibroblasts from patients with Graves' disease is mediated through the insulin-like growth factor I receptor pathway. *Journal of Immunology* 170:6348-6354.

Pritchard, J., N. Horst, W. Cruikshank, and T.J. Smith. 2002. Igs from Patients with Graves' Disease Induce the Expression of T Cell Chemoattractants in Their Fibroblasts. *The Journal of Immunology* 168:942-950.

Radic, M., J. Mackle, J. Erikson, C. Mol, W. Anderson, and M. Weigert. 1993. Residues that mediate DNA binding of autoimmune antibodies. *The Journal of Immunology* 150:4966-4977.

Radic, M., M. Mascelli, J. Erikson, H. Shan, and M. Weigert. 1991. Ig H and L chain contributions to autoimmune specificities. *The Journal of Immunology* 146:176-182.

Rahman, A., D.S. Latchman, and D.A. Isenberg. 1998. The role of in vitro expression systems in the investigation of antibodies to DNA. *Seminars in Arthritis and Rheumatism* 28:130-139.

Rao, P.V., P.F. Watson, A.P. Weetman, G. Carayanniotis, and J.P. Banga. 2003. Contrasting activities of thyrotropin receptor antibodies in experimental models of Graves' disease induced by injection of transfected fibroblasts or deoxyribonucleic acid vaccination. *Endocrinology* 144:260-266.

Rapoport, B., R. Alsabeh, D. Aftergood, and S.M. McLachlan. 2000. Elephantiasic pretibial myxedema: insight into and a hypothesis regarding the pathogenesis of the extrathyroidal manifestations of Graves' disease. *Thyroid : official journal of the American Thyroid Association* 10:685-692.

Rapoport, B., G.D. Chazenbalk, J.C. Jaume, and S.M. McLachlan. 1998. The thyrotropin (TSH) receptor: interaction with TSH and autoantibodies. *Endocrine Reviews* 19:673-716.

Rapoport, B., and S.M. McLachlan. 2007. The thyrotropin receptor in Graves' disease. *Thyroid : official journal of the American Thyroid Association* 17:911-922.

Rapoport, B., R.W. Williams, C.R. Chen, and S.M. McLachlan. 2010. Immunoglobulin heavy chain variable region genes contribute to the induction of thyroid-stimulating antibodies in recombinant inbred mice. *Genes and Immunity* 11:254-263.

Read, S., V. Malmstrom, and F. Powrie. 2000. Cytotoxic T lymphocyte-associated antigen 4 plays an essential role in the function of CD25(+)CD4(+) regulatory cells that control intestinal inflammation. *The Journal of Experimental Medicine* 192:295-302.

Rebuffat, S.A., B. Nguyen, B. Robert, F. Castex, and S. Peraldi-Roux. 2008. Antithyroperoxidase antibody-dependent cytotoxicity in autoimmune thyroid disease. *J Clin Endocrinol Metab* 93:929-934.

Reff, M.E., K. Carner, K.S. Chambers, P.C. Chinn, J.E. Leonard, R. Raab, R.A. Newman, N. Hanna, and D.R. Anderson. 1994. Depletion of B cells in vivo by a chimeric mouse human monoclonal antibody to CD20. *Blood* 83:435-445.

Renne, C., E. Ramos Lopez, S.A. Steimle-Grauer, P. Ziolkowski, M.A. Pani, C. Luther, K. Holzer, A. Encke, R.A. Wahl, W.O. Bechstein, K.H. Usadel, M.L. Hansmann, and K. Badenhoop. 2004. Thyroid fetal male microchimerisms in mothers with thyroid disorders: presence of Y-chromosomal immunofluorescence in thyroid-infiltrating lymphocytes is more prevalent in Hashimoto's thyroiditis and Graves' disease than in follicular adenomas. *J Clin Endocrinol Metab* 89:5810-5814.

Resetkova, E., R. Notenboom, G. Arreaza, T. Mukuta, N. Yoshikawa, and R. Volpé. 1994. Seroreactivity to bacterial antigens is not a unique phenomenon in patients with autoimmune thyroid diseases in Canada. *Thyroid* 4:269-274.

Reusch, R.N. 2012. Insights into the structure and assembly of Escherichia coli outer membrane protein A. *FEBS Journal* 279:894-909.

Reveille, J.D. 2011. The genetic basis of spondyloarthritis. *Ann Rheum Dis* 70:i44-i50.

Riley, G., and S. Toma. 1989. Detection of pathogenic Yersinia enterocolitica by using congo red-magnesium oxalate agar medium. *J. Clin. Microbiol.* 27:213-214.

Ringold, D.A., J.T. Nicoloff, M. Kesler, H. Daves, A. Hamilton, and T. Mack. 2002. Further Evidence for a Strong Genetic Influence on the Development of Autoimmune Thyroid Disease: The California Twin Study *Thyroid* 12:647-653.

Rohde, J.R., J.M. Fox, and S.A. Minnich. 1994. Thermoregulation in Yersinia enterocolitica is coincident with changes in DNA supercoiling. *Mol Microbiol* 12:187-199.

Röthlisberger, D., A. Honegger, and A. Plückthun. 2005. Domain Interactions in the Fab Fragment: A Comparative Evaluation of the Single-chain Fv and Fab Format Engineered with Variable Domains of Different Stability. *Journal of Molecular Biology* 347:773-789.

Ruiz-Riol, M., P. Barnils Mdel, R. Colobran Oriol, A.S. Pla, F.E. Borras Serres, A. Lucas-Martin, E.M. Martinez Caceres, and R. Pujol-Borrell. 2011. Analysis of the cumulative changes in Graves' disease thyroid glands points to IFN signature, plasmacytoid DCs and alternatively activated macrophages as chronicity determining factors. *Journal of Autoimmunity* 36:189-200.

Saitoh, O., N. Abiru, M. Nakahara, and Y. Nagayama. 2007. CD8+CD122+ T cells, a newly identified regulatory T subset, negatively regulate Graves' hyperthyroidism in a murine model. *Endocrinology* 148:6040-6046.

Saitoh, O., and Y. Nagayama. 2006. Regulation of Graves' hyperthyroidism with naturally occurring CD4+CD25+ regulatory T cells in a mouse model. *Endocrinology* 147:2417-2422.

Sakaguchi, S., M. Miyara, C.M. Costantino, and D.A. Hafler. 2010. FOXP3+ regulatory T cells in the human immune system. *Nat Rev Immunol* 10:490-500.

Sakaguchi, S., N. Sakaguchi, M. Asano, M. Itoh, and M. Toda. 1995. Immunologic self-tolerance maintained by activated T cells expressing IL-2 receptor alpha-chains (CD25). Breakdown of a single mechanism of self-tolerance causes various autoimmune diseases. *The Journal of Immunology* 155:1151-1164.

Sale, M.M., T. Akamizu, T.D. Howard, T. Yokota, K. Nakao, T. Mori, H. Iwasaki, S.S. Rich, J.E. Jennings-Gee, M. Yamada, and D.W. Bowden. 1997. Association of autoimmune thyroid disease with a microsatellite marker for the thyrotropin receptor gene and CTLA-4 in a Japanese population. *Proc Assoc Am Physicians* 109:453-461.

Salvi, M., G. Vannucchi, I. Campi, N. Curro, D. Dazzi, S. Simonetta, P. Bonara, S. Rossi, C. Sina, C. Guastella, R. Ratiglia, and P. Beck-Peccoz. 2007. Treatment of Graves' disease and associated ophthalmopathy with the anti-CD20 monoclonal antibody rituximab: an open study. *Eur J Endocrinol* 156:33-40.

Sanders, J., F. Allen, J. Jeffreys, J. Bolton, T. Richards, H. Depraetere, N. Nakatake, M. Evans, A. Kiddie, L.D.K.E. Premawardhana, D.Y. Chirgadze, R.N. Miguel, T.L. Blundell, J. Furmaniak, and B.R. Smith. 2005. Characteristics of a Monoclonal Antibody to the Thyrotropin Receptor that Acts as a Powerful Thyroid-Stimulating Autoantibody Antagonist. *Thyroid* 15:672-682.

Sanders, J., D. Chirgadze, P. Sanders, S. Baker, A. Sullivan, A. Bhardwaja, J. Bolton, M. Reeve, N. Nakatake, M. Evans, T. Richards, M. Powell, R. Miguel, T. Blundell, J. Furmaniak, and B. Smith. 2007. Crystal structure of the TSH receptor in complex with a thyroid-stimulating autoantibody. *Thyroid* 17:395-410.

Sanders, J., M. Evans, L. Premawardhana, H. Depraetere, J. Jeffreys, T. Richards, J. Furmaniak, and B. Smith. 2003. Human monoclonal thyroid stimulating autoantibody. *The Lancet* 362:126-128.

Sanders, J., Evans, M., Betterle, C., Sanders, P., Bhardwaja, A., Young, S., Roberts, E., Wilmot, J., Richards, T., Kiddie, A., Small, K., Platt, H., Summerhayes, S., Harris, R., Reeve, M., Coco, G., Zanchetta,

R., Chen, S., Furmaniak, J and Smith, B. R. 2008. A Human Monoclonal Autoantibody to the Thyrotropin Receptor with Thyroid-Stimulating Blocking Activity. *Thyroid* 18:735-746.

Sanders, J., J. Jeffreys, H. Depraetere, T. Richards, M. Evans, A. Kiddie, K. Brereton, M. Groenen, Y. Oda, J. Furmaniak, and B. Rees Smith. 2002. Thyroid-Stimulating Monoclonal Antibodies. *Thyroid* 12:1043-1050.

Sanders, P., S. Young, J. Sanders, K. Kabelis, S. Baker, A. Sullivan, M. Evans, J. Clark, J. Wilmot, X. Hu, E. Roberts, M. Powell, R. Nunez Miguel, J. Furmaniak, and B. Rees Smith. 2011. Crystal structure of the TSH receptor (TSHR) bound to a blocking-type TSHR autoantibody. *Journal of Molecular Endocrinology* 46:81-99.

Scheid, J.F., H. Mouquet, J. Kofer, S. Yurasov, M.C. Nussenzweig, and H. Wardemann. 2011. Differential regulation of self-reactivity discriminates between IgG+ human circulating memory B cells and bone marrow plasma cells. *Proceedings of the National Academy of Sciences* 108:18044-18048.

Schiellerup, P., K.A. Krogfelt, and H. Locht. 2008. A comparison of self-reported joint symptoms following infection with different enteric pathogens: effect of HLA-B27. *The Journal of Rheumatology* 35:480-487.

Schneider, A.B., K. Ikekubo, and K. Kuma. 1983. Iodine content of serum thyroglobulin in normal individuals and patients with thyroid tumors. *J Clin Endocrinol Metab* 57:1251-1256.

Schroeder Jr, H.W., and L. Cavacini. 2010. Structure and function of immunoglobulins. *Journal of Allergy and Clinical Immunology* 125:S41-S52.

Shiina, T., K. Hosomichi, H. Inoko, and J.K. Kulski. 2009. The HLA genomic loci map: expression, interaction, diversity and disease. *Journal of Human Genetics* 54:15-39.

Shimojo, N., Y. Kohno, K. Yamaguchi, S. Kikuoka, A. Hoshioka, H. Niimi, A. Hirai, Y. Tamura, Y. Saito, L.D. Kohn, and K. Tahara. 1996. Induction of Graves-like disease in mice by immunization with fibroblasts transfected with the thyrotropin receptor and a class II molecule. *Proceedings of the National Academy of Sciences of the United States of America* 93:11074-11079.

Siminovitch, K.A., A. Bakhshi, P. Goldman, and S.J. Korsmeyer. 1985. A uniform deleting element mediates the loss of kappa genes in human B cells. *Nature* 316:260-262.

Simmonds, M.J., and S.C. Gough. 2004a. Genetic insights into disease mechanisms of autoimmunity. *Br Med Bull* 71:93-113.

Simmonds, M.J., and S.C.L. Gough. 2004b. Unravelling the genetic complexity of autoimmune thyroid disease: HLA, CTLA-4 and beyond. *Clinical & Experimental Immunology* 136:1-10.

Simmonds, M.J., J.M.M. Howson, J.M. Heward, H.J. Cordell, H. Foxall, J. Carr-Smith, S.M. Gibson, N. Walker, Y. Tomer, J.A. Franklyn, J.A. Todd, and S.C.L. Gough. 2005. Regression Mapping of Association between the Human Leukocyte Antigen Region and Graves Disease. *The American Journal of Human Genetics* 76:157-163.

Singh, S.P., D. McDonald, T.J. Hope, and B.S. Prabhakar. 2004. Upon thyrotropin binding the thyrotropin receptor is internalized and localized to endosome. *Endocrinology* 145:1003-1010.

Sisson, J.C., P. Kothary, and H. Kirchick. 1973. The Effects of Lymphocytes, Sera and Long-Acting Thyroid Stimulator from Patients with Graves' Disease on Retrobular Fibroblasts. *Journal of Clinical Endocrinology & Metabolism* 37:17-24.

Smith, B.R., S.M. McLachlan, and J. Furmaniak. 1988. Autoantibodies to the Thyrotropin Receptor. *Endocrine Reviews* 9:106-121.

Smith, T.J., C.C. Tsai, M.-J. Shih, S. Tsui, B. Chen, R. Han, V. Naik, C.S. King, C. Press, S. Kamat, R.A. Goldberg, R.P. Phipps, R.S. Douglas, and A.G. Gianoukakis. 2008. Unique Attributes of Orbital Fibroblasts and Global Alterations in IGF-1 Receptor Signaling Could Explain Thyroid-Associated Ophthalmopathy. *Thyroid* 18:983-988.

Soliman, M., E. Kaplan, T. Yanagawa, Y. Hidaka, M.E. Fisfalen, and L.J. DeGroot. 1995. T-cells recognize multiple epitopes in the human thyrotropin receptor extracellular domain. *J Clin Endocrinol Metab* 80:905-914.

Sorisky, A., D. Pardasani, A. Gagnon, and T.J. Smith. 1996. Evidence of adipocyte differentiation in human orbital fibroblasts in primary culture. *J Clin Endocrinol Metab* 81:3428-3431.

Stadanlick, J.E., and M.P. Cancro. 2008. BAFF and the plasticity of peripheral B cell tolerance. *Current Opinion in Immunology* 20:158-161.

Stassi, G., M. Todaro, F. Bucchieri, A. Stoppacciaro, F. Farina, G. Zummo, R. Testi, and R. De Maria. 1999. Fas/Fas ligand-driven T cell apoptosis as a consequence of ineffective thyroid immunoprivilege in Hashimoto's thyroiditis. *Journal of Immunology* 162:263-267.

Stavnezer, J., J.E. Guikema, and C.E. Schrader. 2008. Mechanism and regulation of class switch recombination. *Annual Review of Immunology* 26:261-292.

Takahashi, M., and A. Kimura. 2010. HLA and CTLA4 polymorphisms may confer a synergistic risk in the susceptibility to Graves' disease. *Journal of Human Genetics* 55:323-326.

Takahashi, T., T. Tagami, S. Yamazaki, T. Uede, J. Shimizu, N. Sakaguchi, T.W. Mak, and S. Sakaguchi. 2000. Immunologic self-tolerance maintained by CD25(+)CD4(+) regulatory T cells constitutively expressing cytotoxic T lymphocyte-associated antigen 4. *The Journal of Experimental Medicine* 192:303-310.

Tiller, T., J. Kofer, C. Kreschel, C.E. Busse, S. Riebel, S. Wickert, F. Oden, M.M. Mertes, M. Ehlers, and H. Wardemann. 2010. Development of self-reactive germinal center B cells and plasma cells in autoimmune Fc gammaRIIB-deficient mice. *The Journal of Experimental Medicine* 207:2767-2778.

Tiller, T., M. Tsuiji, S. Yurasov, K. Velinzon, M.C. Nussenzweig, and H. Wardemann. 2007. Autoreactivity in Human IgG+ Memory B Cells. *Immunity* 26:205-213.

Trulzsch, K., T. Sporleder, E.I. Igwe, H. Russmann, and J. Heesemann. 2004. Contribution of the Major Secreted Yops of Yersinia enterocolitica O:8 to Pathogenicity in the Mouse Infection Model. *Infect. Immun.* 72:5227-5234.

Tsatsoulis, A. 2006. The Role of Stress in the Clinical Expression of Thyroid Autoimmunity. *Annals of the New York Academy of Sciences* 1088:382-395.

Tsui, S., V. Naik, N. Hoa, C.J. Hwang, N.F. Afifiyan, A. Sinha Hikim, A.G. Gianoukakis, R.S. Douglas, and T.J. Smith. 2008. Evidence for an association between thyroid-stimulating hormone and insulin-like growth factor 1 receptors: a tale of two antigens implicated in Graves' disease. *Journal of Immunology* 181:4397-4405.

Tunbridge, W.M., D.C. Evered, R. Hall, D. Appleton, M. Brewis, F. Clark, J.G. Evans, E. Young, T. Bird, and P.A. Smith. 1977. The spectrum of thyroid disease in a community: the Whickham survey. *Clinical Endocrinology* 7:481-493.

Ueda, H., J.M. Howson, L. Esposito, J. Heward, H. Snook, G. Chamberlain, D.B. Rainbow, K.M. Hunter, A.N. Smith, G. Di Genova, M.H. Herr, I. Dahlman, F. Payne, D. Smyth, C. Lowe, R.C. Twells, S. Howlett, B. Healy, S. Nutland, H.E. Rance, V. Everett, L.J. Smink, A.C. Lam, H.J. Cordell, N.M. Walker, C. Bordin, J. Hulme, C. Motzo, F. Cucca, J.F. Hess, M.L. Metzker, J. Rogers, S. Gregory, A. Allahabadia, R. Nithiyananthan, E. Tuomilehto-Wolf, J. Tuomilehto, P. Bingley, K.M. Gillespie, D.E. Undlien, K.S. Ronningen, C. Guja, C. Ionescu-Tirgoviste, D.A. Savage, A.P. Maxwell, D.J. Carson, C.C. Patterson, J.A. Franklyn, D.G. Clayton, L.B. Peterson, L.S. Wicker, J.A. Todd, and S.C. Gough. 2003. Association of the T-cell regulatory gene CTLA4 with susceptibility to autoimmune disease. *Nature* 423:506-511.

Uz, E., C. Mustafa, R. Topaloglu, Y. Bilginer, A. Dursun, O. Kasapcopur, S. Ozen, A. Bakkaloglu, and T. Ozcelik. 2009. Increased frequency of extremely skewed X chromosome inactivation in juvenile idiopathic arthritis. *Arthritis Rheum* 60:3410-3412.

Vanderpump, M.P., W.M. Tunbridge, J.M. French, D. Appleton, D. Bates, F. Clark, J. Grimley Evans, D.M. Hasan, H. Rodgers, F. Tunbridge, and et al. 1995. The incidence of thyroid disorders in the

community: a twenty-year follow-up of the Whickham Survey. *Clinical Endocrinology* 43:55-68.

Vannucchi, G., D. Covelli, N. Currò, D. Dazzi, A. Maffini, I. Campi, P. Bonara, C. Guastella, L. Pignataro, R. Ratiglia, P. Beck-Peccoz, and M. Salvi. 2012. Serum BAFF Concentrations in Patients with Graves' Disease and Orbitopathy before and after Immunosuppressive Therapy. *Journal of Clinical Endocrinology & Metabolism* 97:E755-E759.

Verma, R., E. Boleti, and A.J.T. George. 1998. Antibody engineering: Comparison of bacterial, yeast, insect and mammalian expression systems. *Journal of Immunological Methods* 216:165-181.

Vestergaard, P., L. Rejnmark, J. Weeke, H.C. Hoeck, H.K. Nielsen, J. Rungby, P. Laurberg, and L. Mosekilde. 2002. Smoking as a risk factor for Graves' disease, toxic nodular goiter, and autoimmune hypothyroidism. *Thyroid : official journal of the American Thyroid Association* 12:69-75.

Viboud, G.I., and J.B. Bliska. 2005. YERSINIA OUTER PROTEINS: Role in Modulation of Host Cell Signaling Responses and Pathogenesis. *Annual Review of Microbiology* 59:69-89.

Vinuesa, Carola G., and Jason G. Cyster. 2011. How T Cells Earn the Follicular Rite of Passage. *Immunity* 35:671-680.

Vinuesa, C.G., S.G. Tangye, B. Moser, and C.R. Mackay. 2005. Follicular B helper T cells in antibody responses and autoimmunity. *Nature Reviews Immunology* 5:853-865.

Vos, X.G., N. Smit, E. Endert, J.F. Brosschot, J.G.P. Tijssen, and W.M. Wiersinga. 2008. Age and stress as determinants of the severity of hyperthyroidism caused by Graves' disease in newly diagnosed patients. *European Journal of Endocrinology* 160:193-199.

Walker, L.S.K., and D.M. Sansom. 2011. The emerging role of CTLA4 as a cell-extrinsic regulator of T cell responses. *Nat Rev Immunol* 11:852-863.

Walsh, J.P., A.P. Bremner, M.K. Bulsara, P. O'Leary, P.J. Leedman, P. Feddema, and V. Michelangeli. 2005. Parity and the risk of autoimmune thyroid disease: a community-based study. *J Clin Endocrinol Metab* 90:5309-5312.

Wang, Z., Q. Zhang, J. Lu, F. Jiang, H. Zhang, L. Gao, and J. Zhao. 2010. Identification of Outer Membrane Porin F Protein of Yersinia enterocolitica Recognized by Antithyrotopin Receptor Antibodies in Graves' Disease and Determination of Its Epitope Using Mass Spectrometry and Bioinformatics Tools. *Journal of Clinical Endocrinology & Metabolism* 95:4012-4020.

Wardemann, H., S. Yurasov, A. Schaefer, J.W. Young, E. Meffre, and M.C. Nussenzweig. 2003. Predominant Autoantibody Production by Early Human B Cell Precursors. *Science* 301:1374-1377.

Warford, A., S. McLachlan, A. Malcolm, E. Young, J. Farndon, and B. Rees Smith. 1984. Characterization of lymphoid cells in the thyroid of patients with Graves' disease. *Clin Exp Immunol* 57:626-632.

Weetman, A., M. Yateman, P. Ealey, C. Black, C. Reimer, R. Williams, B. Shine, and N. Marshall. 1990. Thyroid-stimulating antibody activity between different immunoglobulin G subclasses. *The Journal of Clinical Investigation* 86:723-727.

Weetman, A.P. 1990. Thyroid peroxidase as an antigen in autoimmune thyroiditis. *Clinical & Experimental Immunology* 80:1-3.

Weetman, A.P. 2000. Graves' disease. *N Engl J Med* 343:1236-1248.

Weetman, A.P. 2004a. Autoimmune thyroid disease. *Autoimmunity* 37:337-340.

Weetman, A.P. 2004b. Cellular immune responses in autoimmune thyroid disease. *Clinical Endocrinology* 61:405-413.

Weinstein, E., E. Peeva, C. Putterman, and B. Diamond. 2004. B-cell biology. *Rheum Dis Clin North Am* 30:159-174.

Weiss, M., S.H. Ingbar, S. Winblad, and D.L. Kasper. 1983. Demonstration of a saturable binding site for thyrotropin in Yersinia enterocolitica. *Science* 219:1331-1333.

Wellmann, U., M. Letz, M. Herrmann, S. Angermüller, J. Kalden, and T. Winkler. 2005. The evolution of human anti-double-stranded DNA autoantibodies. *Proceedings of the National Academy of Sciences* 102:9258-9263.

Wiersinga, W.M. 2011. Autoimmunity in Graves' ophthalmopathy: the result of an unfortunate marriage between TSH receptors and IGF-1 receptors? *J Clin Endocrinol Metab* 96:2386-2394.

Wiersinga, W.M., and L. Bartalena. 2002. Epidemiology and Prevention of Graves' Ophthalmopathy. *Thyroid* 12:855-860.

Wildin, R.S., F. Ramsdell, J. Peake, F. Faravelli, J.-L. Casanova, N. Buist, E. Levy-Lahad, M. Mazzella, O. Goulet, L. Perroni, F. Dagna

Bricarelli, G. Byrne, M. McEuen, S. Proll, M. Appleby, and M.E. Brunkow. 2001. X-linked neonatal diabetes mellitus, enteropathy and endocrinopathy syndrome is the human equivalent of mouse scurfy. *Nat Genet* 27:18-20.

Williams, R.C., Jr., N.J. Marshall, K. Kilpatrick, J. Montano, P.M. Brickell, M. Goodall, P.A. Ealey, B. Shine, A.P. Weetman, and R.K. Craig. 1988. Kappa/lambda immunoglobulin distribution in Graves' thyroid-stimulating antibodies. Simultaneous analysis of C lambda gene polymorphisms. *The Journal of Clinical Investigation* 82:1306-1312.

Wing, K., and S. Sakaguchi. 2009. Regulatory T cells exert checks and balances on self tolerance and autoimmunity. *Nature Immunology* 11:7-13.

Winsa, B., A. Karlsson, R. Bergstrom, H.O. Adami, A. Gamstedt, R. Jansson, U. Adamson, and P.A. Dahlberg. 1991. Stressful life events and Graves' disease. *The Lancet* 338:1475-1479.

Wolf, M., T. Misaki, K. Bech, M. Tvede, J. Silva, and S. Ingbar. 1991. Immunoglobulins of Patients Recovering from Yersinia enterocolitica Infections Exhibit Graves' Disease-like Activity in Human Thyroid Membranes. *Thyroid* 1:

Wren, B.W. 2003. The Yersiniae [mdash] a model genus to study the rapid evolution of bacterial pathogens. *Nat Rev Micro* 1:55-64.

Wucherpfennig, K.W., and D. Sethi. 2011. T cell receptor recognition of self and foreign antigens in the induction of autoimmunity. *Seminars in Immunology* 23:84-91.

Xiang, Z., A.J. Cutler, R.J. Brownlie, K. Fairfax, K.E. Lawlor, E. Severinson, E.U. Walker, R.A. Manz, D.M. Tarlinton, and K.G. Smith. 2007. FcgammaRIIb controls bone marrow plasma cell persistence and apoptosis. *Nature Immunology* 8:419-429.

Yamashita, E., M.V. Zhalnina, S.D. Zakharov, O. Sharma, and W.A. Cramer. 2008. Crystal structures of the OmpF porin: function in a colicin translocon. *EMBO J* 27:2171-2180.

Yanaba, K., J.D. Bouaziz, K.M. Haas, J.C. Poe, M. Fujimoto, and T.F. Tedder. 2008. A regulatory B cell subset with a unique CD1dhiCD5+ phenotype controls T cell-dependent inflammatory responses. *Immunity* 28:639-650.

Yanagawa, T., Y. Hidaka, V. Guimaraes, M. Soliman, and L.J. DeGroot. 1995. CTLA-4 gene polymorphism associated with Graves' disease in a Caucasian population. *J Clin Endocrinol Metab* 80:41-45.

Zakarija, M. 1983. Immunochemical characterization of the thyroid-stimulating antibody (TSAb) of Graves' disease: evidence for restricted heterogeneity. *J Clin Lab Immunol* 10:77-85.

Zamani, M., M. Spaepen, M. Bex, R. Bouillon, and J.J. Cassiman. 2000. Primary role of the HLA class II DRB1*0301 allele in Graves disease. *Am J Med Genet* 95:432-437.

Zembala, M., G.L. Asherson, J. Noworolski, and B. Mayhew. 1976. Contact sensitivity to picryl chloride: the occurrence of B suppressor cells in the lymph nodes and spleen of immunized mice. *Cell Immunol* 25:266-278.

Zhang, H., I. Kaur, DW Niesel, GS Seetharamaiah, JW Peterson, B. Prabhakar, and G. Klimpel. 1997. Lipoprotein from Yersinia enterocolitica Contains Epitopes That Cross-React with the Human Thyrotropin Receptor. *J. Immunol* 158:1976-1983.

Zhang, J., N. Zahir, Q. Jiang, H. Miliotis, S. Heyraud, X. Meng, B. Dong, G. Xie, F. Qiu, Z. Hao, C.A. McCulloch, E.C. Keystone, A.C. Peterson, and K.A. Siminovitch. 2011. The autoimmune disease-associated PTPN22 variant promotes calpain-mediated Lyp/Pep degradation associated with lymphocyte and dendritic cell hyperresponsiveness. *Nature genetics* 43:902-907.

Zhang, M., K.P. Tong, V. Fremont, J. Chen, P. Narayan, D. Puett, B.D. Weintraub, and M.W. Szkudlinski. 2000. The extracellular domain suppresses constitutive activity of the transmembrane domain of the human TSH receptor: implications for hormone-receptor interaction and antagonist design. *Endocrinology* 141:3514-3517.

Zhao, S.-X., S. Tsui, A. Cheung, R.S. Douglas, T.J. Smith, and J.P. Banga. 2011. Orbital fibrosis in a mouse model of Graves' disease induced by genetic immunization of thyrotropin receptor cDNA. *Journal of Endocrinology* 210:369-377.

Zheng, J., Y. Liu, Y.-L. Lau, and W. Tu. 2010. CD40-activated B cells are more potent than immature dendritic cells to induce and expand CD4+ regulatory T cells. *Cell Mol Immunol* 7:44-50.

Zhou, J., M. Bi, C. Fan, X. Song, R. Yang, S. Zhao, L. Li, Y. Li, W. Teng, and Z. Shan. 2012. Regulatory T cells but not T helper 17 cells are modulated in an animal model of Graves' hyperthyroidism. *Clinical and Experimental Medicine* 12:39-46.

Zotos, D., J.M. Coquet, Y. Zhang, A. Light, K. D'Costa, A. Kallies, L.M. Corcoran, D.I. Godfrey, K.M. Toellner, M.J. Smyth, S.L. Nutt, and D.M. Tarlinton. 2010. IL-21 regulates germinal center B cell differentiation and proliferation through a B cell-intrinsic mechanism. *Journal of Experimental Medicine* 207:365-378.

Zuckerman, N.S., W.A. Howard, J. Bismuth, K. Gibson, H. Edelman, S. Berrih-Aknin, D. Dunn-Walters, and R. Mehr. 2010. Ectopic GC in the thymus of myasthenia gravis patients show characteristics of normal GC. *European Journal of Immunology* 40:1150-1161.

Hargreaves CE, Dunn-Walters D, Banga JP.

Abstract 14th International Thyroid Congress, Paris, France, 2010.

Title: Studies on rearranged, germline antibody genes that predispose potentially autoreactive B cells to produce thyroid stimulating antibodies in Graves' disease: expression as recombinant Fab antibody for evaluation of antigen binding specificity.

Graves' disease is an antibody driven autoimmune disease, where antibody to thyroid stimulating hormone receptor (TSHR) stimulate the gland to produce excessive thyroid hormone resulting in hyperthyroidism. Knowledge of factors responsible for production of antibody to TSHR with thyroid stimulating activity is fundamental to gaining a deeper insight into the molecular basis of the condition. To produce antigen specific antibodies, B lymphocytes first produce immunoglobulin (Ig) genes by recombining the different heavy and light chain variable (V)-region gene segments. Subsequent antigenic stimulation leads to class switching and diversification of the antibody repertoire by clonal expansion and somatic hypermutation, leading to increase in antibody affinity. Evidence of the same process is shown in autoimmune disease, although the self antigen (autoantigen) or the environmental agent (pathogen) driving the affinity maturation remains largely unknown. We have initiated studies to determine the antigen binding properties of germline Ig genes whose affinity matured variants have previously been shown to be pathogenic thyroid stimulating antibodies, in order to gain an insight into the *in vivo*

stimulatory events leading to the clonal expansion of B cells resulting in thyroid autoimmunity.

The molecular immunology of two monoclonal antibodies (mAbs) KSAb1 (IgG2b, k) and KSAb2 (IgG2a, k) to TSHR with thyroid stimulating properties have been studied. The mAbs derive from a single mouse undergoing experimental Graves' disease. Despite different subclass, it was striking that KSAb1 and KSAb2 use the same rearrangement of immunoglobulin heavy chain variable region (IGHV) and light chain variable region (IGVL) germlines genes, and arose from a single precursor B cell clone. To study binding properties of the germline antibodies, we have synthesised the rearranged germline IGHV and IGLV genes derived from the Ig gene families of KSAb1 and KSAb2. The synthetic germline IGHV and IGLV genes have been expressed in bacteria as recombinant Fab (rFab) antibody. Successful expression of the germline rFab has been attained, and purified to homogeneity by metal chelation and protein-G chromatography. As controls, rFab of KSAb1 and as negative control, rFab from a mAb to an islet cell antigen in type 1 diabetes, have been expressed and purified in similar manner. Examination of a variety of parameters on whether the germ line configured rFab preparation shows any measurable binding to TSHR or environmental agents such as infectious pathogens are underway to define the antigens that contribute to the clonal expansion and diversification of potentially autoreactive B cell clones implicated in thyroid autoimmune disease. Moreover, such investigations will also give an insight into how potentially autoreactive B cell escape the *in vivo*

immune tolerance mechanisms that prevent the clonal expansion of such rogue B cell clones, which through somatic hypermutation events produce disease-inducing antibodies.

Abstract ESF-JSPS Frontier Science Conference Series for Young Researchers Cutting Edge Immunology and its Clinical Application, Holland, 2011.

Hargreaves CE, Dunn-Walters D, Banga JP.

Title: Anti-TSHR autoantibodies in Graves' disease develop from non-autoreactive precursors

Introduction: Graves' disease (GD) is an antibody driven autoimmune disease, where antibody to thyroid stimulating hormone receptor (TSHR), stimulate the gland to produce excessive thyroid hormone resulting in hyperthyroidism. Knowledge of factors responsible for production of antibody to TSHR with thyroid stimulating activity is fundamental to gaining a deeper insight into the molecular basis of the condition.

We have recently described two monoclonal antibodies (mAbs), KSAb1 (IgG2b, k) and KSAb21 (IgG2a, k), derived from the same mouse with powerful thyroid stimulating antibody (TSAb) properties. V-region sequence analysis showed that both were derived from the same rearranged H- and L-genes. This gave us an opportunity to study the antigenic specificity of the rearranged genes that predispose to the generation of TSAbs.

Methods: To study the binding properties of the rearranged germline (RG) sequence of these antibodies, we synthesised the germline variable region light and heavy genes of KSAb1 and KSAb2. The synthetic RG construct was cloned in pAK19 vector for bacterial expression as recombinant Fab (rFab) preparations and purified to homogeneity by metal chelation. As controls, rFab preparation of KSAb1 and an irrelevant control, rFab 96/3 were expressed and purified in a similar manner.

Reactivity of rFab RG to TSHR was examined by a variety of experimental parameters, including: competitive inhibition of radiolabelled thyroid stimulating hormone (TSH) binding to immobilised TSHR, stimulation of the TSHR second messenger cAMP in CHO cells transfected with full-length TSHR and by flow cytometry.

Results: rFab RG did not inhibit radiolabelled TSH from binding TSHR, did not stimulate cAMP and did not display measurable binding in flow cytometry assays.

Conclusion: This data suggests anti-TSHR autoantibodies develop from non-reactive precursor B cells and this pathogenicity may develop through the process of somatic hypermutation in the periphery. Experiments are currently underway to further define when pathogenicity arises and whether it is an environmental agent that first drives the clonal expansion of such rogue B cells.

Abstract 35th Annual European Thyroid Association, Krakow, Poland, 2011.

Hargreaves CE, Dunn-Walters D, Banga JP.

Title: Somatic hypermutation of the immunoglobulin heavy chain variable-region of thyroid stimulating antibodies determines binding to the TSH-receptor.

Introduction: Graves' disease is an autoimmune disease where antibodies to TSH-receptor (TSHR) stimulate the gland to produce excessive thyroid hormone causing hyperthyroidism. Knowledge of factors responsible for production of the pathogenic thyroid stimulating antibodies (TSAbs) is fundamental to understanding the molecular basis of the condition.

We described two monoclonal TSAbs derived from one mouse undergoing autoimmune hyperthyroidism. Immunoglobulin (Ig) gene sequence analysis showed that both TSAbs were derived from the same clonotype, but varied in their hypermutation, thus providing an opportunity to study the effect of hypermutation on antigenic specificity.

Methods: To study the binding properties of the germline clonotype, we synthesised the germline *IGH* and *IGK* genes shared by the two mAbs (KSAb1 and KSAb2). The synthetic construct was cloned for expression as recombinant Fab (rFab) and purified to homogeneity. We also assessed the contribution of the somatically hypermutated *IGH* and *IGK* by creating two swap constructs: Swap 1 comprises the mutated KSAb1

IGK and germline *IGH*, Swap 2 comprises the mutated KSAb1 *IGH* and the germline *IGK*. Swap constructs were expressed as rFabs; Swap 1 was purified to homogeneity and Swap 2 was partially purified. Binding of rFabs to TSHR was examined by competitive inhibition of ^{125}I-TSH binding to TSHR, stimulation of the TSHR second messenger cAMP and by flow cytometry.

Results: The germline rFab failed to recognise TSHR. Interestingly, Swap 2 rFab inhibited ^{125}I-TSH binding to TSHR, whilst Swap 1 rFab did not, showing the importance of the *IGH* in determining receptor binding.

Conclusion: We show for the first time that TSAbs responsible for Graves' disease develop from non-reactive precursor B cells, which acquire TSHR recognition and pathogenicity as a result of somatic hypermutation. The availability of non-reactive precursor antibody provides an opportunity to examine the role of infectious agents in Graves' disease.